Impact of Diet on Gene Dysfunction in Type 2 Diabetes

by

Merell Pabilona Billacura, MSc

A thesis submitted for a Doctor of Philosophy degree at

Nottingham Trent University

June 2022

Examiners:

Prof. Paul Squires

Professor in Biomedical Science (Diabetes and Endocrinology)

University of Lincoln, United Kingdom

Dr. Alan Hargreaves

Reader/Associate Professor in Biochemistry

Nottingham Trent University, United Kingdom

Declaration

Publications and papers arising from this thesis

Cripps, M.J., Bagnati, M., Jones, T.A., Ogunkolade, B.W., Sayers, S.R., Caton, P.W., Hanna, K., **Billacura, M.P.**, Fair, K., Nelson, C., Lowe, R., Hitman, G.A., Berry, M.D. and Turner, M.D. (2020). Identification of a subset of trace amine-associated receptors and ligands as potential modulators of insulin secretion. Biochemical Pharmacology *171,* 113685.

Lavilla,C., **Billacura, M.P.**, Hanna,K., Boocock,D., Coveney,C., Miles,A., Foulds,G.A., Murphy,A., Tan,A., Jackisch,L., Sayers,S., Caton,P.W., Doig,C.L, McTernan,P.G., Colombo,S.L., Sale,C., and Turner,M.D. (2021). Carnosine protects stimulus-secretion coupling through prevention of protein carbonyl adduction events in cells under metabolic stress. Free Radical Biology and Medicine. 2021 Nov 1;175:65-79. doi: 10.1016/j.freeradbiomed.2021.08.233. Epub 2021 Aug 27. PMID: 34455039.

Billacura, M.P., Lavilla Jr, C., Cripps, M.J., Hanna, K., Sale, C. and Turner, M.D., 2022. β-alanine scavenging of free radicals protects mitochondrial function and enhances both insulin secretion and glucose uptake in cells under metabolic stress. *Advances in Redox Research*, p.100050.

Hanna,K., **Billacura, M.P.**, Cripps,M.J., Jones,T.A., Marshall,C., Ogunkolade,W, Sayers,S., Caton,P.W., Hitman,G.A., and Turner,M.D. (2022). Glucolipotoxic downregulation of HNF-4α gene expression results in decreased expression of multiple protein trafficking molecules, and reduced insulin secretion from pancreatic β-cells. Submission to J. Endocrinol.

Acknowledgement

This work would not be possible without the help and support of the following people and institutions:

I want to thank my director of studies, Mark D. Turner, Ph.D., who helped me secure a Ph.D. scholarship from DOST-Newton Scholarship. Dr. Turner has allowed me to work under his guidance and learn various transferable skills independently. With this, I owe him a lot.

To Prof. Craig Sale, Ph.D., co-supervisor, for the comments and suggestions made to refine this work; Sergio L. Colombo, Ph.D., co-supervisor, for the guidance in the laboratory work and providing answers to my queries; and Carl Nelson, Ph.D., my independent assessor, for the comments and suggestions during meetings.

Newton Agham Programme, a partnership of the British Council Philippines and Department of Science and Technology Philippines, for funding my entire Ph.D. journey. Without your support, I would not be able to come to the UK for a postgraduate study. I would like to special mention and give thanks to the massive support of Josette T. Biyo, Ph.D., Director of DOST-SEI, Andrea Teran and Danie Son Gonzalvo, Newton Fund Managers in the Philippines and Edwin Bondoc Lopez of DOST-SEI. I want to thank Mindanao State University-Marawi and her Officials for granting my study leave. Special thanks to the Philippine Government for funding my Ph.D.

Dr. Paul W. Caton and Dr. Sophie R. Sayers from Diabetes and Nutritional Sciences Division, King's College London, for collaborative *ex-vivo* mouse islet data that supports and increases the validity and impact of this work.

NTU Department of Chemistry and Forensics specially to Christopher Garner, Ph.D., Suniya Khatun, Daniel Cotton and team for the computational screening potential carnosinase inhibitors and synthesis of carnosine mimetics.

I want to thank Marta Bagnati, Ph.D., Tania Jones, Ph.D., Babatundi Ogunkolade, Ph.D., Robert Lowe, Ph.D., and Prof. Graham A. Hitman, Ph.D., from Blizard Institute, Barts and The London School of Medicine and Dentistry, Queen Mary University of London for their contribution to transcriptomic analysis and MetaCore™ pathway analysis.

NTU Technical Staff, especially to Jayne Spence, for always there whenever I need something to sort out in the laboratory;

Charlie A. Lavilla, Jr., Ph.D., and his wife, Misshell L. Lavilla, helped me settle here in the UK and for the fantastic memories, we had from Edale Road, NG2 4HT to Station House, NG6 9AA. Andy and Juvy Davidson-Hogg for the beautiful memories in Station House and for treating Maria and I as family.

Katie Hanna, Ph.D., and Michael Cripps, Ph.D., for providing me data for this project. Laura Gonzales, Ph.D., Akashdeep Singh, Ph.D., and Stephanie Anuta for the memories working in IBRC 009.

Arnold Tan for the technical help in culturing skeletal muscle C2C12 myotubes. With this, I have finalised my Seahorse Mito Stress work.

Maximilian E. Pickup, Jinous Samavat, Ph.D., Nikoletta Kalenderoglou, Ph.D., Satinderdeep Kaur, Justine Hu, Lydia Hardowar, Daniel Dimmock, Nikita Lad, Tameille Nickoya Valentine, Alice Murphy, Ph.D., Nick Weir, Ph.D., Younis Awais and Christian Mifsud for the warm friendship.

Maria Distressa R. Genita-Billacura, my beautiful and loving Wife, for always there in times of adversity and success. You have never left me. For always lifting me up and giving me joy beyond expectation. I can never thank you enough.

To my parents, Marlou Lucero Billacura and Ofelia Intrepido Pabilona Billacura for the love, encouragement, and emotional support. To Saturnino L. Genita Jr. Family for the understanding and taking care of our place in the Philippines whilst we are away. To my families in London, especially to Auntie Anne

Leonor and Auntie Susie Rodriguez for the warm welcome whenever we are in London.

Lastly, to God who strengthens me and guides me throughout this endeavour.

Abstract

Type 2 diabetes (T2D) is an autoinflammatory disease and metabolic disorder characterised by high blood glucose levels, failure/reduction of insulin secretion by the pancreas, and insulin resistance. The International Diabetes Foundation reported in 2019 that 9.3% (463 million) of the adult population were living with diabetes, half of which were undiagnosed. T2D is also strongly linked to obesity, which is the single most highly modifiable risk factor for T2D.

Isolated CD-1 mice islets, INS-1 rat pancreatic β-cells and skeletal muscle C2C12 mouse myotubes were hereby used as cellular models for T2D. The effects of glucolipotoxic (GLT) metabolic stress were investigated by incubating these cells in medium supplemented with chronically elevated glucose and high free fatty acid concentrations that mimic the extracellular environment typically found in patients with poorly controlled T2D. In addition, molecules potentially able to counter these effects were investigated by incubating cells in either: control medium ± 10 mM L-carnosine (or β-alanine); control medium ± 100 µM carnosine analogues; GLT medium ± 10 mM L-carnosine (or β-alanine); GLT medium ± 100 µM carnosine analogues.

The effects of glucolipotoxicity were assessed through transcriptomic analysis utilising microarray data and Illumina-HiSeq gene expression data in combination with non-biased ranked pathway analysis using Metacore^{TM} technology. The results generated from these methods were validated using RT-qPCR and Western blotting. Functional assays were performed to determine cell viability, reactive species scavenging, 3-nitrotyrosine (3-NT) level, 4-hydroxynonenal (4-HNE) level and Seahorse Mito Stress assay utilised to determine the impact of GLT and potential therapeutic agents on mitochondrial function.

Using the above methodologies, hepatocyte nuclear factor 4 alpha (HNF4α) was shown to be a transcription factor that is a central regulator of protein trafficking through control of expression of multiple Rab genes and syntaxin 17. Furthermore, HNF4α was shown to be sensitive to GLT metabolic stress, and targeted HNF4α knocked down inhibited insulin secretion. HNF1α expression was reduced when HNF4α was downregulated, suggesting an association between the two transcription factors. Cell adhesion pathways were also shown to be strongly downregulated by GLT, and targeted knocked down of the extracellular matrix genes encoding matrix metallopeptidase 14 (MMP14), CD44 molecule (CD44) and Erb-B2 receptor tyrosine kinase 4 (ErbB4) expression inhibited insulin secretion.

Carnosine is a physiological histidine-containing dipeptide that has recently been shown to help reduce glycated haemoglobin 1ac (HbA1c) levels in patients with T2D, although the mechanism of action associated with this reduction is poorly understood. Data presented herein show that carnosine, its analogues, and the constituent amino acid, β-alanine, effectively scavenge radical species generated by GLT. GLT was also shown to decrease maximal respiration and reduce mitochondria's ability to generate ATP. However, this decrease was effectively reversed by the supplementation of carnosine and β-alanine to GLT media. Carnosine and carnosine mimetics also consequently increased insulin secretion that was hitherto inhibited by GLT. Importantly, carnosine analogues, M8 and E3, significantly reduced the formation of 3-NT and 4-HNE adducts in both *in vitro* and *in vivo* experiments and were shown to counter obesity and T2D in a 10-week animal study. This therefore indicates a potential role for these molecules as novel therapeutic agents in the treatment and/or prevention of metabolic diseases.

Table of contents

Impact of Diet on Gene Dysfunction in Type 2 Diabetes i
Acknowledgement iv
Abstract vii
Table of contents ix
List of figures xiv
List of tables xviii
Abbreviations xix

Chapter 1
Thesis Overview, Aims and Objectives 1
1.1 Introduction 2
1.2Pancreas 4
1.3 Islets of Langerhans 5
1.3.1 α-cells 6
1.3.2 β-cells 6
1.3.3 δ-cells 8
1.3.4 Pancreatic polypeptide cell 10
1.3.5 Ghrelin-positive and other islet cell types 10
1.4 Insulin and its structure 10
1.4.1 Insulin synthesis, secretion, and action 12
1.4.2 Insulin signalling pathway 15
1.5 Diabetes 16
1.5.1 Symptoms of diabetes 19
1.5.2 Drugs used to combat diabetes 20
1.5.2.1 Glucagon-like peptide-1 20
1.5.2.2 Metformin 21
1.5.2.3 Thiazolidinediones 23
1.5.2.4 Sulfonylureas 24
1.5.2.5 Glinides 25
1.5.2.6 α-Glucosidase inhibitors 26
1.5.2.7 Insulin 27
1.5.2.8 Sodium-glucose co-transporter inhibitors 28
1.5.2.9 Statins 29
1.6 Carnosine 30

1.6.1 L-histidine 33
1.6.2 β-alanine 34
1.7 Glucolipotoxicity 34
1.8 Radical species 36
1.8.1 Radical oxygen species 37
1.8.1.1 Sources of radical oxygen species 38
1.8.2 Reactive nitrogen species 43
1.8.3 Dual role of ROS and RNS 45
1.9 Oxidative stress 48
1.10 Nitrosative stress 49
1.11Aims and objectives 49

Chapter 2
Materials and Methodology 51
2.1 Reagents and buffer solutions 52
2.2 Cell culture 54
2.2.1 INS-1 cells 54
2.2.2 C2C12 cells 55
2.3 Cell culture, propagation, and passaging 55
2.4 Preparation of glucolipotoxic media 56
2.5 Cell counting 56
2.6 Cell plate seeding and cell culture lysate extraction 58
2.7 Determination of total protein concentration in lysates 59
2.8 Cryo-conservation and recovery of frozen cells 60
2.9 Mycoplasma assessment and decontamination 61
2.10 Mice strain, islet extraction and digestion 63
2.11Cell functional analyses 63
2.11.1 Cell viability 63
2.11.2 Radical species detection 64
2.11.3 Insulin secretion assay 65
2.11.4 3-Nitrotyrosine assay 66
2.11.5 4-Hydroxynonenal assay 67
2.11.6 Seahorse mitochondrial function assay 68
2.12 Sodium dodecyl sulphate-polyacrylamide gel electrophoresis 74
2.12.1 Immunoblotting 77

2.12.2 Signal band densitometry 78
2.13 Small interfering RNA transfection 79
2.14 Real-time reverse transcription polymerase chain reaction 79
2.14.1 Primer design 80
2.14.2 Primer validation 82
2.14.3 RNA extraction 83
2.14.4 RNA quality assessment and quantification 85
2.14.5 cDNA synthesis 86
2.14.6 QuantiNova SBYR green PCR 87
2.14.7 RT-qPCR data analysis 89
2.15 RNAsequencing 89
2.15.1 DNase treatment 89
2.15.2 Library preparation 90
2.15.3 Sequencing 91
2.15.4 Data analysis 92
2.15.5 Network analysis 92
2.16 Screening of potential carnosinase inhibitors and carnosine mimetics 93
2.17 Statistical analyses 94

Chapter 3
Hepatocyte Nuclear Factor 4α and Hepatocyte Nuclear Factor 1α 95
3.1 Introduction 96
3.2 Results 98
3.2.1 Effects of GLT on HNF4α and HNF1α 98
3.3 Discussion 109
3.4 Conclusion 115

Chapter 4
Extracellular Matrix Proteins and Cytoskeletal Remodelling 116
4.1 Introduction 117
4.2 Results 120
4.3 Effect of glucolipotoxicity on MMP14, CD44 and ErbB4 protein expression 128
4.3 Effect of MMP14, CD44 and ErbB4 knocked down on insulin secretion 134
4.4 Discussion 145
4.5 Conclusion 149

Chapter 5

L-carnosine and β-alanine: Their Impact on Mitochondrial Bioenergetics 150

5.1 Introduction 151

5.2 Results 156

5.2.1 Effects of L-carnosine and β-alanine in INS-1 cells and C2C12 myotubes viability 156

5.2.2 Scavenging potential of L-carnosine and β-alanine using INS-1 and C2C12 myotubes 163

5.2.3 Effects of L-carnosine on the mitochondrial function exposed to glucolipotoxic condition 169

5.2.4 Effects of β-alanine on the mitochondrial function exposed to glucolipotoxic condition 176

5.3 Discussion 183

5.4 Conclusion 189

Chapter 6

Carnosine, Carnosine Inhibitors and Carnosine Mimetics 191

6.1 Introduction 192

6.2 Results 197

6.2.1 Effects of L-carnosine on glucolipotoxic free radicals and insulin secretion 197

6.2.2 Carnosinase inhibitors as potential scavengers of reactive species and their effect on insulin secretion 205

6.2.3 Carnosine mimetics as a potential scavenger of reactive species and their effect on insulin secretion 212

6.2.4 Effect of carnosinase inhibitor and carnosine mimetic on 4-hydroxynonenal level 219

6.2.5 Effect of carnosinase inhibitor and carnosine mimetic on 3-nitrotyrosine level 221

6.3 Discussion 222

6.4 Conclusion 229

Chapter 7

General Discussion, Summary, and Conclusion 230

7.1 General discussion and summary 231

Chapter 8
Future Work 236
8.1 Histone acetylation 237
8.2 Olfactory receptor agonist ligands its implication to glucolipotoxicity inhibition of insulin secretion 240

References 246
Appendices 318

List of figures

Figure 1.1 Pancreas and islets of Langerhans. 5
Figure 1.2 Structure of $zinc_2$-$insulin_6$ complex 7
Figure 1.3 Structure of somatostatin 9
Figure 1.4 Cleavage of proinsulin to insulin 12
Figure 1.5 Regulation of metabolism by insulin 13
Figure 1.6 Signal transduction in insulin action 15
Figure 1.7 Chemical structure of metformin 22
Figure 1.8 Chemical structures of known glitazones 23
Figure 1.9 Chemical structures of sulfonylureas 25
Figure 1.10 Chemical structures of common glinides 26
Figure 1.11 Chemical structures of known α-glucosidase inhibitors 27
Figure 1.12 Carnosine structure 30
Figure 1.13 Synthesis and hydrolysis of carnosine 31
Figure 1.14 Structure-activity of carnosine 32
Figure 1.15 Generation of reactive oxygen species in the mitochondria 39
Figure 1.16 Cellular sources of radical oxygen species 41
Figure 1.17 Fenton reaction 43
Figure 1.18 Formation of peroxynitrite 44
Figure 1.19 Formation of 3-nitrotyrosine 45

Figure 2.1 Neubauer chamber of the haemocytometer 58
Figure 2.2 Mycoplasma detection test by PCR 62
Figure 2.3 Location and labelling of sensor cartridge ports 70
Figure 2.4 Seahorse XF cell mito stress key parameters and kinetic profile 71
Figure 2.5 Seahorse XF cell mito stress modulators target of action in electron transport chain complexes 72
Figure 2.6 Nitrocellulose membrane with transferred proteins 77
Figure 2.7 RNA integrity number 85
Figure 2.8 RNAseq library preparation 91

Figure 3.1 HNF4α Metacore™ pathway map 99
Figure 3.2 qPCR validation of HNF4α pathway genes 100
Figure 3.3 HNF4 protein expression level exposed in glucolipotoxicity 102
Figure 3.4 HNF1α protein level exposed in glucolipotoxicity 104

Figure 3.5 Effect of HNF4α knocked down on Rab gene expression 105
Figure 3.6 Effect of HNF4α knocked down on insulin secretion 108

Figure 4.1 Extracellular matrix remodelling/actin cytoskeleton MetaCore™ map 123
Figure 4.2 Illumina HiSeq RNA expression data for ECM membrane proteins dysregulated by GLT. 124
Figure 4.3 qPCR expression of the extracellular matrix mRNAs using INS-1 cells 125
Figure 4.4 qPCR expression of the extracellular matrix mRNAs using CD-1 mice pancreatic islet cells 127
Figure 4.5 Protein expression of MMP14 exposed to GLT 129
Figure 4.6 Protein expression of CD44 exposed to GLT. 131
Figure 4.7 Protein expression of ErbB4 exposed to GLT 133
Figure 4.8 Transient knocked down of MMP14 135
Figure 4.9 Transient knocked down of CD44 136
Figure 4.10 Transient knocked down of ErbB4 137
Figure 4.11 Effect of MMP14 knocked down on insulin secretion 139
Figure 4.12 Effect of CD44 knocked down on insulin secretion 141
Figure 4.13 Effect of ErbB4 knocked down on insulin secretion 143

Figure 5.1 Mitochondrial structure and its function 152
Figure 5.2 β-cell function under euglycemia and hyperglycaemia 154
Figure 5.3 Effect of experimental conditions on INS-1 rat pancreatic β-cell morphology 158
Figure 5.4 Effect of experimental conditions on skeletal C2C12 myotubes morphology 160
Figure 5.5 Effect of β-alanine on INS-1 rat pancreatic β-cell viability 161
Figure 5.6 Effect of L-carnosine on C2C12 myotubes viability 162
Figure 5.7 Effect of β-alanine on C2C12 myotubes viability 163
Figure 5.8 Effect of GLT and β-alanine on radical species production using INS-1 cells 164
Figure 5.9 Effect of GLT and carnosine on radical species production using C2C12 myotubes 166
Figure 5.10 Effect of GLT and β-alanine on radical species production using C2C12 myotubes 168

Figure 5.11 Effect of metabolic stress and carnosine on mitochondrial respiration of INS-1cells 170
Figure 5.12 Effect of metabolic stress and carnosine on mitochondrial respiration of C2C12 myotubes 173
Figure 5.13 Effect of metabolic stress and β-alanine on mitochondrial respiration of INS-1cells 177
Figure 5.14 Effect of metabolic stress and β-alanine on mitochondrial respiration of C2C12 myotubes 180

Figure 6.1 Hydrolysis of calcein AM dye to fluorescent calcein by intracellular esterases. 194
Figure 6.2 Mechanism of action of DCFH-DA in the live cell 196
Figure 6.3 Effect of experimental conditions on INS-1 rat pancreatic β-cell morphology. 198
Figure 6.4 Effect of experimental conditions on INS-1 rat pancreatic β-cell viability 199
Figure 6.5 Effect of GLT and carnosine on radical species production 201
Figure 6.6 iNOs protein expression level 202
Figure 6.7 Effect of L-carnosine on iNOS protein expression level 203
Figure 6.8 Effect of carnosine on insulin secretion to glucolipotoxic treated INS-1 rat pancreatic β-cells 204
Figure 6.9 Morphological effect of carnosinase inhibitors to INS-1 rat pancreatic β-cells 207
Figure 6.10 Effect of carnosinase inhibitors on INS-1 rat pancreatic β-cell health 209
Figure 6.11 Effect of carnosinase inhibitors on GLT ROS production 211
Figure 6.12 Effect of carnosinase inhibitors on insulin secretion to glucolipotoxic treated INS-1 rat pancreatic β-cells 212
Figure 6.13 INS-1 cells treated with carnosine mimetics 214
Figure 6.14 Effect of carnosine esters on INS-1 rat pancreatic β-cell health 215
Figure 6.15 Effect of carnosine mimetics on GLT ROS production. 216
Figure 6.16 Effect of carnosine on insulin secretion to glucolipotoxic treated INS-1 rat pancreatic β-cells 218
Figure 6.17 Effect of M8 and E3 on 4-hydroxynonenal production 220
Figure 6.18 Effect of M8 and E3 on 3-nitrotyrosine production 221
Figure 6.19 Tautomeric forms of L-carnosine 224

Figure 6.20 Reaction mechanism of L-carnosine towards hydroxyl radicals 224
Figure 6.21 Proposed reaction mechanism of L-carnosine with 4-HNE 227

Figure 8.1 qPCR validation of genes involved in TCA, fatty acid and cholesterol synthesis 238
Figure 8.2 Effect of glucolipotoxicity inhibited insulin secretion to IDH2 overexpressed INS-1 cells. 239
Figure 8.3 Effect of OLRs on INS-1 rat pancreatic β-cell health 242
Figure 8.4 Effect of OLRs on insulin secretion to glucolipotoxic treated INS-1 rat pancreatic β-cells 243

Figure A1. HNF1α 319
Figure A2. HNF4α 320
Figure A3. MMP14 321
Figure A4. CD44 321
Figure A5. ErbB4 322
Figure A6. iNOS 323

List of tables

Table 1.1 Classification of diabetes. 17

Table 2.1 Media and buffer solutions used in the entire study. 52
Table 2.2 PCR reaction set-up using EZ-PCR mycoplasma kit. 61
Table 2.3 Cycling conditions set by EZ-PCR mycoplasma kit. 61
Table 2.4 Working compound preparation. 70
Table 2.5 Summary of the effects of the modulators in mitochondrial respiration. 72
Table 2.6 Seahorse XF cell mito stress key parameters and how it is calculated. 74
Table 2.7 Recipes for preparation of stacking and resolving gels. 75
Table 2.8 Primary and secondary antibodies used in immunoblotting. 78
Table 2.9 Primers used in the entire study. 81
Table 2.10 Master mix in qPCR. 82
Table 2.11 PCR cycling conditions for reverse transcription. 83
Table 2.12 Reverse transcription cDNA master mix. 86
Table 2.13 PCR cycling conditions for cDNA reverse transcription. 87
Table 2.14 Master mix in RT-qPCR. 88
Table 2.15 Cycling conditions for qPCR. 89

Table 4.1 Pathway map enrichment analysis report of RNAseq data. 121

Abbreviations

3-NT	–	3-nitrotyrosine
4-HNE	–	4-hydoxynonenal
ADP	–	Adenosine diphosphate
AGE	–	Advanced glycation end product
ALE	–	Advanced lipoxidation end product
AMPK	–	5'-adenosine monophosphate-activated protein kinase
ATP	–	Adenosine triphosphate
BCA	–	Bicinchoninic acid assay
BSA	–	Bovine serum albumin
cAMP	–	cyclic adenosine monophosphate
CD44	–	CD44 molecule (Indian blood group)
CN1	–	Carnosinase 1
CNDP1	–	Serum carnosinase
CN2	–	Carnosinase 2
CNDP2	–	Tissue carnosinase
Complex III	–	Ubiquinol-cytochrome c oxidoreductase
CPT-1	–	Carnitine palmitoyl transferase-1
DCFDA	–	2’,7’ - Dichlorofluorescein diacetate
ErbB4	–	Receptor protein-tyrosine kinase ErbB-4
ECM	–	Extracellular matrix
EGF	–	Epidermal growth factor
EGFR	–	Epidermal growth factor receptors
ER	–	Endoplasmic reticulum
ERO1	–	Endoplasmic reticular oxidoreductin 1
FAD	–	Flavin adenine dinucleotide
FASN	–	Fatty acid synthase
FCCP	–	Carbonyl cyanide-4 (trifluoromethoxy) phenylhydrazone
FFAs	–	Free fatty acids
FMN	–	Flavin mononucleotide
GAPDH	–	Glyceraldehyde-3-phosphate dehydrogenase
GIP	–	Glucose-dependent insulinotropic polypeptide
GLP-1	–	Glucagon-like peptide 1
GLT	–	Glucolipotoxicity
Glut2	–	Glucose transporter 2

Glut4	–	Glucose transporter 4
G_{olf}	–	Olfactory G protein
GSIS	–	Glucose stimulated insulin secretion
HbA1c	–	Glycated haemoglobin
HMGC	–	3-hydroxy-3-methylglutaryl coenzyme A
HNF1α	–	Hepatocyte nuclear factor 1 alpha
HNF4α	–	Hepatocyte nuclear factor 4 alpha
IBM	–	Inner boundary membrane
IDH2	–	Isocitrate dehydrogenase 2
IMM	–	Inner mitochondrial membrane
iNOS	–	Inducible nitric oxide synthase
INS-1	–	Insulinoma-1
INS2	–	Insulin
IRS	–	insulin receptor substrate
LADA	–	Latent autoimmune diabetes of adults
MMP14	–	Matrix metallopeptidase 14
MMPs	–	Matrix metalloproteinases
MODY	–	Maturity onset diabetes of the young
NIDDM	–	Non-insulin-dependent diabetes mellitus
nNOS	–	Neuronal nitric oxide synthase
Nrg	–	Neuroregulins
OGDH	–	2-oxoglutarate dehydrogenase E1
OGTT	–	Oral glucose tolerance test
OMM	–	Outer mitochondrial membrane
OXPHOS	–	Oxidative phosphorylation system
p66SHC	–	Src homologous-collagen homologue adaptor protein
PBS	–	Phosphate buffered saline
RIPA	–	Radioimmunoprecipitation assay buffer
RNS	–	Reactive nitrogen species
RONS	–	Reactive oxygen and nitrogen species
ROS	–	Reactive oxygen species
Rot/AA	–	Rotenone/Antimycin
RPMI-1640	–	Roswell Park Memorial Institute-1640
RT-qPCR	–	Quantitative reverse transcription polymerase chain reaction
SC4MOL	–	Sterol-C4-methyl oxidase

SDH	–	Succinate dehydrogenase
SNARE	–	Soluble N-ethylmaleimide sensitive fusion protein attachment receptors
T1DM	–	Type 1 diabetes mellitus
T2DM	–	Type 2 diabetes mellitus
TAARs	–	Trace amine-associated receptors
TBST	–	Tris-buffered saline with Tween-20
TIMPs	–	Tissue inhibitors of metalloproteinases
UCP2	–	Uncoupling protein-2
UQCRC1	–	Ubiquinol-cytochrome c reductase core protein 1 gene

Chapter 1

Thesis Overview, Aims and Objectives

1.1 Introduction

In 2021, International Diabetes Federation (IDF) has reported that 537 million adults aged 20-79 living are with diabetes and this is expected rise to 643 million and 783 million by 2030 and 2045, respectively (IDF, 2021). Notably, the global proportion and number of adults who are living with diabetes is estimated to be 24 million in Africa (over 1 in 2 adults are undiagnosed), 61 million in Europe (over 1 in 3 adults are undiagnosed), 73 million in Middle-East and North Africa (1 in 3 adults are undiagnosed), 51 million in North America and Caribbean (1 in 4 adults are undiagnosed), 32 million in South and Central America (1 in 3 adults are undiagnosed), 90 million in South-East Asia (over 1 in 2 adults are undiagnosed) and 206 million in Western Pacific (over 1 in 2 adults are undiagnosed) (IDF, 2021). Diabetes is responsible for 6.7 million deaths (1 every 5 seconds) in 2021. Over the last 15 years, USD966 billion dollars was the reported health expenditure in diabetes (IDF, 2021). The National Health Service (NHS) spent £10 billion a year on diabetes which is 10% of its entire budget (www.diabetes.org.uk).

World Health Organisation (WHO) has reported that diabetes has entered the top 10 leading causes of death globally with a significant increase of 70% deaths since 2000 with 80% deaths amongst male (WHO, 2020).

Diabetes mellitus is characterised by a high level of sugar in the blood in the absence of treatment resulting from defects in insulin secretion, insulin action or both. Around 90% of people with diabetes is classified as type 2 diabetes mellitus (T2DM), and 8% is type 1 diabetes mellitus (T1DM), and around 2% is the rare type of diabetes (www.diabetes.org.uk/diabetes-the-basics/differences-between-type-1-and-type-2-diabetes). Being overweight and physically inactive are the main contributing factors in T2DM. Complications of diabetes include neuropathy, retinopathy and nephropathy, and people with poorly controlled diabetes are at high risk of diseases in the heart, eyes (cataract), in the peripheral arterial and

cerebrovascular disease, and erectile dysfunction (Amanat et al., 2020; Kobayashi and Zochodne, 2018; Kouidrat et al., 2017; Saini et al., 2021; Taylor et al., 2021).

Many clinical studies conducted in the human population have shown elevated levels of inflammatory factors, including acute-phase proteins, sialic acid, proinflammatory cytokines and chemokines in patients with T2DM (Bae et al., 2021; Donath et al., 2019; Hu et al., 2018). Elevated levels of these circulating proinflammatory mediators are considered hallmarks of chronic inflammation (Robbins et al., 2014). This has been shown to be a key feature in metabolic disease including T2DM (Donath and Shoelson, 2011; Hotamisligil, 2010). T2DM is also the leading cause of kidney failure, nontraumatic lower-limb amputation, and blindness in adults (American Diabetes Association, 2013).

Studies have shown that more than 80% of patients with T2DM are obese (Donath and Shoelson, 2011; Xu, 2013), with the increased abdominal visceral adipose tissue being associated with both cytokine release and insulin resistance (Osborn and Olefsky, 2012). Moreover, the onset of T2DM typically follows the induction of insulin resistance (Monti et al., 2012; White et al., 2021). Insulin resistance happens when cells in the muscle, liver and fat are not responding to insulin and do not take up glucose from the blood. As a result, the pancreas makes more insulin to help glucose enter the cell. This is the common feature of T2DM and progress due to β-cell dysfunction (Lencioni et al., 2008). Studies have shown that long-chain saturated (palmitate, stearate) and monounsaturated (oleic) free fatty acids (FFAs) are highly active as proinflammatory factors to many cell types, while short-chain FFAs by contrast do not induce inflammation (Lee et al., 2004; Nguyen et al., 2007; Senn, 2006; Shi et al., 2006; Song et al., 2006). These FFAs and proinflammatory cytokines have also been demonstrated to impair insulin signalling (Sarmiento-Ortega et al., 2021; Wenzl et al., 2021). Insulin resistance reduces glucose uptake to skeletal and adipose tissues, as well as liver. This causes

pancreatic β-cells to secrete more insulin to compensate, but over time the sustained burden caused by chronic elevated blood sugar levels results in decreased β-cell function. This in turn results in a failure to sustain insulin demand and the onset of T2DM (Osborn and Olefsky, 2012).

Obesity is a strong modifier of diabetes risk. Obesity accounted for a huge proportion of epidemic of type 2 diabetes mellitus in Asia. It has been shown to affect an increasing number of young adult with type 2 diabetes (Pan et al., 2021; Zeng et al., 2021). The range of diabetic subgroups will become even more wide-ranging in the future with improved classification of patients with diabetes.

Whilst the detrimental effects of long-term exposure to high fat, high sugar diets are clear, the associated mechanisms of diabetogenesis remain poorly defined. Previous data from the Turner group has shown that over 3,000 pancreatic genes have 2-fold or greater change in expression that results from exposure to a high sugar and high fat glucolipotoxic (GLT) environment representative of that experienced by patients with poorly controlled type 2 diabetes (Bagnati et al., 2016). The challenge now is to understand which of these changes drive β-cell dysfunction and the decreased insulin secretion that results from a high sugar, high fat diet.

1.2 Pancreas

The pancreas is an organ of the digestive and endocrine systems of the human body. It has an endocrine function (glucose homeostasis) and exocrine function (nutrient digestion) (Paniccia and Schulick, 2017) (see **Figure 1.1**). The exocrine gland is the central part of the organ which is responsible in secreting digestive enzymes via the ductal system into the duodenum whilst endocrine gland function in producing glucagon, insulin, somatostatin, ghrelin, and pancreatic polypeptide (Collombat et al., 2010). The pancreas is involved in glucose homeostasis; i.e., when the blood glucose level is low, it secretes glucagon to compensate for the

needed glucose, and when blood glucose level high, it secretes insulin, the hormone capable of lowering blood glucose concentration (Rorsman et al., 2018).

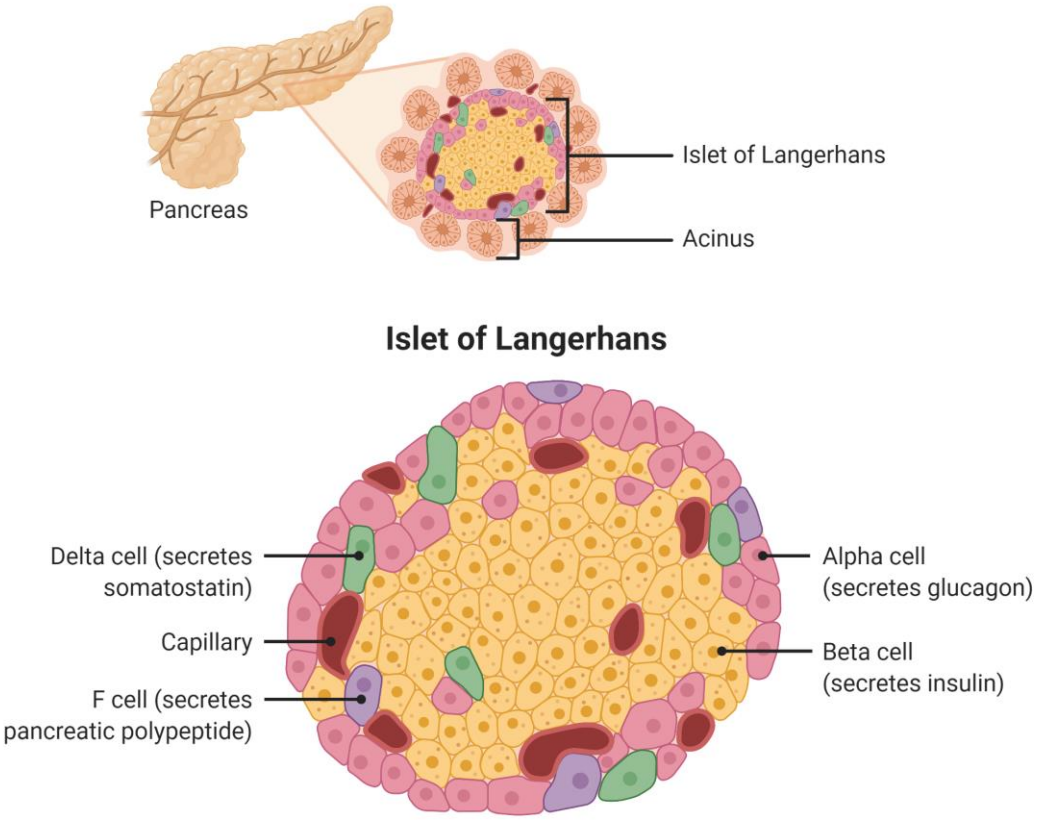

Figure 1.1 Pancreas and islets of Langerhans. Islets of Langerhans are clusters of cells in the pancreas. These groups of cells are responsible for the generation and release of hormones essential in regulating glucose levels. Figure created using Biorender.

1.3 Islets of Langerhans

Islets of Langerhans (see **Figure 1.1**), discovered by Paul Langerhans in 1869, are mixed random islands of endocrine cells found in the pancreas (Da Silva Xavier, 2018) and insulin producing-cells are abundantly present in it (Baetens et al., 1979). Islets of Langerhans are predominantly scattered in the body and tail regions rather than in the head of the pancreas (Baetens et al., 1979; Rorsman and Ashcroft, 2018). Insulin is released in response to elevated levels of nutrients (Lizcano and Alessi, 2002), i.e., glucose, fatty acids and amino acids, by the β-cells.

The pancreatic islet of Langerhans consists of five types of cells, i.e., glucagon-producing α-cells, insulin-releasing β-cells, somatostatin-containing δ-cells, pancreatic polypeptide-secreting cells, and Ghrelin-positive and other islet cell types.

1.3.1 α-cells

Glucagon is a counter hormone to insulin, and is released by the α-cells into the bloodstream when the blood glucose level is low (Svendsen et al., 2018). The interactive regulation of glucagon and insulin secretion is considered a central mechanism for regulating blood glucose. This mechanistic response is to prevent the occurrence of hypoglycaemia, low blood glucose level, and getting back into euglycemia, normal blood glucose level (Cryer, 2012; Gerich, 1988). Under normal conditions, an elevated blood glucose level causes a secretion of insulin from the β-cells which subsequently signals a decrease of glucagon secretion by the α-cells following ingestion of food (Cryer, 2012). Alpha-cells are essential in the regulation of glucose release from the liver (Unger, 2010) and abnormal α-cells function contributes to the development of type 2 diabetes which results from excessive production of glucagon (hyperglucagonemia) and consequently, expressing high level of blood sugar (hyperglycaemia) (Kahn, 2003; Kazda et al., 2017; Knop et al., 2007; Unger and Orci, 1975).

1.3.2 β-cells

Approximately 70-80% of the islet of Langerhans is composed of β-cells (Baetens et al., 1979). β-cells have a polygonal shape with an average diameter size of 13-18 µm (Göpel et al., 1999). Each has approximately 10,000 secretory granules (Olofsson et al., 2002) which contain up to 8-9 fg insulin (1.6-1.8 amol insulin) corresponding to approximately circa 100 mM (Huang et al., 1995; Rorsman and

Renström, 2003). Insulin is packed in the secretory granules as Zn_2-$insulin_6$ complex in a crystalline form (Svendsen et al., 2018).

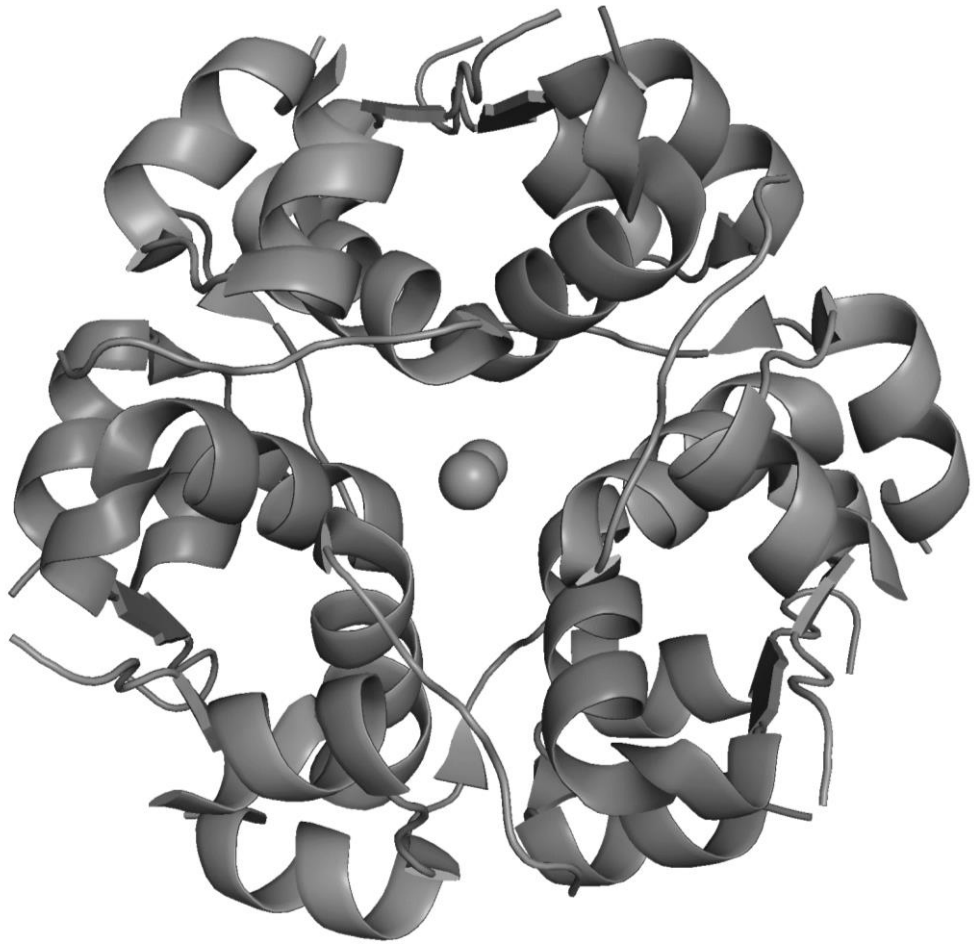

Figure 2.2 Structure of $zinc_2$-$insulin_6$ complex. Molecular structure of insulin hexamer. One of the zinc ions can be seen in the centre whilst the other lies below the plane. Figure was drawn using Pymol.

The critical role of the β-cell is attributed to acting as a glucose sensor by secreting insulin into the bloodstream in response to an elevated glucose concentration. This process was done metabolically by inducing changes in electrical activity, thereby building up the cytoplasmic Ca^{2+} concentration and initiating Ca^{2+}-dependent exocytosis of insulin-containing secretory granules (Rorsman and Ashcroft, 2018). Type 2 diabetes is characterised by chronic hyperglycaemia caused by impaired insulin secretion and action of insulin (Rorsman and Ashcroft, 2018). Approximately 48-56 days (rat) is the lifespan of mature beta-cells, and the pre-existing beta-cells

supplant them through the differentiation and proliferation of new β-cells derived from the pancreatic ducts (Stoffers et al., 2000).

Incretin hormones are synthesised in the gut (Nauck and Meier, 2018) and have the ability to enhance insulin secretion (Irwin and Flatt, 2013). The two most important incretin hormones are glucose-dependent insulinotropic polypeptide (GIP) and glucagon-like peptide-1 (GLP-1) (Fehmann et al., 1995; Holst and Orskov, 2004; Holst, 1999). Enteric hormones such as cholecystokinin (CCK) (Irwin and Flatt, 2013; O'Harte et al., 1998) and oxyntomodulin (OXM) (Irwin and Flatt, 2013) have been found also to stimulate insulin secretion. These gut hormones are used in the treatment for obesity-diabetes (Irwin and Flatt, 2013). CCK has been found to increase β-cell survival by directly reducing the cytokine-induced and endoplasmic reticulum-induced cell death (Lavine et al., 2010).

In pancreatic β-cells, glucose metabolism is tightly controlled by the activity of glucokinase (Bonner et al., 2015; Doliba et al., 2012) and glucose transporters (GLUT 1 and GLUT 2 in humans, and GLUT2 in mice) (Heimberg et al., 1995; McCulloch et al., 2011) because the only substrate for glucokinase is D-glucose. Glucokinase is only functional at high glucose levels because it has a low binding affinity towards glucose (She et al., 2022).

1.3.3 δ-cells

Somatostatin (see **Figure 1.3**) secreting cells (δ-cells) comprise 10% of the islet of Langerhans. Delta-cells are also observed to be present in the stomach and pancreas (Arimura et al., 1975), hypothalamus (Luft et al., 1978), central nervous system, peripheral neurons (Hökfelt et al., 1975), and the gastrointestinal tract (Hökfelt et al., 1975).

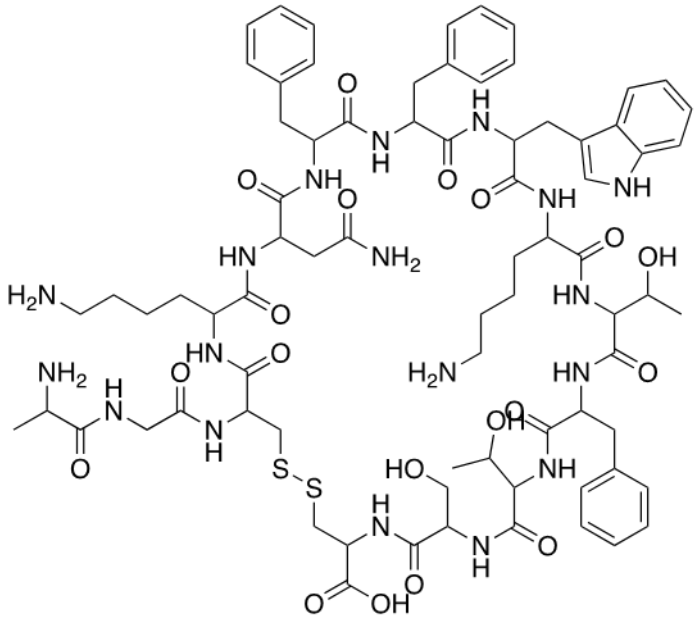

Figure 3.3 Structure of somatostatin.

Somatostatin acts as a negative regulator of insulin, glucagon, and pancreatic polypeptide secretion (Ensinck et al., 1989; Hauge-Evans et al., 2009; Kailey et al., 2012), and is also involved in Ca^{2+} signalling (Berts et al., 1996; Braun et al., 2009; Zhang et al., 2007). Somatostatin was also found to inhibit epinephrine (Kailey et al., 2012; Lacey et al., 1990), ghrelin (Wierup et al., 2014), galanin (Renström et al., 1996), and leptin (Seufert et al., 1999). Somatostatin acts as an inhibitory hormone in the release of pituitary hormones and modulator of nervous functions as its role as a direct depressant on neural activity and decreases motor activity (Luft et al., 1978). Aside from being an important component of islet architecture and intercellular communication (Brereton et al., 2015), δ-cells are electrically excitable (Kanno et al., 2002). δ-cells have been reported to transdifferentiate into β-cells (Chera et al., 2014), although this remains the subject of controversy, as some studies do not support transdifferentiation of δ-cells to β-cells as a viable means to replenish β-cell mass (Da Silva Xavier, 2018).

1.3.4 Pancreatic polypeptide cell

Pancreatic polypeptide (PP) cells comprise 1-2% of the islet of Langerhans (Clark et al., 1988; Stefan et al., 1982; Sundler et al., 1977). Glucose stimulates the secretion of PP from PP-containing cells, and this has been shown to an inhibitor of glucagon (Aragón et al., 2015). It was also observed that PP could be stimulated by 10 mM arginine, but not glucagon (Weir et al., 1979).

1.3.5 Ghrelin-positive and other islet cell types

Ghrelin, serotonin (enterochromaffin cells), gastrin (G-cells) and small granules of unknown content (P/D1-cells) were also found to be present in the islet of Langerhans (Alumets et al., 1978; Bordi et al., 1986; Capella et al., 1978; Rindi et al., 2002; Rindi et al., 2002; Solcia et al., 1987; Wierup et al., 2002; Wierup et al., 2007; Wierup et al., 2014). Unfortunately, there are no further studies found yet on the function of the other cells except for ghrelin-positive cells. It was observed that ghrelin concentration increased during fasting (Dornonville de la Cour et al., 2001; Toshinai et al., 2001; Tschöp et al., 2000) and it was shown to have an insulin secretion inhibitory effect in humans and rodents (Broglio et al., 2001; Broglio et al., 2003; Colombo et al., 2003; Egido et al., 2002; Reimer et al., 2003; Wierup and Sundler, 2004). Hence, ghrelin has an inversely proportional relationship with insulin (Dezaki et al., 2008; Korbonits et al., 2004), i.e., as plasma insulin concentration increases, plasma ghrelin concentration decreases. Studies have also shown that ghrelin was able to regulate the release of glucagon, somatostatin, and pancreatic polypeptide (Arosio et al., 2003; Egido et al., 2002; Olofsson et al., 2002).

1.4 Insulin and its structure

The β-cells synthesise insulin in the endocrine pancreas. It is a polypeptide hormone wherein its active form is composed of A- and B-chains (see **Figure 1.4**). Two

interchain disulphide bonds link the two chains. However, the A-chain has an intrachain disulphide bond. Impaired folding of proinsulin can cause the development of endoplasmic reticulum stress, β-cell apoptosis, and diabetes mellitus (Weiss et al., 2000).

Insulin chains A and B are secondary in structure. Chain A has two α-helical segments that are nearly antiparallel. These two helices are connected by non-canonical turn which brings into proximity the N-chain and C-chain termini. N-chain terminus is the start of the protein or polypeptide, and this refers to the free amino group at the end of the polypeptide whilst C-chain terminus is the end of the protein or polypeptide, and this refers to the free carboxyl group at the end of the polypeptide. On the other hand, the B-chain has a central α-helix flanked by disulphide bonds and β-turns (Weiss et al., 2000).

The process of insulin biosynthesis starts with the translation of the 110 amino acids containing polypeptide known as preproinsulin (which contains the N-terminal signal peptide), followed by the B chain, then the C-peptide (the connecting peptide) and the C-terminal A chain. When they are translocated into the endoplasmic reticulum, the N-terminal signal peptide is detached, transforming preproinsulin into proinsulin. Disulfide bonds between the B and A chains are formed as well. Proinsulin left the endoplasmic reticulum and moved through the Golgi complex to the trans-Golgi network, sorted by the membrane-enclosed organelles known as secretory granules. After this event, proinsulin is converted into mature insulin by cleavage of the C-peptide. This mature insulin, consisting of A and B chains only, is stored in the secretory granules, which will be fused with the plasma membrane to release insulin or are intracellularly degraded by autophagy or direct delivery of lysosomes (see **Figure 1.4**).

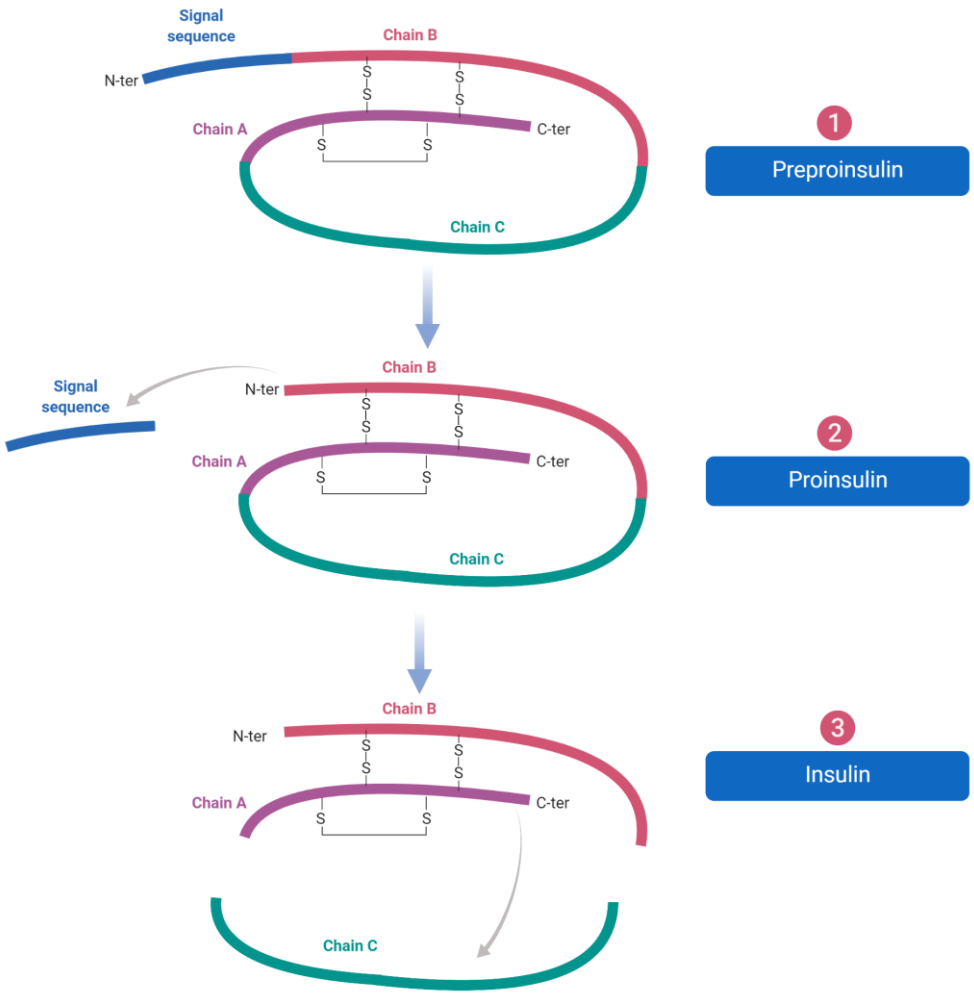

Figure 4.4 Cleavage of proinsulin to insulin. Insulin, a hormone with 51-residue, is secreted by β-cells in the islets of Langerhans. Insulin is composed of A- and B-chains, containing 21 and 30 residues, respectively, connected by two disulfide bonds. A-chain has an intrachain disulfide bond. C-chain is the linker between A-chain and B-chain of proinsulin and considered as inert byproduct of insulin synthesis. Preproinsulin (1) is transformed into a proinsulin (2) by proteolytic action and proinsulin is converted to insulin (3) by pancreatic beta-cells. Figure created using Biorender.

1.4.1 Insulin synthesis, secretion, and action

Pancreatic β-cells secretes insulin into the bloodstream in response to the high levels of nutrients, i.e., carbohydrates, fatty acids, and amino acids, circulating in the blood. Insulin stimulates the uptake of these nutrients, which in turn triggers the elevation of enzyme activity involved in glycogen, lipid and protein synthesis and storage in the liver, adipose tissue, and muscle, respectively. Whilst this is

happening, insulin inhibits enzymes involve in catalyse degradation and release of these nutrients back into the blood circulation (Saltiel and Kahn, 2001) (see **Figure 1.5**).

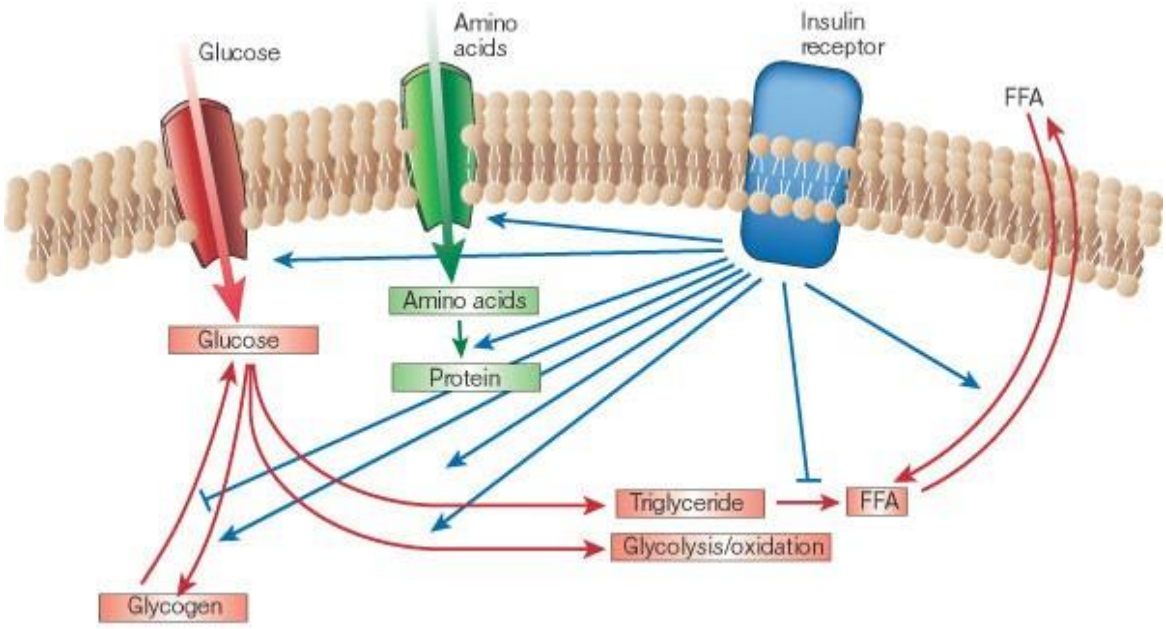

Figure 5.5 Regulation of metabolism by insulin. Insulin does promotes the synthesis and storage of lipids, carbohydrates, and proteins, whilst suppressing their degradation and release into the circulation. Permission to use the image granted by Saltiel and Kahn (2001).

Glucose enters the β-cell via a facilitative glucose transporter, GLUT2 which is widely distributed in the liver, kidney, serosal surface of intestinal mucosa cells and pancreatic β-cell (Naseri et al., 2021; Wang et al., 2021). As the glucose enters the cell, it is enzymatically phosphorylated by glucokinase and converted into glucose-6-phosphate. This substrate is then metabolised through glycolysis, tricarboxylic acid cycle, and oxidative phosphorylation (Morrissey et al., 2021; Zhang et al., 2021). This series of metabolic reactions results in an increase in ATP levels within the β-cell, thereby increasing the ATP/ADP ratio which triggers the channel closing of ATP-dependent K^+ channels. With this, the membrane undergoes depolarisation and this activates Lc-type Ca^{2+} channels, thereby allowing Ca^{2+} to enter the β-cell and thereby significantly increasing intracellular [Ca^{2+}] in the area around the Ca^{2+}

channel (Backes et al., 2021). This effect stimulates the fusion of insulin-containing granules with the plasma membrane and results in the secretion of insulin (Lieberman and Peet, 2018). Lc-type Ca^{2+} channel is a C class calcium channel which play a role in synapses and secretory cells. As an example, it was found that in retinal bipolar cells, Ca^{2+} entry through the Lc channels triggers ultrafast exocytosis, whilst in pancreatic beta-cells it was observed that evoked secretion is highly sensitive to Ca^{2+} (Wiser et al, 1999).

The insulin receptor, a member of the tyrosine kinase family of receptors, is a dimer with each half containing an α- and β-subunit. Insulin binds to α-subunits, and when this happens, the β-subunits cross the plasma membrane and protrude into the cytosol, autophosphorylate each other, and activate the insulin receptor (Lawrence, 2021). The autophosphorylated receptor binds the insulin receptor substrate (IRS) at multiple sites, i.e., Shc and Cbl, and form a binding site for proteins with SH2 domains such as Grb2, phospholipase Cγ(PLCγ), PI 3-kinase, and downstream PtdIns(3,4,5)P_3-dependent protein kinases, ras and the MAP kinase cascade, and Cbl/CAP and the activation of TC10 (Meijles et al., 2021). These pathways involved would act in a coordinated fashion in regulating of enzyme activation and inactivation, vesicle trafficking, gene expression, and protein synthesis. These processes would result in the regulation of lipid, protein and glucose metabolism (see **Figure 1.6**) (Saltiel and Kahn, 2001).

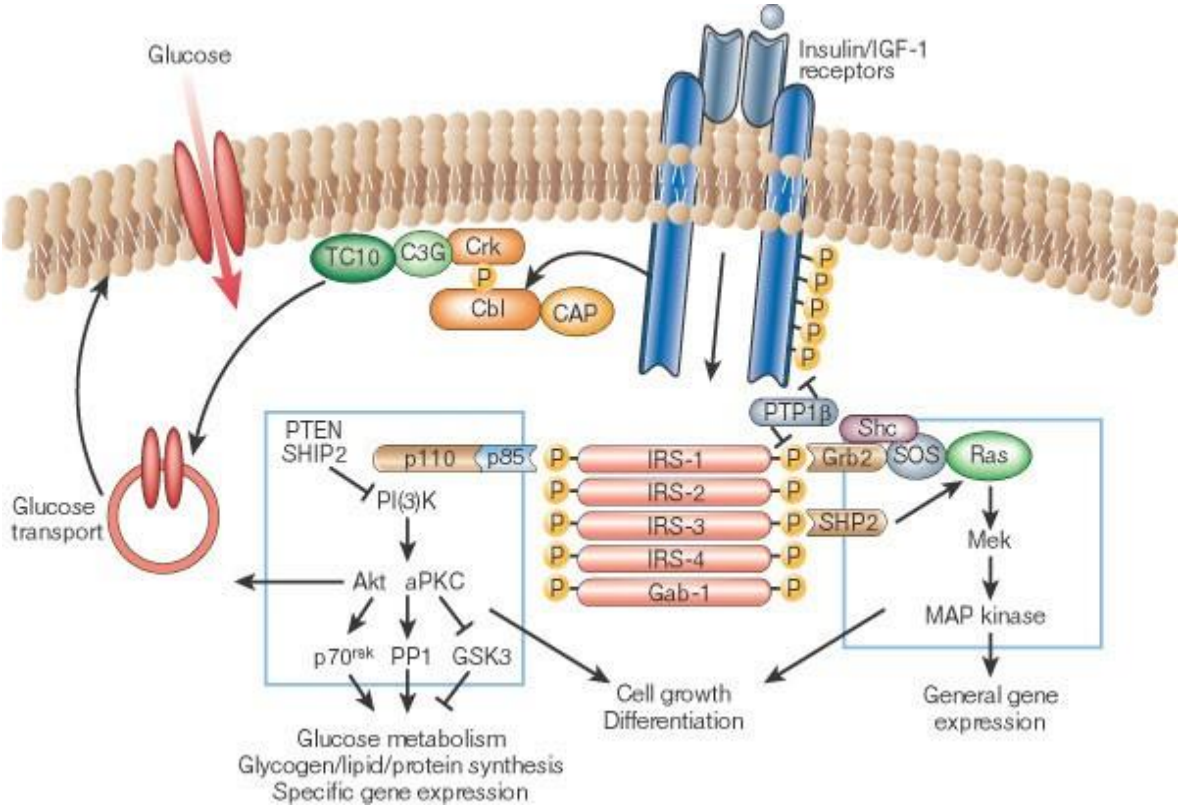

Figure 6.6 Signal transduction in insulin action. Insulin receptors undergo autophosphorylation and catalyse the phosphorylation on the cellular proteins of the IRS family, Shc and Cbl. On phosphorylation of specific tyrosine residues, these proteins interact with the signalling molecules through their SH2 domains and result in the activation of PI(3)K, PtdIns(3,4,5)P3-dependent protein kinases, Cbl/CAP and TC10, and ras and the MAP kinase cascade. Permission to use the image granted by Saltiel and Kahn (2001).

1.4.2 Insulin signalling pathway

All animals have an unpredictable pattern of feeding and starvation that develops between meals. This caused significant stress to the animals. However, humans have the ability to store nutrients which can be used during periods of fasting. Insulin is the driving force that controls this process by responding to elevated levels of nutrients such as glucose in the bloodstream.

Adipose tissue, skeletal muscle, and liver are the primary tissues responsive to insulin in the body (Fuchs et al., 2021). The binding of insulin to its receptor stimulate the transport of nutrients (glucose, fatty acids, and amino acids) from the bloodstream into the tissues. This event consequently converts the nutrients to

stored macromolecules (proteins, glycogen, and lipids) (James et al., 2021; Takahashi et al., 2021). Dysregulation of the uptake and storage of nutrients reliably following feeding results in diabetes.

1.5 Diabetes

Diabetes is a chronic metabolic disorder of hyperglycaemia and insulin resistance in the absence of treatment. It is traditionally classified as one of two main types (although there are other forms), namely type 1 diabetes mellitus (the pancreas cannot produce insulin as result of autoimmune attack) and type 2 diabetes mellitus (the pancreas is unable to release sufficient insulin to cope with the demand imposed by insulin resistance and obesity) (Arneth et al., 2019). Diabetes in each case is defined by abnormalities in pancreatic β-cell function that lead to either β-cell stress, dysregulation, or loss. With this, treatments could be targeted to mediated pathways of hyperglycaemia in a specific patient.

Reclassification of types of diabetes was revisited by WHO in 2019 (see **Table 1.1)** for the new classification of diabetes with reasons provided as follows:

1. The phenotypes of type 1 diabetes mellitus (T1DM) and type 2 diabetes mellitus (T2DM) are becoming less distinguishable with high obesity frequency at a very young age. Increasing reported cases of T1DM in adulthood and T2DM in young people.
2. Developments in molecular genetics have aided doctors and clinicians in identifying subtypes of diabetes. This leads to important suggestions for choice of treatment in some cases.
3. Growing understanding of pathophysiology has resulted in a trend towards evolving personalised therapies and precise medication. Unlike the previous classification, “hybrid types of diabetes” and “unclassified diabetes” were added

as the new types of diabetes. This inclusion would provide practical guidance to clinicians for assigning a type of diabetes to individuals at the time of diagnosis.

Table 1.1 Classification of diabetes.

Types of diabetes	**Brief description**	**Change from previous classification**
Type 1 diabetes	β-cell destruction (mostly immune- mediated) and absolute insulin deficiency; onset most common in childhood and early adulthood	Type 1 sub-classes removed
Type 2 diabetes	Most common type, various degrees of β-cell dysfunction and insulin resistance; commonly associated with overweight and obesity	Type 2 sub-classes removed
Hybrid forms of diabetes		**New type of diabetes**
Slowly evolving, immune-mediated diabetes of adults	Similar to slowly evolving type 1 in adults but more often has features of the metabolic syndrome, a single GAD autoantibody and retains greater β-cell function	Nomenclature changed – previously referred to as latent autoimmune diabetes of adults (LADA)
Ketosis-prone type 2 diabetes	Presents with ketosis and insulin deficiency but later does not require insulin; common episodes of ketosis, not immune-mediated	No change

Other specific types		
Monogenic diabetes -Monogenic defects of β-cell function -Monogenic defects in insulin action	Caused by specific gene mutations, has several clinical manifestations requiring different treatment, some occurring in the neonatal period, others by early adulthood Caused by specific gene mutations; has features of severe insulin resistance without obesity; diabetes develops when β-cells do not compensate for insulin resistance	Updated nomenclature for specific genetic defects
Disease of exocrine pancreas	Various conditions that affect the pancreas can result in hyperglycaemia (trauma, tumor, inflammation, etc.)	No change
Endocrine disorders	Occurs in diseases with excess secretion of hormones that are insulin antagonists	No change
Drug- or chemical-induced	Some medicines and chemicals impair insulin secretion or action, some can destroy β-cells	No change
Infection-related diabetes	Some viruses have been associated with direct β-cell destruction	No change
Uncommon specific forms of immune-mediated diabetes	Associated with rare immune-mediated diseases	No change

Other genetic syndromes sometimes associated with diabetes	Many genetic disorders and chromosomal abnormalities increase the risk of diabetes	No change
Unclassified diabetes	Used to describe diabetes that does not clearly fit into other categories. This category should be used temporarily when there is not a clear diagnostic category especially close to the time of diagnosis	New types of diabetes
Hyperglycaemia first detected during pregnancy		
Diabetes mellitus in pregnancy	Type 1 or type 2 diabetes first diagnosed during pregnancy	No change
Gestational diabetes mellitus	Hyperglycaemia below diagnostic thresholds for diabetes in pregnancy	Defined by 2013 diagnostic criteria

Adapted from https://www.who.int/publications/i/item/classification-of-diabetes-mellitus

1.5.1 Symptoms of diabetes

Typical clinical manifestations of diabetic patients are thirst, polyuria, weight loss, genital yeast infection, blurring of vision or even blindness in the absence of effective treatment. However, these symptoms may develop slowly in type 2 diabetes mellitus and therefore can often initially go unnoticed, depending on the progression of hyperglycaemia to pathological and functional changes that may be present for a long time before a diagnosis is made.

In 2011, a report in consultation with World Health Organisation, four diagnostic tests and its measurement for diabetes were recommended such as fasting plasma glucose values of ≥ 7.0 mmol/L (126 mg/dL), 2-hour post-load

plasma glucose after a 75 g oral glucose tolerance test (OGTT) values of ≥ 11.1 mmol/L (200 mg/dL), random blood glucose ≥ 11.1 mmol/L (200 mg/ dL) in the presence of signs and symptoms of diabetes, and glycated haemoglobin (HbA1c) ≥ 6.5% (48 mmol/mol) (Jensen et al., 2021; Kaur et al., 2020; Owora, 2018).

1.5.2 Drugs used to combat diabetes

Insulin resistance and impaired β-cell function are the major causes of type 2 diabetes. Currently, here are the list of drugs available used to treat diabetes.

1.5.2.1 Glucagon-like peptide-1

Glucose-dependent insulinotropic polypeptide (GIP), and glucagon-like peptide 1 (GLP-1) are incretin hormones secreted from the intestine after food ingestion (Mathiesen et al., 2019). They may potentiate roundly to 70% of the postprandial insulin response in healthy individuals (Puddu et al., 2013). It has been found that one of the most important pathophysiological changes observed in type 2 diabetes is the disorder of GLP-1 secretion (Puddu et al., 2013).

There were studies on GLP-1 receptor agonists or dipeptidyl peptidase-4 (DPP4) inhibitors (the enzyme responsible for GLP-1 inactivation) as focus on the treatment of diabetes (Perfetti et al., 2000; Pospisilik et al., 2003; Tourrel et al., 2002; Wang and Brubaker, 2002). It has shown that GLP-1 receptor agonists helped in improve glucose tolerance and preserving islet β-cell mass by facilitating the proliferation of islet endocrine cells and decrease of cellular apoptosis (Farilla et al., 2002), and GLP-1 increases insulin biosynthesis (Pospisilik et al., 2003). Yagihashi and coworkers observed that long-period DPP4 inhibitor vildagliptin's effects on islet morphology improved insulin secretion and glucose tolerance. They suppressed hyperglucagonemia by elevating the plasma active glucagon-like peptide-1 concentration (Inaba et al., 2012). Long-term DPP4 inhibition resulted in increased

GLUT-2 expression and insulin secretion, and there was an observed protection from islet size increase in insulin resistance (Stoffers et al., 2000). The binding of GLP-1 to its receptor GLP-1R bring about its biological action. GLP-1R is a specific seven-transmembrane receptor guanine nucleotide-binding protein coupled receptor (GPCR) (Puddu et al., 2013).

In the pancreas, GLP-1 has been shown to amplify glucose-induced insulin secretion via cAMP release and associated signalling pathways, help to improve pancreatic β-cell regeneration, proliferation, and reduction of apoptosis, and also be involved in the inhibition of glucagon secretion from pancreatic α-cells, thus, restoring glucose homeostasis (Brubaker and Drucker, 2004).

Glucagon-like peptide 1 (GLP-1) is released by cells in the small intestine after eating, and GLP-1 is found to be commonly low in patients with diabetes (Gadsby, 2007). Dipeptidyl peptidase four (DPP-4) is present in various tissues including the immune system, and has the ability to degrade GLP-1 (Richter et al., 2008). Sitagliptin and vildagliptin are classified as DPP-4 inhibitors that are able to increase the half-life of endogenous GLP-1. However, they have been found to cause hypoglycaemia when administered (Richter et al., 2008) and have also been reported to increase nasopharyngitis, urinary tract infection and upper respiratory infection (Gadsby, 2007). The primary concern of these drugs is also their long-term effect on the immune system (Gadsby, 2007; Richter et al., 2008).

1.5.2.2 Metformin

Biguanides are oral glucose-lowering agents used to treat non-insulin-dependent diabetes mellitus (NIDDM). Metformin (see **Figure 1.7**) and phenformin were introduced in 1957 for NIDDM treatment, however, phenformin causes lactic acidosis hence was withdrawn from the market (Bailey, 1992) whereas metformin

does not demonstrate the same risk with appropriate prescription (Sulkin et al., 1997).

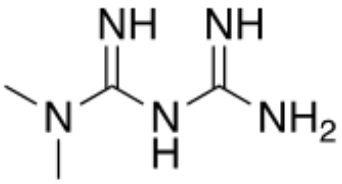

Figure 7.7 Chemical structure of metformin.

Metformin is an antidiabetic drug most commonly used to treat type 2 diabetes (Nathan et al., 2009), either as a monotherapy or in combination with a sulfonylurea (Bailey, 1992). Insulin resistance is often treated with metformin (Cho and Kieffer, 2011). Metformin is an anti-hyperglycaemic drug that does not cause clinical hypoglycaemia. It is also able to combat hypertriglyceridemia and does not facilitate weight gain. In addition it has been proposed to exert a vasoprotective property (Bailey, 1992).

The anti-hyperglycaemic potential of metformin (Kirpichnikov et al., 2002) is attributed to the glucose and fatty acids uptake within the muscle and fat tissues mediated by the 5'-adenosine monophosphate-activated protein kinase (AMPK) (EC 2.7.11.31), a major cellular regulator of lipid and glucose metabolism (Zhou et al., 2001) and subsequently inhibited complex 1 of the electron transport chain (El-Mir et al., 2000; Owen et al., 2000).

Metformin was found to restore insulin secretory pattern when rat pancreatic islet was exposed to high glucose or high fatty acids (Patanè et al., 2000). It has also been shown that metformin was able to increase insulin content, insulin release, and reduced apoptosis (Marchetti et al., 2004). It has also been shown that metformin interferes with vitamin B_{12} absorption but is not associated with anaemia (Bailey et al., 1996). Metformin is also found not to be bound to plasma proteins

hence it is not readily metabolised or excreted rapidly by the kidney (Bailey, 1992) by organic cation transporters (Puddu et al., 2013).

1.5.2.3 Thiazolidinediones

Glitazones (see **Figure 1.8**) commonly known as thiazolidinediones are insulin-sensitising drugs used in the treatment for type 2 diabetes mellitus, and its hypoglycaemic effect is exerted by activating the PPAR*γ* (Kersten et al., 2000; Spiegelman, 1998). Troglitazone, rosiglitazone and pioglitazone were approved for use in poorly controlled type 2 diabetic (Kersten et al., 2000). Amongst these PPARγ ligands rosiglitazone has the highest affinity to the PPAR followed by troglitazone and pioglitazone (Kersten et al., 2000).

By activating PPAR*γ* by glitazone ligands in effect protects pancreatic beta-cells from cell apoptosis (Zeender et al., 2004) by preventing nuclear factor-*κ*B (NF-*κ*B) activation (Ao et al., 2010; Liu et al., 2016; Saitoh et al., 2008).

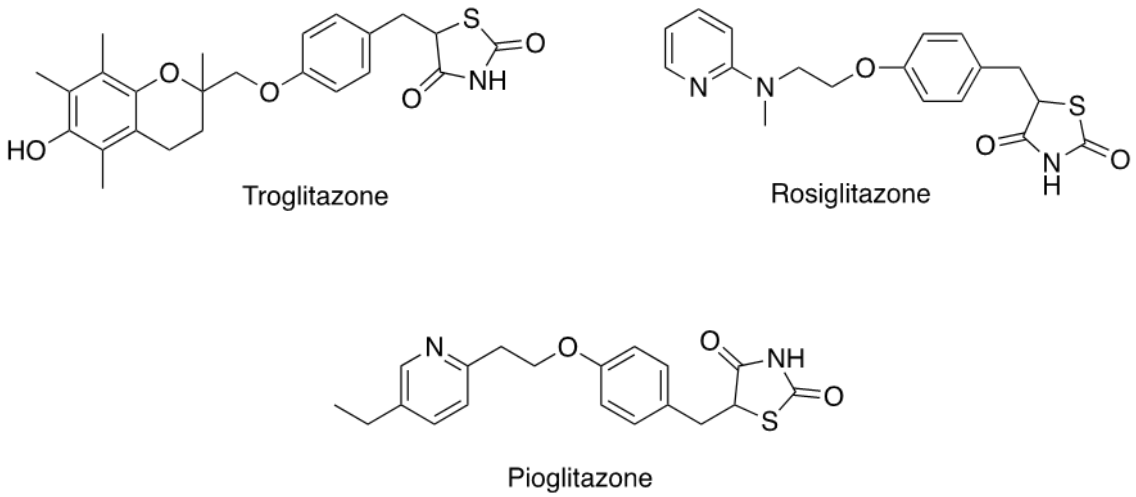

Figure 8.8 Chemical structures of known glitazones.

Studies have found that glitazones not only improve insulin sensitivity and insulin secretion (Diani et al., 2004; Miyazaki and DeFronzo, 2008), but also prevent β-cell mass loss and morphological damage in the islet (Ishida et al., 2004; Kawasaki et

al., 2005; Zeender et al., 2004) and maintain islet function (Campbell and Mariz, 2007; Kawasaki et al., 2005). However, studies published in 2007 show that diabetic patients treated with glitazones gain weight and have increased risk of heart failure (Home et al., 2007; Singh et al., 2007), and an increase in risk for myocardial infarction (Nissen and Wolski, 2007; Singh et al., 2007).

1.5.2.4 Sulfonylureas

Sulfonylureas stimulate insulin release from the β-cell (Nathan et al., 2009) in response to glucose and non-glucose secretagogue such as amino acids (Sola et al., 2015) and appear to have similar efficacy as metformin (DeFronzo and Goodman, 1995) but can significantly improve glycemic control when in combination with metformin (Derosa et al., 2010; Derosa et al., 2011; Hirst et al., 2013; Nestler, 2008). First generation sulfonylureas such as chlorpropamide and glibenclamide (see **Figure 1.9**) were found to cause side effects such as hypoglycaemia and cardiovascular risk (Sola et al., 2015) in comparison to second-generation sulfonylureas such as gliclazide, glimepiride, and glipizide (see **Figure 1.9**) (Gangji et al., 2007; Holstein et al., 2001) which were equally effective in lowering blood glucose level (Sola et al., 2015). However, newer prolonged-release preparations of sulfonylureas are safer for reducing the risk of hypoglycaemia (Sola et al., 2015). Sulfonylureas can however cause weight gain (Nathan et al., 2009).

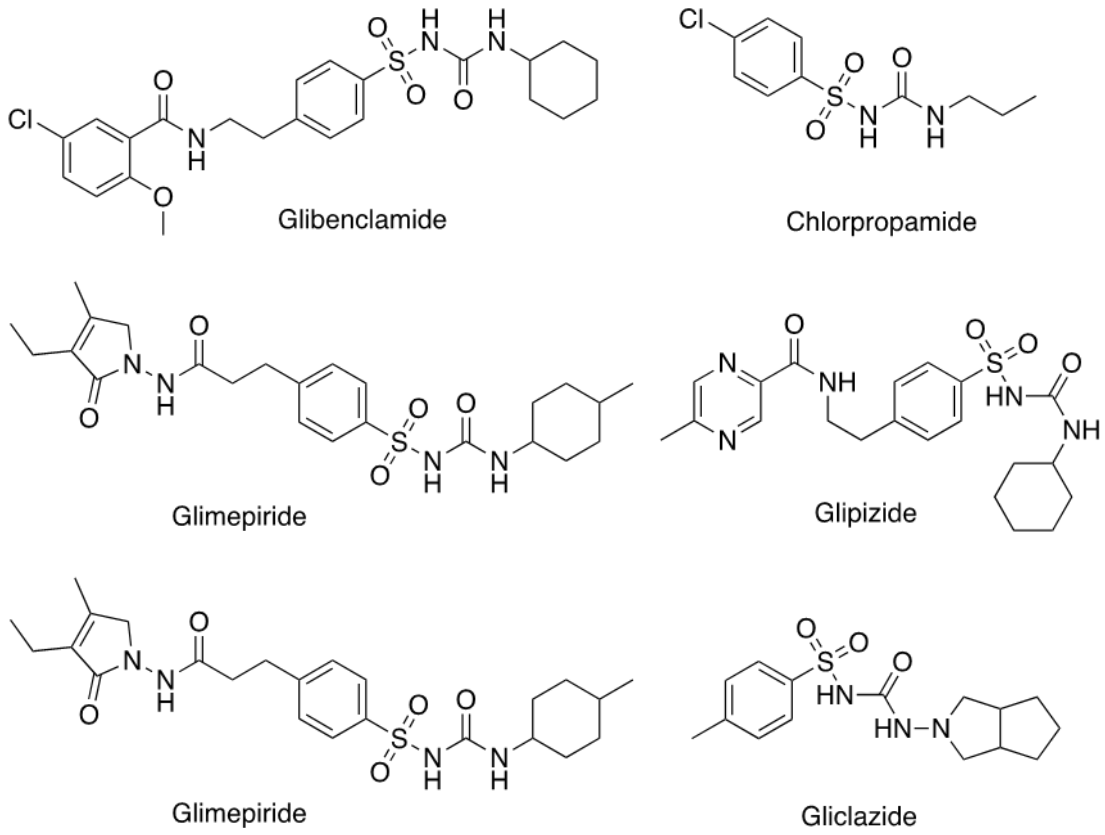

Figure 9.9 Chemical structures of sulfonylureas.

1.5.2.5 Glinides

Glinides (see **Figure 1.10**) have a shorter circulating half-life than sulfonylureas and bind to a different site within the sulfonylurea receptor (Malaisse, 2003). The two most common glinides are repaglinide and nateglinide. Between the two, repaglinide is more effective in decreasing HbA1c level. It has been reported that repaglinide is comparatively effective to metformin and sulfonylureas with or without combination therapy (Gerich et al., 2005; Rosenstock et al., 2004). HbA_{1C} - glycated haemoglobin, which reflects the blood sugar levels over ~3 month period, and which should be at a level less than 7% as recommended by the American Diabetes Association (American Diabetes Association, 2002; DeWitt and Hirsch, 2003). Patients taking glinides have been found to be less at risk of undesirable hypoglycaemia, but similarly have risk in gaining weight in using sulfonylureas (Damsbo et al., 1999; Gerich et al., 2005).

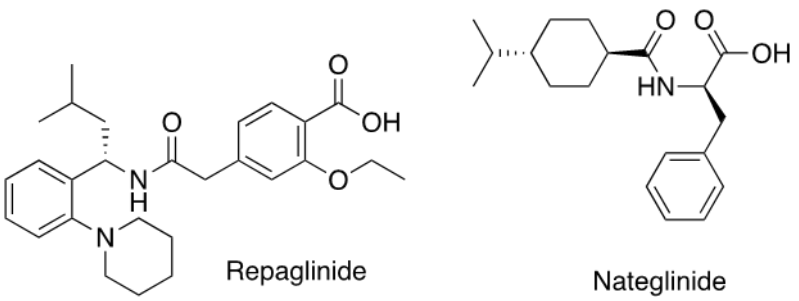

Figure 10.10 Chemical structures of common glinides.

1.5.2.6 α-Glucosidase inhibitors

Alpha-glucosidase inhibitors (see **Figure 1.11**), miglitol, voglibose, and acarbose, are widely used drugs for treatment of type 2 diabetes (Moelands et al., 2018; van de Laar et al., 2005; Yin et al., 2014). These α-glucosidase inhibitors have been proved in reversing impaired glucose tolerance to normal glucose tolerance. However, acarbose has shown an additional potential to reduce inflammation and disabling carotid plaques (Derosa et al., 2012). Alpha-glucosidase inhibitors delay the rate of digestion of carbohydrates in the small intestine and hence lowering postprandial glucose concentration and insulin levels without causing hypoglycaemia (Kumar et al., 2011; Nathan et al., 2009; van de Laar et al., 2005). However, its efficacy in lowering blood glucose concentration is less compared to metformin and sulfonylureas (van de Laar et al., 2005). Common adverse effects in using α-glucosidase inhibitors are increased flatulence, and gastrointestinal symptoms (Chiasson et al., 2003; van de Laar et al., 2005) and they should not be used with patients having inflammatory bowel disease, colonic ulceration, and partial or predisposed to intestinal obstruction (Derosa and Maffioli, 2012).

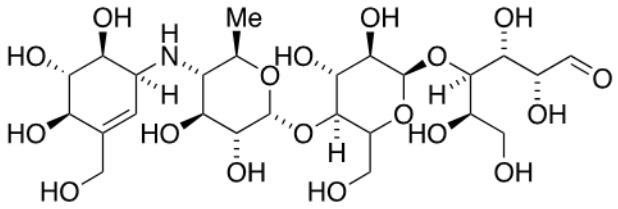

Acarbose

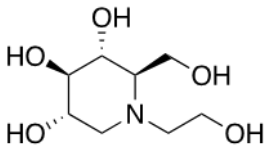

Miglitol

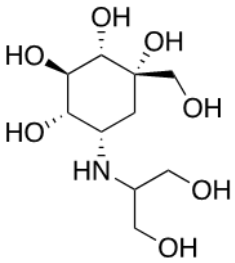

Voglibose

Figure 11.11 Chemical structures of known α-glucosidase inhibitors.

1.5.2.7 Insulin

Since its discovery in 1921, insulin is the most essential compound used to combat diabetes mellitus and since then various insulin formulation has been developed (Greco et al., 1995). Insulin therapy is the treatment with the most clinical experience and most effective in lowering blood glucose (Puddu et al., 2013). It has been reported that insulin therapy may preserve β-cell function, enhance lipid metabolism and improve patients' long-term survival with myocardial infarction (Juneja et al., 2001; Linn et al., 1996; Malmberg, 1997; Rivellese et al., 2000).

In type 1 diabetes mellitus, lifelong administration of insulin is required with its goal to avoid acute complications and prevent long-term microvascular and macrovascular complications (Malik and Taplin, 2014). Type 1 diabetes mellitus patients have been observed to require multiple injections to attain a desirable HbA_{1C} - glycated haemoglobin (American Diabetes Association, 2002; DeWitt and Hirsch, 2003).

Administration of insulin to type 2 diabetes mellitus patients has been reported to compensate for decreased endogenous insulin secretion and increase

glucose uptake (Cheng et al., 2021; Koivisto, 1993; Sędzikowska and Szablewski, 2021). Insulin therapy for type 2 diabetic patients is administered when their HbA_{1C} level reaches 10.4% in the United States of America (Abdelgani et al., 2021; Hayward et al., 1997; McVean and Miller, 2021) and when there is a 50% β-cell function decline following diagnosis (UKPDS, 1998).

The main concerns of insulin therapy are weight gain, hyperinsulinemia, hypoglycemia, and possibly sodium and fluid retention. Hypoglycemia is the most common adverse effect of insulin therapy (Pérez et al., 2020; Perkins et al., 2021; Tamborlane and Amiel, 1992) along with weight gain, hyperinsulinemia, and sodium and fluid retention (Calcaterra et al., 2021; Koivisto, 1993; Petersen and Shulman, 2018; Stenvers et al., 2019).

1.5.2.8 Sodium-glucose co-transporter inhibitors

Sodium-glucose co-transporter 1 (SGLT1) and sodium-glucose co-transporter 2 (SGLT2) are essential mediators of epithelial glucose transport. SGLT1 is responsible primarily for the glucose uptake in the intestine. SGLT2 is responsible for the reabsorption of glucose in the tubular system of the kidney, and whilst doing this, SGLT1 act on the reabsorption of the excess filtered glucose (Rieg and Vallon, 2018). It was observed that mutation of the SGLT1 gene could cause difficulty in absorbing glucose and galactose. Mutation in the SGLT2 gene is linked with glucose in the urine, termed glucosuria (Rieg and Vallon, 2018).

Phlorizin, a glucoside, was found to have the potential efficacy in competitively inhibiting the action of SGLT1 and SGLT2; however, its use was stopped due to intestinal side effects and a short life (Mehta et al., 2020; Rieg and Vallon, 2018; Wang et al., 2019).

Sodium-glucose co-transporter-2 inhibitors (SGLT2i) are used in individuals with type 2 diabetes to reduce the sugar that the kidney absorbs with additional

benefits of blood pressure reduction and loss of weight (Brown et al., 2021; Cowie and Fisher, 2020). SGLT2i are found to be most effective when used for glucose lowering if the estimated glomerular filtration rate is more than 60 mL per minute per $73m^2$ at initiation to avoid diabetic ketoacidosis (Brown et al., 2021). SGLT2i can prevent and treat heart failure (Brown et al., 2021; Neuen et al., 2019; Vallon and Verma, 2021). SGLT2i are inhibitors of renal glucose reabsorption resulting in substantial presence of sugars in the urine (glycosuria). Brands such as Forxiga ®, Jardiance ®, Steglatro ® and Invokana ® are recommended for patients with type 2 diabetes (www.diabetes.org.uk).

1.5.2.9 Statins

Statins are often prescribed to patients with diabetes because of the risk of heart diseases such as stroke and heart attack (www.diabetes.org.uk). Statins inhibit the conversion of 3-hydroxy-3-methylglutaryl coenzyme A (HMGC) to mevalonate by HMGC reductase. This step is crucial in the synthesis of cholesterol. By doing so, statins have been found to have a strong potential to lower the levels of lipids, thus reducing cardiovascular risk and mortality rate. The effects of statins have been shown to reach beyond their potential to lower cholesterol levels. As statins affect the mevalonate pathway, it has also influenced the inflammatory response, endothelial function, and coagulation (Pinal-Fernandez et al., 2018). However, there are recently reported studies that long-term use of statins is linked to the development of diabetes mellitus, which elevates the risk of cardiovascular diseases (Abbasi et al., 2021; Barter et al., 2018; Guber et al., 2021; Kamran et al., 2018; Wallemacq, 2019; Yandrapalli et al., 2019).

1.6 Carnosine

Over time, injectable and oral medications often become less beneficial, and there are limited options to treat type 2 diabetes. Hence, there is an urgent need to find new drugs that could be synthesised and used to combat diabetogenesis and find novel treatment strategies. The promising effectiveness of carnosine in lowering fasting plasma glucose has been reported (de Courten et al., 2015), and there is an absence of literature working on the action of carnosine in the pancreas.

Carnosine (β-alanyl-L-histidine) (see **Figure 1.12**), a histidine-containing dipeptide, is an abundant nonprotein nitrogen-containing compound of meat discovered by V.S. Gulewitch, a Russian chemist, in 1900 in Liebig's meat extract (Gulewitsch and Amiradžibi, 1900).

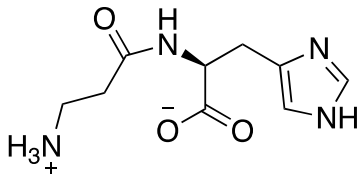

β-alanyl-L-histidine
(Carnosine)

Figure 12.12 Carnosine structure.

It is a structurally bioactive compound synthesised by carnosine synthase, EC 6.3.2.11, from β-alanine, and L-histidine and it is present in mammalian tissues (Unno et al., 2008). A large amount of carnosine can be found in skeletal muscle and it can also be present in brain regions, body fluids and other tissues. However, the concentration is 10- to 1000- fold lower than in muscle tissue (Boldyrev, A. A., 2012; Boldyrev et al., 2013). Only two tissues, skeletal muscle and olfactory bulb, contain carnosine in the millimolar range in mammals.

A methylated form of carnosine was found and identified in goose and chicken muscle (anserine), snake muscle (ophidine), and whale muscle (balenine)

(Boldyrev et al., 2013). Mostly, mammals have both carnosine and one of the methylated forms in their skeletal muscle. Variable high concentrations of carnosine and anserine are found in vertebrate skeletal muscle and brain tissue, whilst in marine mammals and reptilian species, balenine is more common (Kwiatkowski et al., 2018).

Carnosine has a pKa value of 6.72, which is relatively close to physiological pH and more so than that of free L-histidine which has a pKa value of 6.0. The pH buffering capacity of carnosine is attributed to the presence of the imidazole ring of L-histidine. Amide bond formation of L-histidine with a nonproteinogenic amino acid (a β-amino acid) makes the peptide bond relatively difficult for dipeptidases to hydrolyse. However, the opposite result can be seen if L-histidine is bound to a proteinogenic amino acid (Boldyrev et al., 2013).

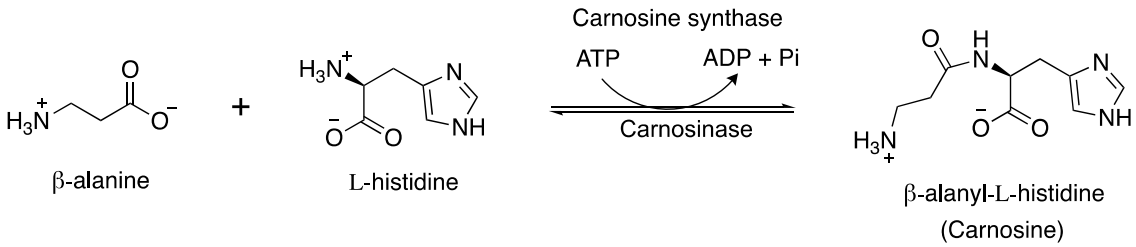

Figure 13.13 Synthesis and hydrolysis of carnosine. β-alanine and L-histidine are the components in synthesising carnosine.

Carnosine inhibits the formation of advanced lipoxidation and glycation end products (ALEs/AGEs). Indeed, Anderson et al. (2018) observed that when L-carnosine was supplemented to experimental mice it does reduce the metabolic effects of a high-fat diet, including the reduction of 4-HNE levels. L-carnosine has also been used as a lubricant component for eye drops, and clinicians observed their effectiveness and advantage for patients with oxidation-linked ocular disease (Babizhayev et al., 2009).

Carnosine is susceptible to hydrolysis by carnosinase. The hydrolytic enzyme carnosinase exists in two different forms, serum carnosinase (CN1 or CNDP1 or CNDP dipeptidase 1) and tissue carnosinase, a cytosolic nonspecific dipeptidase (CN2 or CNDP2 or CNDP dipeptidase 2) (Otani et al., 2005; Teufel et al., 2003). It was identified by Hanson and Smith from porcine kidney in 1949. Crystallographic data shows the presence of two domains in the molecular structure, domain A has a catalytic and metallic binding activity and domain B provides for the homodimer formation (Unno et al., 2008).

Building from this information, it is possible to design novel carnosine derivatives that are resistant to this enzymatic hydrolysis through computational chemistry and chemical synthesis. Consequently, these carnosine derivatives are intended to have an improved therapeutic potential (Bellia et al., 2014). Carnosine derivatives stability against degradation has already been published in some works (Bellia et al., 2014; Vistoli et al., 2009).

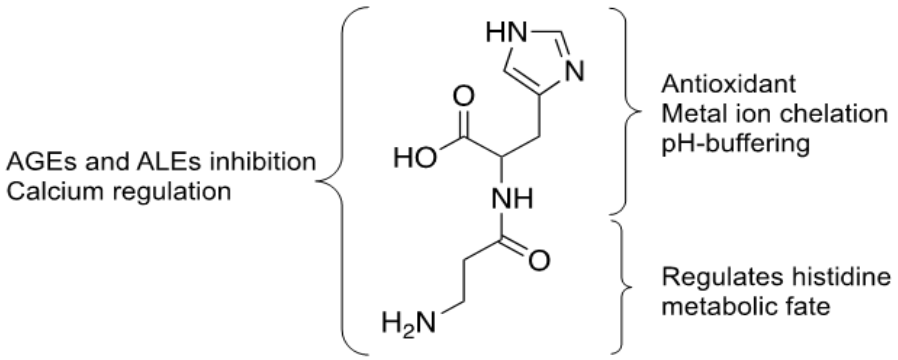

Figure 14.14 Structure-activity of carnosine. β-alanine regulates L-histidine metabolic fate. The imidazole ring essential for its antioxidant, metal-ion chelation and pH buffering effect. Carnosine inhibits AGEs and ALEs formation and function in calcium regulation.

Supplementation of carnosine close to the physiological concentration found in skeletal muscle (20-50mM) has the potential to increase viability of cells. This could be attributed to a decrease in DNA methylation or reduction of telomere fragments of chromosomes (Holliday and McFarland, 2000). Potential in healing wounds by

administration of carnosine (100 mg/kg injected daily) to wounded mice has also been observed. These researchers also noticed an increase in growth factors and cytokine genes involved in wound healing (Ansurudeen et al., 2012).

Daily supplementation of 6mg/kg body weight of carnosine to obese type 2 diabetes patients has been shown to result in a moderate reduction in both glucose and HbA1c levels. It has also been observed that oxidative stress and serum hydroperoxide levels are significantly reduced in patients with type 2 diabetes (Karkabounas et al., 2018).

1.6.1 L-histidine

L-histidine is an amino acid containing an imidazole ring that attributes its chemical properties such as proton buffering capacity, chelation of metals, and antioxidant properties. In diet, L-histidine has been reported as a requirement for maintaining body weight, and its dietary deficiency causes anaemia, hypoproteinaemia, and loss of weight (Fuller et al., 1947).

Owing to the proton buffering capacity of histidine, it has been used as a component in solutions used for organ preservation in transplant surgery and myocardial protection (Edelman et al., 2013). Chinese women with metabolic syndrome were given histidine as a supplement and shown to improve insulin sensitivity and loss of body fat (DiNicolantonio et al., 2018).

The ROS scavenging activity of L-carnosine is attributed to the imidazole ring of L-histidine which has been shown to inhibit peroxynitrite-induced tyrosine nitration (Fontana et al., 2002) whilst β-alanine has shown to be ineffective as an antioxidant itself (Decker et al., 2000).

1.6.2 β-alanine

β-alanine is a non-proteogenic amino acid endogenously produced in the liver (Trexler et al., 2015). Humans obtain β-alanine from eating poultry and meat. Studies have shown that β-alanine is the rate-limiting reactant in the biosynthesis of L-carnosine (Dunnett and Harris, 1999; Harris et al., 2006). β-alanine has a high Michaelis constant (K_M) for carnosine synthase and is thus rapidly converted to carnosine (Ng and Marshall, 1978; Skaper et al., 1973), whereas L-histidine has a lower K_m for carnosine synthase (Horinishi et al., 1978). Muscle carnosine concentration has been shown to significantly increase by supplementation of β-alanine for 4- and 10-weeks by 64% (Harris et al., 2006) and 80% (Hill et al., 2007), respectively. However, stopping of β-alanine supplementation has been seen to decrease muscle carnosine concentration by 2-4% on average per week (Baguet et al., 2010). It was also shown that the carnosine concentration is lower in women than men regardless of the baseline levels, and carnosine gradually decreases as age increases (Everaert et al., 2011).

In sprint-trained athletes, oral β-alanine supplementation has been shown to increase muscle carnosine and significantly attenuate muscle fatigue (Derave et al., 2007). In addition, β-alanine supplementation had a significant overall ergogenic effect on exercise (Saunders et al., 2017) by increasing intracellular buffering capacity during exercise (Sale et al., 2010).

1.7 Glucolipotoxicity

Unger et al. introduced the idea of glucotoxicity and lipotoxicity (Unger and Grundy, 1985; Unger, 1995). They have reported that even a mild hyperglycaemia can reduce the insulin secretory function of pancreatic β-cell and excess levels of fatty acids can be harmful to β-cells. Elimination of hyperglycaemia and hyperlipidaemia

can halt the development of metabolic deterioration (Gryczyńska et al., 2021; Solis-Herrera et al., 2000; Triposkiadis et al., 2021; Unger and Grundy, 1985).

Prolonged exposure to high glucose, and increased fatty acids have been reported to deleteriously affect pancreatic β-cell function and mass, thus impairing insulin secretion (Chueire and Muscelli, 2021; Poitout, 2008), to inhibit insulin gene expression (da Silva Rosa et al., 2021; Hagman et al., 2005; Kelpe et al., 2003; Tremblay et al., 2021), proinsulin biosynthesis (Fontés et al., 2010), and induce β-cell death (Lupi et al., 2002; Maestre et al., 2003; Shimabukuro et al., 1998). Glucotoxicity and lipotoxicity have interrelated common mechanisms of action (Prentki et al., 2002). Hyperglycaemia is a prerequisite for lipotoxicity to ensue (Briaud et al., 2001; Briaud et al., 2002; El-Assaad et al., 2003; Harmon et al., 2001; Jacqueminet et al., 2000) and hence, glucolipotoxicity is the applicable term used to describe deleterious effects of lipids on β-cell function (Poitout and Robertson, 2008).

When glucose concentration is low and normal, carnitine-palmitoyl transferase-1 (CPT-1) transports fatty acids into the mitochondria for fatty acid β-oxidation breaking down into energy. However, in the presence of high glucose and high fatty acids, intracellular metabolism of glucose forms citrate and malonyl-CoA in the cytosol. Effectively malonyl-CoA inhibits the enzymatic action of CPT-1 which in turn regulates fatty acid β-oxidation and accumulation of long-chain acyl-CoA esters in the cytosol (Prentki, and Corkey, 1996). This is primarily because fatty acid synthase activity in β-cell was observed to be lower than that of acetyl-CoA carboxylase (Brun et al., 1996). The accumulation of long-chain acyl-CoA esters in cytosol adversely affects β-cell function by lowering insulin gene expression and impairs glucose-induced insulin secretion (Poitout and Robertson, 2002). It is also shown to activate the esterification pathway leading to the cytosolic accumulation of ceramide, diglycerides, phosphatidic acid, phospholipids and triglycerides (Poitout

et al., 2010). In INS-1 cells, exposure to high glucose suppressed fatty acid β-oxidation, leading to coordinated induction of glycolytic and lipogenic genes and altered lipid partitioning (Roche et al., 1998).

It was observed that an acute elevation of free fatty acids can enhance insulin secretion (Carpentier et al., 1999); however, prolonged exposure to free fatty acids causes deterioration of β-cell function (Paolisso et al., 1995). Free fatty acid elevation significantly inhibits the stimulatory effect of hyperglycaemia on β-cell function when lipids are co-infused with glucose (Leung et al., 2004).

1.8 Radical species

Free radicals have been reported in chemistry since the 20th century (Gomberg, 1900) and investigations of critical biological processes discovered that free radicals occur as reaction intermediates (Commoner et al., 1954). Free radicals are very reactive chemical species containing unpaired electrons (Kehrer and Klotz, 2015). They are continuously produced in cells as normal by-products during metabolism (Kehrer and Klotz, 2015; Valko et al., 2007). In living systems, free radical species in low amounts can serve as a molecular signal activating stress responses that are significantly beneficial to organisms. A high concentration of radical species can however cause oxidative damage and tissue dysfunction (Di Meo et al., 2016). In cells, radical species can oxidise biomolecules and cause cell death and tissue injury. However, cells have developed defence mechanisms to limit the radical species' deleterious effects, including enzymes capable of decomposing peroxides. Chemical compounds with the ability to scavenge free radicals can also be introduced into the cell to sequester free radical species (Cheeseman and Slater, 1993).

1.8.1 Radical oxygen species

Radical oxygen species (ROS) are a set of derived oxygen molecules such as oxygen radicals (superoxide, hydroxyl, peroxyl, and alkoxyl radicals) and nonradical species but classified as oxidising agents (hypochlorous acid, ozone, and hydrogen peroxide) (Bedard and Krause, 2007). Amongst the oxygen radicals, hydroxyl radicals are considered the most toxic because of their ability to pass readily through membrane barriers and into the nucleus where they can interact strongly with DNA to cause mutations (Robertson et al., 2003).

ROS are produced during cellular metabolic processes or may be introduced via toxic extracellular mediators (Puddu et al., 2013). Also, ROS are by-products of cellular metabolism, primarily in the mitochondria (Thannickal and Fanburg, 2000). ROS are generated from a series of reactions which usually starts with superoxide which is catalysed by superoxide dismutase to form hydrogen peroxide, or superoxide reacts with nitric oxide and forms peroxynitrite (Bedard and Krause, 2007). In addition, ROS can interact with biomolecules such as proteins, lipids, carbohydrates and nucleic acids (Bedard and Krause, 2007; Thannickal and Fanburg, 2000) and crucially irreversibly alter the function of the target molecule (Puddu et al., 2013).

In the β-cell, elevated levels of ROS have been reported to effectively contribute to β-cell dysfunction (Evans et al., 2003; Robertson et al., 2003), thereby contributing to the pathogenesis of many human diseases (Thannickal and Fanburg, 2000), including type 2 diabetes (Rovira-Llopis et al., 2017a). Primarily this major problem is due to the relatively low production and activity of enzymes involved in the antioxidant defence system including superoxide dismutase, catalase, and glutathione peroxidase (Robertson et al., 2003; Tiedge et al., 1997). Hence, β-cells are strongly affected by oxidative stress (Olofsson et al., 2007).

Superoxide anion, an unstable molecule and very reactive, is converted to a less reactive molecule hydrogen peroxide (H_2O_2) by superoxide dismutase, then H_2O_2 is converted into water and oxygen by H_2O_2 inactivating enzymes such as catalase and glutathione peroxidases (Rhee et al., 2005). Amongst the different redox couples in the cell, the glutathione disulphide-glutathione couple is the most abundant and serves as an essential indicator of the redox environment (Schafer and Buettner, 2001). As such, the reduced form of glutathione (GSH) is considered as crucial defence against ROS (Liu et al., 2022; Muri and Kopf, 2021; Numazawa et al., 2008). Hence, changes in the GSH/GSSG half-reduction potential could be an indicator to understand the redox biochemistry of the cell under oxidative stress (Park, 2021; Schafer and Buettner, 2001; Zitka et al., 2012).

1.8.1.1 Sources of radical oxygen species

Mitochondria, membrane-bound organelles and powerhouses of the cell, are the primary source of reactive oxygen species (ROS) (Xiao et al., 2017) and represents the central regulatory node for ROS synthesis (Hauck et al., 2019). It has been shown that excess mitochondrial ROS causes mitochondrial dysfunction leading to type 2 diabetes, non-alcoholic fatty liver disease, heart failure (Hauck et al., 2019) and induced cardiac inflammation via mitochondrial DNA damage pathway (Yao et al., 2015). Respiratory chain complexes are the major source of ROS produced in the mitochondria (Yang and Lian, 2020). However, ROS can also be produced as a by-product that occurs in peroxisomes, cytochrome *P*-450, and other cellular elements (Balaban et al., 2005; Gonzalez, 2005; Harrison, 2004; Pritchard et al., 2001; Schrader and Fahimi, 2004; Thannickal and Fanburg, 2000).

Oxidative stress occurs when the antioxidant system is disturbed by the overproduction of oxidative radical species (Rani et al., 2016) and ROS (Betteridge, 2000) potentially leading to cell and tissue damage (Sies, 2015). Oxidative

degradation of lipids, lipid peroxidation, occurs when ROS attacks polyunsaturated fatty acids (PUFA) in the mitochondrial membrane. This reaction will lead to production of reactive lipids such as 4-hydroxynonenal and subsequently compromise mitochondrial function (Xiao et al., 2017).

Reactive oxygen species produced in excess could damage lipids, nucleic acids, and proteins. These effects on the cellular biomolecules could lead to several cellular functions, including genetic mutations, reduction of energy metabolism, altered cellular transport mechanisms, inflammation, immune activation, cell cycle control, impaired cell signalling, and reduced biological activity (Rani et al., 2016). Nutritional stress caused by a high-sugar and high-fat diet could lead to oxidative stress and consequently elevate protein carbonylation and lipid peroxidation products, reducing glutathione (GSH) levels and antioxidant system (Rani et al., 2016).

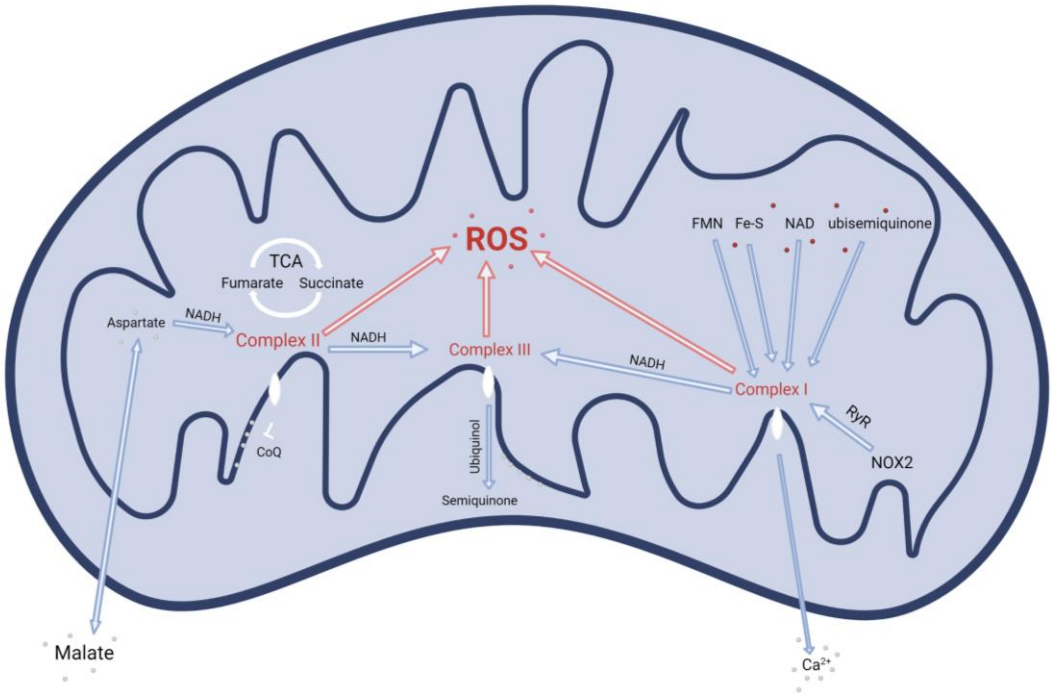

Figure 15.15 Generation of reactive oxygen species in the mitochondria. Significant factors in reactive oxygen species generation are the respiratory chain complexes. Figure created using Biorender.

Cellular reactive oxygen species are mostly generated in the mitochondria (Di Meo et al., 2016; Yang and Lian, 2020) and NADPH oxidases (Dan Dunn et al., 2015). Mitochondrial ROS have been shown to integrate in signalling pathways such as regulating the immune responses and autophagy (Dan Dunn et al., 2015). NADPH oxidase is an enzyme which primarily transports electrons across the plasma membrane and functions to produce superoxide and other downstream ROS (Bedard and Krause, 2007). NADPH and NADH participation in the respiratory chain and cellular metabolism contributes to ROS generation in cells (Yang and Lian, 2020).

NADH-ubiquinone oxidoreductase (complex I) is composed of flavin mononucleotide, Fe-S cluster ubisemiquinone, and NAD (Zorov et al., 2014). Complex I is considered as the major source of mitochondrial ROS. In normal condition, complex I generates a small amount of ROS to effect oxidative damage. Most of the ROS developed in this complex is from complex II through the tricarboxylic acid cycle (TCA) (Bhardwaj et al., 2021; De Grandis et al., 2021; Vranas et al., 2021). Mutation of the gene encoding NADH dehydrogenase subunit 6 caused a deficiency in respiratory complex I NADH (reduced form of nicotinamide adenine dinucleotide) dehydrogenase subunit 6 (ND6). These mutations produced a deficiency in respiratory complex I activity linked to the generation of overproduction of reactive oxygen species (Ishikawa et al., 2008).

Succinate dehydrogenase (SDH) (complex II) is composed of hydrophilic proteins (SDHA and SDHB) and hydrophobic proteins (SDHC and SDHD). The hydrophobic proteins bind to ubiquinone. Complex II has a crucial role in the TCA cycle and respiratory chain. Accumulation of TCA intermediate succinate is a metabolic signature of ischaemia-reperfusion (Chouchani et al., 2014). During reperfusion, accumulated succinate is reoxidised by SDH thereby increasing ROS

generation from an overproduction of fumarate and malate/aspartate shuttle (Chouchani et al., 2014; Yang and Lian, 2020).

Ubiquinol-cytochrome c oxidoreductase (complex III) is encoded by ubiquinol-cytochrome c reductase core protein 1 gene (UQCRC1) and received equivalents from complexes I and II. The reducing equivalents are then progressed with ubiquinol and generate semiquinone for proton transfer. Src homologous-collagen homologue adaptor protein ($p66^{SHC}$) produced mitochondrial ROS as apoptosis signal via cytochrome c oxidation in the mitochondrial electron transfer chain (Yang and Lian, 2020).

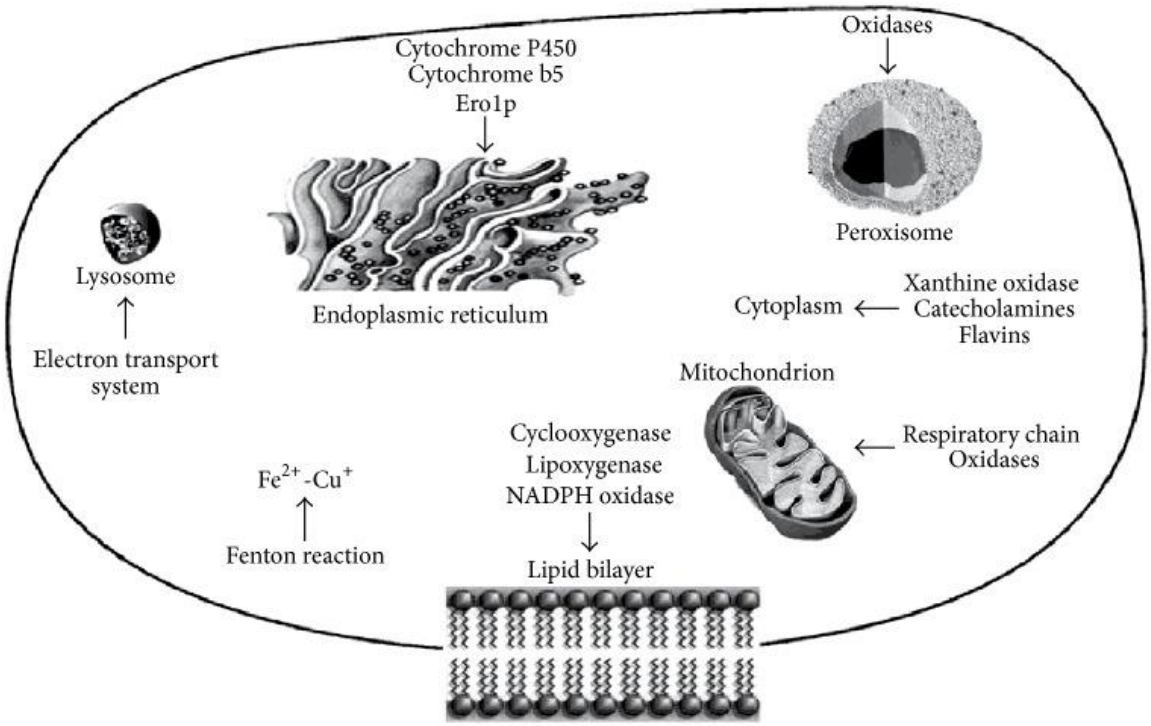

Figure 16.16 Cellular sources of radical oxygen species. Several sites for ROS generation have been identified localised in the cytosol, in the peroxisomes, on the plasma membrane, on membranes of mitochondria, and on membranes of endoplasmic reticulum. Soluble cell components and organelles were shown to be involved in the generation of radical species. Figure adapted from Di Meo et al (2016) and Venditti et al (2015).

In adipose biology, crucially ROS have a positive role as they can inactivate the tensin homolog protein as well as the dual-specificity of lipid and protein

phosphatase in enabling the action of insulin (Kwon et al., 2004). It was found also that ROS could oxidised UCP1, a component of thermogenesis and which is involved in the production of beige fat cells (Chouchani et al., 2016).

The endoplasmic reticulum is a membrane-bound organelle that is involved primarily in lipid and protein biosynthesis (Thannickal and Fanburg, 2000). Endoplasmic reticular oxidoreductin 1 (ERO1) oxidase is a protein disulfide oxidase of the endoplasmic reticulum that transfers electrons from the reduced protein disulfide isomerase to O_2 and produces H_2O_2 as a consequence of protein folding and secretion (Zito, 2015). Aside from the importance of ERO1 in the endoplasmic reticulum oxidative stress, it may be a significant source of intracellular ROS along with mitochondrion or xanthine dehydrogenase system.

Catecholamines, flavins, hydroquinones, and thiols have been shown to participate in redox reactions and contributed to the production of intracellular reactive oxygen species (Freeman and Crapo, 1982).

Hypoxanthine is oxidised to xanthine by xanthine oxidase. Then, xanthine is reduced to uric acid by xanthine dehydrogenase. This oxidoreduction process involve in the production of ROS by generating superoxide and hydrogen peroxide (Furuhashi et al., 2020). This process utilises NAD^+ as oxidising substrate (McCord et al., 1985).

The superoxide produced within mitochondria via autooxidation of electron carriers is converted into hydrogen peroxide through superoxide dismutase. Hydrogen peroxide reacts with ferrous ion, which produces hydroxyl radicals is known as the Fenton reaction (see **Figure 1.17**).

Figure 17.17 Fenton reaction.

Peroxisomes are involved in the synthesising bile acids, cholesterol, dolichol, plasmalogens, and β-oxidation of fatty acid. Peroxisomes are also implicated in amino acid metabolism, synthesis of lipidic compounds, glyoxylate metabolism, and generation of reactive oxygen species (Singh, 1997). During the activity of the enzymes involved in these reactions, ROS are generated (Antonenkov et al., 2010).

Peroxisomes contain xanthine oxidase (Angermüller et al., 1987), which produces superoxide and inducible nitric oxide synthase (Stolz et al., 2002), which generates nitric oxide. Peroxisomes are thereby a potential source of damaging reactive oxygen and nitrogen species.

1.8.2 Reactive nitrogen species

Like ROS, reactive nitrogen species (RNS) are by-products of cellular metabolism and ionising radiation usually involved in the release of hydroxyl radical, hydrogen peroxide, and superoxide anion radical (Kurutas, 2016). Examples of nitrogen species are nitric oxide, nitrogen dioxide, and peroxynitrite.

Nitric oxide (NO) is shown to be vital in regulating cellular function and as the mediator of cellular damage (Pacher et al., 2007). Nitric oxide contains an unpaired electron which makes it a radical and is produced during the metabolism of arginine to citrulline by nitric oxide synthase (Kurutas, 2016). Protein kinase C (ε isoform) is activated by nitric oxide and this activation stimulates a specific family of tyrosine kinases to induce apoptosis (Castrillo et al., 2001).

In an aqueous and lipid environment, NO is soluble and diffuses rapidly through the cytoplasm and plasma membrane. In an extracellular environment NO

reacts with oxygen and water to produced nitrate and nitrite anions (Kurutas, 2016). Oxyhaemoglobin reacts with NO to form methaemoglobin and nitrate (Helms and Kim-Shapiro, 2013). This process regulates NO synthesis from reacting with oxygen to produced nitrogen dioxide significantly. But, simultaneous synthesis of NO and superoxide anion radicals transforms the biological action of NO in generating a more damaging and reactive species, peroxynitrite (Pacher et al., 2007).

Nitrogen dioxide is classified as an indoor and outdoor air pollutant from cigarette smoke, car emission, gas stoves heaters to name a few (Persinger et al., 2002). Exposure to nitrogen dioxide can trigger inflammation, cell injury, and pulmonary edema (Moldéus, 1993) and increase thiobarbituric acid reactive substance (TBARS), a marker of lipid oxidation in the lungs (Sagai et al., 1984). Peroxynitrite is produced from the reaction of superoxide anion and nitric oxide (see **Figure 1.18**) (Blough and Zafiriou, 2002).

Figure 18.18 Formation of peroxynitrite.

Peroxynitrite exceeds significantly the effectiveness of the Fenton reaction and Haber-Weiss reaction in producing hydroxyl radicals (Beckman et al., 1990) and peroxynitrite has also been reported to generate nitrogen dioxide, an oxidant thought only produced from cigarette smoke and pollution from the air (Pacher et al., 2007). Peroxynitrite reacts with tyrosine, tryptophan and lipids to form nitrotyrosine, nitrotryptophan, and nitrated lipids, respectively, which are considered as biological markers *in vivo* (see **Figure 1.19**).

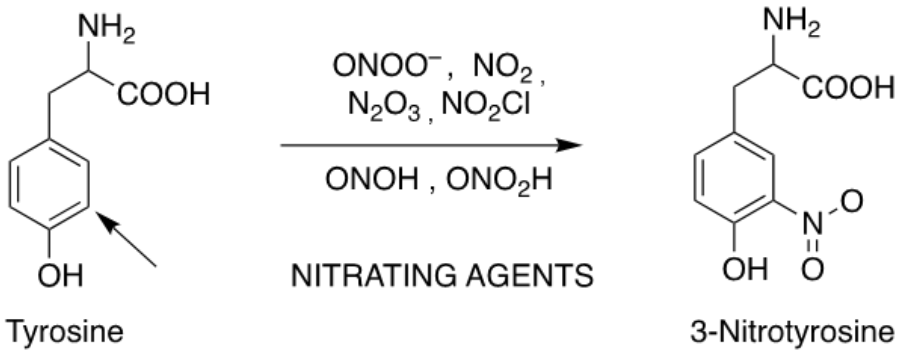

Figure 19.19 Formation of 3-nitrotyrosine. Nitration at the ortho position of the OH group of tyrosine is the preferred site of reaction to form 3-nitrotyrosine.

Peroxynitrite generated by the immune cells has been shown to kill endocytosed bacteria (Pacher et al., 2007). The formation of nitrotyrosine is a biological marker of inflammation and nitrosative stress (Pacher et al., 2007). A significant increase of inducible NO synthase (iNOS)-derived peroxynitrite formation in type 1 and type 2 diabetic platelets has been shown to damage human platelets (Tannous et al., 1999). However, inhibition of the excess production of iNOS and peroxynitrite prevents the development of diabetes (Mabley et al., 2004; Suarez-Pinzon et al., 1997; Suarez-Pinzon et al., 2001; Szabó et al., 2002).

1.8.3 Dual role of ROS and RNS

The mechanism of type 2 diabetes is not fully understood and elucidated; however, studies show that ROS andRNS, collectively known as RONS, play a role not only in insulin resistance but also in the β-cell dysfunction, thereby progressing the development of type 2 diabetes (Ahmad et al., 2017; Singh et al., 2009; Wang, X. and Hai, 2011).

At low concentration, RONS plays a significant role in signalling pathways as regulatory mediators. However, when the level of RONS is moderate or high, they cause deleterious effects in living organisms by inactivating important cellular molecules (Di Meo et al., 2016). For example, at low concentration, nitric oxide is

identified as a signalling molecule in blood vessel modulation and at high concentration, nitric oxide can mediate cellular toxicity damaging metabolic enzymes and nitric oxide can also generate peroxynitrite from the reaction with superoxide (Zapol, 2019).

In pancreatic β-cells, ROS plays a crucial role in the normal insulin transduction (Puddu et al., 2013) and ROS generation has been shown to occur due to glucose stimulation (Bindokas et al., 2003; Tanaka et al., 2002). Leloup et al. have shown that transient mitochondrial ROS production is associated with glucose-induced insulin secretion (Leloup et al., 2009).

The hydroxyl radical is a very toxic radical species as it quickly passes the cell membrane, enters the nucleus, and interacts with DNA to cause mutation (Robertson et al., 2003). The cyclic guanosine monophosphate (cGMP) pathway is implicated in the pathogenesis of malaria, fibrosis, neurodegeneration, and inflammation (Friebe et al., 2020). Hydroxyl radical is generated from the reaction of superoxide and hydrogen peroxide. Formation of hydroxyl radical activates guanylate cyclase. Hydroxyl radical was found to stimulate cGMP production (Mittal and Murad, 1977).Through this mechanism, cGMP is formed and allowed the physiological regulation of guanylate cyclase during an altered redox and formation of free radical in tissues in response to hormones (Mittal and Murad, 1977).

ROS have been shown to regulate protein phosphorylation, transcription factors and ion channels at normal physiological processes, and it is shown to be implicated in thyroid hormone production and crosslinking of the extracellular matrix (Brieger et al., 2012). ROS have also been shown to regulate apoptosis, growth, and other signalling cascades and even contributed to the regulation of blood pressure, immune function, and cognitive function (Brieger et al., 2012).

Nitric oxide has a broad spectrum of signalling functions associated in physiological and pathophysiological processes (Bogdan, 2001). Nitric oxide plays

a role as a signalling molecule in blood vessel modulation (Ignarro et al., 1987) and is a potent mediator in cellular toxicity damaging metabolic enzymes such as increasing mtDNA content, MitoTracker fluorescence (an indicator of mitochondrial membrane potential), expression of cytochrome *c* oxidase subunit IV of the mitochondrial respiratory chain, cytochrome *c*, and mitochondrial mass (Lee-Huang et al., 2021). The effects of the stimulated by NO were brought about by guanosine 3′,5′-monophosphate-dependent increased expression of peroxisome proliferator-activated receptor γ coactivator 1α, nuclear respiratory factor 1, and mitochondrial transcription factor A. All of these are crucial mediators of gene expression for mitochondrial biogenesis (Knott and Bossy-Wetzel, 2010). The cytotoxicity attributed to nitric oxide is due to peroxynitrite generated from the reaction of nitric oxide and superoxide anion radical (Pacher et al., 2007). Nitric oxide and its derivatives and reactive oxygen intermediates are species which are toxic to the immune system and shown to control tumours and intracellular microbes *in vivo* (Bogdan et al., 2000).

Nitric oxide synthases (NOS) converts L-arginine and oxygen to nitric oxide and L-citrulline. This conversion requires flavin mononucleotide (FMN), reduced nicotinamide adenine dinucleotide (NADPH), tetrahydrobiopterin (BH_4), flavin adenine dinucleotide (FAD), and thiol as cosubstrates or cofactors (Hanusch et al., 2022; Picciano and Crane, 2019). There are three isoforms of NOS, and all of them bind to calmodulin and contain a haem group (Förstermann and Sessa, 2012). Haem is crucial for the interdomain transfer of electrons from the flavin to the haem of the opposite monomer (Abu-Soud and Stuehr, 1993). Neuronal NOS, known as nNOS/NOS I, are expressed in central and peripheral neurons which could involved in controlling blood pressure, and smooth muscle relaxation vasodilation via peripheral nitrergic nerves. Residual nNOS is needed for the action of phosphodiesterase-5 inhibitors.

Inducible NOS, known as iNOS/NOS II, is expressed in response to cytokines and contributes to inflammatory disease pathophysiology. iNOS is regulated at the transcriptional and post-transcriptional level, which involves signal transduction pathways and molecules (Bogdan et al., 2000). Endothelial NOS, known as eNOS/NOS III, is expressed in endothelial cells that function to dilate blood vessels, control blood pressure and have vasoprotective and anti-atherosclerotic effects (Förstermann and Sessa, 2012). NOS isolated from neuronal and endothelial cells are calmodulin-dependent. Due to the differences in the calmodulin-binding domain, neuronal NO synthase and endothelial NO synthase require elevated Ca^{2+} for their catalytic activity whilst inducible NO synthase has a high affinity to calmodulin without Ca^{2+}.

1.9 Oxidative stress

Elevated oxidative stress indicates the progressive development of diabetes and its complications (Maritim et al., 2003). Oxidative stress is described as the imbalance of ROS production and antioxidant defences (Betteridge, 2000) in favour of the ROS (Sies, 1997). Possible mechanisms in the development of oxidative stress are activation of transcription factors, protein kinase C and formation of advanced glycated end products (AGEs) (Maritim et al., 2003). Under oxidative stress, AGEs activate NF-κB (Mohamed et al., 1999), which enhances the production of nitric oxide (Maritim et al., 2003) and, as a consequence, causes islet β-cell damage. Oxidative stress has been shown to decrease the level of reduced glutathione (Cheng and González, 1986), thus impairing glucose homeostasis *in vivo* (Pitocco et al., 2010) and cause depletion of NADPH levels (Cheng and González, 1986; Gonzalez et al., 1986).

Hyperglycaemia and hyperlipidaemia are conditions that can induce oxidative stress. Hyperlipidaemia can only occur at a high glucose level, and

hyperglycaemia is a pre-requisite for its effect (El-Assaad et al., 2003; Harmon et al., 2001). Thus, glucolipotoxicity is the better term used to describe the impact of lipotoxicity between lipids and β-cell functions (Pitocco et al., 2010).

ROS and RNS were identified as factors in various pathologies such as hypertension, ischemia and reperfusion injury, neurodegenerative diseases (Parkinson's disease and Alzheimer's disease), ageing, rheumatoid arthritis, cancer, cardiovascular disease, atherosclerosis, and diabetes mellitus (Valko et al., 2007).

1.10 Nitrosative stress

Stamler and co-workers defined nitrosative stress as dysregulation of nitric oxide and nitric-oxide derivatives of radical nitrogen species (Hausladen and Stamler, 1999). Like oxidative stress, nitrosative stress accounts for the chemical modification of proteins through crucial amino acids reacting with RNS which consequently causes irreversible loss or reversible regulation of protein function (Klatt and Lamas, 2000). This occurs when the antioxidant defence system cannot neutralise the excess nitrating oxidants produced during inflammatory processes (Valko et al., 2007).

1.11 Aims and objectives

The harmful effects of long-term exposure to excess nutrients (high glucose and high fat) are evident in various studies; however, diabetogenesis mechanisms remain poorly established. Previous data from the Turner group has shown that over 3,000 pancreatic genes have 2-fold or more significant change in gene expression that results from exposure to a high sugar and high fat glucolipotoxic (GLT) environment representative of that experienced by patients with poorly controlled type 2 diabetes. The challenge now is to understand which of these genes drives β-

cell dysfunction and the decreased insulin secretion that results from high sugar and high-fat diet.

Generally, this study has the following objectives, and the specific objectives of each study is stated in each chapter.

1. To identify whether glucolipotoxicity affects HNF4α expression and whether this effect is involved in the inhibition of insulin secretion using INS-1 cell.
2. To evaluate the effect of glucolipotoxicity on the extracellular matrix remodelling and cell adhesion pathways using INS-1 cells.
3. To assess the effects of carnosine and its analogues on radical species generation and insulin secretion inhibition by glucolipotoxicity using INS-1 cells.
4. To determine the effects of L-carnosine and β-alanine on mitochondrial bioenergetics using INS-1 cells and C2C12 myotubes.

Chapter 2

Materials and Methodology

2.1 Reagents and buffer solutions

All reagents were purchased from Sigma-Aldrich, Haverhill, UK and plasticwares were purchased from ThermoFisher, UK and VWR, UK unless otherwise stated.

Table 2.1 Media and buffer solutions used in the entire study.

Name	Components
Roswell Park Memorial Institute-1640 complete medium (RPMI-1640 complete medium)	RPMI-1640 (Cat. No. R6504-10X1L) containing 11 mM of D-glucose ($C_6H_{12}O_6$), 26 mM sodium bicarbonate ($NaHCO_3$), 10 mM 4-(2-hydroxyethyl)piperazine-1-ethanesulfonic acid ($C_8H_{18}N_2O_4S$, HEPES), 50 µM β-mercaptoethanol ($HSCH_2CH_2OH$), 1% v/v sodium pyruvate ($C_3H_3O_3Na$) (Gibco by Life Technologies, Cat. No. 11360-070), 1% v/v penicillin/streptomycin (Gibco by Life Technologies, Cat. No. 15140-122), 10% v/v heat inactivated fetal bovine serum (Gibco by Life Technologies, Cat. No. 16140-071)
Glucolipotoxic medium (GLT media)	RPMI-1640 complete medium supplemented with 17 mM D-glucose ($C_6H_{12}O_6$), 200 µM oleic acid ($CH_3(CH_2)_7CHCH(CH_2)_7COONa$), 200 µM palmitic acid ($CH_3(CH_2)_{14}COOH$), 2% bovine serum albumin (BSA) (Cat. No. A7030-500G)
RPMI-1640 medium + L-carnosine	RPMI-1640 medium supplemented with 10 mM L-carnosine
RPMI-1640 medium + β-alanine	RPMI-1640 medium supplemented with 10 mM β-Alanine
L-carnosine + GLT	GLT medium supplemented with 10 mM L-carnosine

β-alanine + GLT	GLT medium supplemented with 10 mM β-alanine
100 mM oleic acid stock solution	0.0304 g sodium oleate ($CH_3(CH_2)_7CHCH(CH_2)_7COONa$), 0.5 mL ethanol ($CH_3CH_2OH$), 0.5 mL distilled H_2O
100 mM palmitic acid stock solution	0.0255 g palmitic acid ($CH_3(CH_2)_{14}COOH$), 1 mL ethanol (CH_3CH_2OH)
RadioImmunoPrecipitation Assay buffer (RIPA buffer)	150 mM sodium chloride, NaCl, 0.1% Triton X-100, 0.5% sodium deoxycholate, $C_{24}H_{39}NaO_4$, 0.1% sodium dodecyl sulphate (SDS), 50 mM Tris-base, pH 8.0, protease inhibitor (Roche Applied Science, Cat. No. 11697498001)
Protein loading buffer	950 µL 4X Laemmli buffer (Bio-rad, Cat. No. 1610747), 50 µL β-mercaptoethanol ($HSCH_2CH_2OH$)
Lower buffer	1.5 M Tris-base ($NH_2C(CH_2OH)_3$), pH 8.8
Upper buffer	0.5 M Tris-base ($NH_2C(CH_2OH)_3$), pH 6.8
Running buffer	250 mM Tris-base ($NH_2C(CH_2OH)_3$), 1.92 M glycine, 35 mM SDS, pH 8.3
Transfer buffer	60% 5X Trans Blot Turbo transfer solution (Bio-rad, Cat. No. 10026938), 20% distilled H_2O, 20% ethanol
Phosphate buffered saline (PBS) 10X	137 mM sodium chloride (NaCl), 2.7 mM potassium chloride (KCl), 10 mM sodium phosphate dibasic (Na_2HPO_4), 2 mM potassium phosphate monobasic (KH_2PO_4)
Tris-buffered saline (TBST) 10X	1.5 M sodium chloride (NaCl), 0.5M Tris-base ($NH_2C(CH_2OH)_3$), 1.0% Tween-20, pH 7.6
TAE buffer 10X	400 mM Tris-acetate,10 mM ethylenediamine tetra-acetic acid (EDTA), pH 8.2

Krebs-Ringer buffer solution	125 mM NaCl, 1.2 mM KH_2PO_4, 5 mM KCl, 2 mM $MgSO_4$, 1.67 mM D-glucose, 0.1% w/v bovine serum albumin (BSA), 25 mM HEPES, pH 7.4
Secretagogue cocktail	1 mM Tolbutamide, 10 mM Leucine, 10 mM Glutamine, 1 mM 3-isobutyl-1-methylxanthine (IBMX), 1 µM phorbol 12-myristate 13-acetate (PMA) and 10 mM D-glucose

2.2 Cell culture

Two experimental cellular models of type 2 diabetes have been established in the Turner group using immortalised cells. This enables individual variables to be manipulated in isolation and cells subjected to various experimental conditions, reflecting either T2D disease pathophysiology or to test the therapeutic potential of potential new drugs. For this research, rat insulinoma cell line INS-1 and mouse skeletal muscle C2C12 cells were used in the entire study. The initial passage number of these cell lines stored from the nitrogen tank were noted and these cells were split up to twenty (20) passage only.

2.2.1 INS-1 cells

INS-1 pancreatic β-cell line is an insulin secreting cell line derived from a transplantable rat insulinoma by x-ray irradiation. This cell line can synthesise proinsulin I and II (Asfari et al., 1992). Morphological features shown by native β-cells are also displayed by this cell line. This cell is dependent on β-mercaptoethanol for its growth and survival, as removal of the thiol compound from the medium was shown to cause a 15-fold drop in the total cellular glutathione levels (Asfari et al., 1992). One of the possible explanations for this was the activation of cystine uptake, which has been shown to lead to an increased level of glutathione (Ishii et al., 1987;

Pruett et al., 1989). INS-1 cells have also been shown to retain differentiated characteristics for insulin biosynthesis, and storage is about 30-40 times higher than other transplantable rat insulinoma such as RINm5F and other rat insulinoma derived cell lines (Carrington et al., 1986; Clark et al., 1990).

2.2.2 C2C12 cells

C2C12 cells are immortalised cell line generated by Blau, Chiu, and Webster in 1983. C2C12 cells grow and proliferate as undifferentiated myoblasts in high serum and differentiate into myotubes in low serum conditions. These are robust cells that have been used by multiple groups to successfully investigate glucose metabolism, insulin resistance, reactive nitrogen and oxygen species and glucose transporters, both at molecular and cellular levels (Abdelmoez et al., 2020; Chen, L. et al., 2019; Sanvee et al., 2019; Shen et al., 2019; Wong et al., 2020). The immortal C2C12 cells were originally derived from the thigh muscle of a 2-month-old female C3H mouse donor 70 hours after a crush injury (Brenner et al., 2021; Diokmetzidou et al., 2016).

2.3 Cell culture, propagation, and passaging

INS-1 rat pancreatic β-cells were cultured in Roswell Park Memorial Institute (RPMI-1640) medium containing 11 mM D-glucose then supplemented with 26 mM sodium bicarbonate, 10 mM HEPES, 50 µM β-mercaptoethanol and the pH was adjusted to 7.4. The medium was then supplemented with 10% v/v fetal bovine serum, 1% v/v sodium pyruvate (100 nM, Cat. No. 11360070) and 1% v/v penicillin streptomycin (10,000 U/mL, Cat. No. 15140122). INS-1 cells were then plated in a Nunc™ cell culture polystyrene T75 flask and incubated at 37 ^{o}C in an environment of 95% air/5% CO_2 (Bagnati et al., 2016; Cripps et al., 2017; Marshall et al., 2007).

Mercaptoethanol is a potent reducing agent supplemented in cell culture media to reduce toxic levels of oxygen radicals (Castillo-Martín et al., 2014).

When 80-85% confluence of cells was achieved, cells were passaged by aspirating the medium and washing the cells with 5 mL sterile of Dulbecco's phosphate buffered saline (DPBS) solution. INS-1 cells were then incubated with 5 mL of 0.05% Trysin-EDTA (1X) to detach the INS-1 cells at 37 ^{o}C for 3 minutes. INS-1 cells were harvested by gently pipetting back and forth with 5 mL of complete RPMI-1640 medium. Cell pellets were collected through centrifugation at 200 x g for 5 minutes at room temperature. Harvested cells were re-suspended with 5 mL of complete RPMI-1640 medium and re-plated and grown in polystyrene T75 flask or 6-well plates (Bagnati et al., 2016; Cripps et al., 2017; Marshall et al., 2007).

2.4 Preparation of glucolipotoxic media

To mimic conditions typically experienced by a diabetic patient with poorly controlled type 2 diabetes *in vitro*, INS-1 rat pancreatic β-cells were incubated with glucolipotoxic (GLT) media. To prepare the GLT medium, RPMI-1640 media was supplemented with an additional 17 mM glucose (28 mM final concentration), followed by 2% fatty acid free bovine serum albumin (BSA), and 200 µM oleic acid, and 200 µM palmitic acid conjugated to the BSA by incubating at 37 ^{o}C for at least 1 hour. The medium was filtered using a 0.2 µM Millipore PES membrane filter.

2.5 Cell counting

INS-1 rat pancreatic β-cells were incubated in complete RPMI-1640 medium in a Nunc™ cell culture polystyrene T75 flask to 70-80% confluency, then passaged by aspirating the medium and washing the cells with 5 mL of sterile Dulbecco's phosphate buffered saline (DPBS) solution. Cells were then incubated with 5 mL of 0.05% Trysin-EDTA (1X) to detach the cells at 37 ^{o}C for 3 minutes. Cells were

harvested by gently pipetting back and forth with 5 mL of complete RPMI-1640 medium. Cell pellets were collected through centrifugation at 200 x g for 5 minutes at room temperature. Harvested cells were re-suspended with 5 mL of complete RPMI-1640 medium and re-plated and grown in T75 flask or 6-well plates .

To seed the required number of cells on the plate, correct counting is a must, and this was done manually using a haemocytometer. A 10 µL of cell suspension was loaded into a Neubauer chamber and to identify the living cells from the necrotic cells, 10 µL of 0.2% Trypan Blue was added to it and mixed thoroughly. Ten (10) µL of the mixture was then loaded into a Neubauer chamber then cells were counted from the four squares (see **Equation 1** and **Figure 2.1**) and the cell concentration calculated using the formula below:

$$\text{Concentration} = (\text{Number of cells x } 10{,}000)/(\text{Number of squares x dilution factor})$$

Equation 2.1 Formula in calculating the cells concentration using haemocytometer.

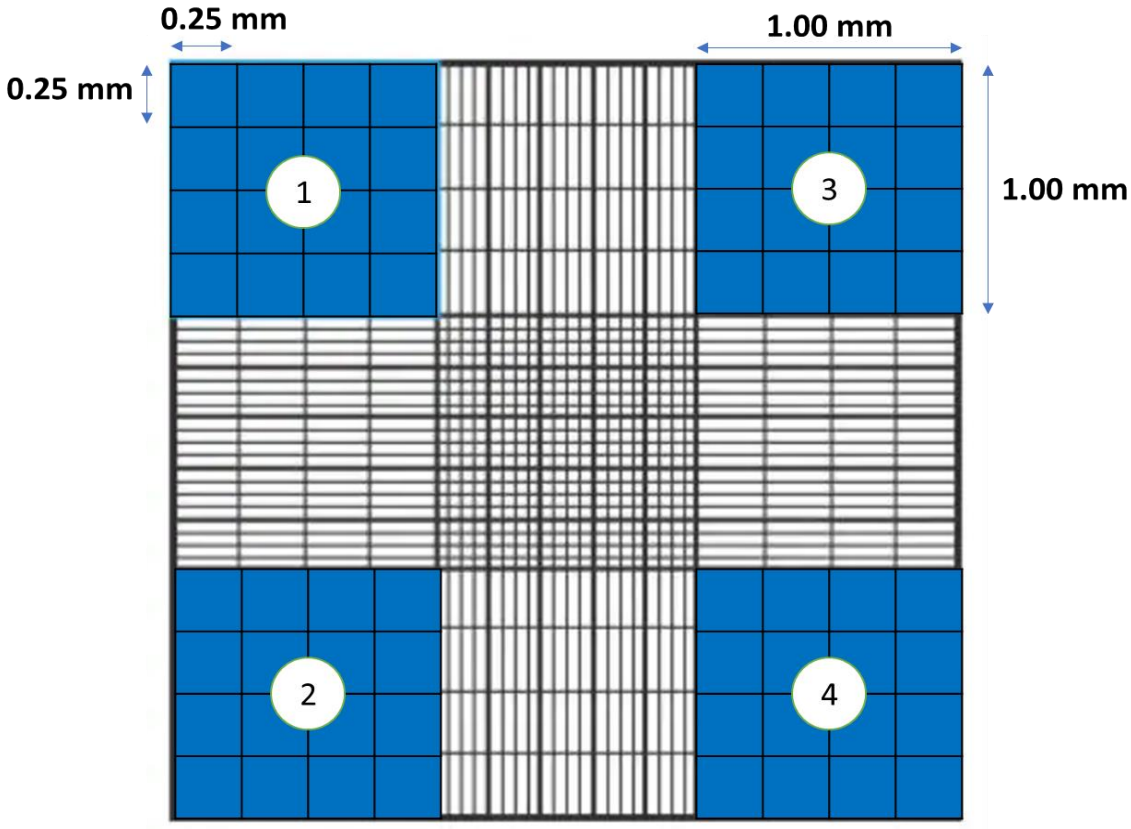

Figure 2.1 Neubauer chamber of the haemocytometer. The live and dead cells found in the labelled squares were counted in a north-west clockwise direction.

2.6 Cell plate seeding and cell culture lysate extraction

The number of initially seeded cells on a nunclon delta 6- or 12-well polystyrene plate were 50,000- and 25,000 INS-1 cells per well, respectively. These cells were then incubated for 5 days whilst changing the medium on the 3rd day.

INS-1 cells plated in 6-well plates were treated with RPMI-1640 medium, or RPMI-GLT medium, and incubated for 5 days whilst changing the required medium solution, respectively, on the 3rd day of treatment. After 5 days of incubation, INS-1 cells were washed twice with cold DPBS and lysed in 150 µL cold RadioImmunoPrecipitation Assay (RIPA) buffer with protease inhibitor (Roche Applied Science, Basel, Switzerland). Sterile scrapers were used to detach cells from each well. Lysates were collected in pre-cooled 2 mL microcentrifuge tubes and vortex-mixed for 3 minutes and centrifuged at 20,000 x g for 20 minutes at 4 ^{o}C.

The supernatants containing the total cellular protein were transferred into pre-cooled 2 mL sterile microcentrifuge tubes and stored at -80 ^{o}C for future use and analysis.

2.7 Determination of total protein concentration in lysates

Biochemical analysis of protein depends on the accurate determination of protein concentration in order to subsequently be able to normalise data (Bainor et al., 2011; Olson et al., 2007). Bicinchoninic acid assay (BCA) sodium salt, introduced by Smith et al (1985), is a water-soluble compound which gives an intense purple colour when reacts with cuprous ion in basic solution (Smith et al., 1985). Nowadays, it is a popular colorimetric method for quantification of total proteins and used to determine the exact amount of total protein for the exact loading in sodium dodecyl sulphate-polyacrylamide gel electrophoresis (SDS-PAGE) gels. In this assay, amide bonds in proteins reduces cupric ion (Cu^{2+}) to cuprous ion (Cu^{+}) resulting to a faint blue-violet colour reaction. Then cuprous ion is chelated by two molecules of BCA sodium salt to form an intense, purple-coloured BCA-Copper complex that highly absorbs at a wavelength of 562 nm. Its absorbance increases as the total protein concentration in sample increases.

In this project, the Pierce^{TM} BCA Protein Assay Kit (Thermo Scientific, Loughborough, UK) was used to determine the total cellular protein of the cells exposed to various experimental conditions. Bovine serum albumin is included in the kit to establish the standard calibration curve for total protein quantification. The preparation of the working solution and sample were done using the protocol in the kit.

To conduct the assay, 10 µL of protein lysates and BSA standard calibrators were pipetted into the nunclon polystyrene 96-well plate and added with 200 µL working solution (50:1 v/v reagent A:reagent B). The plate was then incubated at

37 °C for 30 minutes and absorbance was read at 562 nm (Infinite M Plex by Tecan, Reading, UK). Corrected absorbance of the BSA standard calibrator against its respective concentration was plotted. Using the linear equation from the standard curve, the unknown total protein concentration of each lysates was determined and the required loading volume (30 µg) for SDS-PAGE was calculated.

Using the linear equation from the standard curve, the total cellular protein concentration of each lysate was determined, in order to calculate the required loading volume of 30 µg per well for SDS-PAGE.

2.8 Cryo-conservation and recovery of frozen cells

Following passaging of INS-1 cells (detailed above) cells were harvested by gently pipetting back and forth with 5 mL of RPMI-1640 medium. Cell pellets were collected through centrifugation at 200 x g for 5 minutes at room temperature. Harvested cells were resuspended with 5 mL of Synth-a-Freeze medium (Life Technologies, UK) and transferred into equally into 5 cryovials. Synth-a-Freeze medium is a liquid cryopreservation medium containing 10% v/v dimethylsulfoxide (DMSO) that promotes high cell viability and recovery after thawing. INS-1 cells in cryovials with synth-a-freeze medium were labelled, then placed into a Mr. Frosty freezing container for a slow cooling rate of -1 °C per minute and stored in a -80 °C freezer for 24 hours before being transferred to a liquid nitrogen container for long-term storage.

To recover frozen INS-1 cells stored in a liquid nitrogen, a cryovial was defrosted and the cell solution carefully added into a 15 mL polystyrene conical tube containing 5 mL of RPMI-1640 medium. The mixture was then centrifuged at 200 x g for 5 minutes, then the supernatant decanted. The pellet was washed twice with RPMI-1640 media before it was resuspended with 5 mL of RPMI-1640 medium and

seeded into a polystyrene T75 flask containing 15 mL RPMI-1640 medium. INS-1 cells were incubated at 37 °C in a 95% air/5% CO_2 environment condition.

2.9 Mycoplasma assessment and decontamination

INS-1 rat pancreatic β-cell culture medium was periodically tested for potential mycoplasma infection. To do this, EZ-PCR mycoplasma test kit (Biological Industries, CT, USA, Cat. No. 20-700-20) was used. 1 mL of cell growth medium was taken and centrifuged at 200 x g for 5 minutes to settle any cells or debris in the medium. The supernatant was carefully transferred into a 2 mL sterile polypropylene centrifuge tube and further centrifuged at 20,000 x g for 10 minutes in order to precipitate mycoplasma. Supernatant was discarded, then 50 µL of buffer solution was added to the pellet and the tube heated at 95 °C for 3 minutes.

The mixture underwent a simple PCR (see **Table 2.2** and **Table 2.3** for PCR set-up and cycling conditions) to amplify the amount of mycoplasma present.

Table 2.2 PCR reaction set-up using EZ-PCR mycoplasma kit.

Reagents	**Volume per reaction, µL**
H_20	35
Reaction mix	10
Test sample	5

Table 2.3 Cycling conditions set by EZ-PCR mycoplasma kit.

Phase	**Temperature, ºC**	**Time**	**Number of cycles**
Initial denaturation	94	30 s	-
Denaturation	94	30 s	35
Annealing	60	120 s	
Extension	72	60 s	
Final Extension	72	5 min	-

After the sample underwent PCR, 2% agarose dissolved in 1X tris-acetate-EDTA (TAE) buffer was made and added with 5 µL of SYBR® Safe DNA gel stain (10,000X in DMSO) (Thermo Fisher, MA, USA, Cat. No. S33102). It was then solidified in the gel cassette. Into each PCR samples, 2 µL of 10X DNA loading buffer (Thermo Fisher, MA, USA, Cat. No. 10816015) was added. DNA electrophoresis was conducted by loading 20 µL of each sample into the wells along with the positive control and 100 bp DNA ladder (Cleaver Scientific, UK, CSL-MDNA-100BP) and was run at 70 V for 45 minutes. After running the electrophoresis, the entire agarose gel (see **Figure 2.2**) was visualised using GeneSnap software.

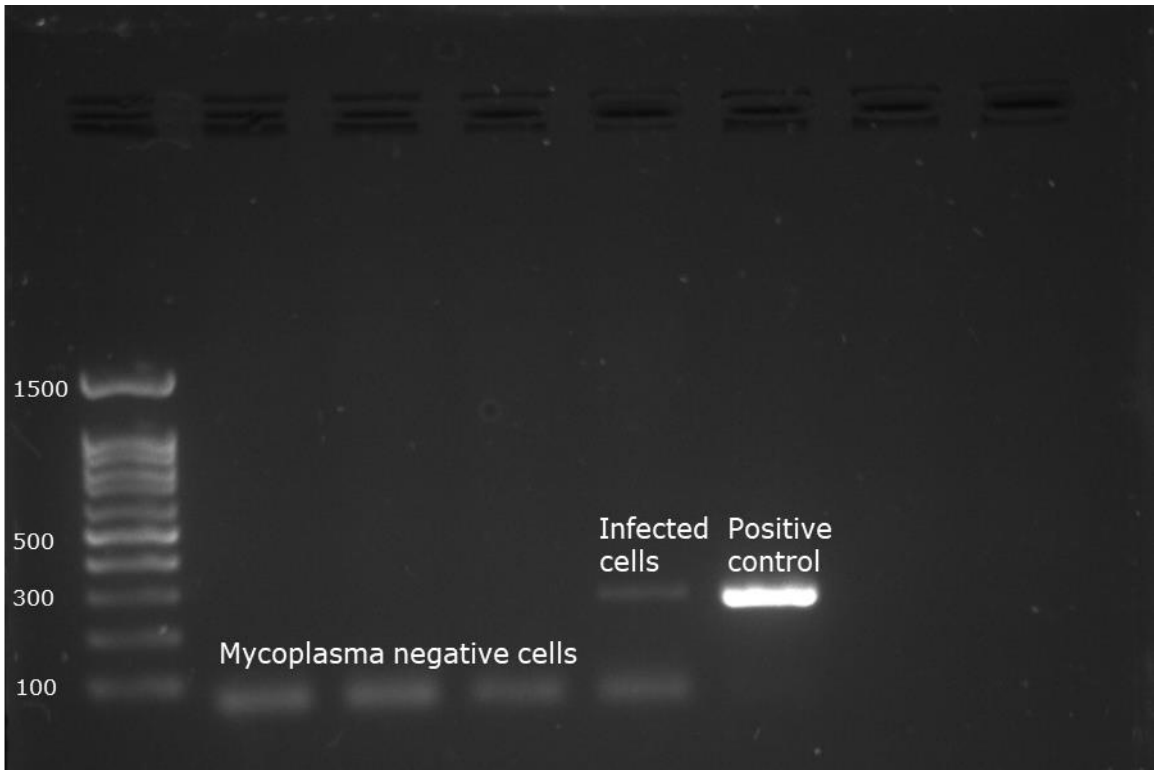

Figure 2.2 Mycoplasma detection test by PCR. PCR reaction was performed on the supernatant of INS-1 rat pancreatic β-cells cultured in RPMI-1640 medium for 5 days. None of my cells (first three columns after the ladder) were infected by mycoplasma relative to control, showing no band at 270 bp. The cells on the fourth column came from a student in a different lab, and these were shown to be contaminated by mycoplasma.

2.10 Mice strain, islet extraction and digestion

In this study, male CD-1 mice (Charles River, UK) were used. Mice were maintained in a 12-hour light/12-hour dark cycle and fed a standard rodent diet. The mice were sacrificed after 10 weeks by overdose of sedative and the pancreas excised. The pancreas was digested by directly injecting of ice-cold 1mg/ml collagenase P (Roche Applied Science, Switzerland) and 0.15 mg/ml DNAse 1 (Roche Applied Science, Switzerland) diluted in RPMI-1640 into the pancreatic duct. Upon pancreatic inflation, it was excised and cut into small pieces by surgical scissors and placed in ice cold RPMI. Samples were sealed with parafilm and incubated at 37°C for 7 minutes under static conditions followed by forceful shaking every minute post incubation until suitable pancreatic tissue digestion. Digested tissue was allowed to settle before supernatant removal and transfer to black bottomed container. Islets were picked by hand using a light microscope and p200 pipette, then cultured in a flask containing RPMI 1640 and incubated at 37°C in a 95% air/5% CO_2 atmosphere. All animal procedures were undertaken by Dr. Sophie Sayers at King's College London and this was approved by King's College London Ethics Committee. Protocols were carried out in accordance with the UK Home Office Animals (Scientific Procedures) Act 1986.

2.11 Cell functional analyses

2.11.1 Cell viability

Calcein AM or calcein acetoxymethyl ester was used to assess the cellular health of INS-1 rat pancreatic β-cells exposed to various experimental conditions. Calcein AM, a cell permanent dye, is a non-fluorescent cell-permeable dye that is converted to a green-fluorescent calcein after acetoxymethyl ester hydrolysis by intracellular esterases. The measured intensity of calcein is directly proportional to the activity of cellular esterases which is also proportional to cell viability.

In this experiment, INS-1 rat pancreatic β-cells were incubated in polystyrene nunclon delta 12-well plate for 5 days in RPMI-1640 medium ± 10 mM L-carnosine or RPMI-1640 medium ± 100 µM carnosine analogues or GLT medium (RPMI-1640 medium supplemented with 17 mM D-glucose, 200 µM oleic acid and 200 µM palmitic acid) ± 10 mM L-carnosine or GLT medium ± 100 µM carnosine analogues. After the incubation period, the media was aspirated, and cells were washed thrice with Krebs-Ringer buffer solution (KRBS). A final concentration of 5 µM calcein AM was added to make 1 mL Krebs-Ringer buffer solution. This was loaded into each well for 1 hour before washing again thrice with Krebs-Ringer buffer solution. After washing, 1 mL of Krebs-Ringer buffer solution was loaded to each well. Cell viability was measured via fluorescence using excitation and emission at 490 nm and 520 nm, respectively, with cell viability expressed as the percentage change ± S.E.M. in comparison to control.

2.11.2 Radical species detection

Oxidative stress could be a result of low levels of antioxidants or high production of reactive oxygen and nitrogen species (RONS) (Myhre et al., 2003). The generation of high levels of intracellular oxidant levels could result in damaging biological molecules and activation of signalling pathways (Myhre et al., 2003). 2',7'-Dichlorofluorescin diacetate (DCFH-DA) or 2',7'-dichlorodihydrofluorescin diacetate (DCFH2-DA), a non-fluorescent cell-permeable probe that diffuses easily across the plasma membrane. Cellular esterases cleave the acetate moiety to form a more hydrophilic 2',7'-dichlorodihydrofluorescein (DCFH2) which is retained in the cytosol. DCFH2 is then oxidised to 2',7'-dichlorofluorescein (DCF) which can be measured spectrofluorometrically. Detection of intracellular oxidative stress using DCFH-DA is limited to *in vitro* (Reiniers et al., 2017). DCFH-DA can also be used to measure

radical species not limited to the reactive oxygen species, including some nitrogen species (Kalyanaraman et al., 2012).

In this experiment, INS-1 rat pancreatic β-cells were incubated in polystyrene nunclon delta 12-well plate for 5 days in RPMI-1640 medium ± 10 mM L-carnosine or RPMI-1640 medium ± 100 µM carnosine analogues or GLT medium (RPMI-1640 medium supplemented with 17 mM D-glucose, 200 µM oleic acid and 200 µM palmitic acid) ± 10 mM L-carnosine or GLT medium ± 100 µM carnosine analogues. After the incubation period, the medium was aspirated, and cells were washed thrice with Krebs-Ringer buffer solution. A final concentration of 20 µM DCFH-DA was added to make a 1 mL Krebs-Ringer buffer solution. It was loaded into each well for 1 hour before washing again thrice with Krebs-Ringer buffer solution. After washing, 1 mL of Krebs-Ringer buffer solution was loaded to each well. Detection of radical species was measured via fluorescence using excitation and emission at 495 nm and 530 nm, respectively, with radical species detection, expressed as a percentage change in comparison to control.

2.11.3 Insulin secretion assay

In this experiment, INS-1 rat pancreatic β-cells were incubated in polystyrene nunclon delta 12-well plate for 5 days in RPMI-1640 medium ± 10 mM L-carnosine or RPMI-1640 medium ± 100 µM carnosine analogues or GLT medium (RPMI-1640 medium supplemented with 17 mM D-glucose, 200 µM oleic acid and 200 µM palmitic acid) ± 10 mM L-carnosine or GLT medium ± 100 µM carnosine analogues. After the incubation period, the medium was aspirated, and INS-1 cells were washed thrice with 0.5 mL Krebs-Ringer buffer solution. Subsequently, the cells were incubated for 3 hours with 1mL Krebs-Ringer buffer solution ± insulin secretagogue cocktail (10 mM glutamine, 1 mM tolbutamide, 1 µM phorbol 12-myristate 13-acetate, 10 mM leucine, 1 mM 3-isobutyl-1-methylxanthine, and 10 mM D-glucose). After 3

hours of incubation period, the supernatant was collected, and pipetted in a labelled 2 mL tube, then centrifuged at 1000 x g for 2 minutes to remove cell debris. The insulin concentration of each supernatant was analysed following the procedures set by Mercodia High Range Rat Insulin ELISA as follows: A 1:10 dilution of the supernatant: Krebs-Ringer buffer solution was made. 10 µL of the samples, control and calibrators was pipetted into the precoated wells respectively and into it, 50 µL of enzyme conjugate (dilution of 1:10 of enzyme conjugate:enzyme buffer) was pipetted. The plate was then covered with aluminium foil and was shaken at 900 rpm at room temperature for 2 hours. After the incubation period, the reaction mixture was discarded. The wells were then washed 5 times with 1X wash buffer and tapping it against a tissue between washings. Then, 200 µL TMB was pipetted into each well. The plate was covered with aluminium foil then incubated for 15 minutes at room temperature. After the incubation period, 50 µL of stop solution was pipetted into each well. The plate was shaken briefly for 5 seconds to ensure mixing and was read at 450 nm.

The total cellular protein content of each respective wells was determined and assayed with bicinchoninic acid protein assay, which was used to normalise the data of the insulin secretion assay experiment.

2.11.4 3-Nitrotyrosine assay

Reactive-nitrogen species (RNS) such as peroxynitrite ($ONOO^-$) reacts with tyrosine to form 3-nitrotyrosine. Peroxynitrite is a product by the reaction of nitric oxide (•NO) and superoxide (O_2^-•), and nitryl chloride (NO_2Cl) and •NO_2 (Tsikas and Duncan, 2014). Formation of 3-nitrotyrosine provides an evidence of production of RNS (Halliwell, 1997).

In this experiment, CD-1 mice were fed with high fat diet ± 100 µM carnosine analogues. After feeding, the plasma was extracted and the plasma samples were

prepared following the protocol in the ELISA kit (Fine test, Wuhan Fine Biotech Co., Ltd.) as follow: plasma was added with heparin as anticoagulant and the samples were centrifuge for 5 minutes at 200 x g at 4 ^{o}C. The supernatant was collected and assayed immediately. The total protein concentration of the supernatant was determined using BCA protein assay (PierceTM BCA Protein Assay Kit, ThermoFisher Scientific, UK).

To carry out the assay, the plate was washed twice with washing buffer before adding the 50 µL standard, sample and blank into each well. Into each well, 50 µL of biotin-labelled antibody were added and was gently tapped to ensure uniformity of the mixture before incubating for 45 minutes at 37 ^{o}C. After the incubation period, the solution mixture was aspirated, and the plate was washed with washing buffer thrice. A volume of 100 µL of SABC working solution was added into each well and incubate for 30 minutes at 37 ^{o}C. The solution mixture was aspirated, and the plate was washed for 5 times with washing buffer. Into the plate, 90 µL of TMB substrate solution were added and the plate was incubated for 20 minutes at 37 ^{o}C. After this, 50 µL of stop solution were added and the plate was immediately read at 450 nm.

2.11.5 4-Hydroxynonenal assay

In this experiment, CD-1 mice were fed with high fat diet ± 100 µM carnosine analogues. After feeding, the plasma was extracted and the plasma samples were prepared following the protocol in the ELISA kit (Fine test, Wuhan Fine Biotech Co., Ltd.) as follows: plasma was mixed with heparin as anticoagulant and the samples were centrifuge for 5 minutes at 200 x g at 4 ^{o}C. The supernatant was collected and assayed immediately. The total protein concentration of the supernatant was determined using BCA protein assay (PierceTM BCA Protein Assay Kit, ThermoFisher Scientific, UK).

To carry out the assay, the plate was washed twice with washing buffer before adding the 50 µL standard, sample and blank into each well. Into each well, 50 µL of biotin-labelled antibody were added and was gently tapped to ensure uniformity of the mixture before incubating for 45 minutes at 37 ^{o}C. After the incubation period, the solution mixture was aspirated, and the plate was washed with washing buffer thrice. A 100 µL volume of SABC working solution was added into each well and incubate for 30 minutes at 37 ^{o}C. The solution mixture was aspirated, and the plate was washed for 5 times with washing buffer. Into the plate, 90 µL of TMB substrate solution were added and the plate was incubated for 20 minutes at 37 ^{o}C. After this, 50 µL of stop solution were added and the plate was immediately read at 450 nm.

2.11.6 Seahorse mitochondrial function assay

The Agilent Seahorse XF Cell Mito Stress Test measures key parameters of mitochondrial function by directly measuring the oxygen consumption rate (OCR) of cells on the Seahorse XFe24 Extracellular Flux Analyzers (Agilent Technologies, Milton Keynes, UK). It is a plate-based live cell assay that allows the monitoring of OCR in real time. The assay uses the built-in injection ports on XF sensor cartridges to add modulators of respiration into each cell well during the assay to reveal the key parameters of mitochondrial function. The modulators included in this assay kit are oligomycin, carbonyl cyanide-4 (trifluoromethoxy) phenylhydrazone (FCCP), rotenone, and antimycin.

INS-1 rat pancreatic β-cells were plated at a density of 100,000 cells/well in polystyrene nunclon delta 6-well plate and initially treated for 3 days in complete RPMI-1640 medium ± 10 mM L-carnosine or GLT medium ± 10 mM L-carnosine, and incubated at 37 ^{o}C in 95% air/5% CO_2 atmosphere. On the third day, 5,000 cells of the treated INS-1 cells were seeded into the Seahorse XF24 cell culture microplate and further exposed to same treatment for 2 days.

C2C12 myoblasts were seeded at a density of 10,000 cells/well in growth medium [DMEM with 10% foetal bovine serum and 1% penstrep glutamine (100X, Cat. No. 10378016)] in Seahorse XF24 cell culture microplate and cultured at 37 ^{o}C in 95% air/5% CO_2 atmosphere. In the next day, cells were differentiated with DMEM supplemented with 5% horse serum instead of FBS. After two days, multinucleated myotubes were treated with control differentiation medium ± 10 mM L-carnosine or GLT medium ± 10 mM L-carnosine for 5 days with a medium change on the third day.

One day prior to the assay, the Seahorse XFe24 sensor cartridge was hydrated by pipetting 1 mL of Seahorse XF calibrant into each well. This was incubated at 37 ^{o}C in a humidified non-CO_2 incubator overnight. The Seahorse XFe24 Analyzer was warmed up at 37 ^{o}C overnight or for a minimum of 5 hours prior to use.

On the day of the assay, spent medium was aspirated, and C2C12 myotubes and INS-1 cells washed twice with 0.5 mL Seahorse XF DMEM and Seahorse XF RPMI-1640 media (both supplemented with 1 mM pyruvate, 2 mM L-glutamine, and 10 mM D-glucose), respectively, initially warmed at 37 °C prior to use. After washing, 0.5 mL assay medium was pipetted into the C2C12 myotubes and INS-1 cells, and the microplates were incubated in a non-CO_2 incubator for 45 minutes to 1 hour before the assay. Seahorse XF calibrant in the hydrated sensor cartridges was replaced with fresh 1 mL Seahorse XF Calibrant warmed at 37 °C. From the stock solution of 100 µM oligomycin, 100 µM carbonyl cyanide-4 (trifluoromethoxy) phenylhydrazone (FCCP), and 50 µM Rot/AA, a working solution of 1.5 µM oligomycin (first injected to inhibit ATP synthase and determines the ATP cellular production), 2.0 µM FCCP (second injected to collapse proton gradient and disrupts the mitochondrial membrane potential and used to measure spare respiratory capacity), and 0.5 µM Rot/AA (third and last injected to collapse mitochondrial

respiration to measure non-mitochondrial respiration driven by processes outside the mitochondria) (see **Table 2.4** for preparation) were loaded respectively into the injection ports (A, B, and C) (see **Figure 2.3**) of the sensor cartridge. Into the warmed Seahorse XFe24 Analyzer, loaded sensor cartridge was placed in the instrument tray for O_2 and pH calibration. When the calibration step was completed, the utility plate was replaced by the microplate containing C2C12 myotubes or INS-1 cells. Then following the protocol set in the Wave program, the mito stress test was conducted. When the assay ended, the data were given and expressed as mean ± S.E.M.

Table 2.4 Working compound preparation.

Compound	Final well, µM	Stock solution volume, µL	Medium volume, µL	Volume added to the port, µL
Oligomycin, Port A	1.5	450	2,550	56
FCCP, Port B	2.0	600	2,400	62
Rot/AA, Port C	0.5	300	2,700	69

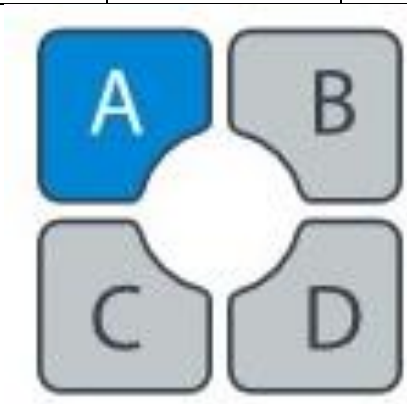

Figure 2.3 Location and labelling of sensor cartridge ports. Oligomycin was pippeted into port A, FCCP into port B and Rot/AA into port C.

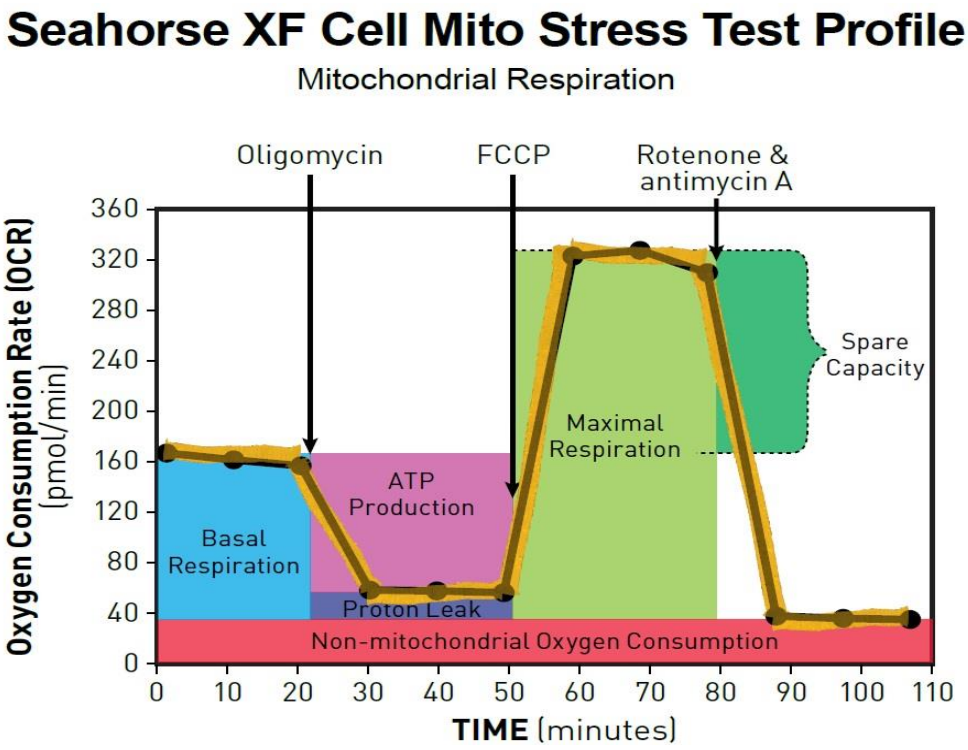

Figure 2.4 Seahorse XF cell mito stress key parameters and kinetic profile. Shows the injection sequence such that oligomycin is injected first followed by FCCP and lastly, Rot/AA.

The effects of the modulators on the electron transport chain is specifically depicted in **Figure 2.5**. Oligomycin is first injected into the assay, causing a reduction of the electron flow in the electron transport chain. Oligomycin inhibits ATP synthase at this stage (complex V). Carbonyl cyanide-4 (trifluoromethoxy)phenylhydrazone (FCCP) is the second modulator that is injected. It is an uncoupling agent causing a collapse of the proton gradient and disrupts the mitochondrial membrane potential. Thereby causing an uninhibited flow of electrons in the electron transport chain resulting in a maximum oxygen consumption rate at complex IV. Rotenone and antimycin A inhibits complex I and complex III, respectively. This inhibition causes shutting down of the mitochondrial respiration, and by doing so, nonmitochondrial respiration driven by the processes, i.e., glycolysis, outside of the mitochondria can be assessed.

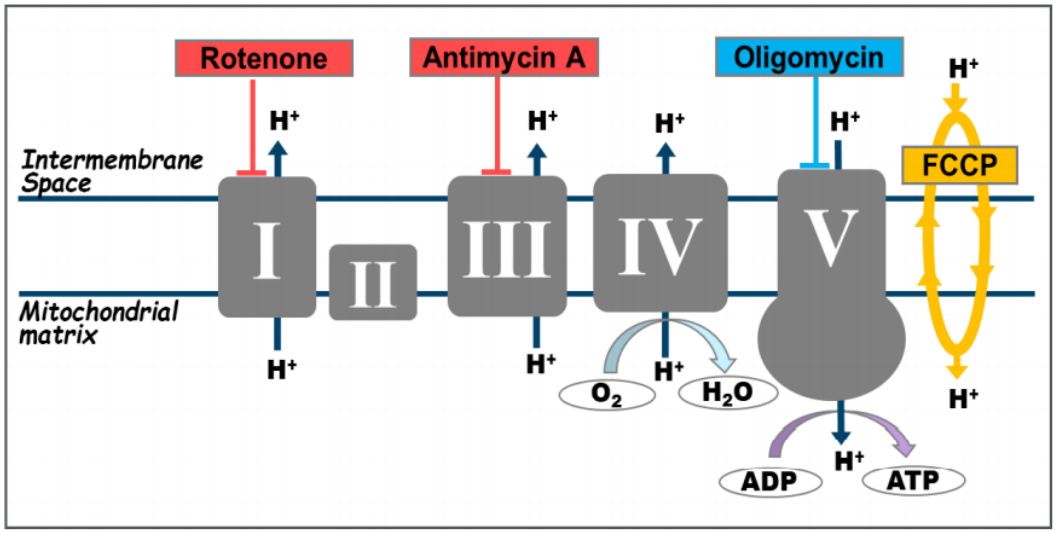

Figure 2.5 Seahorse XF cell mito stress modulators target of action in electron transport chain complexes. Oligomycin inhibits complex V, rotenone inhibits complex I, antimycin A inhibits complex III and FCCP shuttle protons across inner membrane.

Table 2.5 Summary of the effects of the modulators in mitochondrial respiration.

Modulators	Electron transport chain target	Effect of oxygen consumption rate
Oligomycin	ATP synthase (complex V)	Decrease
FCCP	Inner mitochondrial membrane	Increase
Rotenone/Antimycin A	Complex I and complex III, respectively	Decrease

Basal respiration-Oxygen consumption used to meet cellular ATP demand resulting from mitochondrial proton leak. Shows energetic demand of the cell under baseline conditions.

ATP production-The decrease in oxygen consumption rate upon injection of the ATP synthase inhibitor oligomycin represents the portion of basal respiration that

was being used to drive ATP production. Shows ATP produced by the mitochondria that contributes to meeting the energetic needs of the cell.

Proton leak-Remaining basal respiration not coupled to ATP production. Proton leak can be a sign of mitochondrial damage or can be used as a mechanism to regulate the mitochondrial ATP production.

Maximal respiration-The maximal oxygen consumption rate attained by adding the uncoupler FCCP. FCCP mimics a physiological “energy demand” by stimulating the respiratory chain to operate at maximum capacity, which causes rapid oxidation of substrates (sugars, fats, and amino acids) to meet this metabolic challenge. Shows the maximum rate of respiration that the cell can achieve.

Spare respiratory capacity-This measurement indicates the capability of the cell to respond to an energetic demand as well as how closely the cell is to respiring to its theoretical maximum. The cell's ability to respond to demand can be an indicator of cell fitness or flexibility.

Non-mitochondrial oxygen consumption-Oxygen consumption that persists due to a subset of cellular enzymes that continue to consume oxygen after the addition of rotenone and antimycin A. This is important to get an accurate measure of mitochondrial respiration.

Based on the Seahorse kinetic profile (see **Figure 2.4**), key parameters were calculated as follows.

Table 2.6 Seahorse XF cell mito stress key parameters and how it is calculated.

Parameter	Equation
Non-mitochondrial oxygen consumption	Minimum rate measurement after rotenone / antimycin A injection
Basal respiration	(Last rate measurement before first injection) – (Non-mitochondrial respiration rate)
Maximal respiration	(Maximum rate measurement after FCCP injection) – (Non-mitochondrial respiration rate)
H^+ (proton) leak	(Minimum rate measurement after oligomycin injection) – (Non-mitochondrial respiration rate)
ATP production	(Last measurement after before oligomycin injection) – (Minimum rate measurement after oligomycin injection)
Spare respiratory capacity	(Maximal respiration) – (Basal respiration)

2.12 Sodium dodecyl sulphate-polyacrylamide gel electrophoresis

Sodium dodecyl sulphate-polyacrylamide gel electrophoresis is widely used in biomedical research and other life sciences disciplines as a protein separation technique (Rath et al., 2009). To make sure proper protein separation, SDS is mixed with protein samples to denature the three-dimensional structure formed to interactions of noncovalent bonds. This SDS-protein interaction also allows the entity to acquire a net negative charge. Then protein in its primary structure will polymerise with acrylamide monomers. By applying an electric field, proteins will move into a single direction and the resolving gel leads to separation of proteins based on their molecular weight (Saraswathy and Ramalingam, 2011).

Various gel percentages were made during the entire duration of the study to separate the protein of interest from the total cellular proteins. To do this, a simple rule was followed to detect the protein of interest: for low molecular weight proteins, use high percentage of resolving gel and for high molecular weight proteins, use low percentage of resolving gel. Resolving and stacking gels were made according to the recipes supplied by Bio-Rad (www.bio-rad.com/webroot/web/pdf/lsr/literature/Bulletin_6040.pdf) as follows:

Table 2.7 Recipes for preparation of stacking and resolving gels.

Compounds	**Stacking gel**	**Resolving gel**		
	4%	**7.5%**	**10%**	**12%**
30% acrylamide/bis	1.98 mL	3.75 mL	5.0 mL	6.0 mL
0.5 M Tris-HCl, pH 6.8	3.78 mL	-	-	-
1.5 M Tris-HCl, pH 8.8	-	3.75 mL	3.75 mL	3.75 mL
10% SDS	150 µL	150 µL	150 µL	150 µL
Distilled water	9 mL	7.28 mL	6.02 mL	5.03 mL
TEMED	15 µL	7.5 µL	7.5 µL	7.5 µL
10% APS	75 µL	75 µL	75 µL	75 µL
Total volume	15 mL	15 mL	15 mL	15 mL

Prior to pouring the resolving gel, a glass cassette sandwich was assembled using 1.0 mm spacer, gel thickness. Resolving gel mixture was poured into the glass plate leaving 1 cm from the top of the plate and immediately 70% ethanol (CH_3CH_2OH) was spread on top of the resolving gel to make the gel linear. This set-up was left for around 30-45 minutes to let the polymerisation reaction occur and to make the gel solidify. After polymerisation, ethanol was removed and the top part of the gel was 4-5 times washed with distilled water to eliminate the alcohol residue. After this, stacking gel mixture was poured on top of the resolving gel and a ten teeth comb

with 50 µL volume capacity was quickly inserted in place. This was allowed to polymerise again for 30 minutes. After the top gel was polymerised, the comb was removed and the gel placed in an electrophoretic tank and 1X running buffer was pouredinto the tank. Prior to loading of protein samples into each well, 30 µg of protein was added with 4X Laemmli loading buffer (950 µL denaturing buffer with 50 µL β-mercaptoethanol) and heated at 95 ^{o}C for 5 minutes. Mercaptoethanol is added to reduce the disulfide linkages in solubilising proteins, and it also reduces excess oxidative polymerisation of catalysts. This denatured protein samples were then loaded, along with one lane of the reference protein ladder (Cat. No. ab116028, Abcam, Cambridge, UK). The gel was run initially at 60 V for 10-15 minutes to allow samples to stack before changing its voltage to 90 V for 120 minutes or continued until the dye reached near the bottom of the glass plate.

After running the proteins in the gel, the separated proteins were transferred to a 0.45 µm nitrocellulose membrane using the Bio-Rad Trans-Blot Turbo^{TM} machine using a semi-dry transfer pre-programmed protocol such as 10-, 7- and 5-minutes for high-, mixed- and low-molecular weight proteins, respectively. The gel was placed on top of the pre-soaked nitrocellulose membrane in transfer buffer (Bio-Rad, UK) then it was sandwiched with stacks of six pre-soaked filter papers in transfer buffer on top and bottom. Air bubbles was removed by rolling the sandwich with a gel roller. Nitrocellulose membrane was soaked with Ponceau S solution for a minute to check if proteins were successfully transferred onto the membrane (see **Figure 2.6**) The membrane was then washed initially with distilled water and subsequently with 1X Tris-buffered saline, containing 0.1% v/v Tween 20 (TBST) until proteins bands were not visible anymore.

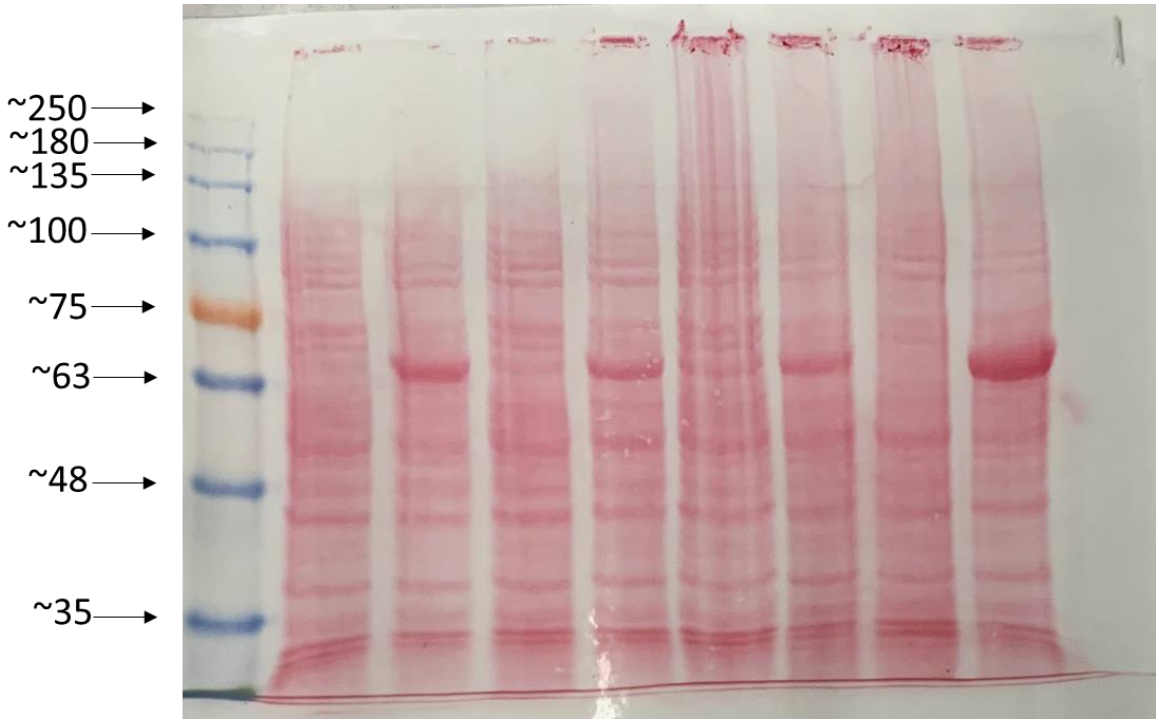

Figure 2.6 Nitrocellulose membrane with transferred proteins. Proteins were separated in 7.5% SDS-PAGE gel and transferred to 0.45 µm nitrocellulose membrane using Trans-blot Turbo™ in a setting of mixed molecular weights; 25 volts for 7 minutes.

2.12.1 Immunoblotting

Western blotting or immunoblotting involves electrophoretic separation of proteins by SDS-PAGE and transfer to nitrocellulose membrane or polyvinylidene difluoride (PVDF). This is followed by staining with Ponceau S solution to check if the proteins successfully bound onto the membrane. The membrane is then incubated in 5% skimmed milk to block the non-specific binding sites and then incubated in primary antibody of the target protein and then with secondary antibody with chemiluminescent detection. Immunoblotting techniques use antibodies to identify specific target proteins, distinguishing them from other unrelated proteins in the same sample.

With the proteins transferred into the nitrocellulose membrane, the membrane was blocked with 5% w/v milk powder in TBST for 1 hour and incubated with specific primary antibody (diluted in 5% w/v milk with TBST) overnight at 4 ^{o}C on a benchmark tube roller. After incubation, the nitrocellulose membrane was

washed with TBST thrice and incubated with appropriate blotting-grade horseradish peroxidase secondary antibody conjugate (anti-mouse, -goat or -rabbit IgG) (diluted in 5% m/v milk with TBST) for 1 hour at room temperature. The nitrocellulose membrane was washed thrice with TBST and the band signals were viewed using G:BOX Chemi XX6 and XX9 gel doc systems using enhanced chemiluminescence (ECL) (Cat. No. RPN2209, GE Healthcare, UK) as antibody binding detection system.

Table 2.8 Primary and secondary antibodies used in immunoblotting.

Type	Antibody	Source	Supplier
Primary	GAPDH	Rb	Bio-Rad Laboratories, Ltd., UK
	β-Actin	Mouse	Bio-Rad Laboratories, Ltd., UK
	iNOS	Mouse	Bio-Rad Laboratories, Ltd., UK
	HNF4α	Mouse	Santa Cruz Biotechnology, Inc., UK
	HNF1α	Mouse	Santa Cruz Biotechnology, Inc., UK
	MMP14	Mouse	Santa Cruz Biotechnology, Inc., UK
	ErbB4	Mouse	Santa Cruz Biotechnology, Inc., UK
	CD44	Mouse	Santa Cruz Biotechnology, Inc., UK
Secondary, HRP conjugate	Mouse IgG	Goat	Bio-Rad Laboratories, Ltd., UK
	Rabbit IgG	Goat	Bio-Rad Laboratories, Ltd., UK

Note: Manufacturer's recommended dilution was followed.

2.12.2 Signal band densitometry

After immunoblotting, the band signals of the protein of interest were quantified using ImageJ software which was downloaded at https://imagej.nih.gov/ij/. This free downloadable imaging software from the National Institute of Health has been used for scientific image analysis (Schneider et al., 2012). ImageJ was developed by Wayne S. Rasband in 1997 (Rueden et al., 2017) and since then has been useful to research particularly in life sciences (Arena et al., 2017). Western blot

housekeeping genes such as β-actin and GAPDH were used to normalise the band intensity obtained from the protein of interest.

2.13 Small interfering RNA transfection

To transiently knocked down cellular protein, small interference RNA (siRNA) technology from Dharmacon (Dharmacon, GE Healthcare, Colorado USA) were purchased and Lipofectamine RNAiMAX (ThermoFisher, Massachussetts, USA) was used as transfection reagent. Into a 6-well plate, 200,000 INS-1 cells were seeded and on the next day they were transfected for 24 hours prior to being exposed to growth medium and GLT. To prepare the siRNA-transfection reagent complex, 2 µL of siRNA (20 µM) were diluted in 48 µL of serum-free Optimem medium and mixed gently. In a separate Eppendorf tube, 3 µL of the transfection reagent were diluted with 47 µL of serum-free Optimem medium and mixed gently. The mixtures were incubated for 20 minutes before mixing them, and then incubated for 10 minutes at room temperature. The spent medium was discarded and replaced with 900 µL RPMI-1640 medium without antibiotic and 100 µL transfection solution was pipetted into each well. After 24 hours, the spent medium was removed and the cells were washed twice with DPBS before exposing to RPMI-1640 medium or GLT medium for 3 days. After the incubation period, INS-1 cells were lysed and analysed by qPCR to validate the knocked down.

2.14 Real-time reverse transcription polymerase chain reaction

For quantification of mRNA expression, the method of choice selected was real-time reverse transcription polymerase chain reaction (RT-qPCR) (Nolan et al., 2006), as it is accurate, sensitive and fast in measuring gene expression (Derveaux et al., 2010). In real-time PCR, the amount of DNA is measured after each cycle via

fluorescent dyes that yield increasing fluorescent signal in direct proportion to the number of PCR product molecules, amplicons, generated.

To perform RT-qPCR, there are three steps that need to be undertaken:

a. the reverse transcriptase dependent conversion of RNA into cDNA
b. the amplification of cDNA using PCR
c. the detection and quantification of amplification products in real time

2.14.1 Primer design

To undertake RT-qPCR, primer design is an essential parameter to which one needs to pay attention. To accomplish this, a combination of design tools available online were used, including National Center for Biotechnology Information (NCBI) and Integrated DNA Technologies. To design the primers for the gene of interest the NCBI gene search engine (https://www.ncbi.nlm.nih.gov/gene) was used to obtain the specific mRNA of the species of interest (rat, mouse, human and etc.). Then, the mRNA sequence was loaded into the Primer Quest Tool (https://eu.idtdna.com/site/account/login?returnurl=%2FPrimerquest%2FHome%2FIndex) and from this primers pairs were obtained. These primers were then processed using NCBI Primer-BLAST (https://www.ncbi.nlm.nih.gov/tools/primer-blast/) to check the specificity of the primers obtained from primer quest tool and also noting that these primers will not amplify any other unwanted transcripts. PCR primers with 17-25 nucleotides in length, G + C content between 40-55%, and a melting point temperature between 57-62 °C were chosen to obtain a 100-140 bp amplicon. The designed primers were then purchased from Sigma-Aldrich in desalted form with a concentration of 100 µM upon dissolution with water.

Table 2.9 Primers used in the entire study.

Species	Target gene	Sequence forward (5'-3')	Sequence reverse (5'-3')
Rat	ErbB4	AGTGGTCTGTCATTGCTTATCC	TGCTGTTGTCCGTGATGTAG
	Syntaxin 17	TGACCAGATCCACAACCATTG	AAGTCCGCTTCTAAGGTTTCC
	CD44	GCCTGGTACGGAGTCAAATAC	TCATCAATGCCTGATCCAGAAA
	MMP14	GGTGTGTGTCCAACCCTATTT	GGATGGAAGAGAAGCAGATGAC
	MMP15	CTAGACTGCCCATGTTCTCTTT	GACCTCTGGTACCCTAGTATGT
	MMP16	GGACCAACAGACCGAGATAAAG	ACCAATACAAGGAGGCCATAAG
	GAPDH	CATCTCCCTCACAATTCCATCC	GAGGGTGCAGCGAACTTTAT
Mouse	ErbB4	GTGAGCTTGGCTAGAGTGTTAG	GAAGGAAGACCACCAGAGAAAG
	Syntaxin 17	GGTGCAGAATTTGGGACAAG	CATTCGCTTCAAAAGGACCAG
	CD44	CAGTCACAGACCTACCCAATTC	GTGTGTTCTATACTCGCCCTTC
	MMP14	CAGGAGTGGGCACATCTTATT	CAATTCCTACCCTTGCCTTCT
	MMP15	CACCCACCTGGATTGGATTT	GAGGGAAGATTCTGGAGGTAAAG
	MMP16	GGACCAACAGACCGAGATAAAG	ACCAATACAAGGAGGCATAAGG
	HNF1α	ACACCCATGAAGACACAGAAG	TCTTAGTTGGCAGCTCATCG
	HNF4α	CCCTGGAGTTTGAAAATGTGC	AGGCTGTTGGATGAATTGAGG
	Rab1b	GAACCCCGAATATGACTACCTG	CGAATCTTGAAATCCACACCG

	Rab2a	ACAGACAAGAGGTTTCAGCC	GTGTGATAGAACGAAAGGACTCC
	Rab4b	CAGAAGTGGAAAGGAGCTGAG	TCACCAGGAATTTGAAGAGGAAG
	Rab10	AGGGAACAAGTGTGACATGG	TCAGCTAATGTGAGGAACGC
	CD40	CTGTGAGGATAAGAACTTGGAGG	AGAGAAACACCCCGAAAATGG
	GAPDH	CTTTGTCAAGCTCATTTCCTGG	TCTTGCTCAGTGTCCTTGC

2.14.2 Primer validation

Upon the arrival of the lyophilised primers from Sigma-Aldrich Taq-polymerase master mix (Qiagen, Hilden, Germany, Cat. No. 201203) was prepared containing both forward and reverse primers and the sample cDNA. This mix was put into the thermocycler (see **Tables 2.10** and **2.11** for reaction set up and amplification conditions, respectively) and PCR conducted to check for single product amplification. PCR products were then electrophoresed in a 2% agarose gel at 70 V for 30 minutes. The gel was then visualized using GeneSnap software (Syngene, Bangalore, India).

Table 2.10 Master mix in qPCR.

Components	**Volume**
Taq PCR Master Mix	10 µL
Forward primer, 10 µM	0.8 µL
Reverse primer, 10 µM	0.8 µL
cDNA sample, 25 ng	0.33 µL (25 ng)
RNAse and DNAse free water	8.07 µL
Total volume	20 µL

Table 2.11 PCR cycling conditions for reverse transcription.

Step	Temperature, ºC	Time, seconds	Cycles
Initial denaturation	94	180	1
Denaturation	94	45	35
Annealing	61.5	45	
Extension	72	30	
Final extension	72	600	1

2.14.3 RNA extraction

In this experiment, INS-1 rat pancreatic β-cells were incubated in polystyrene nunclon delta 6-well plate for 5 days in RPMI-1640 medium or GLT medium (complete RPMI-1640 medium supplemented with 17 mM D-glucose, 200 µM oleic acid and 200 µM palmitic acid). After the incubation period, the medium was aspirated, and INS-1 cells washed with DPBS and incubated using 0.5 mL of 0.05% Trypsin-EDTA (1X) for a minute then added with 1.0 mL of RPMI-1640 medium to inactivate the trypsin. The mixture was then transferred into a 2.0 mL DNAse/RNAse free polypropylene tube and centrifuged at 300 x g for 5 minutes. The supernatant was discarded, and the pellet was washed thrice with DPBS before resuspending with 1 mL of DPBS and centrifuged at 300 x g for 5 minutes. This was done to ensure that no growth medium was left in the tube, for if so it would inhibit lysis and cause dilution of the lysate - which could then affect the binding condition of RNA to the RNeasy membrane.

After centrifugation, the supernatant was discarded and protocols in RNeasy® Micro Kit (Qiagen, Hilden, Germany, Catalogue No.74004) followed to isolate total RNA from treated INS-1 cells (<500,000 cells). To the pelleted cells, 350 µL of RLT buffer (10 µL β-mercaptoethanol per 1 mL RLT buffer) were added then the mixture was vortex-mixed for a minute to ensure homogenisation and efficient lysis. To the homogenised lysate, 350 µL of 70% ethanol (CH_3CH_2OH) were added and pipetted back and forth to ensure homogenisation of the lysate and

this also promotes selective binding of RNA to the RNeasy membrane. The homogenised lysate was transferred into a RNeasy® Mini spin column placed inside a 2 mL collection tube and centrifuged for 15 seconds at 1600 x g. The flow through was discarded. The next step was to ensure there was no presence of genomic DNA contaminant from the RNA solution by adding 80 µL DNase solution (10 µL DNase I in 70 µL RDD buffer) (Qiagen, Hilden, Germany, Cat. No. 79254). This was added dropwise directly into RNeasy® Mini spin column membrane and incubated at room temperature for 15 minutes. After the incubation period, 700 µL of RW1 buffer were added into the RNeasy® Mini spin column membrane to wash the membrane-bound RNA. Then, RNeasy® Mini spin column was centrifuged at 1600 x g for 15 seconds and discarded the collection tube containing the flow through. The RNeasy® Mini spin column was put into in a new 2 mL collection tube and 500 µL RPE buffer (4 volumes of ethanol were added to the RPE buffer concentrate to obtain a working solution) were pipetted into the column membrane to remove traces of salts left in the column due to buffers used and was centrifuged at 8000 x g for 15 seconds and discarded the flow through. Another 500 µL RPE buffer were pipetted into the column membrane and this time it was centrifuged at 1600 x g for 2 minutes and discarded the collection tube with flow through. The RNeasy® Mini spin column was put into a new collection tube and centrifuged at 22,000 x g for a minute to ensure removal of RPE buffer or any residual flow-through in the membrane. The RNeasy® Mini spin column was put into a new 1.5 mL collection tube and 20 µL of DNAse/RNAse free water pipetted into the centre of the membrane and the RNeasy® Mini spin column centrifuged at 1600 x g for a minute to elute the RNA. The RNA sample then underwent quantification and quality assessment and stored at -80 ºC until used for analysis.

2.14.4 RNA quality assessment and quantification

RNA is a thermodynamically stable molecule and can easily be degraded due to poor handling or enzymatic degradation due to an abundance of RNase in the sample. RNA molecules transfer information encoded in the genome to generate various proteins. Hence, determining the quality of RNA sample is a crucial step prior to performing RT-qPCR, microarray analysis, next generation sequencing (NGS), and RNA blotting (Auer et al., 2003). RNA quality can be assessed by using a 2100 Bioanalyzer Instrument (Agilent Technologies, Inc, USA). RNA molecules are stained with intercalating dye, then electrophoretically separated using a microfabricated chips and detected using laser-induced fluorescence detection (Schroeder et al., 2006). The Bioanalyzer software then generates an electropherogram, gel-like image, from which the ratio of the 18S to 28S ribosomal subunits can be determined. These parameters are used in assessing RNA quality. Aside from these parameters, RNA concentration is also provided at a concentration of ng/µL.

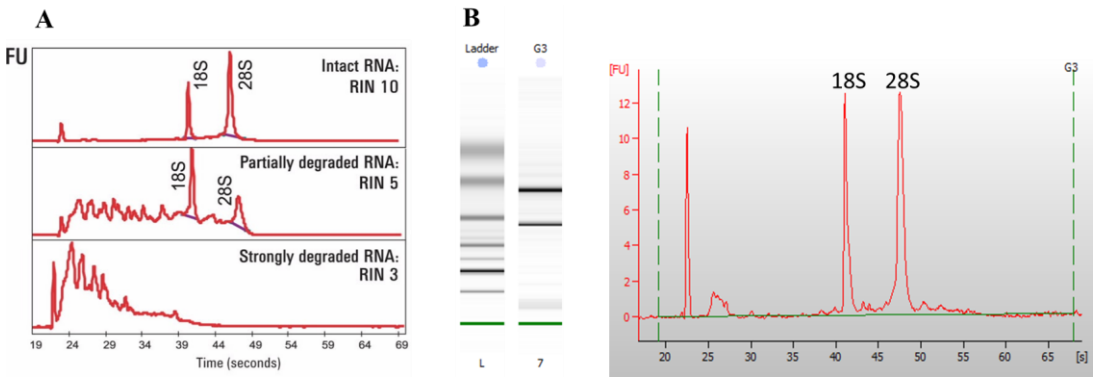

Figure 2.7 RNA integrity number. RIN scores provides integrity of RNA samples. A. RNA samples from fully intact RNA (RIN 10) to strongly degraded RNA (RIN 3) (Adapted from Agilent Technologies) B. Representative electropherogram of a good quality of RNA sample (RIN 9.9).

Agilent RNA 6000 Nano Kit (Agilent Technologies, Inc, USA) was used to analyse RNA samples. Microfluidic chips were preloaded with gel and fluorescent dye then

1 µL of RNA sample and reference ladder was pipetted into the wells. This chip was vortex-mixed for 10 minutes then loaded to the Agilent 2100 Bioanalyzer Instrument and run using Agilent Bioanalyser software. Traditionally, RIN score of 2.0 and higher is considered of high quality (Schroeder et al., 2006), however, in this experiment, RNA samples with RIN score of 8 and above were only considered for further analysis.

2.14.5 cDNA synthesis

The quantified and quality assessed total RNA sample was reverse transcribed to a single-stranded complementary DNA using High Capacity cDNA Reverse Transcription kit (Cat. No. 4368814, Thermo Fisher, MA, USA). 1.5 µg of total RNA were pipetted in each well of 200 µL PCR plate and added to and equal of a pre-mixed 2X reverse transcription master mix (see **Table 2.12** for the components) then pipetted down and up to mix, before sealing the plate. The PCR tube was briefly centrifuged to spin down all the components and to eliminate air bubbles. The PCR tube was then placed in a programmed PCR thermal cycler for single-stranded transcription (see **Table 2.13** for the cycling conditions).

Table 2.12 Reverse transcription cDNA master mix.

Components	**Volume**
Reverse transcription buffer	2 µL
dNTPs	0.8 µL
Random primers	2 µL
Reverse transcription reverse	1 µL
RNA sample	(1.0 µg)
RNAse and DNAse free water	Variable
Total volume	20 µL

Table 2.13 PCR cycling conditions for cDNA reverse transcription.

Step	Temperature, ºC	Time, minutes
Primer annealing	25	10
DNA polymerisation	37	120
Enzyme deactivation	85	5
Maintenance	4	15

2.14.6 QuantiNova SBYR green PCR

Real-time reverse transcription polymerase chain reaction is a good, useful and fast screening method in detecting gene expression in real-time. SYBR® Green I dye is a fluorescent DNA-binding dye that binds to the minor groove of any double-stranded DNA. Excitation of DNA-bound SYBR® Green dye produces a much stronger fluorescent signal compared to unbound dye. During the amplification step (40 cycles long), a fluorescent dye binds to the DNA molecules and fluorescence values are recorded for each cycle. The fluorescence signal is directly proportional to the DNA concentration over a broad range, and the point at which fluorescence is first detected as statistically significant above the background is called the cycle threshold or CT value. The higher the initial amount of sample DNA, the sooner the accumulated product is detected and therefore the lower the CT value. The QuantiNova SYBR Green PCR Kit has been developed for use in a two-step cycling protocol, with a denaturation step at 95 ºC, and a combined annealing/extension step at 60 ºC. This protocol will also work for primers with a Tm well below 60 ºC. Within 2 minutes of raising the temperature to 95 °C, QuantiNova Antibody and QuantiNova Guard are denatured and QuantiNova DNA Polymerase is activated, enabling PCR amplification.

In this experiment, INS-1 rat pancreatic β-cells were incubated for 72 hours in RPMI-1640 medium ± GLT. After incubation, INS-1 cells were lysed, and total RNA was extracted. RNA quality was assessed using Agilent RNA 6000 Nano Kit

(Agilent Technologies, Inc, California, USA) or it can be quickly assessed and quantified using NanoDrop™ One/One^{C} Microvolume UV-Vis Spectrophotometer (Thermo Fisher, Loughborough, UK). After RNA quality was evaluated, it underwent reverse-transcription to single-stranded cDNA using a cDNA synthesis kit (Cat. No. 4368814, ThermoFisher, MA, USA), then RT-qPCR performed using specific primers. On each batch of experiment, a negative internal control composed of master mix with no cDNA was included to examine any sign of contamination on the reagents used. A housekeeping gene, GAPDH, was used as reference gene in normalising gene expression of the gene of interest.

To perform the experiment, the protocol from QuantiNova SYBR® Green PCR kit (Qiagen, Hilden, Germany, Cat. No. 208054) was followed. A reaction mixture was prepared according to **Table 2.14** and was pipetted into each well of the 96-well PCR plate. This was then placed into the Applied Biosystems™ QuantStudio™ 7 Flex Real-Time PCR System (Applied Biosystems, UK) and run according to the cycling programme set in **Table 2.15**.

Table 2.14 Master mix in RT-qPCR.

Components	**Volume**
2X SYBR green mix	10 µL (1X)
Forward primer	1 µL (0.7 µM)
Reverse primer	1 µL (0.7 µM)
cDNA sample	0.33 µL (100ng)
QN ROX reference dye	2 µL (1X)
RNAse and DNAse free water	variable
Total volume	20 µL

Legend: *1:200 dilution for low-ROX dye cyclers (i.e., Applied Biosystems ViiA7 Real-Time PCR Systems).

Table 2.15 Cycling conditions for qPCR.

Temperature, ºC	Time	Step	Number of cycles
95	2 minutes	Initial activation	
95	5 seconds	Denaturation	40
60	19 seconds	Combined annealing/extension	
4	∞		

2.14.7 RT-qPCR data analysis

To analyse the generated data from the RT-qPCR, $\Delta\Delta C_t$ method was employed (Livak and Schmittgen, 2001; Rao et al., 2013). This comparative quantification technique compares the results of the experimental samples with a calibrator, *untreated sample* and a normaliser, housekeeping gene. With this $\Delta\Delta C_t$ method, the C_t values for the target gene in both the test sample and calibrator sample were adjusted in relation to a normaliser gene C_t from the same two samples. The resulting $\Delta\Delta C_t$ value was incorporated to determine the fold difference in expression.

The fold change relative to the calibrator sample was calculated as follows:

1. ΔC_t = C_t target gene – C_t reference gene (normalization to housekeeping gene, GAPDH, to minimize sample to sample variation).
2. $\Delta\Delta C_t$ = ΔC_t sample (treated) - ΔC_t calibrator (untreated).
3. Fold difference, 2-$\Delta\Delta C_t$ = gene fold change of treated sample relative to the calibrator sample.

2.15 RNA sequencing

2.15.1 DNase treatment

RNA samples were treated with DNA-free DNA removal kit (Life Technologies, Loughborough, UK) to remove any presence of contaminant genomic DNA. To do this, 0.1 volume of 10X DNAse buffer was pippeted into RNA samples and samples

incubated at 37 ^{0}C for 10 minutes with gentle agitation. After the incubation period, 0.1 volume of DNAse activation agent was pippeted in the sample and incubated at room temperature for 2 minutes with agitation. The mixture was centrifuged at 200 x g for 90 seconds and RNA samples transferred to Eppendorf tubes.

2.15.2 Library preparation

Known high quality RNA (RIN score >8) was sent to the Sarah Lamble laboratory in Oxford for subsequent library preparation and sequencing using Illumina mRNA seq sample preparation kit (Illumina, San Diego, USA). Initially, samples were ribo-depleted, removing the majority of rRNA and allowing increased sensitivity and analysis power of transcriptomes and less abundant sequences. The process of ribo-depletion was conducted using a rRNA depletion kit (Cat. No. K155003, ThermoFisher, Leicester, UK) where rRNA was captured by complimentary oligonucleotides that are coupled to paramagnetic beads, after which the bound rRNA was precipitated and removed from the reaction. Using magnetic beads is considered the most efficient way to get high quality RNA (Zhao et al., 2018).

The library was then generated with the fragmentation of small pieces of mRNA using cations under increased temperatures, before reverse transcription with random primers and resultant cDNA strand synthesis. Double strand cDNA was synthesised by removing the RNA template and synthesising a replacement cDNA strand. The fragments were then ‘end-repaired’ by blunting the overhanging sequence ends using T4 DNA polymerase and Klenow DNA polymerase (Scamrov and Beabealashvilli, 1988; Yang, Yanling and LiCata, 2018). The 3’ to 5’ exonuclease activity of the added enzymes removes the 3’ end overhand, whilst the polymerase activity fills in the 5’ overhang. The fragments were then prepared for ligation to adapters that have a T base overhang at their 3’ end by adenylation at the 3’ end (A base added to 3’ end) through the Klenow antibody polymerase activity.

Adapters were subsequently ligated to the DNA fragments. Fragments were size selected (~200bp) and purified on a gel for downstream enrichment before amplification via PCR with primers that target the adapters. The resultant library was validated, and quality control assured using Agilent Bioanalyser method described previously, before sequencing.

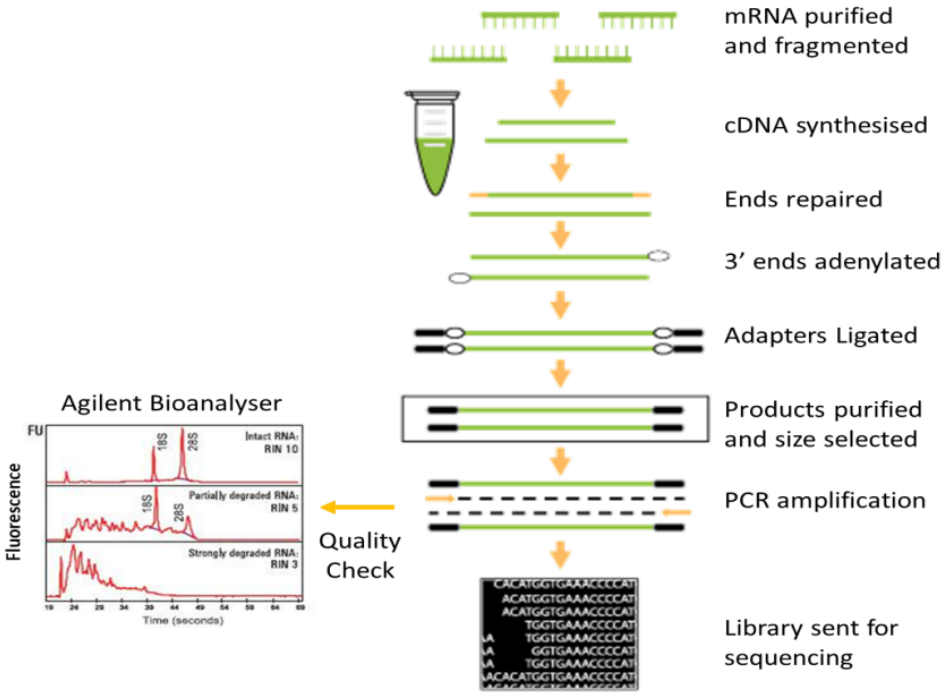

Figure 2.8 RNAseq library preparation. RNA is purified by removing rRNA and fragmented into small pieces. Double stranded cDNA is synthesised via reverse transcription before the ends are repaired and adenylated. Adapters are ligated, and samples are size selected and purified before quality check, amplification and resultant library sequencing. Figures adapted from EpiGentek and Agilent websites.

2.15.3 Sequencing

The aforementioned library was used to perform paired end sequencing over one lane of a flow cell on Illumina-HiSeq 2000 instrument in Oxford Genomics Centre, Oxford, United Kingdom. This technology depends on random fragmented genomic DNA attachment to an optically transparent planar surface. The attached DNA is extended and amplified to produce an ultra-high-density sequencing flow cell, containing hundreds of millions of DNA clusters, each consisting of roughly 1000

copies of each template. The templates were sequenced using a four-colour DNA sequencing by synthesis technology used reversible terminators with removable fluorescent dyes.

2.15.4 Data analysis

The raw RNAseq data was analysed by Dr. Rob Lowe at the Blizard Institute, Barts and The London School of Medicine and Dentistry. The output sequencing data (compressed FASTQ files) from the Illumina machine run were aligned to an annotated reference genome using Top Hat v 2.0.9: http://tophat.cbcb.umd.edu. Reads that were aligned to exons, genes and splice junctions were counted using a reference genome 'rn4' extracted from UCSC (http://genome.ucsc.edu/goldenPath/credits.html#rat_credits). Using the HTseq-count programme (http://wwwhuber.embl.de/users/anders/HTSeq/doc/count.html), data was visualised and interpreted, calculating gene and transcript expression, and then citing variations in expression between samples and conditions. Using the programme DEseq (http://www.bioconductor.org/packages/devel/bioc/html/DEseq.html) samples were normalised to correct in-sample distributional differences. Statistical significance of gene expression fold changes was then calculated by comparing read counts from experimental samples to that of corresponding control samples with p values adjusted using the Bonferroni formula. To conduct a Bonferroni correction, the critical p value is divided by the number of comparisons being made simultaneously on a single data set. To conduct a Bonferroni correction, divide the critical p value by the number of comparisons being made.

2.15.5 Network analysis

To identify enriched pathways and functions between differentiated expressed genes, data were analysed by Dr. Tania A. Jones (Blizard Institute, Barts and The

London School of Medicine and Dentistry, UK). Data was loaded into pathway analysis programmes: PANTHER (http://www.pantherdb.org/) and Metacore™, version 6.34 from Thomson Reuters (http://thomsonreuters.com/metacore/) which identify enriched networks, pathways, molecular functions, biological processes, cellular components, protein classes and diseases associated with the resultant list of differentially expressed genes. Enrichment is calculated with statistical values for genes within a specific pathway and considered significant if more genes of a given pathway are listed than would be expected by chance, based on the complete number of genes associated with that pathway. Bespoke enriched networks were created indicating directionality and expression change of genes within that pathway.

2.16 Screening of potential carnosinase inhibitors and carnosine mimetics

Carnosine has been found to be hydrolysed by the enzymatic action of carnosinase and to overcome this hydrolysis reaction, one of the proposed strategies is to design slowly-hydrolysable carnosine analogues. In collaboration with Dr. Christopher Garner and his team from NTU Department of Chemistry and Forensics, the MayBridge library (https://www.maybridge.com) containing over 53,000 diverse compounds was prepared in (https://www.eyesopen.com/omega) for virtual screening (https://www.eyesopen.com/rocs). ROCS was used in order to identify compounds with similar structure, shape and conformation to that of carnosine, and determine those compounds least likely to be effectively hydrolysable by carnosinase. From more than 53,000 screened compounds, and using Tanimoto scoring function, only the top 50 hits were selected to undergo further analysis by docking to the binding site of carnosinase. To do this, their ability to efficiently and effectively dock into the active site of the carnosinase was evaluated using the programme GOLD https://www.ccdc.cam.ac.uk/solutions/csddiscovery/components/gold/. Bestatin, a nonspecific competitve inhibitor of carnosinase, was used as an

internal control to identify any error in the method. From the results, 14 potential carnosinase inhibitors were purchased. These compounds were then dissolved in ethanol and diluted with sterile KREBS-Ringer buffer solution to a final concentration of 100 µM. In this thesis, only 5 (M4, M8, M14, M21, M28) were evaluated for actions on insulin secretion assay and radical species scavenging, as the other compounds were found to be toxic in C2C12 myotubes in experiments conducted by a colleague in the lab.

For carnosine mimetics, these are carnosine ester derivatives synthesised by Dr. Christopher Garner and his team. These compounds have a similar function and activity to that of carnosine, whilst being designed to be slowly-hydrolysable by carnosinase enzymes.

2.17 Statistical analyses

GraphPad Prism 8 (GraphPad Software) was used as a statistical software tool. T-test, One-way ANOVA and Tukey's test (*post-hoc test*) were conducted. Unpaired t-test was used when comparing means of two independent groups to determine the significant difference between groups. One-way analysis of variance (ANOVA) was conducted in comparing two or more groups defined by one factor. An ANOVA test can tell if the overall results are significant but would not tell exactly which of the groups are different. In order to do this, a *post-hoc* Tukey test based on the studentised range distribution, was implemented to determine which specific group means were different from each other. A p-value was calculated from a statistical test and p values less than 0.05 are considered as significant. Data were presented as mean ± S.E.M. Statistical significance was defined as *p<0.05, **p<0.01, ***p<0.001, ****p<0.0001**.**

Chapter 3

Hepatocyte Nuclear Factor 4α and Hepatocyte Nuclear Factor 1α

3.1 Introduction

Mutations in the human genes encoding hepatocyte nuclear factor 1alpha (HNF1α) and hepatocyte nuclear factor 4alpha (HNF4α) have the potential to cause pancreatic β-cell dysfunction, particularly impairing insulin secretion, and consequently cause diabetes mellitus and maturity onset diabetes of the young (MODY) (Boj et al., 2001; Hansen et al., 2002). MODY is often misdiagnosed as either type 1 diabetes or type 2 diabetes (Pihoker et al., 2013; Thanabalasingham et al., 2012; Thirumalai et al., 2013) as the diagnosis of diabetes relied on blood glucose level in a timed sample collection and also based on clinical criteria such as body mass index, and the age of the onset of diabetes (McDonald and Ellard, 2013). However, MODY does not fit with the classic clinical diagnosis of diabetes and now it is known that MODY result from autosomal dominant mutations in a single gene (Miedzybrodzka et al., 1999). Laboratory based assessment on the serum C-peptide, and islet autoantibodies can be a good way to know and differentiate MODY from type 1 and type 2 diabetes (Ellard et al., 2008; Owen et al., 2009). MODY accounts for 3.6% of diabetes cases in individuals diagnosed younger than 30 years in the United Kingdom (Shields et al., 2017) and 1-6% in all diabetic cases in Asia (Yang et al., 2020). Protein misfolding, defective transcriptional regulation, dysfunctional ion channels, impaired signal transduction and/or abnormal metabolic enzymes are the possible mechanisms implicated in the development of MODY (Nkonge et al., 2020).

Hepatocyte nuclear factor 4α (HNF4α) is a member of the nuclear receptor superfamily (Vető et al., 2017). HNF4 is an orphan member of the nuclear receptor superfamily with a zinc finger DNA binding domain and a putative ligand binding domain (Sladek et al., 1990). It functions as a transcription factor (Sladek et al., 1990) in kidney, intestine, liver and pancreatic islets (Ihara et al., 2005) and binding sites for HNF4 have been found in the regulatory regions of many genes (Nkonge

et al., 2020) including the gene for the transcription factor HNF1α (Sladek, 1994). It has a major role in hepatic development and is considered a master gene regulator (Odom et al., 2004) in differentiated hepatocytes (Vető et al., 2017). HNF4α also controls genes with important roles in amino acid metabolism, bile acid synthesis, and inflammation (Vető et al., 2017). However, genes of lipid and glucose metabolism transporters such as glucose transporter protein type 1, glucose transporter type 4 and fatty acid synthase (Kadota et al., 2016), and transcription factors are among the most important targets of the HNF4α protein (Stoffel and Duncan, 1997).

HNF4α has two promoter sites (P1 and P2) and nine splice variants. P2 promoter is located 46 kb upstream of P1 promoter and whilst P2 promoter is active in pancreatic β-cells and hepatocytes, P1 promoter is active in hepatocytes (Boj et al., 2001; Hansen et al., 2002; Thomas et al., 2001). HNF4α is considered as an important positive regulator of HNF1α (Guo and Lu, 2019; Santangelo et al., 2011) and its expression has shown to be dependent on HNF1α in mouse pancreatic islets and exocrine cells (Hansen et al., 2002). This interaction is through binding of HNF1α to P2 promoter site located 45.6 kb upstream from HNF4α P1 promoter site (Hansen et al., 2002). Like HNF4α, HNF1α is also expressed in liver, pancreas, kidney, and intestine (Cereghini, 1996; Jang, 2020; Ott et al., 1991). HNF1α is a dimeric homeodomain containing transcription factor (Ott et al., 1991) that was found to regulate the expression of insulin, glucose transporter 1, glucose transporter 2, and sodium-dependent glucose co-transporter 2 (Haliyur et al., 2019; Valkovicova et al., 2019).

Autosomal dominant mutations of human HNF1α gene (also known as MODY3) cause β-cell dysfunction due to progressive development of hyperglycaemia during childhood, and decreased insulin secretion (Yamagata et al., 1996). Patients with HNF1α-MODY3 are at high risks of developing diabetes

primarily due to reduced insulin secretion at a younger age before 25 (Valkovicova et al., 2019; Yamagata et al., 1996) . Given its role in MODY, I therefore decided to investigate potential links to T2D, and in particular β-cell dysfunction resulting from exposure of INS-1 rat pancreatic β-cells to glucolipotoxicity.

3.2 Results

3.2.1 Effects of GLT on HNF4α and HNF1α

Islets of patients with type 2 diabetes have been shown to have significantly downregulated HNF4α expression (Gunton et al., 2005). However, the mechanism by which this occurs remains poorly defined. To investigate this, INS-1 rat pancreatic β-cells were exposed to GLT medium for 3 days, RNA extracted and isolated, then comparative transcriptomic analysis performed using Affymetrix microarrays. Utilising MetaCore™ technology, a non-biased software analysis platform from Clarivate Analytics, HNF4α was shown to be the central regulator, depicted in **Figure 3.1**, of multiple protein trafficking genes, including Syntaxin 17 and several Ras-associated binding (Rab) proteins (Rab1b, Rab2a, Rab4b and Rab10) which are associated with secretory pathway protein trafficking.

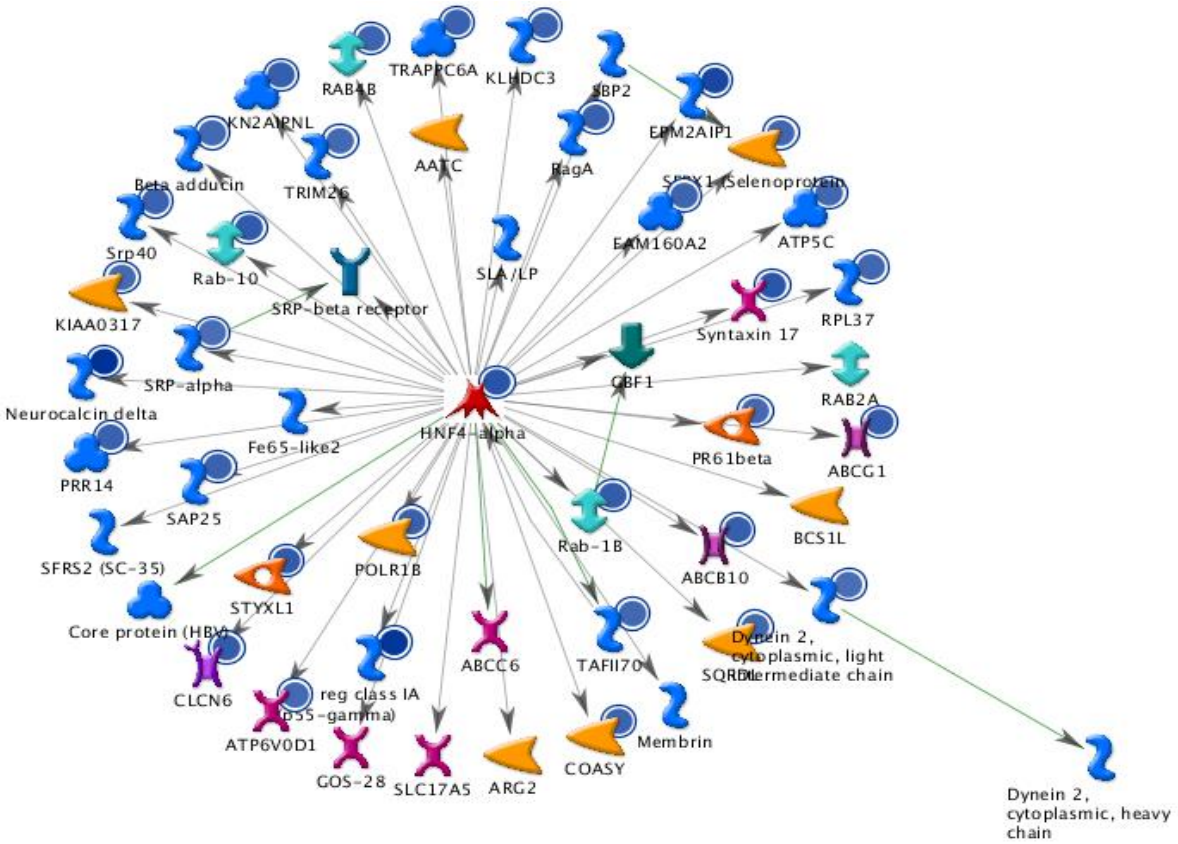

Figure 3.1 HNF4α Metacore™ pathway map. Non-biased interaction analysis identified genes affected by glucolipotoxicity (GLT). HNF4α is shown as the central hub and interacted with other genes. Blue circles indicate statistically significant downregulated gene expression and the arrows between hubs demonstrate the direction of association. Map generated by Dr. Tania A. Jones (Queen Mary, University of London).

As shown in the MetaCore™ map (**Figure 3.1**), HNF4α is the central regulator of multiple trafficking genes, including Syntaxin 17 and Rab proteins. As transformed β-cell lines are not always fully representative of primary β-cell biology however, it is important to determine whether these findings are indicative of whole animal physiology. With this and in collaboration with Dr. Paul W. Caton and Dr. Sophie Sayers from King's College London, pancreatic islet cells from CD-1 mice were isolated and cultured in RPMI-1640 medium or RPMI-1640 medium supplemented with 17 mM D-glucose, 200 μM oleic acid and 200 μM palmitic acid. Cells were lysed, then RNA was extracted and reverse transcribed, and RT-qPCR performed using primers specific for the target genes.

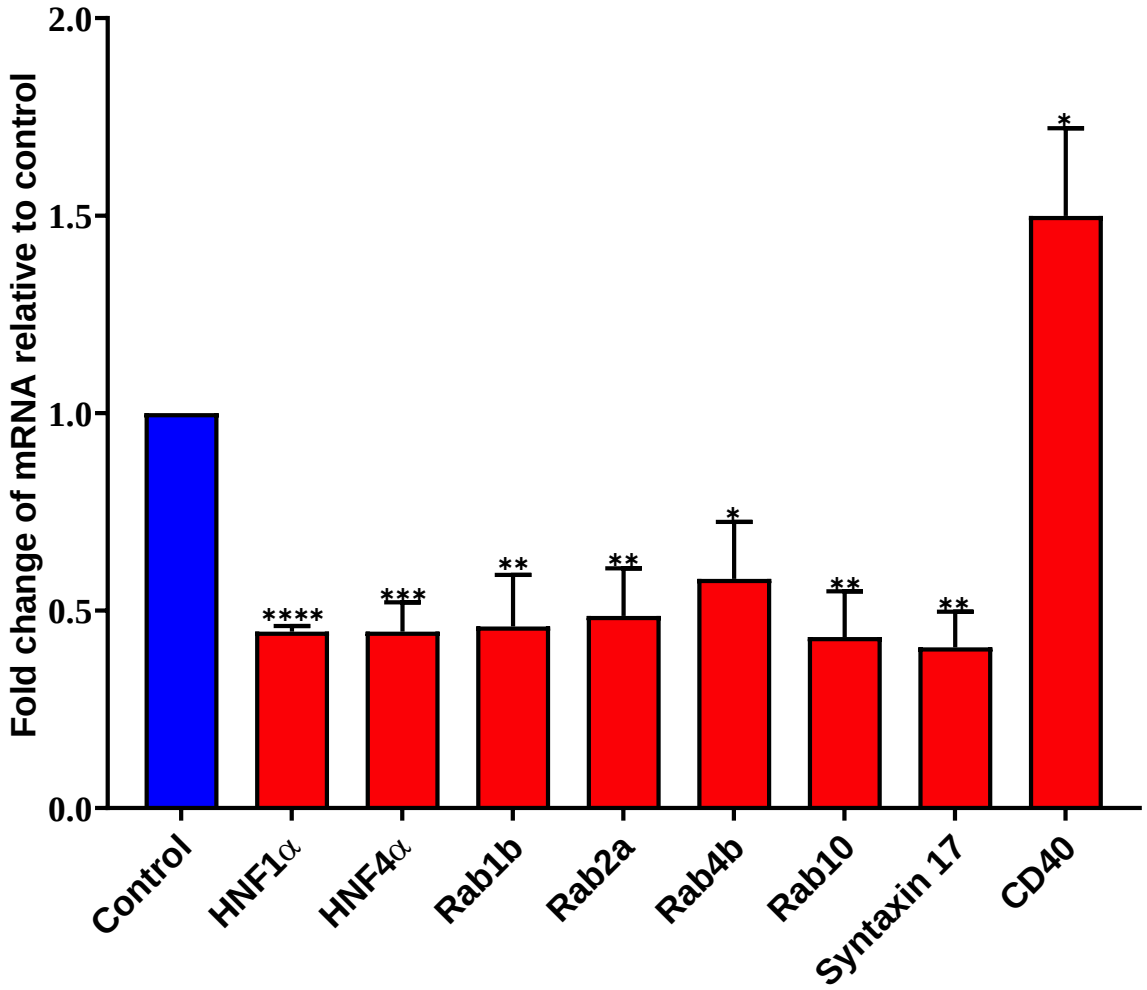

Figure 3.2 qPCR validation of HNF4α pathway genes. Pancreas was surgically removed from mice and islets isolated, then cultured for 72h in RPMI-1640 medium or RPMI-1640 medium supplemented with 17 mM D-glucose, 200 μM oleic acid and 200 μM palmitic acid. Cells were then lysed, RNA extracted and cDNA synthesised, and RT-qPCR performed using primers specific for the target genes. Data are presented as ΔΔCt values expressed as fold change relative to cells grown in control medium. Data shown is the mean ± S.E.M. of three independent experiments. *p<0.05, **p<0.01, ***p<0.001, ****p<0.0001

HNF4α mRNA expression level (shown in **Figure 3.2)** was significantly downregulated in mouse pancreatic islets following exposure to GLT medium, to 0.45 ± 0.01 (55.00% reduction, p=0.0009) relative to control. Similarly, HNF1α mRNA expression was also significantly downregulated to 0.45 ± 0.01 (55.00% reduction, p<0.0001) compared to control. It was also observed that mRNA expression of Rab genes was also significantly decreased, such that Rab1b, Rab2a,

Rab4b and Rab10 were downregulated to 0.46 ± 0.13 (54.00% reduction, p=0.0072), 0.49 ± 0.12 (51.00% reduction, p=0.0064), 0.58 ± 0.14 (42.00% reduction, p=0.0220), 0.43 ± 0.12 (57.00% reduction, p=0.0040) fold expression relative to control. Syntaxin 17 was also significantly downregulated to 0.41 ± 0.09 (p=0.0014) expression relative to control.

GLT has previously been shown to upregulate CD40 expression by the Turner Group (Bagnati et al., 2016). As such, this was therefore used as a positive control to verify that downregulation of other genes is not a non-specific artefact of GLT incubation. CD40 was confirmed to be significantly upregulated upon exposure to GLT to 1.50 ± 0.22 (p=0.0440).

As mRNA level does not always equate to protein expression level, I next incubated INS-1 cells for 5 days in RPMI-1640 medium or RPMI-1640 medium supplemented with 17 mM D-glucose, 200 μM oleic acid, and 200 μM palmitic acid. After the 5-day incubation period, INS-1 cells were lysed with RIPA buffer solution and total cellular protein was separated using 10% polyacrylamide gel in sodium dodecyl sulphate-polyacrylamide gel electrophoresis (SDS-PAGE). The separated proteins were then transferred onto a nitrocellulose membrane and blocked with 5% milk powder for an hour at room temperature. The membrane was then incubated overnight in a roller at 4 ^{o}C with anti-HNF4α primary antibody (1:1000 dilution). As shown in **Figure 3.3,** HNF4α protein expression level was significantly downregulated to 0.76 ± 0.08 (p=0.0475) upon exposure to GLT compared to control.

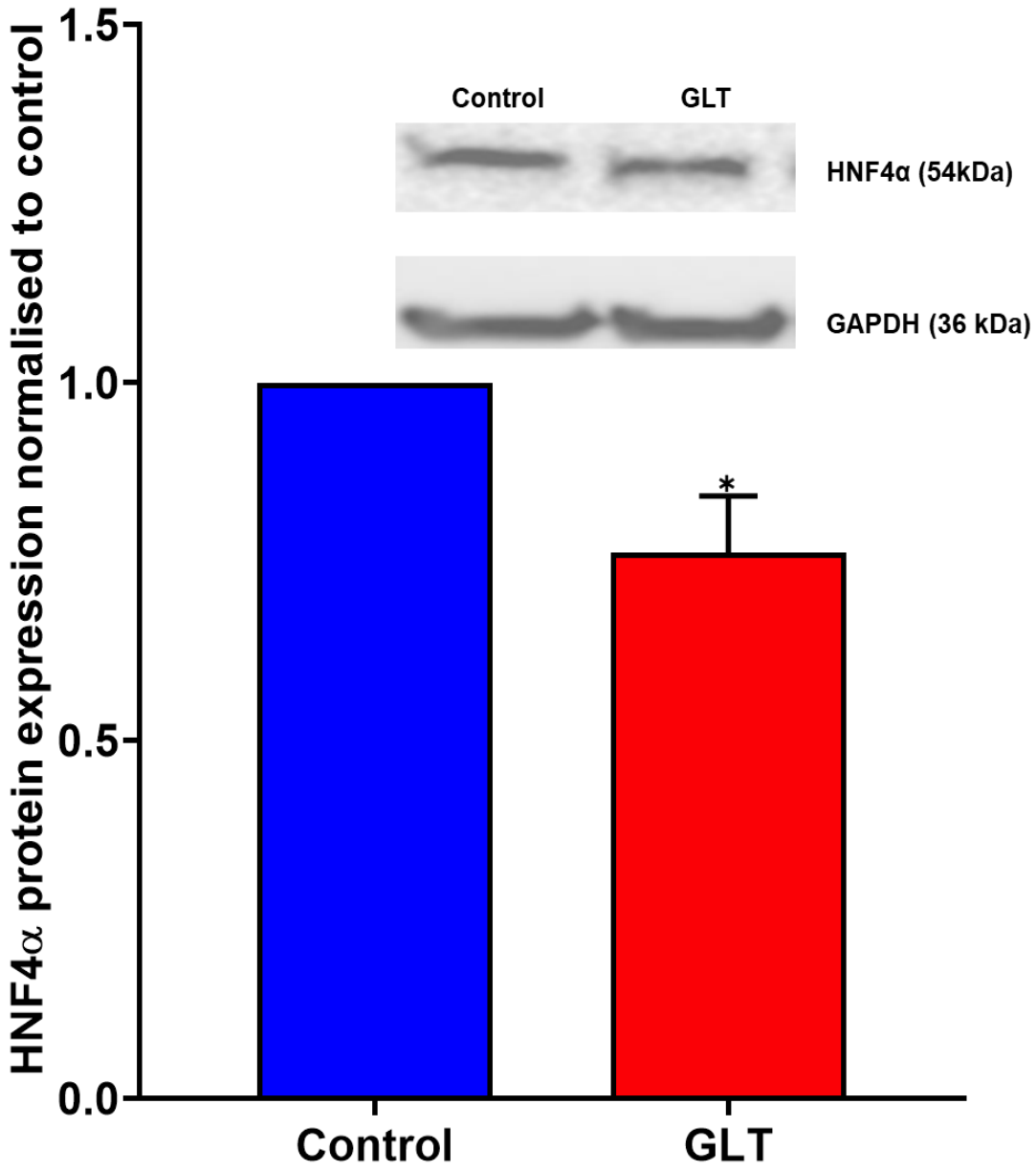

Figure 3.3 HNF4 protein expression level exposed in glucolipotoxicity. INS-1 rat pancreatic β-cells were cultured for 5 days in complete RPMI-1640 medium or RPMI-1640 medium supplemented with 17 mM D-glucose, and 200 µM oleic acid, 200 µM palmitic acid. After the incubation period, INS-1 cells were lysed with RIPA buffer and protein was separated using 10% polyacrylamide gel. The separated proteins were then transferred onto a nitrocellulose membrane and blocked with 5% milk powder for an hour. The membrane was then incubated overnight at 4 ^{o}C with HNF4α antibody (1:1000 dilution). Western blots are representative of 3 independent experiments and densitometric analysis was carried out using imageJ software. Bands were normalised using GAPDH as loading control. T-test was conducted for the analysis of the data. *$p<0.05$

The result of HNF1α mRNA expression was also validated with HNF1α protein expression level. To do this, INS-1 cells were incubated for 5 days in RPMI-1640 medium ± GLT. After the incubation period, INS-1 cells were lysed with RIPA buffer solution, total cellular protein was separated in a 10% polyacrylamide gel then transferred onto a nitrocellulose membrane and immunoblotted against HNF1α antibody (1:1000 dilution) for overnight at 4 ^{0}C.

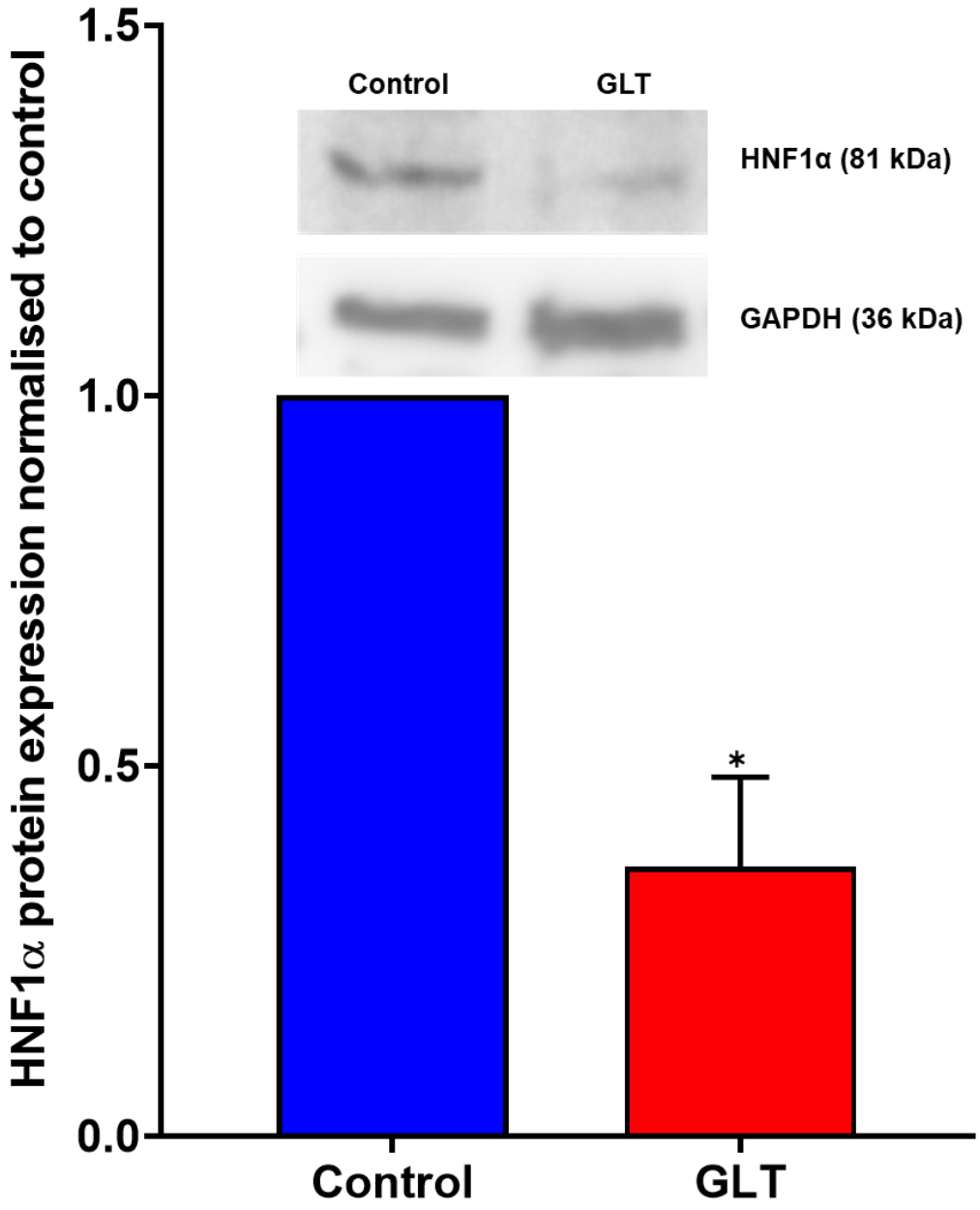

Figure 3.4 HNF1α protein level exposed in glucolipotoxicity. INS-1 rat pancreatic β-cells were cultured for 5 days in complete RPMI-1640 or RPMI-1640 supplemented in 17 mM D-glucose, 200 µM oleic acid, and 200 µM palmitic acid. After the incubation period, INS-1 cells were lysed with RIPA buffer solution and total cellular protein was separated using 10% polyacrylamide gel. The gel was then transferred onto a nitrocellulose membrane and blocked with 5% milk powder for an hour. The membrane was then incubated overnight at 4 ^{o}C with HNF4α antibody (1:1000 dilution). Western blots are representative of 3 independent experiments and densitometric analysis was carried out using imageJ software. Bands were normalised using GAPDH as loading control. T-test was conducted for the analysis of the data. *$p<0.05$.

The results shown above indicate that the protein expression level of HNF1α was significantly downregulated to 0.36 ± 0.12 (64% reduction, p=0.0342) expression relative to control following exposure to GLT medium.

To determine whether Rab protein dysregulation was driven by the reduced expression of HNF4α, HNF4α was knocked down by 24h siRNA incubation (Dharmacon, UK), and INS-1 cells subsequently exposed to glucolipotoxic medium for 3 days. RNA was then extracted and reverse transcribed, and RT-qPCR performed using Rab-specific primers.

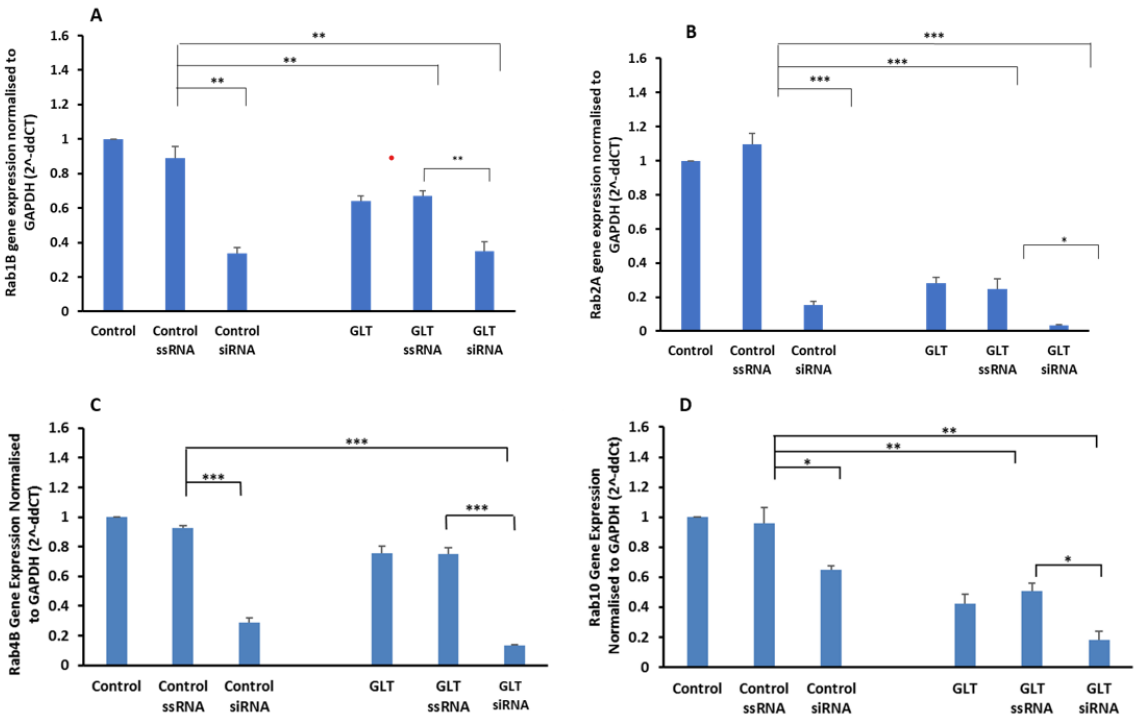

Figure 3.5 Effect of HNF4α knocked down on Rab gene expression. INS-1 rat pancreatic β-cells were transfected ± HNF4α ssRNA or siRNA for 24h, then incubated ± GLT for 72h. Cells were then lysed, RNA was extracted, reverse transcribed (cDNA synthesis) and RT-qPCR performed using primers specific for the target Rab genes. *p<0.05, **p<0.01, ***p<0.001. Dr. Katie Hanna performed this experiment.

Depicted in **Figure 3.5** is the effect of HNF4α knocked down on Rab gene expression. It was shown that HNF4α knocked down for siRNA has an efficiency of 35.38-84.8% relative to the untreated control. Results show that Rab1b was

significantly downregulated by 67.00% relative to control ssRNA (p=0.0087) and was significantly downregulated by 63.00% relative to the untreated control (p=0.0076). Furthermore, in GLT treated cells it was shown that Rab1b was significantly decreased by 47.77% relative to GLT ssRNA treated (p=0.0065) and was significantly downregulated by 45.32% relative to INS-1 cell under normal GLT condition (p=0.0053). Rab1b was also significantly decreased by 64.97% in GLT relative to control (p=0.0034).

Rab2a was significantly decreased by 86.16% in control relative to control ssRNA (p=0.0003) and was shown to be significantly decreased by 84.80% compared to control (p=0.000006). Rab2a was significantly decreased by 85.73% compared to GLT ssRNA (p=0.0264) and was shown to significantly decreased by 87.50% relative to normal GLT (p=0.0040). It was also observed that Rab2a gene expression was significantly decreased by 71.90% (p=0.00007) upon exposure to a GLT medium for 5 days.

Rab4b was significantly decreased by 68.89% in control relative to ssRNA control (p=0.00028) and was shown to significantly decreased by 71.18% compared to control (p=0.000068). Rab4b was significantly decreased by 88.55% compared to GLT ssRNA (p=0.000043) and was shown to significantly decreased by 88.63% relative to normal GLT (p=0.00012). It was also observed that Rab4b gene expression was decreased by 12.94% (p=0.0690) upon exposure to a GLT medium relative to control, albeit this was not statistically significant.

Rab10 was significantly decreased by 32.66% in control cells relative to control ssRNA (p=0.0490) and was shown to be significantly decreased by 73.58% compared to control (p=0.0410). Rab10 was significantly decreased by 64.39% compared to GLT ssRNA (p=0.0487) and was shown to significantly decreased by 64.39% relative to normal GLT (p=0.00012).

Rab proteins function as key regulators in membrane trafficking and are involved in transport, docking, fusion of lipid bilayer and the insulin secretory vesicle fusion process (Xiong et al., 2017). With this in mind, the impact of the dysregulation of HNF4α on insulin secretion was investigated. To do this, HNF4α was knocked down using siRNA (Dharmacon, UK) for 24h, and INS-1 cells subsequently exposed to glucolipotoxic medium for 3 days. After the incubation period, INS-1 cells were washed twice with Krebs-Ringer buffer solution (KRBS). The cells were then incubated with KRBS ± secretagogue cocktail (1 mM tolbutamide, 10 mM leucine, 10 mM glutamine, 1 mM 3-isobutyl-1-methylxanthine (IBMX), 1 µM phorbol 12-myristate 13-acetate (PMA) and 10 mM D-glucose). Insulin secretion was measured using Mercodia High Range Rat Insulin ELISA (Uppsala, Sweden).

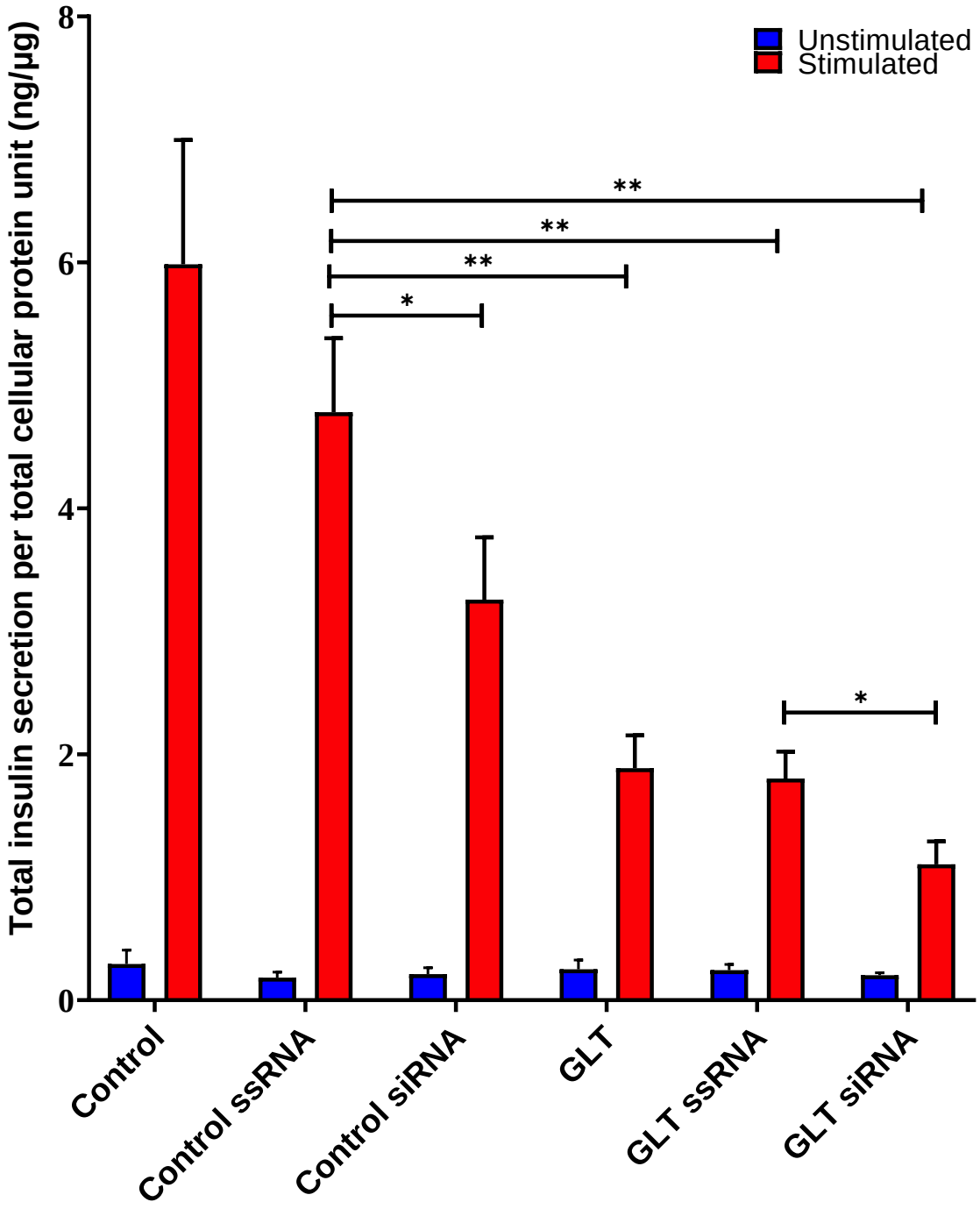

Figure 3.6 Effect of HNF4α knocked down on insulin secretion. INS-1 rat pancreatic β-cells were transiently transfected ± HNF4α ssRNA or siRNA for 24h. Cells were then incubated ± GLT for 72h, prior to secretagogue incubation for 1h [(unstimulated) blue, (stimulated) red]. Insulin secretion was determined using ELISA kit. The data shown are the mean ± S.E.M of three independent experiments. *p<0.05, **p<0.01. Dr. Katie Hanna performed the knocked down assay and Dr. Michael Cripps conducted the insulin secretion assay experiment.

Upon treatment of INS-1 cells with control siRNA, insulin secretion was shown to have a significant reduction to 3.19 ± 0.71 ng/µg (33.82% reduction) relative to control ssRNA (4.82 ± 0.85 ng/µg) (depicted in **Figure 3.6**). GLT ssRNA was significantly decreased to 1.58 ± 0.03 ng/µg (67.22% reduction, p=0.0035) relative to control ssRNA and it was significantly decreased further to 1.05 ± 0.25 ng/µg (78.22% reduction, p=0.0011) upon treatment with GLT siRNA relative to control ssRNA. Furthermore, GLT ssRNA was significantly decreased to 1.58 ± 0.03 ng/µg relative to GLT siRNA (1.05 ± 0.03 ng/µg, 33.54% reduction, p=0.0259).

In summary, HNF4α is the central regulator of multiple protein trafficking genes associated with the secretory pathway. In Metacore™ map, HNF4α expression was significantly downregulated upon exposure to GLT along with Syntaxin 17 and Rab proteins (Rab1b, Rab2a, Rab4b and Rab10). This observation was validated in RT-qPCR in CD-1 mice pancreatic islet cells and similar results were observed. Furthermore, immunoblotting showed that HNF4α and HNF1α protein expression level were both significantly downregulated. It was also shown that Rabs gene expression levels were significantly decreased, and insulin secretion was inhibited following HNF4α knocked down.

3.3 Discussion

In this study, the Metacore™ network analysis showed that HNF4α was significantly downregulated by GLT and this result was validated in western blotting which confirmed a downregulation of the protein expression using INS-1 cells exposed to GLT. This result suggests that HNF4α might be involved in maintaining normal glucose homeostasis. To further investigate this, HNF4α was transiently knocked down and an insulin secretion assay was conducted. It was determined that reduction (35.38-84.8%) of HNF4α resulted in the inhibition of the insulin secretion. This reduction of insulin secretion was further enhanced in the presence of GLT,

suggesting that GLT disrupted HNF4α expression during the onset of type 2 diabetes.

HNF1α regulates expression of pancreatic genes encoding insulin, GLUT2 (Pontoglio et al., 2000), L-pyruvate kinase, aldolase B, 3-hydroxy-3-methylglutaryl coenzyme A reductase and mitochondrial 2-oxoglutarate dehydrogenase E1 (OGDH) and the functions of the gene products are crucial for metabolism and secretion of insulin from pancreatic β-cells (Ryffel, 2001). These genes also contain HNF1 binding sites in their promoter or enhancer regions (Ryffel, 2001). Similarly, HNF4α was shown to regulate expression of insulin, GLUT2, L-pyruvate kinase, and aldolase B, genes that are involved in glucose transport and glycolysis (Wang et al., 2000). In addition, HNF4α also regulates expression of 2-oxoglutarate dehydrogenase (OGDH) E1 subunit and mitochondrial uncoupling protein-2 (UCP2) in pancreatic cells (Ryffel, 2001). OGDH constitutes the rate-limiting enzyme in the mitochondrial Krebs cycle, and UCP2 uncouples respiration from oxidative phosphorylation and inhibits the efficiency of ATP synthesis (Shih et al., 2001). UCP2 belongs to a family of mitochondrial transporter proteins that may uncouple the transport of protons across the inner mitochondrial membrane from the electron transport chain and the synthesis of ATP from ADP, hence generating heat rather than energy (Jia et al., 2009). In the presence of an active UCP2, the proton motive force used to primarily fuel the synthesis of ATP is dissipated as proton leak and this means that less energy can be used for ATP production (Nagy et al., 2004). This UCP2-induced decrease in the ATP:ADP ratio was shown to reduce glucose-stimulated insulin secretion (Brand and Esteves, 2005; Nagy et al., 2004). This suggests a possible reason for having a decreased insulin secretion when HNF4α was transiently knocked down and this reduction of HNF4α was determined using insulin secretion assay (see **Figure 3.6**).

It was reported that HNF4α acts upstream of HNF1α which shown to have a critical role in hepatocyte gene expression. In pancreas, HNF1α stimulates the activation of HNF4α gene transcription via P2 promoter site which in turn activates HNF1α transcription (Ellard et al., 2006). Hence, HNF4α is required for HNF1α expression in pancreatic β-cells (Li et al., 2000). The loss of HNF4α function in the liver has been found to dysregulate glucose homeostasis in HNF4α-MODY1 patients as they were observed to have a decrease in insulin secretion (Li et al., 2000) and dysregulated triglyceride metabolism (Lehto et al., 1999) as well. Therefore, the loss or reduction of HNF4α and HNF1α expression and function could lead to dysregulation of pancreatic β-cell function resulting in increased glucose.

Also shown in the Metacore^{TM} network was the association of HNF4α with the Rab proteins. It was illustrated that downregulation of HNF4α did affect the expression of Rab proteins. i.e., their expression was downregulated as well. To determine if HNF4α expression downregulation affected Rab proteins, HNF4α was transiently knocked down for 24 hours and exposed to GLT for 3 days. In the result, it was shown that reduction of HNF4α resulted in the downregulation of Rab proteins. This result suggests that HNF4α plays a crucial role in the expression of the Rab proteins.

Rab proteins are family of small guanosine triphosphatases (Du and Novick, 2001; Seto et al., 2014; Yap and Winckler, 2009) with molecular weight of 23-28 kDa (Goldenring et al., 2001). Rab proteins found to regulate protein transport along the endocytic, exocytic and recycling pathways in all cell types (McCaffrey and Lindsay, 2013; Yap and Winckler, 2009). Rab proteins are seen to be involved in vesicle docking as soluble *N*-ethylmaleimide sensitive fusion protein attachment receptors (SNARE) pairing regulators (Novick and Zerial, 1997) and have also been shown to play a role in membrane fusion at a target compartment, vesicle budding and formation of transport vesicles, and interactions with the cytoskeleton (Li and

Marlin, 2015; Yap and Winckler, 2009). Hence, Rab proteins have crucial roles as regulators in cell development and differentiation, and signal transduction.

In this study, Rab proteins (Rab1b, Rab2a, Rab4b and Rab10) were significantly downregulated after INS-1 cells were exposed to GLT medium. Also, when HNF4α was transiently knocked down, Rab1b, Rab2a, Rab4b and Rab10 were subsequently downregulated as well. This downregulation observed is the same as depicted in the Metacore™ pathway analysis. This result suggests that HNF4α regulates Rabs gene expression and consequently affects insulin secretion. Wu and his colleagues reported that Rab1a overexpression was critical to insulin secretion and insulin content by interacting with golgin-84. This interaction is crucial in maintaining the Golgi ribbon structure for the conversion of proinsulin to insulin (Liu et al., 2016).

It was reported that the Rab family is involved in the regulation insulin maturation in pancreatic β-cells (Dodson and Steiner, 1998). Studies reported the association of Rab family proteins with insulin containing secretory granules and involvement in the regulation of their exocytosis. For example, overexpression of Rab27a enhanced insulin secretion (Yi et al., 2002), Rab11 is implicated in insulin granule exocytosis (Sugawara et al., 2009), Rab37 decreased expression contributed to impaired exocytosis of insulin in β-cells illustrated in pre-diabetic and diabetic conditions (Ljubicic et al., 2013), and Rab3 was implicated in the exocytosis of insulin (Cazares et al., 2014).

Reports show that Rab proteins are localised and target distinct membrane compartment. Rab1 is a transport vesicle intermediate isolation membrane and autophagosome and Rab2 is associated as transport vesicle intermediate between compartments of endoplasmic reticulum and Golgi (Chavrier et al., 1990; Tisdale and Balch, 1996). It was also found that Rab4 is involved in recycling endosome, and Rab10 to GLUT4 storage vesicle (Li and Marlin, 2015). It was seen that Rab2a,

localise to the endoplasmic reticulum-Golgi intermediate compartment, regulates vesicular transport of proinsulin from the Large Ubiquitinated protein-associated ERGIC (endoplasmic reticulum-Golgi intermediate compartment) to Golgi and it is considered as essential for glucose stimulated insulin secretion (GSIS) under high glucose exposure (Sugawara et al., 2014). Inactivation of Rab2a under exposure to high sugar was implicated to high production of radical oxygen species in the endoplasmic reticulum. And it is known that glucose essentially induces proinsulin biosynthesis in the endoplasmic reticulum (Sugawara et al., 2014) in which in turn caused oxidative stress on pancreatic β-cells. It was also observed that loss of GSIS in insulinoma cells has reduced intracellular Ca^{2+} ion level, high production of reactive oxygen species, and lowered mitochondrial membrane potential (Hu et al., 2019).

Studies show that Rab proteins expression and activity varies for example Rab25 was observed to overexpress in ovarian cancer and breast cancer (Cheng et al., 2004) whilst it was seen to downregulate in colon cancer (Nam et al., 2010). It was shown also that Rab5 and Rab7 overexpression increased the production and accumulation of amyloid β-peptide in the brain and this event is considered as a hallmark of Alzheimer's disease (Ginsberg et al., 2010).

Glucose transporter 4 (GLUT4) is known to facilitate the transport of blood glucose into the muscle and adipose tissue (Huang and Czech, 2007). However, study revealed that GLUT4 is also present in mouse, rat, and human endocrine pancreas (Bähr et al., 2012). In pancreatic β-cells, high glucose level increased GLUT4 expression and this increased GLUT4 level is reduced by an increase of insulin expression (Bähr et al., 2012). It was reported that abnormal trafficking of GLUT4 was observed in individuals with type 2 diabetes (Corbeel and Freson, 2008) and insulin signal transduction activates Rab10 which consequently triggers the stimulation of the translocation of GLUT4 intracellular vesicles to the plasma

membrane and muscle cells for glucose uptake and metabolism. This suggests that dysregulation in membrane trafficking would lead to insulin resistance (Garvey et al., 1998). Rab10 is localised on transferrin receptor negative structures containing GLUT4 and inhibition of Rab10 expression could lead to dysregulation of GLUT4 translocation process whilst its activation could deliver GLUT4 to the cell periphery (Chen and Lippincott-Schwartz, 2013). Rab4 was also found to be involved in GLUT4 biosynthesis (Corbeel and Freson, 2008) and shown that Rab4a and Rab4b recycled GLUT4 through the endosomal system (Chen et al., 2012). Rab2A was shown to be present in GLUT4 vesicles and to be implicated in GLUT4 translocation (Mîinea et al., 2005).

SNARE proteins are crucially involved machinery of membrane fusion both in the secretory pathway and endocytic pathway (Yoon and Munson, 2018). SNARE mediated exocytic pathway was implicated in insulin signalling for glucose transporter trafficking (Yoon and Munson, 2018). It has been reported that stimulation of insulin release is controlled by the amount of SNARE proteins (Oh et al., 2014). It was reported in one study that islets of individuals with type 2 diabetes had a low expression level of Syntaxin 4, however, when it was replenished improvement of β-cell function through increased insulin secretion (Oh et al., 2014; Oh et al., 2018). This enrichment could be possibly achieved through gene therapy or transcriptional upregulation (Oh et al., 2014). In this study, Syntaxin 17, an autophagic SNARE protein (Arora et al., 2021; Itakura and Mizushima, 2013), had its gene expression significantly downregulated upon exposure to high sugar and high fat diet. This result suggests that syntaxin 17 was affected by GLT in INS-1 β-cells and possibly affects insulin secretion. Based on the literature available, this is the first observation of the association of HNF4α and syntaxin17, which were both shown to be downregulated. Hence, in future study, it would be of interest to check

the effect of HNF4α knocked down on syntaxin17 expression, and possibly to knocked down syntaxin17 and assess its effect on insulin secretion.

3.4 Conclusion

In conclusion, non-biased MetaCore™ network analysis identified HNF4α to be the central regulator of multiple genes involved in protein trafficking and HNF4α, HNF1α Syntaxin 17 and Rab genes (Rab1b, Rab2a, Rab4b and Rab10) mRNA expression were downregulated using primary islets exposed to high glucose and high fat diet. Rab proteins which were found to be downstream of HNF4α and involved in the secretion pathway were downregulated following HNF4α knocked down and suggest that HNF4α regulates Rab proteins involved in insulin gene expression. These results indicate that HNF4α has a key role in maintaining normal glucose homeostasis.

Chapter 4

Extracellular Matrix Proteins and Cytoskeletal Remodelling

4.1 Introduction

The extracellular matrix (ECM) is a non-cellular three-dimensional macromolecular network composed of collagens, proteoglycans/glycosaminoglycans, elastin, fibronectin, laminins, and several other glycoproteins (Theocharis et al., 2016). The ECM interacts with cells to regulate diverse functions such as proliferation, migration and differentiation (Bonnans et al., 2014) and is considered to be vital for maintaining normal homeostasis (Theocharis et al., 2016), and disease progression (Ford and Rajagopalan, 2018). The ECM has been shown to have roles in structural and biochemical support, and control of molecular signalling and tissue repair in various organs, including the pancreas (Llacua et al., 2018). Dysregulation of ECM composition, structure, stiffness and abundance can lead to fibrosis and invasive cancer (Bonnans et al., 2014). Further impairment in pancreatic function can be detected by alterations in pancreatic ECM proteins following the development of diabetes (Law et al., 2012). ECM acts through specific combinations of integrin α/β-heterodimers on islet cells and has been shown to affect β-cell survival, function and insulin production. Some ECM components induce release of growth factors to facilitate tissue repair (Llacua et al., 2018).

Matrix metalloproteinases (MMPs), known as matrixins (Visse and Nagase, 2003), are a family of calcium-dependent and zinc-containing endopeptidases that are categorised as collagenases (MMP1, MMP8, MMP13), gelatinases (MMP2, MMP9), stromelysin (MMP3, MMP10, MMP11), matrilysin (MMP7, MMP26), membrane-type MMPs (MT-MMPs) (MMP14, MMP15, MMP16, MMP17, MMP24, MMP25), and elastase (MMP12) (Nagase et al., 2006; Thrailkill et al., 2009). MMPs were discovered in 1962 during a study of collagen remodelling (Gross and Lapiere, 1962) and have been shown to be the main enzymes involved in ECM breakdown and turnover (Bonnans et al., 2014; Mittal et al., 2016). MMPs have common functional domains in their structure, including hemopexin-like domain, pro-peptide

domain, catalytic domain, and signal peptide domain (Bonnans et al., 2014; Tallant et al., 2010). Most MMPs are secreted as zymogens and activated in the extracellular space. MMP activation primarily occurs via proteolytic cleavage or oxidation of the thiol entity (Bonnans et al., 2014). Under normal conditions, MMP activities are regulated at the transcription level, activation of its zymogens, interaction with specific ECM components, and inhibition by endogenous inhibitors (Visse and Nagase, 2003). However, MMP activities have been shown to increase during repair or remodelling processes as well as in diseased or inflamed tissue. MMPs are produced either as soluble or cell membrane-anchored proteinases and cleave ECM components with wide substrate specificities (Bonnans et al., 2014).

Membrane-type matrix metalloproteinase (MT-MMPs) are composed of type I transmembrane proteins (MMP14, MMP15, MMP16, and MMP24) and glycosylphosphatidylinositol (GPI) anchored proteins (MMP17 and MMP25). MT-MMPs can degrade ECM molecules and are capable of activating proMMP2 apart from MMP17. MMP14 has been shown to hydrolyse collagens I, II, III and IV (Holmbeck et al., 1999). MMP14 is crucial in connective tissue metabolism primarily in the development and maintenance of the hard tissues of the skeleton (Holmbeck et al., 1999) and are also shown to have a vital role in the formation of new blood vessels (Pepper, 2001).

MMPs have been linked to inflammatory diseases (Butler and Overall, 2009; Dufour, 2015; Hu et al., 2007) and their proteolytic function extends not only to ECM components but also to cytokines, chemokines and cell surface receptors (Cauwe and Opdenakker, 2010; Dean et al., 2008; Dufour et al., 2018; Marchant et al., 2014; Starr et al., 2012).

It was reported that high blood sugar concentration can either directly or indirectly increase MMPs via oxidative stress or advanced glycation products (Chung et al., 2006) whilst low enzymatic activity of MMPs was presented in a study of diabetic

nephropathy (Han et al., 2006; Inada et al., 2005). In addition, diabetic foot ulcers have been identified to be caused by upregulated levels of MMPs, which could lead to excessive matrix breakdown and increased risk of nonhealing foot ulceration in diabetic patients (Wall et al., 2003).

CD44, a facultative proteoglycan (Yu et al., 2002), is a cell surface adhesion molecule involved in cell-cell and cell-matrix interactions (Naor et al., 1997), as well as in tumour migration, survival and invasion processes (Senbanjo and Chellaiah, 2017; Yu et al., 2002). CD44 is a receptor for hyaluronic acid, collagens, osteopontin, and MMPs, and has been identified as a marker for stem cells of several types (Senbanjo and Chellaiah, 2017).

When epidermal growth factor (EGF) interacts with the ErbB family of receptors, this binding influences a network of signalling pathways from cell division to death, and motility to adhesion (Sliwkowski and Yarden, 2001). Erb-b2 receptor tyrosine kinase 4 (ErbB4/HER4) is part of the tyrosine protein kinase family and belongs to the EGF receptor subfamily along with ErbB1/HER1), ErbB2/Neu/HER2, and ErbB3/HER3 (Olayioye et al., 2000; Roskoski, 2019; Wang, Zhixiang, 2017). EGF receptors are composed of a glycosylated extracellular domain, a single hydrophobic transmembrane segment, and an intracellular portion with a juxta membrane segment, a protein kinase domain, and a carboxyterminal tail (Roskoski, 2014). The ErbB proteins function as homo and heterodimers. Dimerisation promotes tyrosine kinase activity and initiates autophosphorylation of specific tyrosine residues within the cytoplasmic domain. The resulting phosphorylated residues are the docking sites for signalling molecules implicated in the regulation of intracellular signalling cascades. Eventually this can cause downstream effects on gene expression which can determine the biological response to receptor activation (Olayioye et al., 2000).

The role of MMPs in development of complications of type 2 diabetes (DM) is not fully understood and hence, this study aimed to assess whether glucolipotoxic (GLT) exposure of INS-1 pancreatic β-cells influences gene dysregulation in extracellular matrix proteins, and cytoskeletal remodelling specifically on MMP-14, MMP-15, MMP16, CD44 and ErbB4.

4.2 Results

From Turner research group microarray data, and subsequent confirmation analysis using Illumina-HiSeq gene expression data, transcripts showing significant changes in INS-1 rat pancreatic β-cells exposed to GLT were examined. **Table 4.1** shows the rank of the pathway maps with number of genes significantly dysregulated by exposure to high glucose and high fat diet. It was shown in the table that cell adhesion-ECM remodelling ($p=2.365 \times 10^{-9}$), cell adhesion-cell matrix glycoconjugates ($p=2.815 \times 10^{-9}$) and cell adhesion-integrin inside-out signalling in neutrophils ($p=7.989 \times 10^{-6}$), ranked as 2nd, 3rd and 8th, respectively, are major pathways which were significantly dysregulated on gene expression by exposing INS-1 cells to GLT treatment for 3 days.

Table 4.1 Pathway map enrichment analysis report of RNAseq data.

Number	Maps	Total gene number	p Value	Minimum false detection limit
1	Immune response T cell co-signalling receptors, schema	55	9.980×10^{-12}	8.184×10^{9}
2	Cell adhesion_ECM remodeling	53	2.365×10^{-9}	7.695×10^{7}
3	Cell adhesion_Cell-matrix glycoconjugates	38	2.815×10^{-9}	7.695×10^{7}
4	Protein folding and maturation_Bradykinin / Kallidin maturation	32	1.478×10^{-7}	3.030×10^{5}
5	Rheumatoid arthritis (general schema)	50	1.620×10^{-6}	2.657×10^{4}
6	Blood coagulation_Blood coagulation	39	2.137×10^{-6}	2.920×10^{4}
7	Role of cell adhesion in vaso-occlusion in Sickle cell disease	43	7.313×10^{-6}	8.188×10^{4}
8	Cell adhesion_Integrin inside-out signalling in neutrophils	77	7.989×10^{-6}	8.188×10^{4}
9	Development_Neural stem cell lineage commitment (schema)	38	9.976×10^{-6}	9.089×10^{4}
10	Development_BMP7 in brown adipocyte differentiation	39	7.563×10^{-5}	6.202×10^{3}

From the data depicted in **Table 4.1**, MetaCore^{TM}, a non-biased integrated knowledge database, was used to provide interaction data for the dysregulated genes. Matrix metalloproteins (MMPs) [MMP14, MMP15 and MMP16], CD44 (cell surface glycoprotein), and ErbB4 (receptor tyrosine-protein kinase) were shown to be significantly downregulated following INS-1 rat pancreatic β-cells exposure to GLT conditions for 3 days. These proteins are also amenable to study at the protein level, as they are in the β-cell membrane surface.

(**A**)

(**B**)

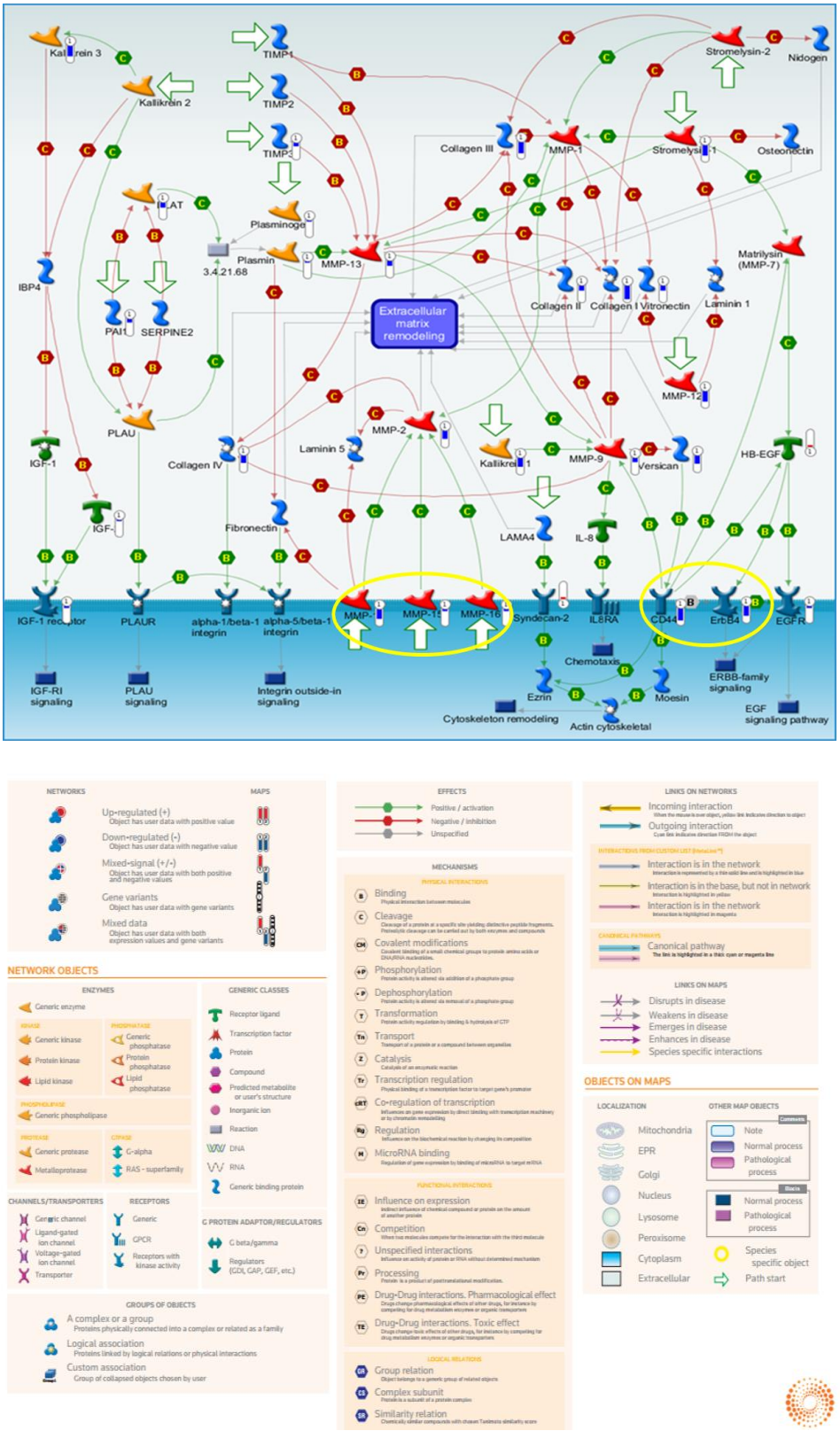

Figure 4.1 Extracellular matrix remodelling/actin cytoskeleton MetaCore™ map. (A) Thermometer icons next to individual genes indicate the significant extent of fold change. Blue bars represent downregulation by glucolipotoxicity and red bars represent upregulation by glucolipotoxicity in INS-1 rat pancreatic β-cells cultured in RPMI-1640 medium or GLT medium for 72 hours. (B) Legend used in the illustration in (A). The map was generated as part of a collaboration with Dr. Tania A. Jones (Queen Mary, University of London, UK).

Depicted in **Figure 4.1**, MetaCore™ network map generation shows that matrix metalloproteins (MMP14, MMP15 and MMP16), CD44 and ErbB4 were downregulated (encircled in yellow in **Figure 4.1**) affecting the extracellular matrix remodelling, actin cytoskeleton and ErbB signalling pathways. It can also be seen that metalloproteinase inhibitor 3 (TIMP3), collagen I, collagen II, collagen III and collagen IV were downregulated upon exposure to high sugar and high fat diet. However, dysregulation of collagen family and TIMP family will not be included in the study.

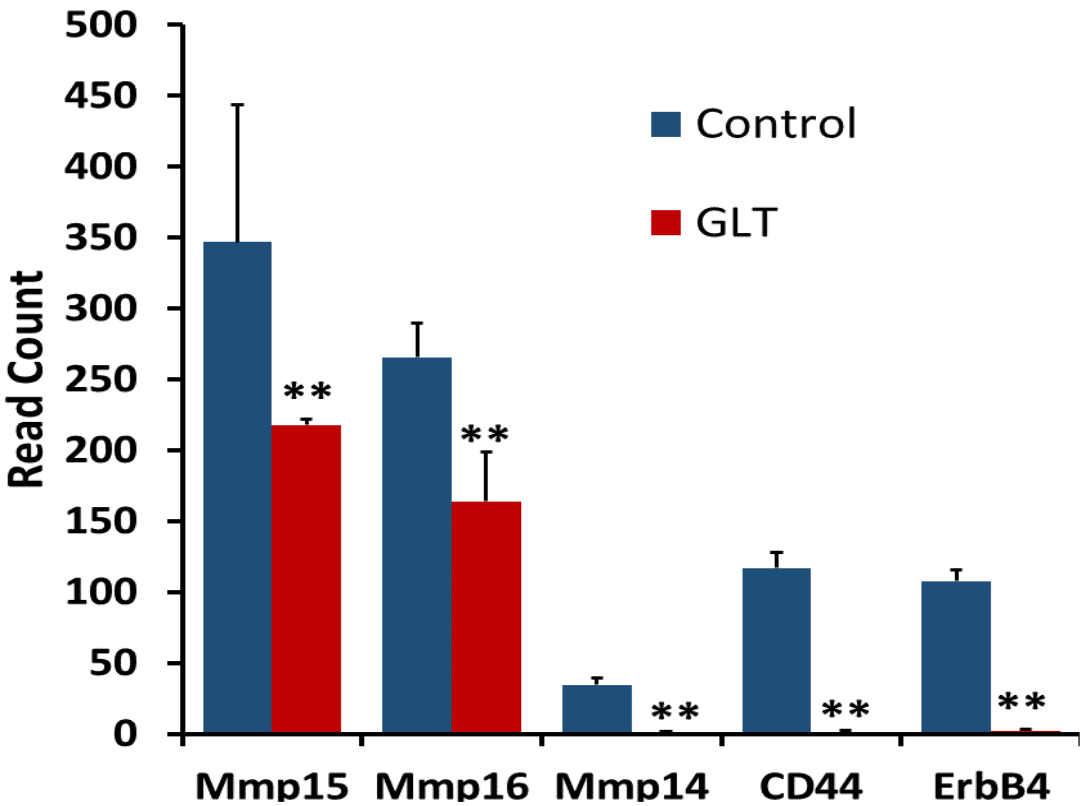

Figure 4.2 Illumina HiSeq RNA expression data for ECM membrane proteins dysregulated by GLT. INS-1 cells were cultured for 72h in RPMI-1640 medium or GLT medium. RNA was extracted, and quality was assessed before Illumina HiSeq sequencing, and analysis was undertaken. Data are expressed as mean RNA read counts ± S.E.M. per condition of MMP15, MMP16, MMP14, CD44 and ErbB4, from 3 independent RNAseq analyses per condition. **p<0.01.

As shown in **Figure 4.2**, exposure of INS-1 cells for 3 days to GLT significantly downregulated the RNA read counts by 98.1 ± 1.9% ($p=9.55 \times 10^{-9}$) in MMP14, 37.2 ± 1.3% (p=0.001) in MMP15, 38.3 ± 13.2% ($p=4.67 \times 10^{-6}$) in MMP16, 99.1 ± 0.9% ($p=7.89 \times 10^{-13}$) in CD44, and 98.1 ± 0.9% ($p=8.68 \times 10^{-10}$) in ErbB4 relative to control. These results were similar to what is shown in the Metacore™ map.

In order to validate what was observed in the RNAseq data analysis shown in **Figure 4.2**, INS-1 cells were exposed for 3 days in RPMI-1640 medium or GLT medium (RPMI-1640 medium supplemented with 17 mM D-glucose, 200 µM oleic acid and 200 µM palmitic acid). After the incubation period, RNA was extracted then underwent cDNA synthesis, RT-qPCR run and analysis (**Figure 4.3**).

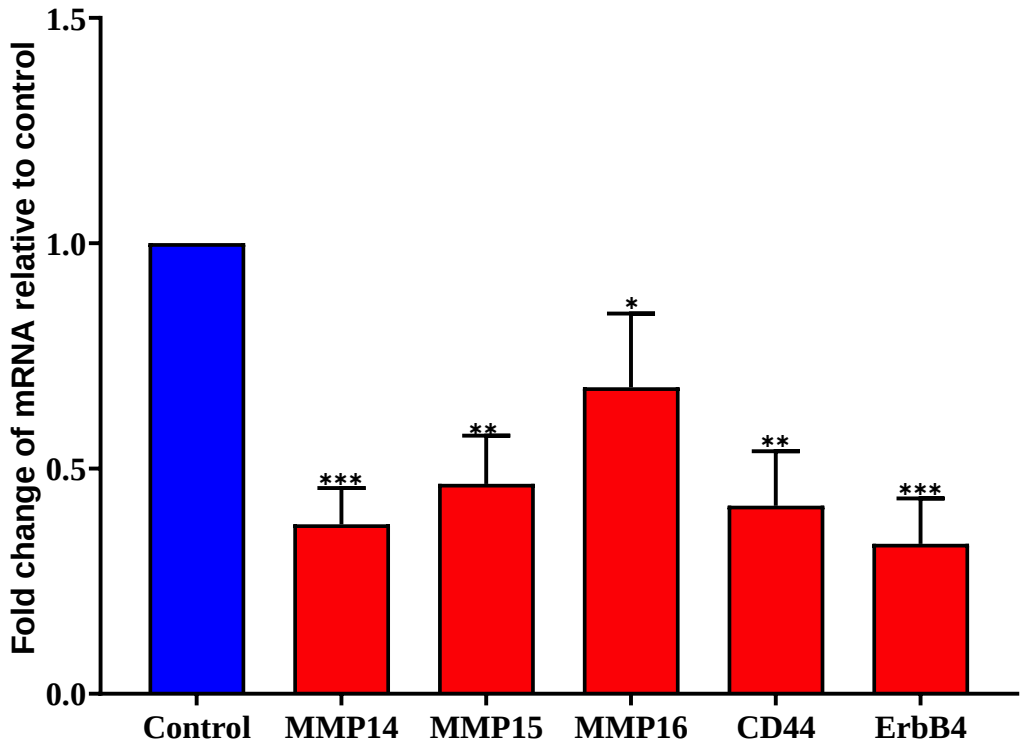

Figure 4.3 qPCR expression of the extracellular matrix mRNAs using INS-1 cells. INS-1 rat cells were incubated for 72 hours in RPMI-1640 or RPMI-1640 supplemented with 17 mM D-glucose, 200 µM oleic acid and 200 µM palmitic acid. Cells were then trypsinised, lysed, RNA extracted, then subjected to cDNA synthesis via reverse transcription and RT-qPCR performed using primers specific for the target genes. Data represent changes in mRNA expression compared to control using ΔΔCt values expressed as a fold change compared to cells grown in RPMI-1640. Control in blue and GLT in red. Data shown are from three independent experiments. *p<0.05, **p<0.01, ***p<0.001.

Extracellular matrix remodelling/actin cytoskeleton pathway analysis of transcriptomic data showed that matrix metalloproteins (MMP14, MMP15 and MMP16), CD44 and ErbB4 were downregulated, and qPCR validation data confirmed that these genes were significantly downregulated following exposure of INS-1 cells to glucolipotoxicity for 3 days. MMP14, MMP15, MMP16, CD44 and ErbB4 were observed to decrease significantly to 0.38 ± 0.08 (p=0.0001), 0.47 ± 0.12 (p=0.0016), 0.68 ± 0.16 (p=0.0333), 0.42 ± 0.12 (0.0015), and 0.33 ± 0.10 (p=0.0003) in fold change relative to control.

The qPCR data generated here were further validated, and in collaboration with Dr. Paul W. Caton and Dr. Sophie Sayers from King's College London, pancreatic islet cells from CD-1 mice were exposed to similar experimental conditions for 3 days, after which RNA was extracted and sent to NTU for further analysis. The integrity of RNA samples was assessed prior to analysis, with a RIN score of 8 or more required for further analysis. RNA samples were then reverse transcribed (cDNA synthesis) and subjected to RT-qPCR using specific primers (see **Table 2.9** for the list of primers used).

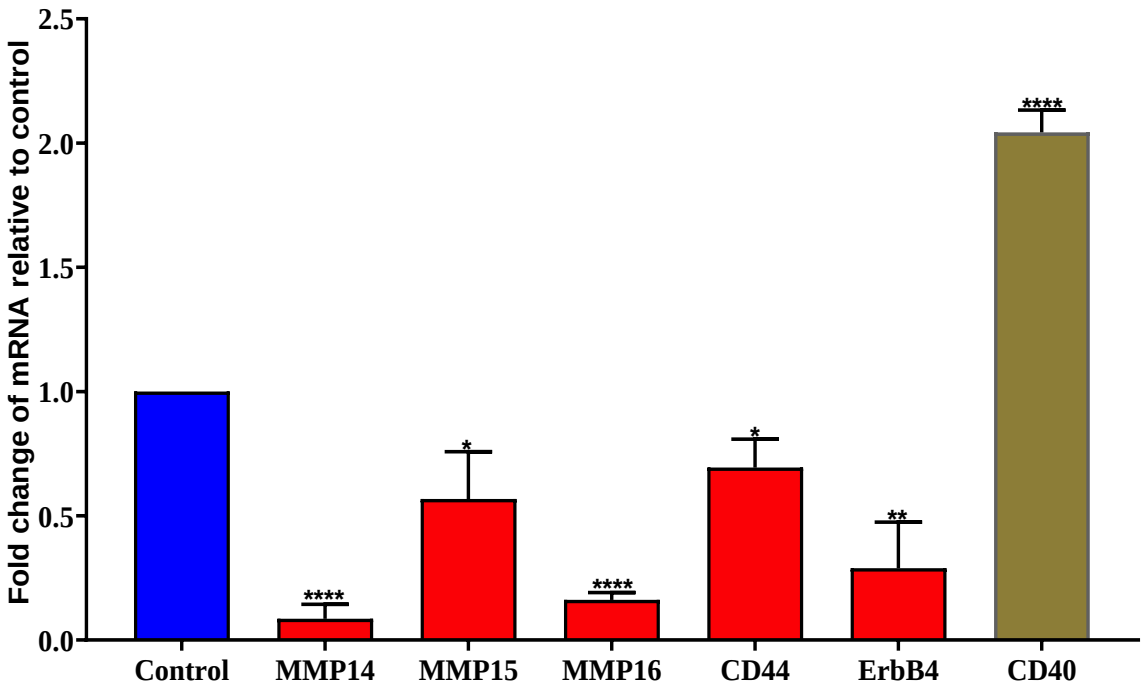

Figure 4.4 qPCR expression of the extracellular matrix mRNAs using CD-1 mice pancreatic islet cells. Pancreas was surgically removed from mice, islets isolated, then cultured for 72h in RPMI-1640 medium or RPMI-1640 medium supplemented with 17 mM D-glucose, 200 µM oleic acid and 200 µM palmitic acid. Cells were then trypsinised, lysed, RNA extracted, cDNA synthesis carried out via reverse transcription and qPCR performed using primers specific for the target genes. Data are shown as changes in mRNA expression compared to control using ΔΔCt *values* expressed as a fold change relative to control. Control is in blue colour and GLT is in red colour. Data shown are of three independent experiments. *p<0.05, **p<0.01, ****p<0.0001.

Results shown in **Figure 4.4** depicted that MMP14, MMP15, MMP16, CD44, and ErbB4 were significantly downregulated after exposure to high sugar and high fat diet. MMP14, MMP15, MMP16, CD44 and ErbB4 were observed to decrease significantly to 0.09 ± 0.06 (p<0.0001), 0.57 ± 0.19 (p=0.0317), 0.16 ± 0.03 (p<0.0001), 0.69 ± 0.11 (p=0.0185), and 0.29 ± 0.19 (p=0.0030) in fold change relative to control. CD40 has previously been shown to be overexpressed in INS-1 cells, mouse islets, and human islets exposed to metabolic stress (Bagnati et al., 2016). CD40 was therefore used as a positive control, and shown to significantly increase to 2.04 ± 0.09 (p<0.0001) relative to control.

4.3 Effect of glucolipotoxicity on MMP14, CD44 and ErbB4 protein expression

Initial results from RNAseq and mRNA expression both from rat and mouse models has shown GLT to downregulate the expression of MMPs, CD44 and ErbB4. However, mRNA expression level does not always equate to protein expression, so the amount of protein expression was also investigated. Only the protein expression of MMP14, CD44 and ErbB4 were determined as they are the most downregulated in RNAseq and mRNA expression. To observe the effects of GLT medium on protein expression level of MMP14, CD44 and ErbB4, INS-1 cells were exposed for 5 days to RPMI-1640 medium ± GLT. After the incubation period, INS-1 cells were lysed with RIPA (radioimmunoprecipitation assay) buffer solution and protein was separated using 10% resolving polyacrylamide gel. The separated total cellular protein was then transferred onto a nitrocellulose membrane and blocked with 5% milk powder for an hour at room temperature. After which, the membrane was then incubated overnight in a roller at 4 ^{o}C against respective primary antibodies.

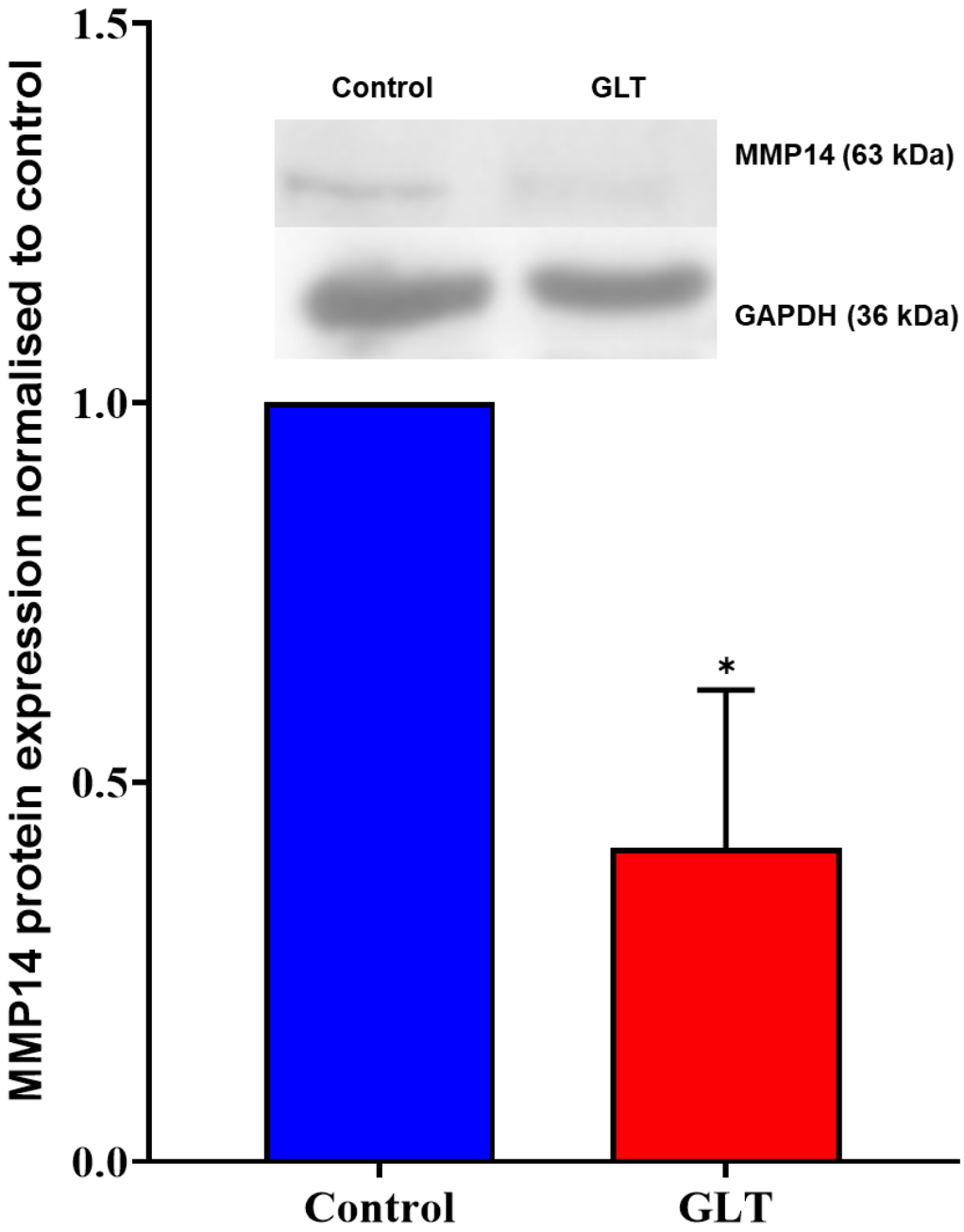

Figure 4.5 Protein expression of MMP14 exposed to GLT. INS-1 cells were incubated ± GLT for 5 days then lysed using RIPA buffer solution. Total cellular proteins were quantified using BCA protein assay and loaded to 10% polyacrylamide gel and separated through SDS-PAGE. Separated proteins were transferred onto a nitrocellulose membrane and immunoblotted against MMP14 specific antibody. Data were normalised to GAPDH and expressed as fold change compared to the control. Data shown are expressed as mean ± S.E.M. of three independent experiments. T-test was conducted for the analysis of the data.*p=0.05.

MMP14 is a member of proteins of the matrix metalloproteinase family which are involved in normal physiological processes such as embryonic development, reproduction, and tissue remodelling. Also, they are involved in disease processes of arthritis and metastasis. As shown in **Figure 4.6**, MMP14 protein expression level was significantly downregulated when exposed to GLT to 0.41 ± 0.21 ($p=0.0478$) fold relative to control.

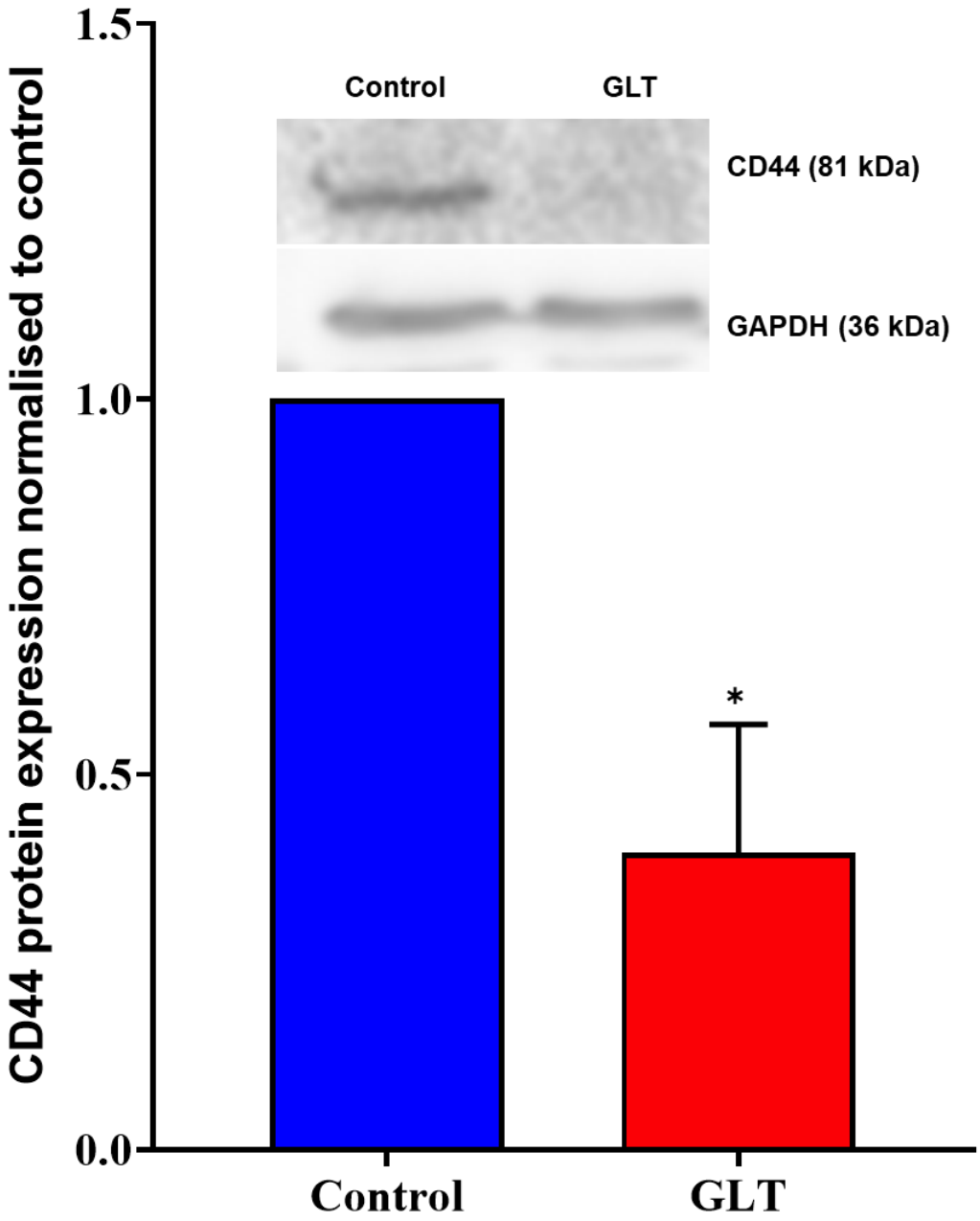

Figure 4.6 Protein expression of CD44 exposed to GLT. INS-1 cells were incubated ± GLT for 5 days prior to lysing using RIPA buffer solution. Total cellular proteins were quantified using BCA assay and loaded to 10% polyacrylamide and separated through SDS-PAGE. Separated proteins were transferred onto a nitrocellulose membrane and immunoblotted against CD44 specific antibody. Data was normalised to GAPDH and expressed as fold change compared to the control. Data shown is expressed as mean ± S.E.M. of three independent experiments. T-test was conducted for the analysis of the data. *p=0.05

Protein expression of CD44 was also evaluated. CD44 is a cell-surface receptor that plays a crucial role in cell-cell interactions, cytoplasmic spreading, and cell adhesion, invasion, and migration. Shown in **Figure 4.6**, CD44 protein expression was significantly downregulated when exposed to GLT to 0.40 ± 0.17 ($p=0.0383$) fold relative to control. CD44 expression was also downregulated upon exposure to GLT as shown in the Metacore^{TM}.

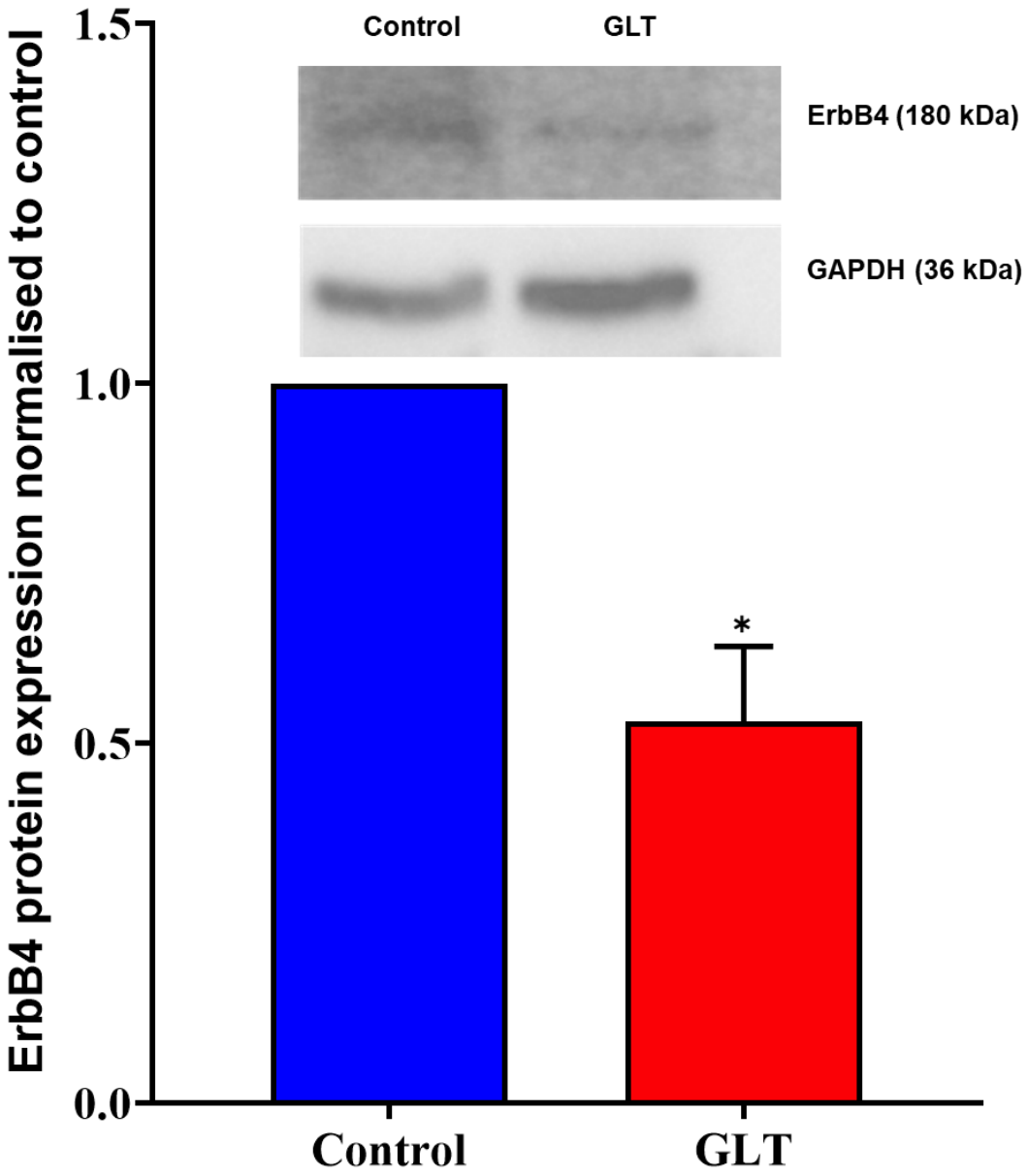

Figure 4.7 Protein expression of ErbB4 exposed to GLT. INS-1 cells were incubated ± GLT for 5 days prior to lysing using RIPA buffer solution. Total cellular proteins were quantified using BCA assay and loaded to 10% polyacrylamide and separated through SDS-PAGE. Separated proteins were transferred onto a nitrocellulose membrane and immunoblotted against ErbB4 specific antibody. Data were normalised to GAPDH and expressed as fold change compared to the untreated control. Data shown are expressed as mean ± S.E.M. of three independent experiments. T-test was conducted for the analysis of the data. *$p<0.05$

ErbB4 has an essential role as cell surface receptor for neuregulins and EGF family members. It is also involved in cell proliferation, differentiation, migration and

apoptosis. **Figure 4.7** shown that ErbB4 was significantly downregulated when exposed to GLT by 0.53 ± 0.11 (p=0.0460) fold change compared to control.

4.3 Effect of MMP14, CD44 and ErbB4 knocked down on insulin secretion

Using siRNA (24 hr) knocked down in INS-1 cells, the expression of MMP14, CD44 and ErbB4 was reduced prior to treatment with control (RPMI-1640) or GLT media for 5 days. After the incubation period, INS-1 cells were trypsinised, lysed, RNA extracted, cDNA synthesis done via reverse transcription, and RT-qPCR performed using primers of the target genes.

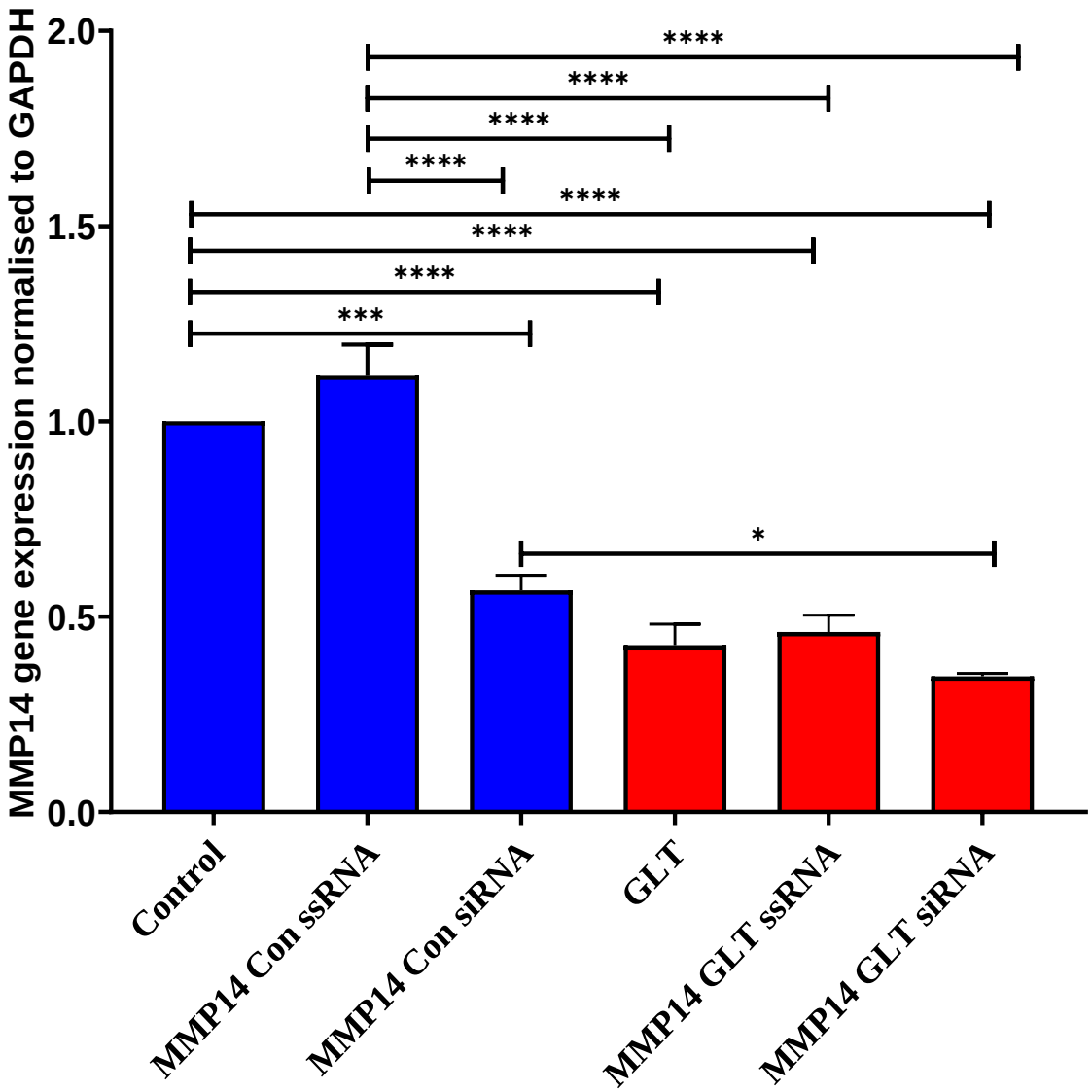

Figure 4.8 Transient knocked down of MMP14. MMP14 was transiently knocked down using siRNA for 24 hours in INS-1 cells, and after incubation, it was exposed to RPMI-1640 ± GLT for 5 days whilst changing the medium on the third day. After the incubation period, INS-1 cells were trypsinised, lysed, RNA extracted, cDNA synthesis carried out via reverse transcription, and RT-qPCR performed using MMP14 primers. The data shown are from three independent experiments. Statistical analyses were carried out by one-way ANOVA followed by Tukey's multiple comparisons test as post hoc test (*p<0.05, ****p<0.0001).

As shown in **Figure 4.8**, MMP14 mRNA expression was significantly decreased when exposed to GLT (0.43 ± 0.05, 57% reduction relative to control untreated, p<0.0001). Using siRNA (24 hour) knocked down in INS-1 cells, the expression of MMP14 was significantly reduced to 0.57 ± 0.04 (43% reduction relative to control

untreated). This reduction was decreased further to 0.35 ± 0.01 when the cells were treated with GLT but the reduction was not significantly different with each other.

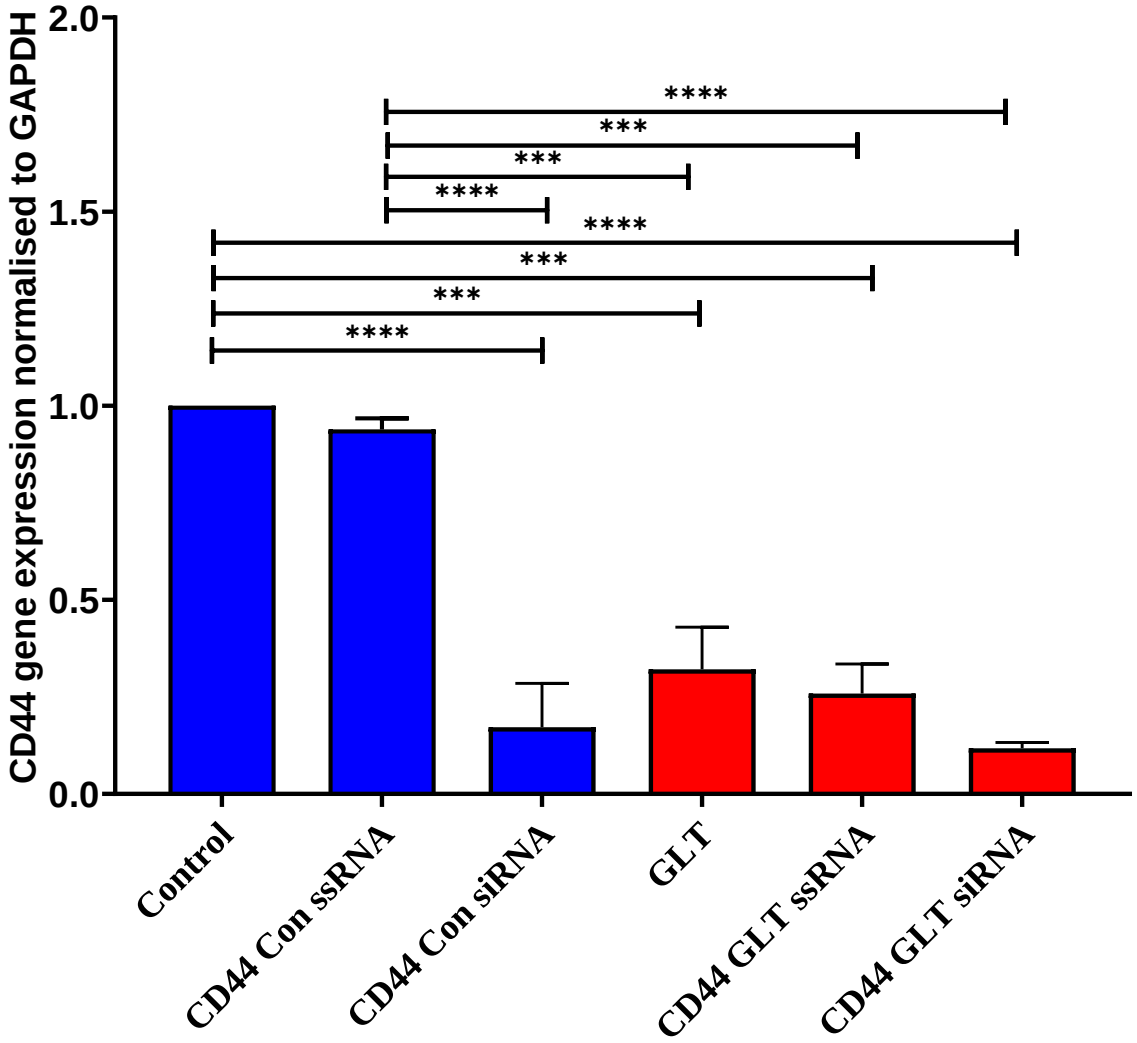

Figure 4.9 Transient knocked down of CD44. CD44 was transiently knocked down using siRNA for 24 hours in INS-1 cells, and after incubation, it was exposed to RPMI-1640 ± GLT for 5 days changing the medium on the third day. After the incubation period, INS-1 cells were trypsinised, lysed, RNA extracted, cDNA synthesis carried out via reverse transcription, and RT-qPCR performed using CD44 primers. The data shown are from three independent experiments. Statistical analyses were carried out by one-way ANOVA followed by Tukey's multiple comparisons test as post hoc test (***p<0.001, ****p<0.0001).

As shown in **Figure 4.9**, CD44 mRNA expression was significantly decreased when exposed to GLT (0.32 ± 0.11, 68% reduction relative to control untreated, p<0.0003) relative to control untreated. Using siRNA (24 hour) knocked down in INS-1 cells,

the expression of CD44 was significantly reduced to 0.17 ± 0.11 (83% reduction relative to control untreated). This reduction was decreased further to 0.12 ± 0.01 when the cells were treated with GLT but the reduction was not significantly different with each other.

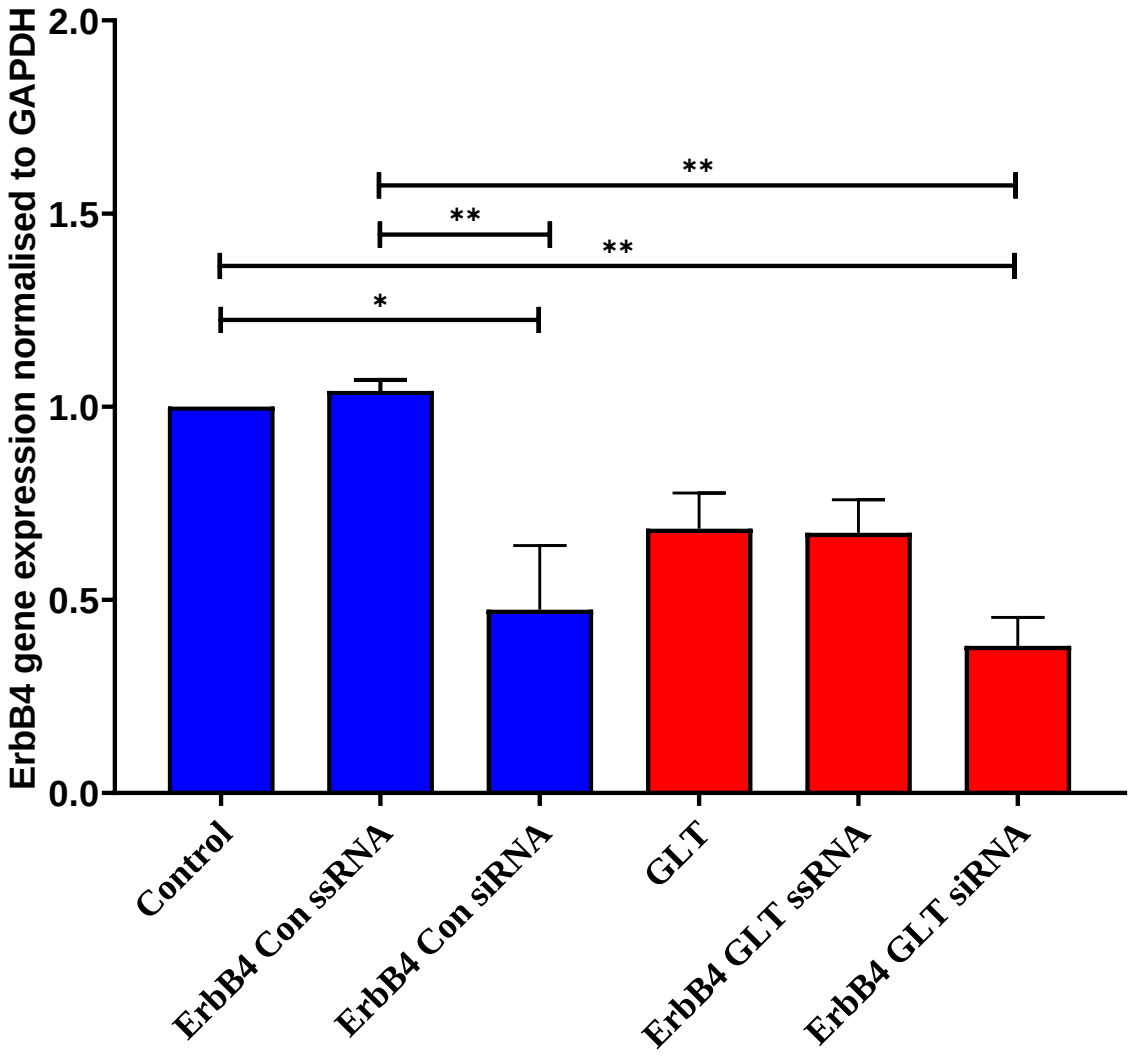

Figure 4.10 Transient knocked down of ErbB4. ErbB4 was transiently knocked down using siRNA for 24 hours in INS-1 cells, and after incubation, it was exposed to RPMI-1640 ± GLT for 5 days changing the media on the third day. After the incubation period, INS-1 cells were trypsinised, lysed, RNA extracted, cDNA synthesis carried out via reverse transcription, and RT-qPCR performed using ErbB4 primers. The data shown are from three independent experiments. Statistical analyses were carried out by one-way ANOVA followed by Tukey's multiple comparisons test as post hoc test (*p<0.05, **p<0.01).

As shown in **Figure 4.10**, ErbB4 mRNA expression was significantly decreased when exposed to GLT (0.68 ± 0.09, 32% reduction relative to control untreated, $p<0.0003$). Using siRNA (24 hour) knocked down in INS-1 cells, the expression of ErbB4 was significantly reduced to 0.47 ± 0.17 (53% reduction relative to control untreated). This reduction was decreased further to 0.38 ± 0.07 when the cells were treated with GLT but the reduction was not significantly different with each other.

To determine the effect of the knocked down of the target genes on insulin secretion, High Range Rat Insulin ELISA (Uppsala, Sweden) was conducted.

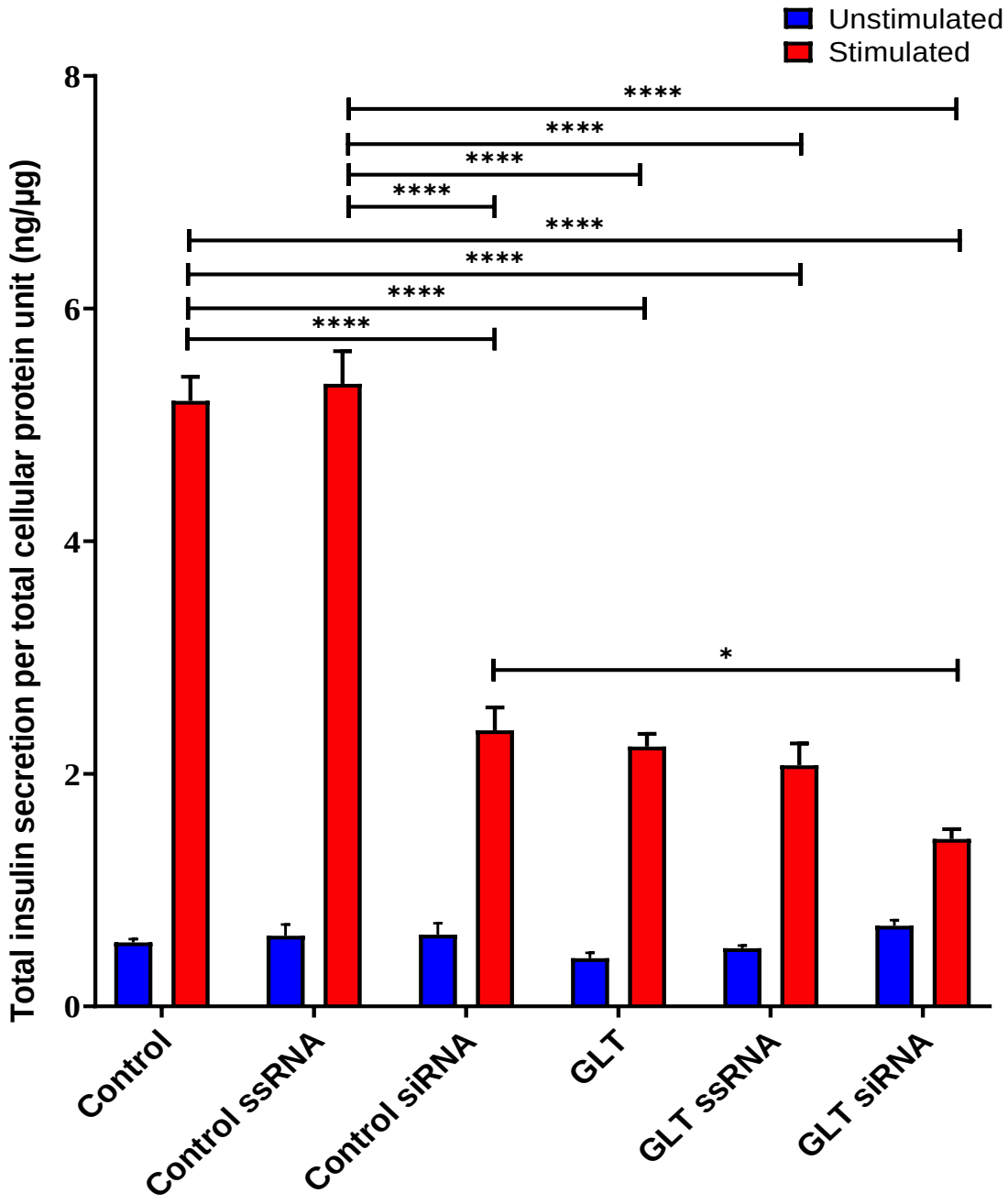

Figure 4.11 Effect of MMP14 knocked down on insulin secretion. MMP14 was transiently knocked down using siRNA for 24 hours in INS-1 cells, and after incubation, it was exposed to RPMI-1640 ± GLT for 5 days changing the medium on the third day. High Range Rat Insulin ELISA determined insulin secretion following incubation ± secretagogue cocktail for 3 hours. Unstimulated is in blue and stimulated is in red with data normalised to total cellular protein. The data shown are from three independent experiments. Statistical analyses were carried out by one-way ANOVA followed by Tukey's multiple comparisons test as post hoc test (*p<0.05, ****p<0.0001 on GLT stimulated).

As shown in **Figure 4.11**, treatment of INS-1 cells with GLT reduced the insulin secretion significantly decreased to 2.23 ± 0.11 ng/µg (57.20% reduction, p<0.0001)

relative to control untreated (5.21 ± 0.21 ng/µg). Using siRNA (24 hour) knocked down in INS-1 cells, the insulin secretion of MMP14 control siRNA was significantly reduced to 2.37 ± 0.20 ng/µg ($p<0.0001$) relative to control untreated. This reduction of insulin secretion in control siRNA was significantly reduced further to 1.44 ± 0.08 ng/µg (GLT siRNA, $p=0.0398$) when treated with GLT. Then using siRNA (24 hour) knocked down in INS-1 cells, the insulin secretion of GLT siRNA was reduced to 1.44 ± 0.08 ng/µg relative to GLT treated INS-1 cells (2.23 ± 0.11 ng/µg). However, this reduction was found to be not significantly different with each other.

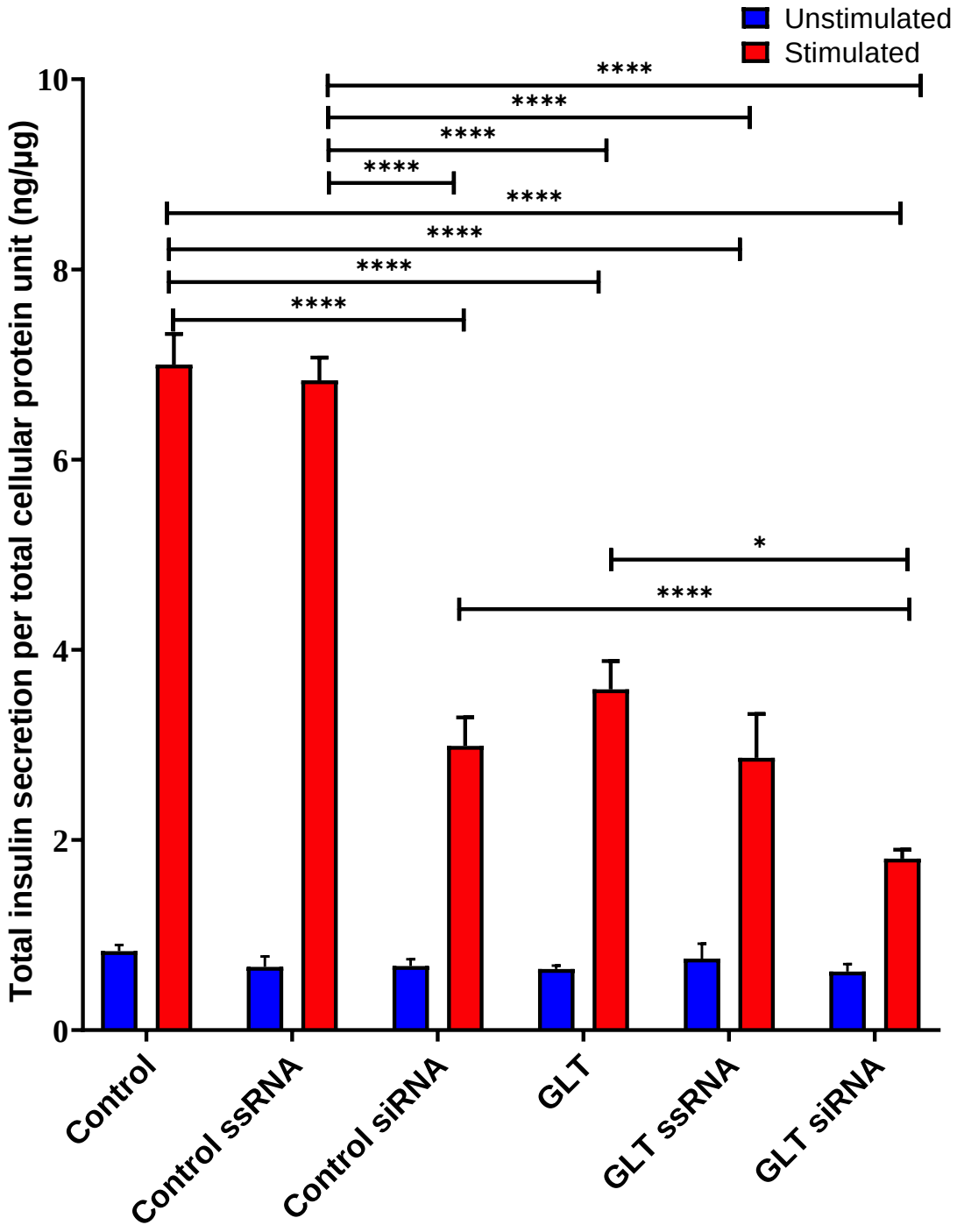

Figure 4.12 Effect of CD44 knocked down on insulin secretion. CD44 was transiently knocked down using siRNA for 24 hours in INS-1 cells, and after incubation, it was exposed to RPMI-1640 ± GLT for 5 days changing the medium on the third day. High Range Rat Insulin ELISA determined insulin secretion following incubation ± secretagogue cocktail for 3 hours. Unstimulated is in blue and stimulated is in red with data normalised to total cellular protein. The data shown are from three independent experiments. Statistical analyses were carried out by one-way ANOVA followed by Tukey's multiple comparisons test as post hoc test (*p<0.05, ****p<0.0001 on GLT stimulated).

As shown in **Figure 4.12**, treatment of INS-1 cells with GLT reduced the insulin secretion significantly decreased to 3.58 ± 0.30 ng/µg (48.86% reduction, $p<0.0001$) relative to control untreated (7.00 ± 0.32 ng/µg). Using siRNA (24 hour) knocked down in INS-1 cells, the insulin secretion of CD44 control siRNA was significantly reduced to 2.99 ± 0.30 ng/µg ($p<0.0001$) relative to control untreated. This reduction of insulin secretion in control siRNA was significantly reduced further to 1.80 ± 0.09 ng/µg (GLT siRNA, $p<0.0001$) when treated with GLT. Then using siRNA (24 hour) knocked down in INS-1 cells, the insulin secretion of GLT siRNA was significantly reduced to 1.80 ± 0.09 ng/µg ($p=0.0140$) relative to GLT treated INS-1 cells (3.58 ± 0.30 ng/µg).

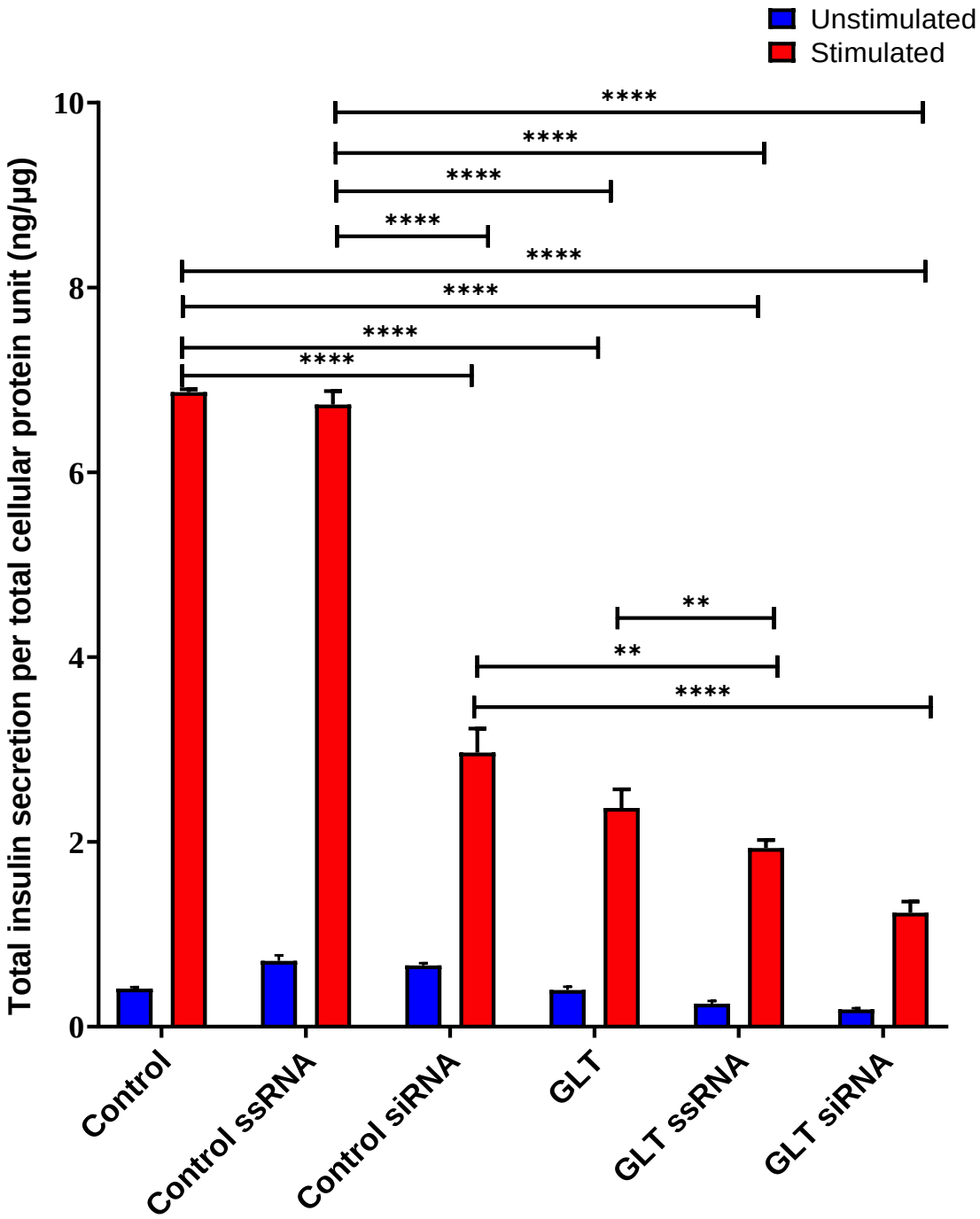

Figure 4.13 Effect of ErbB4 knocked down on insulin secretion. ErbB4 was transiently knocked down using siRNA for 24 hours in INS-1 cells, and after incubation, it was exposed to RPMI-1640 ± GLT for 5 days changing the medium on the third day. High Range Rat Insulin ELISA determined insulin secretion following incubation ± secretagogue cocktail for 3 hours. Unstimulated is in blue and stimulated is in red with data normalised to total cellular protein. The data shown are from three independent experiments. Statistical analyses were carried out by one-way ANOVA followed by Tukey's multiple comparisons test as post hoc test (**p<0.01, ****p<0.0001 on GLT stimulated).

As shown in **Figure 4.13**, treatment of INS-1 cells with GLT reduced the insulin secretion significantly decreased to 2.37 ± 0.20 ng/µg (65.50% reduction, $p<0.0001$) relative to control untreated (6.87 ± 0.03 ng/µg). Using siRNA (24 hour) knocked down in INS-1 cells, the insulin secretion of ErbB4 control siRNA was significantly reduced to 2.97 ± 0.26 ng/µg ($p<0.0001$) relative to control untreated. This reduction of insulin secretion in control siRNA was significantly reduced further to 1.23 ± 0.12 ng/µg (GLT siRNA, $p<0.0001$) when treated with GLT. Then using siRNA (24 hour) knocked down in INS-1 cells, the insulin secretion of GLT siRNA was reduced to 1.23 ± 0.12 ng/µg relative to GLT treated INS-1 cells (2.37 ± 0.20 ng/µg). However, these reductions were found to be not significantly different from each other.

In summary, all gene expression of target genes in control ssRNA is relatively the same as the control. However, when INS-1 cells were treated with siRNA, the gene expression of all target genes was reduced. In the case of gene expression of the target genes exposed in GLT, it was shown that all of them had reduced expression relative to the control. However, gene expression of target genes exposed to GLT ssRNA are relatively the same as GLT, but it was depicted that the gene expression of target genes exposed to GLT siRNA was reduced relative to GLT ssRNA.

In terms of insulin secretion, it was illustrated in the insulin secretion assay experiment that knocked down of the target genes and reduction of their gene expression affects insulin secretion by decreasing it release relative to the control and GLT.

The effect of GLT on insulin secretion is further discussed in Chapter 6. It is also discussed in that chapter the effect of GLT in the production of radical species.

4.4 Discussion

When INS-1 rat pancreatic β-cells were incubated with media supplemented with high glucose and high fatty acid, RNA was extracted for next generation sequencing and it was shown that pathways involved in cell adhesion were significantly downregulated. It was shown also that matrix metalloproteinases (MMPs) [MMP14, MMP15 and MMP16], CD44 and ErbB4 were significantly downregulated as presented in the MetaCore^{TM} network map. These results were then validated in RT-qPCR and western blotting. Exposing INS-1 cells and CD-1 mouse pancreatic islets with GLT media resulted in downregulation of mRNA expression of genes involved in extracellular matrix remodelling and the actin cytoskeleton, specifically MMP14, MMP15 and MMP16, CD44 and ErbB4. It was also observed that protein expression of MMP14, CD44 and ErbB4 was also significantly downregulated, consistent with the results shown in RNAseq data analysis and mRNA expression analysis.

Degradation of ECM is crucial in the release of growth factor and hormones, and matrix metalloproteinases are involved in the degradation mechanism. However, biological action of MMPs is strictly regulated from gene transcription, translation, pro-enzyme activation and inhibition by metalloproteinases inhibitors (TIMPs). TIMPs regulate MMPs activity and thereby preventing excessive matrix degradation (Galliera et al., 2015). MMPs are zinc-dependent enzymes and peptide hydrolases (Tallant et al., 2010) secreted by cells or bound to the cell membrane of cells such as fibroblasts, vascular smooth muscle (VSM), and leukocytes (Cui et al., 2017). Although MMPs can cause ECM protein degradation of collagen and elastin, they have found to be implicated in endothelial cell function as well as VSM cell migration, proliferation, Ca^{2+} signalling, and contraction (Cabral-Pacheco et al., 2020; Raffetto and Khalil, 2008; Wang et al., 2018).

MMPs have been shown to have roles in various physiological processes (morphogenesis, wound repair, embryogenesis, and angiogenesis) and pathological conditions (fibrotic disorders, myocardial infarction, and cancer) (Amălinei et al., 2010; Cui et al., 2017). Studies have also shown that MMPs were involved in tissue repair after acute injury (García-Irigoyen et al., 2015), and implicated in the disassembly of intercellular junctions and the degradation of ECM, thus lessening the physical constraint to cell movement (Mauris et al., 2014) . MMPs were shown to be implicated in ischemic stroke pathophysiology and clinical outcome, however, this might be influenced by ethnic background (Chang et al., 2016). In addition, MMPs have been shown to have a crucial role in viral infection, inflammation and remodelling of the airway, specifically in respiratory syncytial virus (RSV) which is an important pathogen of bronchiolitis, asthma, and severe lower respiratory tract disease in infants and young children (Hirakawa et al., 2013).

Increase levels of MMPs are biomarkers indicative of diabetic nephropathy, diabetic retinopathy, diabetic chronic wound healing inability and diabetic cardiovascular risk (Galliera et al., 2015; Santos et al., 2013; Van Geest et al., 2013). Activation of cytosolic MMP9 and MMP2, and their increased level in the mitochondria can damage them, leading to a vicious production of reactive oxygen species (Santos et al., 2013). By contrast, decreased activity of MMPs expressed in nephrons can lead to abnormal ECM deposition which is a hallmark of diabetic nephropathy (Han et al., 2006; Inada et al., 2005; McLennan et al., 2002). A study conducted by Lewinski and colleagues in 2011 has shown that MMP2 and MMP9 have a lower level in patients with type 2 diabetes (Lewandowski et al., 2011) and there were studies reporting that MMP14 expression level in diabetes was downregulated (Boucher et al., 2006; Dolan et al., 2003; Lenz et al., 2000; McLennan et al., 2002; Portik-Dobos et al., 2002). Relative to our results, these

studies have shown to be in similar results we have MMPs (MMP14, MMP15 and MMP16) were downregulated upon exposure to high sugar and high fat diet.

Within the islet, β-cells contact the extracellular matrix (ECM), which is deposited primarily by intra-islet endothelial cells, and this significant interaction has been shown to modulate cell proliferation and survival (Townsend and Gannon, 2019). Cell-to-cell interactions via gap junctional communication and connexon hemichannels are involved in the pathogenesis of diabetes. Gap junctions are highly specialized transmembrane structures that are formed by connexon hemichannels, which are further assembled from proteins called “connexins” (Wright et al., 2012). In the islet, gap junctions composed of connexin36 provide electrical and metabolic coupling between β-cells, which regulates electrical activity and insulin secretion (Farnsworth and Benninger, 2014). Under high glucose, gap junctions facilitate the coordination of electrical activity across the islet which leads to synchronized release of insulin from individual β-cells (Farnsworth and Benninger, 2014) and β-cells with uncoupled connexin junctions show poor insulin gene expression and secretion in response to glucose compared to coupled β-cells (Meda et al., 1990).

As shown in the Metacore^{TM} map network (illustrated in **Figure 4.1**), collagen family (collagen I, collagen II, collagen III and collagen IV) were all downregulated upon exposure to high sugar and high fat medium. Hence, this can cause dysregulated coordination of electrical activity between ECM and gap junctions in response to glucolipotoxicity and would likely to contribute to the failure of β-cell function such as insulin secretion observed in type 2 diabetes. Studies showed that the ECM is important for islet health *in vivo* and *ex vivo*; however, understanding of the interactions between ECM and islet cells is not yet clear (Townsend and Gannon, 2019).

Results shown here indicate that CD44 was downregulated upon exposure of cells to high sugar and high fat. The CD44 transmembrane glycoprotein family

participates in signal transduction processes by establishing specific transmembrane complexes and organising signalling cascades through the actin cytoskeleton (Ponta et al., 2003). CD44 and its associated partner proteins monitor changes in the extracellular matrix that influence cell growth, survival, and differentiation (Ponta et al., 2003). The actin cytoskeleton is also a highly dynamic structure that is remodelled in response to a variety of signals (Tomas et al., 2006). Its particular main role in pancreatic β-cells is to control glucose homeostasis in which insulin-containing granules undergo regulated exocytosis in response to extrinsic stimuli (such as glucose) that lead to an elevation in cytosolic calcium (Ashcroft et al., 1994; Easom, 2000).

ErbB4/HER4 is a member of the protein-tyrosine kinase family including epidermal growth factor receptors (EGFR) (Roskoski, 2014). EGFR provides information on the relationship between receptor overexpression and oncogenesis (Thompson and Gill, 1985). As the ErbB family are protein-tyrosine kinases, they act as dimers or higher oligomers (Roskoski, 2014). It was shown in genetic studies that ErbB4, type 2 diabetes and obesity are linked together (Böger and Sedor, 2012; Locke et al., 2015; López-Soldado et al., 2016; Maeda et al., 2013; Wang et al., 2014) . From data presented here, ErbB4 was shown to be downregulated in the MetaCore^{TM} map network and this decreased expression was also observed upon qPCR and western blot analysis of cells exposed to high sugar and high fat conditions. ErbB receptors can be activated by binding to their ligands. ErbB4 can be activated by heparin-binding EGF (HB-EGF), epiregulin, betacellulin, and neuroregulins (Nrg) 1-4. These ligands have a crucial role in glucose transport, browning of the adipocytes, glucose homeostasis, energy expenditure, prevention of high fat diet induced obesity, and improvement of insulin sensitivity (Christian, 2015; Ma et al., 2016; Yan et al., 2017). Nrg4 has been shown to be highly expressed in adipose tissue and was enhanced in brown fat, and during brown

adipocyte (Blüher, 2019; Gavaldà-Navarro et al., 2022; Wang et al., 2014). However, Nrg4 expression was shown to decrease in rodent and human obesity (Wang et al., 2014). In addition, ErbB deletion mice were shown to develop obesity, dyslipidemia, hyperglycemia, and insulin resistance (Wang et al., 2014). With this, ErbB4 may therefore have a crucial wider role in glucose homeostasis.

4.5 Conclusion

This work has shown that extracellular matrices are sensitive to nutrient stress, and specifically that the genes MMP14, MMP15, MMP16, CD44 and ErbB4 were dysregulated by glucolipotoxicity, and this may play a crucial role in the dysregulation of insulin secretion observed in type 2 diabetes.

Chapter 5

L-carnosine and β-alanine: Their Impact on Mitochondrial Bioenergetics

5.1 Introduction

Mitochondria are a subcompartment of the cell-bound by a double membrane, the outer membrane and inner membrane which comprise intermembrane space and matrix compartments (Nunnari and Suomalainen, 2012). Mitochondria are commonly known as the powerhouse of the cell. Mitochondria house various metabolic pathways, including the Krebs cycle, fatty acid β-oxidation, urea cycle and oxidative phosphorylation, which enable them to generate ATP to sustain cellular function (Manoli et al., 2007). Mitochondria also play a role in intracellular signalling and apoptosis, intermediate metabolism, and metabolism of lipids, steroids, amino acids and nucleotides (Chinnery and Schon, 2003).

Mitochondria are involved in many cellular pathways and processes such as apoptosis, cell signalling involving production and regulation of ROS, stimulation of Ca^{2+} could increase ATP production by altering the activity of calcium-sensitive mitochondrial matrix enzymes, bioenergetic pathways during the oxidation of glucose, and β-oxidation of fatty acids (Herst et al., 2017). In addition, mitochondria are associated with many cellular functions (**Figure 5.1a**).

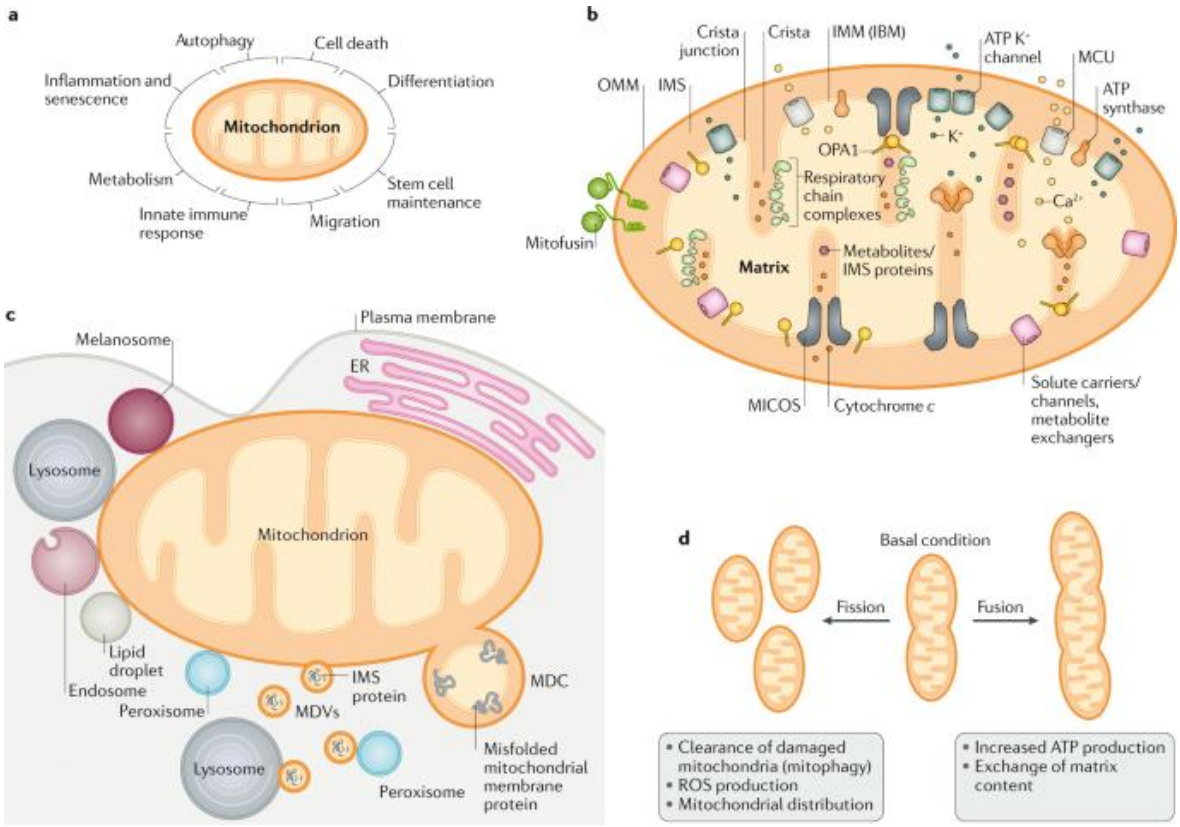

Figure 5.1 Mitochondrial structure and its function. Figure adapted from Giacomello et al (2020).

As shown in **Figure 5.1b**, the mitochondrial matrix is comprises two membranes: the outer mitochondrial membrane (OMM) and the inner mitochondrial membrane (IMM). Krebs cycle, protein biosynthesis, and mitochondrial DNA replication occur in the mitochondrial matrix, which is enclosed by IMM. The OMM acts as a diffusion barrier and facilitates signal transduction in and out of the mitochondria. The IMM is composed of an inner boundary membrane (IBM) and mitochondrial cristae. The IBM hosts many channel transporters that shuttle ions, ADP, ATP, and metabolites between the matric and cytoplasm.

On the other hand, the site where oxidative phosphorylation, iron-sulphur cluster biogenesis and mitochondrial DNA maintenance occur, is in mitochondrial cristae. In **Figure 5.1c**, the OMM interacts with other organelles that regulate mitochondrial function such as the endoplasmic reticulum (ER), lysosomes and endosomes, peroxisomes, plasma membrane, and melanosomes. Released by the

mitochondria, mitochondrial derived vesicles (MDVs) can communicate with lysosomes and peroxisomes, whilst mitochondrial-derived compartments (MDCs) can remove misfolded proteins from the mitochondrial membranes. Mitochondrial fusion favours increased ATP production and exchange of matrix content whilst mitochondrial fission favours increased production of ROS and removal of superfluous mitochondria by mitophagy (**Figure 5.1d**) (Giacomello et al., 2020).

Mitochondrial dysfunction can inhibit mitochondrial metabolism and block insulin secretion (Rocha et al., 2020). Mitochondrial function under normal conditions and type 2 diabetes is shown in **Figure 5.2**.

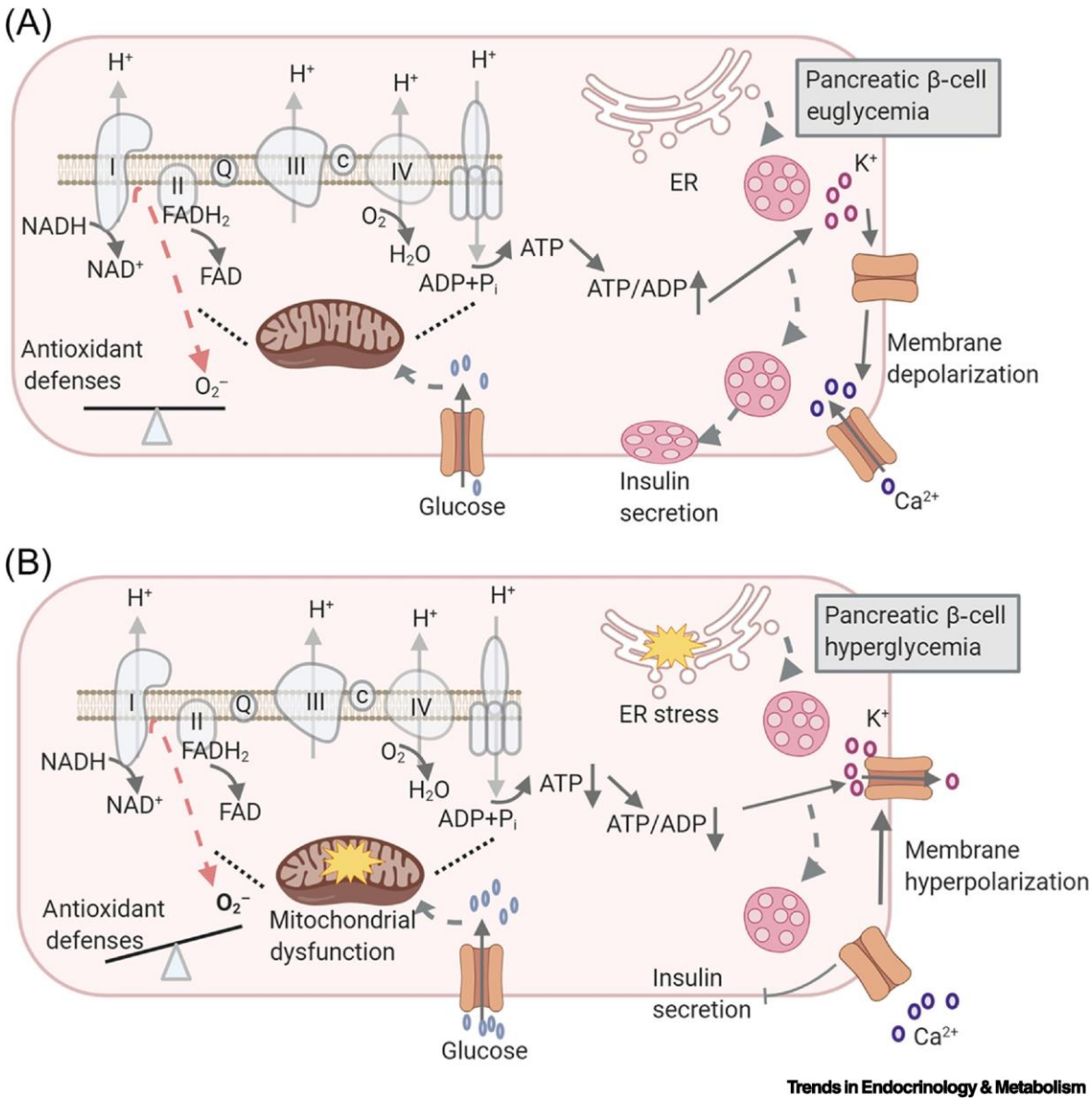

Figure 5.2 β-cell function under euglycemia and hyperglycaemia. (A) In pancreatic β-cell under normal conditions, the glucose is metabolised in glycolysis and generating ATP. As a consequence, the ATP/ADP ratio is high, and potassium (K^+) channels are closed. The plasma membrane is depolarised favouring Ca^{2+} influx into the cell, triggering the release of endoplasmic reticulum-synthesised insulin. (B) In type 2 diabetes, ATP synthesis is weakened and can open ATP-sensitive potassium channels. The plasma membrane is hyperpolarised and blocks the calcium ion influx into the cell, thereby inhibiting insulin secretion. Figure adapted from Rocha et al (2020).

Most of the ATP is produced in the mitochondria (Lee and Wei, 2000) via mitochondrial oxidative phosphorylation system (OXPHOS) (Nunnari and Suomalainen, 2012). Electron carriers (NADH and $FADH_2$) produced from glucose and fatty acid β-oxidation are transferred through mitochondrial respiratory chain

complexes I-IV (Manoli et al., 2007). Protons are generated and pumped out from complexes I, III, and IV into the intermembrane space, which produces an electrochemical gradient to drive the phosphorylation of ADP to ATP via rotary turbine-like ATP synthase machine (complex V), hence the production of ATP (Okuno et al., 2011; Stock et al., 1999).

Since mitochondria use more than 80-90% of the cell's oxygen (Manoli et al., 2007; Paradies et al., 2010), it is the primary source of cellular ROS aside from NAPDH oxidases (Dan Dunn et al., 2015). Mitochondrial activity generated ROS includes superoxide anions, hydrogen peroxide and hydroxyl radicals. In addition, monoamine oxidase present in the mitochondrial outer membrane catalyses the biogenic amines to undergo oxidative deamination to generate in excess hydrogen peroxide, which contributes to the steady-state concentration of ROS both in the cytosol and mitochondrial matrix (Cadenas and Davies, 2000).

Mitochondrial ROS are involved in regulating immune responses and autophagy (Dan Dunn et al., 2015). However, when mitochondrial ROS are produced in excess this can result in lipid peroxidation, OXPHOS dysfunction, and mitochondrial DNA damage. To some extent, oxidative stress ensues, which can cause cellular damage, carcinogenesis and mutagenesis (Manoli et al., 2007; Wei and Lee, 2002). This problem mainly arises due to the low production and activity of enzymes involved in the antioxidant defence system including superoxide dismutase, catalase, and glutathione peroxidase (Robertson et al., 2003; Tiedge et al., 1997), which scavenge excess ROS.

The primary function of mitochondria is the production of ATP for cell survival. In addition, mitochondria generate and detoxify reactive oxygen species implicated in cytoplasmic and mitochondrial matrix calcium regulation, synthesis and catabolism of metabolites, and apoptosis. However, irregularity of these functions can be classified as mitochondrial dysfunction (Brand and Nicholls, 2011).

Mitochondrial dysfunction can be assessed by measuring the rate of ATP production, coupling efficiency, spare respiratory capacity, proton leak and maximum respiratory rate (Brand and Nicholls, 2011).

This part of the study aimed to evaluate whether L-carnosine and β-alanine could affect the production of reactive oxygen species generated by GLT and whether exposure to L-carnosine and β-alanine influences mitochondrial bioenergetics by measuring the oxygen consumption rate using Seahorse Mito Stress assay. Specifically, the purpose of this study was to determine the effect of GLT on basal respiration, ATP production, proton leak, maximal respiration, spare respiratory capacity, and non-mitochondrial oxygen respiration and to determine whether supplementation of medium with L-carnosine and β-alanine could inhibit GLT effects.

5.2 Results

Before assessing the effects of L-carnosine and β-alanine to the effects of glucolipotoxicity to the mitochondrial bioenergetics, the effects of L-carnosine and β-alanine on the cell viability, and radical species scavenging were evaluated using INS-1 cells and C2C12 myotubes. These functional assays were conducted as type 2 diabetes is characterised by excess generation of reactive oxygen species, low ATP level and mitochondrial dysfunction (Rovira-Llopis et al., 2017).

5.2.1 Effects of L-carnosine and β-alanine in INS-1 cells and C2C12 myotubes viability

The effects of supplementation of L-carnosine and β-alanine to the growth medium of INS-1 cells and differentiation medium of C2C12 myotubes were assessed using the calcein-AM assay. In this experiment, INS-1 rat pancreatic β-cells or C2C12 myotubes were incubated in polystyrene nunclon delta 12-well plate for 5 days in

complete growth medium (INS-1 cells) or DMEM supplemented with 5% v/v horse serum and 1% v/v penstrep with L-glutamine (for C2C12 myotubes) ± 10 mM L-carnosine (or 10 mM β-alanine) or GLT medium ± 10 mM L-carnosine (or 10 mM β-alanine). After the 5-day incubation period, cell viability using calcein-AM protocol was measured. The treated INS-1 cells and C2C12 myotubes were visualised using Olympus CKX53 model microscope at 20x objective before and after the treatment of calcein-AM solution.

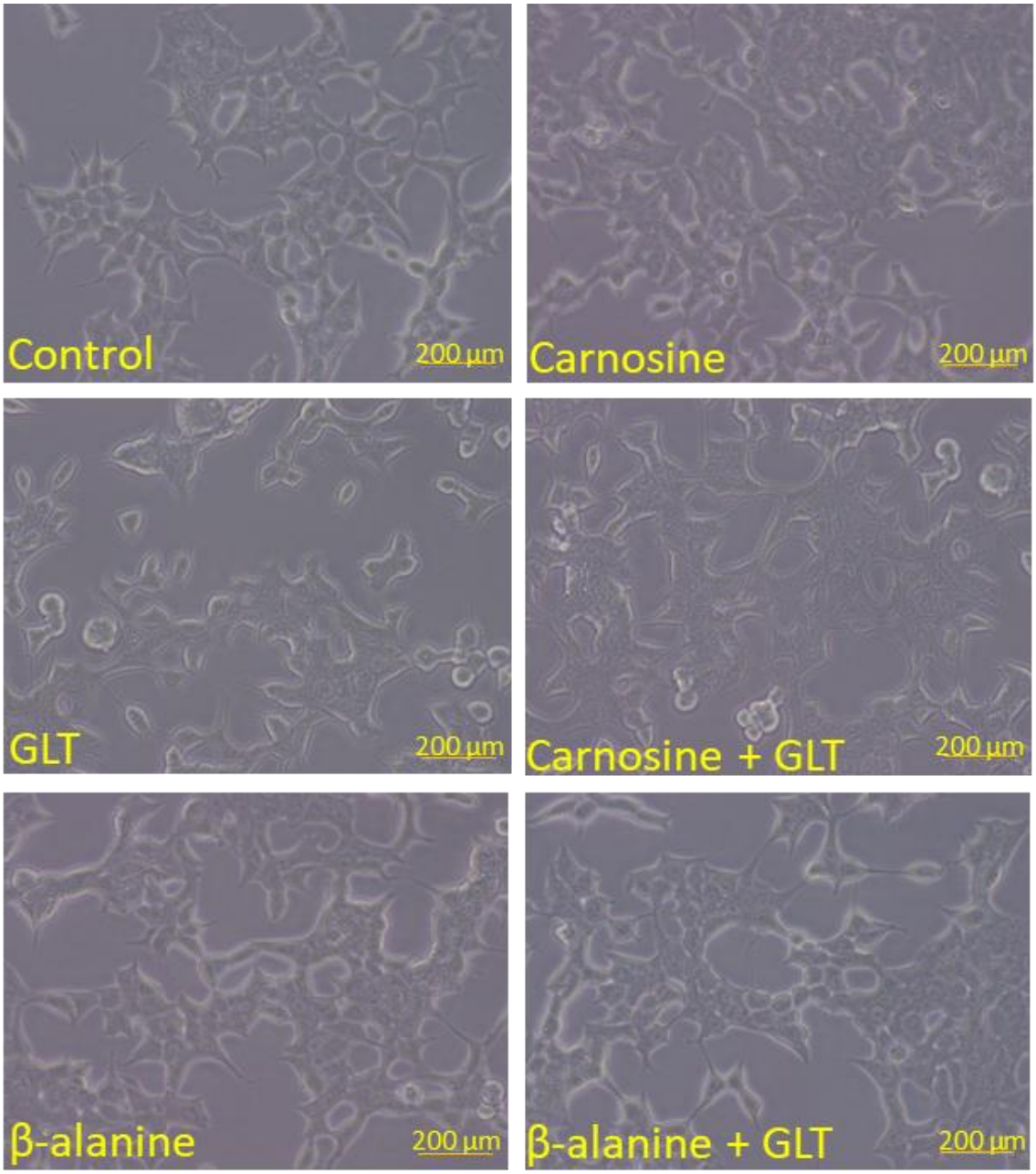

Figure 5.3 Effect of experimental conditions on INS-1 rat pancreatic β-cell morphology. INS-1 cells were incubated for 5 days in complete RPMI-1640 medium ± 10 mM L-carnosine (or β-alanine) or GLT medium ± 10 mM L-carnosine (or β-alanine). Images were taken using Olympus CKX53 model microscope with camera using a 20x objective.

As depicted in **Figure 5.3**, INS-1 cells were exposed to the experimental conditions (carnosine, β-alanine, GLT + carnosine and GLT + β-alanine) and show no observable change in cell morphology relative to control. It was observed that the treatment conditions did not reduce cell adherence onto the surface of the plate. Cells also appeared to have few or no circular/rounded shapes in all conditions

except in GLT condition in which few rounded shape cells were seen. Increased cell death was not significant, and there were few floating cells observed in the plate.

As depicted in **Figure 5.4**, C2C12 myotubes were exposed to the experimental conditions (GLT, carnosine, β-alanine, GLT + carnosine and GLT + β-alanine) and show no observable change in cell morphology relative to control. It was observed that the treatment conditions did not reduce cell adherence onto the surface of the plate. C2C12 myotubes appeared to be in tubular form. There were no or few floating cells observed in the plate.

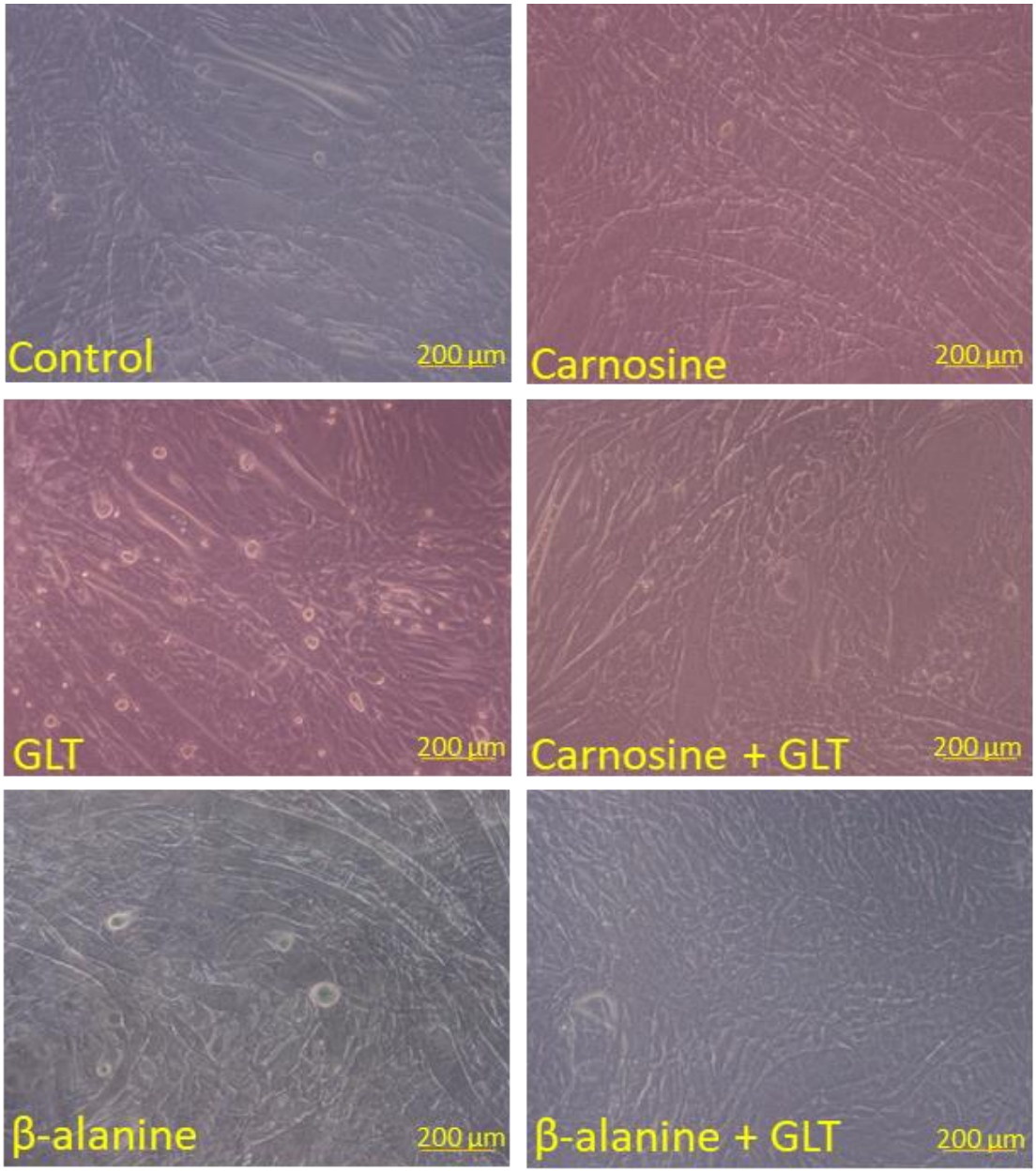

Figure 5.4 Effect of experimental conditions on skeletal C2C12 myotubes morphology. C2C12 myotubes were incubated for 5 days in DMEM ± 10 mM L-carnosine (or β-alanine) or DMEM ± 10 mM L-carnosine (or β-alanine). Images were taken using Olympus CKX53 model microscope with camera using a 20x objective.

Functional analysis on INS-1 cells and C2C12 myotubes viability was performed using the calcein-AM assay. As depicted in **Figure 5.5** (INS-1 cells) **and Figures 5.6, and 5.7** (C2C12 myotubes), INS-1 cells and C2C12 myotubes treated with various experimental conditions, i.e., growth medium ± L-carnosine or β-alanine and GLT ± L-carnosine or β-alanine, shown little or no significant change in cell viability relative to control. This result demonstrated that supplementation of 10 mM L-

carnosine or 10 mM β-alanine does not affect the cell morphology of the cell model used in this experiment.

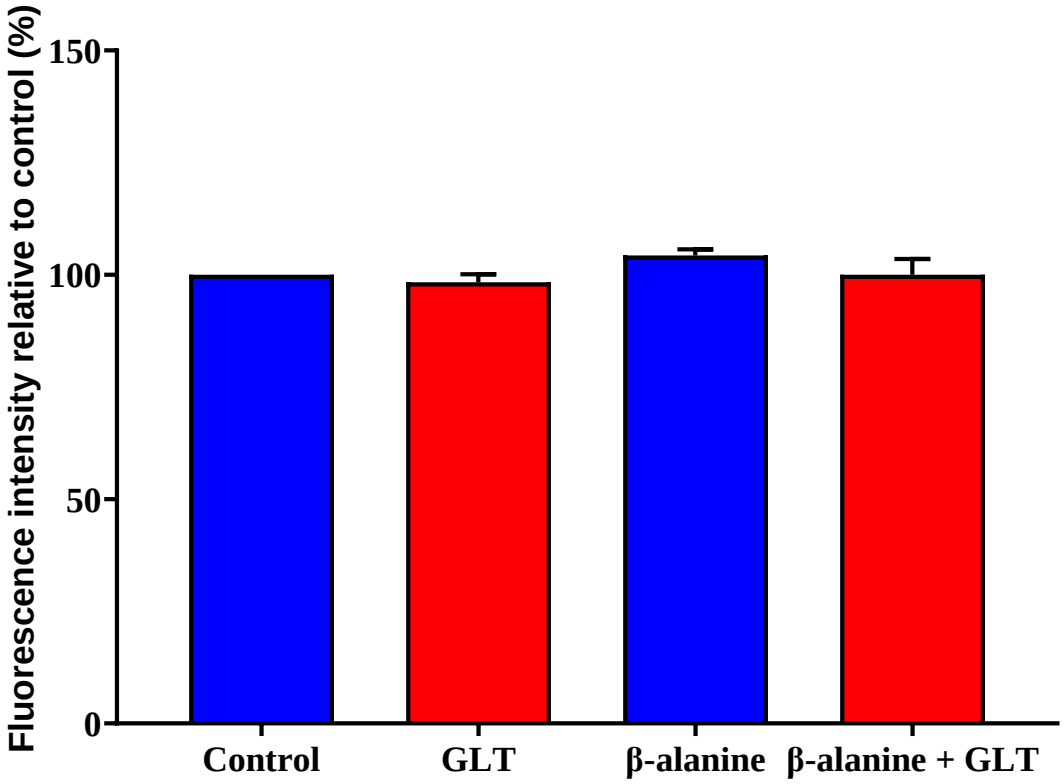

Figure 5.5 Effect of β-alanine on INS-1 rat pancreatic β-cell viability. INS-1 cells were incubated for 5 days in RPMI-1640 medium ± 10 mM β-alanine or GLT medium ± 10 mM β-alanine. After 1 hour incubation with 5 μM solution of calcein-AM, fluorescence intensity was measured using excitation and emission at 490 nm and 520 nm. W is in blue colour and stimulated is in red colour with data normalised to total cellular protein. Cell viability is expressed as percentages of control values ± S.E.M. in comparison to control from three independent experiments.

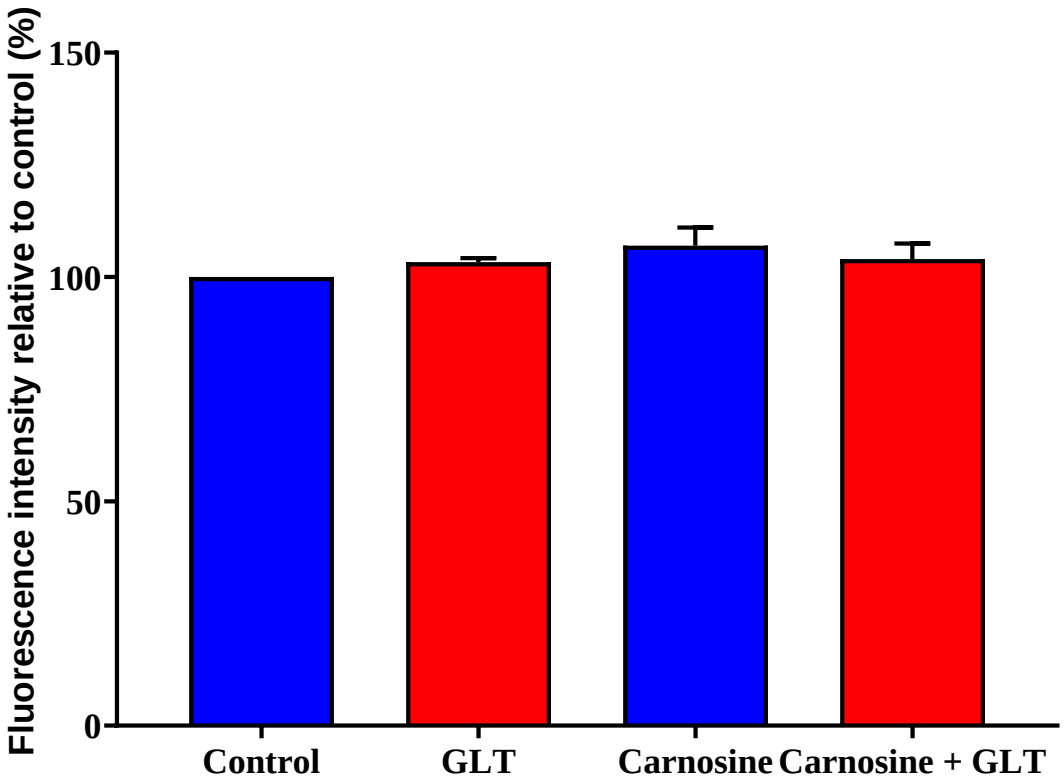

Figure 5.6 Effect of L-carnosine on C2C12 myotubes viability. C2C12 myotubes were incubated for 5 days in DMEM supplemented with 5% v/v horse serum and 1% v/v penstrep with glutamine ± 10 mM L-carnosine or GLT medium ± 10 mM L-carnosine. After 1 hour incubation with 5 μM solution of calcein-AM, fluorescence intensity was measured using excitation and emission at 490 nm and 520 nm. Cell viability is expressed as percentages of control values ± S.E.M. in comparison to control from three independent experiments.

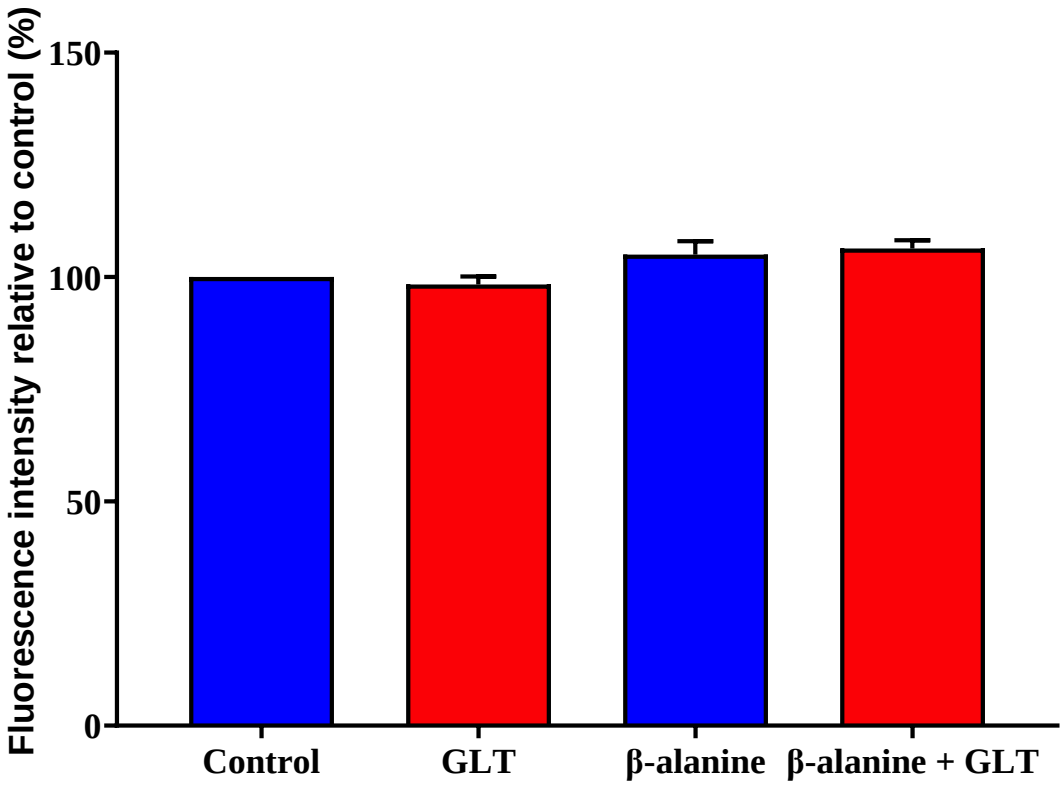

Figure 5.7 Effect of β-alanine on C2C12 myotubes viability. C2C12 myotubes were incubated for 5 days in DMEM supplemented with 5% v/v horse serum and 1% v/v penstrep with glutamine ± 10 mM β-alanine or GLT medium ± 10 mM β-alanine. After 1 hour incubation with 5 µM solution of calcein-AM, fluorescence intensity was measured using excitation and emission at 490 nm and 520 nm. Cell viability is expressed as percentages of control values ± S.E.M. in comparison to control from three independent experiments.

5.2.2 Scavenging potential of L-carnosine and β-alanine using INS-1 and C2C12 myotubes

To determine the level of radical species produced, INS-1 cells and C2C12 myotubes were incubated for 5 days in growth medium (INS-1 cells) or differentiation medium (C2C12 myotubes) ± 10 mM L-carnosine (or β-alanine) or GLT ± 10 mM L-carnosine (or β-alanine). DCFDA (20 µM) was added in Krebs-Ringer buffer solution for 1h, and reactive species formation was detected via fluorescence with excitation (495 nm) and emission (530 nm).

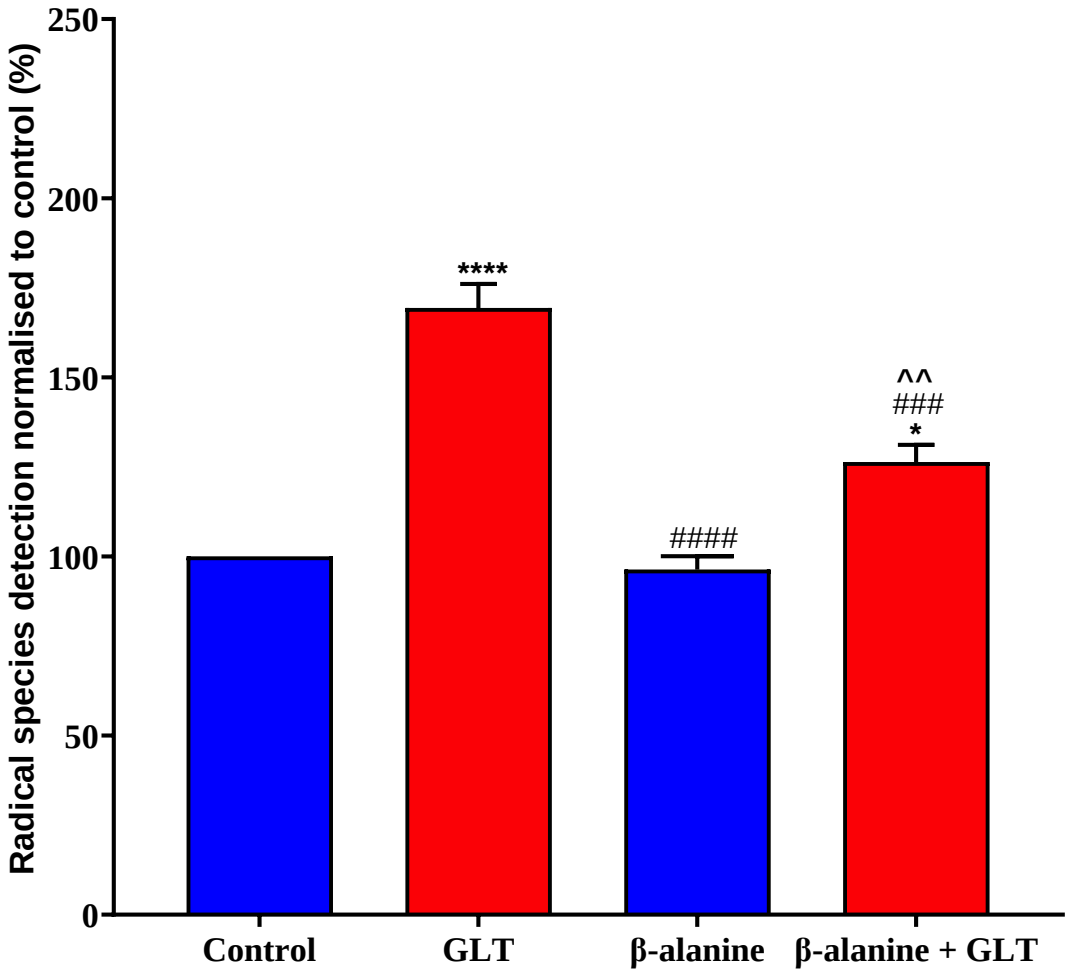

Figure 5.8 Effect of GLT and β-alanine on radical species production using INS-1 cells. INS-1 cells were incubated for 5 days in RPMI-1640 medium ± 10 mM β-alanine or GLT ± 10 mM β-alanine. DCFDA was added in Krebs-Ringer buffer solution for 1 hour, and reactive species production was detected via fluorescence with excitation (495 nm) and emission (530 nm). Reactive species are expressed as percentages of control values ± S.E.M. and data presented are from 3 independent experiments. Statistical analyses were carried out by one-way ANOVA followed by Tukey's multiple comparisons test as post hoc test (*p<0.05, ****p<0.0001 relative to control; $^{\#\#\#}$p<0.001, $^{\#\#\#\#}$p<0.0001 relative to GLT; ^p<0.05 relative to β-alanine).

Figure 5.8 shows the amount of production of reactive species generated in each condition. Exposure of INS-1 cells to GLT resulted in an increase in radical species of 69.33 ± 6.74% (p<0.0001) relative to control. The increase of radical species generation in β-alanine (96.33 ± 3.71, p<0.0001) was significantly lower than GLT. It was also observed that reactive species production in the presence of β-alanine

(96.33 ± 3.71) was lower but not significantly different relative to control. The increase of the radical species production in β-alanine + GLT (126.33 ± 4.81, p=0.0145) was significantly different to control. On the other hand, β-alanine + GLT (126.33 ± 4.81, p=0.0007) was significantly lower than GLT (169.33 ± 6.74). It was also observed that the increase of radical species in β-alanine + GLT (126.33 ± 4.81, p=0.0069) to β-alanine was significantly different. This indicates the effectiveness of β-alanine supplementation in reactive species scavenging in the INS-1 model.

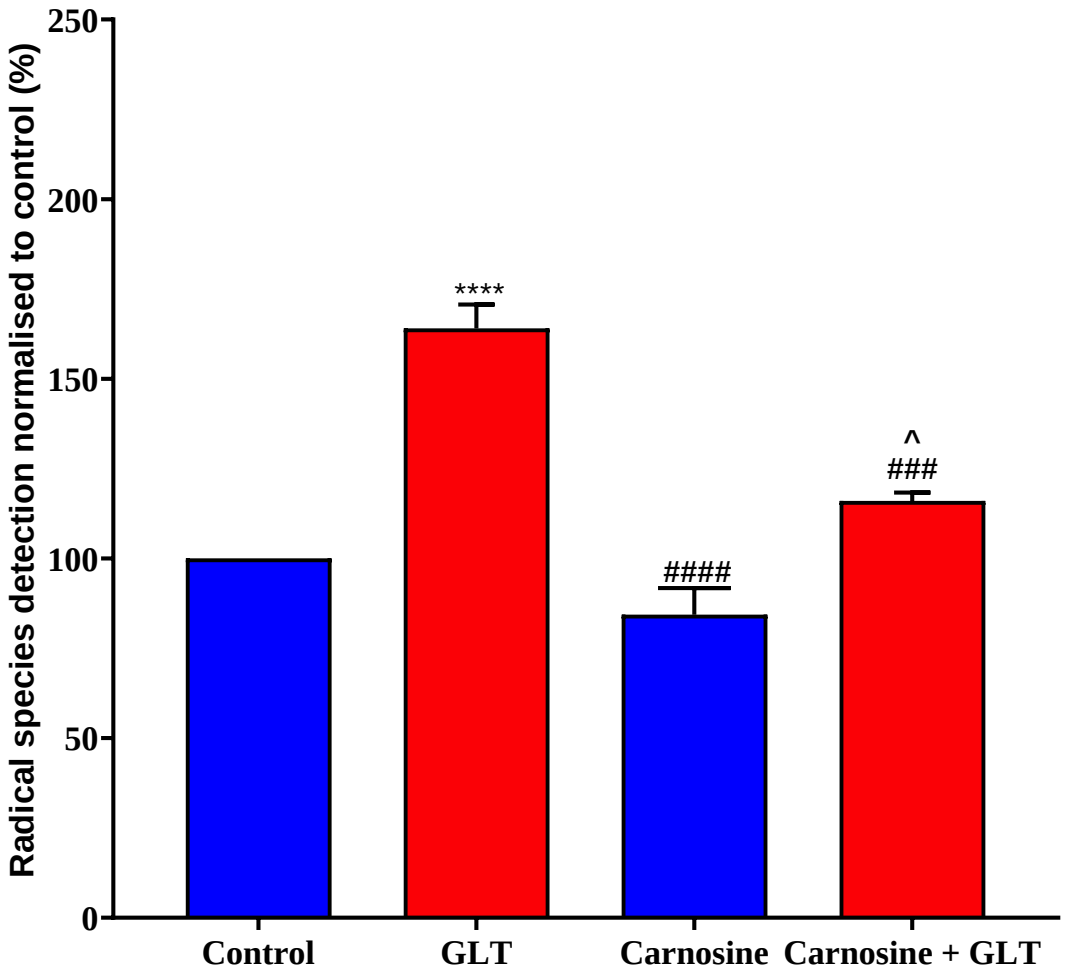

Figure 5.9 Effect of GLT and carnosine on radical species production using C2C12 myotubes. C2C12 myotubes were incubated for 5 days in DMEM supplemented with 5% v/v horse serum and 1% v/v penstrep with glutamine ± 10 mM L-carnosine or GLT ± 10 mM L-carnosine. DCFDA was added in Krebs-Ringer buffer solution for 1 hour, and reactive species production was detected via fluorescence with excitation (495 nm) and emission (530 nm). Reactive species are expressed as percentages of control values ± S.E.M. and data presented was from 3 independent experiments. Statistical analyses were carried out by one-way ANOVA followed by Tukey's multiple comparisons test as post hoc test (****$p<0.0001$ relative to control; $^{###}p<0.001$, $^{####}p<0.0001$ relative to GLT; ^$p<0.05$ relative to L-carnosine).

Figure 5.9 shows the amount of production of reactive species generated by exposing C2C12 myotubes to various experimental conditions. Exposure of C2C12 myotubes to GLT resulted in an increase in radical species of 64 ± 6.66% ($p<0.0001$) relative to control. It was also observed that reactive species production in the

presence of L-carnosine (84.33 ± 7.45%) was lower but not significantly different relative to control. Similarly, L-carnosine + GLT (116 ± 2.31%, p=0.0008) was significantly lower than the GLT (164 ± 6.66%). It was also observed that the increase of radical species in L-carnosine + GLT (116 ± 2.31%, p=0.0102) to L-carnosine was significantly different. This indicates the effectiveness of L-carnosine supplementation in scavenging reactive species in the C2C12 myotubes model.

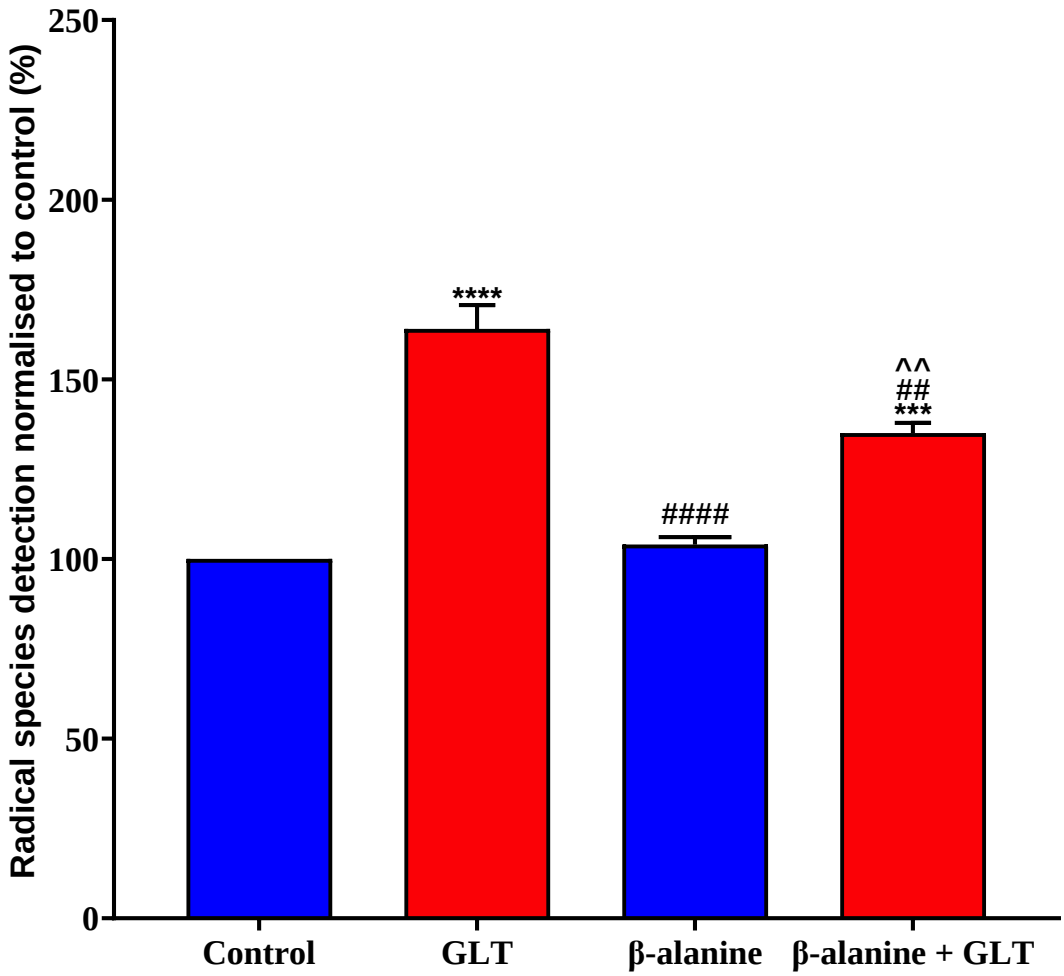

Figure 5.10 Effect of GLT and β-alanine on radical species production using C2C12 myotubes. C2C12 myotubes were incubated for 5 days in DMEM supplemented with 5% v/v horse serum and 1% v/v penstrep with glutamine ± 10 mM β-alanine or GLT ± 10 mM β-alanine. DCFDA was added in Krebs-Ringer buffer solution for 1 hour, and reactive species production was detected via fluorescence with excitation (495 nm) and emission (530 nm). Reactive species are expressed as percentages of control values ± S.E.M. and data presented was from 3 independent experiments. Statistical analyses were carried out by one-way ANOVA followed by Tukey's multiple comparisons test as post hoc test (***$p<0.001$, ****$p<0.0001$ relative to control; $^{\#\#}p<0.01$, $^{\#\#\#\#}p<0.0001$ relative to GLT; ^^$p<0.01$ relative to β-alanine).

Figure 5.10 shows the exposure of C2C12 myotubes to GLT resulted in an increase in radical species of 64 ± 6.66% ($p<0.0001$) relative to control. However, the radical species generation in GLT (164 ± 6.66%, $p<0.0001$) was significantly higher than β-alanine (104 ± 2.08%). The increase of radical species generation in β-alanine + GLT (35 ± 2.89%, $p=0.0008$) was significantly higher than control. On the other

hand, β-alanine + GLT (135 ± 2.89%, p=0.0028) was significantly lower than the GLT (164 ± 6.66%). It was also observed that the radical species production in β-alanine + GLT (35 ± 2.89%, p=0.0018) is significantly higher than β-alanine. This indicates the effectiveness of β-alanine supplementation in scavenging reactive species in the C2C12 myotubes model.

5.2.3 Effects of L-carnosine on the mitochondrial function exposed to glucolipotoxic condition

The Agilent Seahorse XFp Cell Mito Stress Test was used to assess the mitochondrial function of INS-1 cells and C2C12 myotubes exposed to high glucose and high fatty acid diet for 5 days. This measurement is directly involved by measuring the oxygen consumption rate of the cells in real-time via Seahorse XFp Extracellular Flux Analyser.

The assay used built-in injection ports where chemical modulators such as oligomycin, carbonyl cyanide-4 (trifluoromethoxy)phenylhydrazone (FCCP), and rotenone and antimycin are added in sequence into cell wells during the assay to reveal the key parameters of mitochondrial function.

Exposure of pancreatic β-cell to high glucose and high fatty acid has previously been shown to cause β-cell failure (Barlow and Affourtit, 2013). To determine whether L-carnosine has an effect on the damaging impact of GLT on mitochondrial function, the oxygen consumption rate (OCR) was measured using Agilent Seahorse XF analyser. The results shown that there was a reduction of the key parameters of the mitochondrial respiration as illustrated in **Figure 5.11** for INS-1 cells in GLT.

(A)

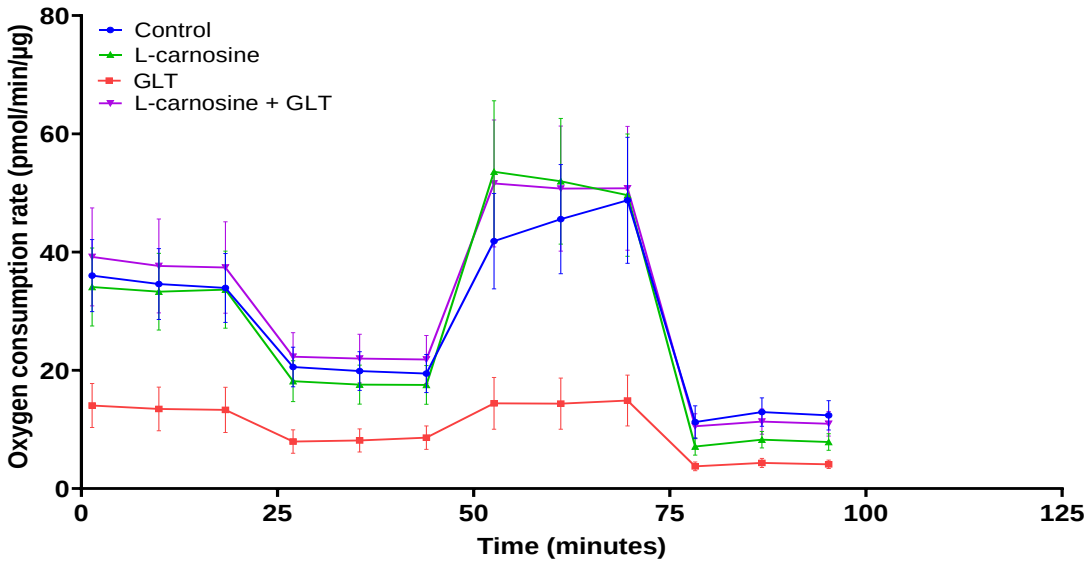

(B)

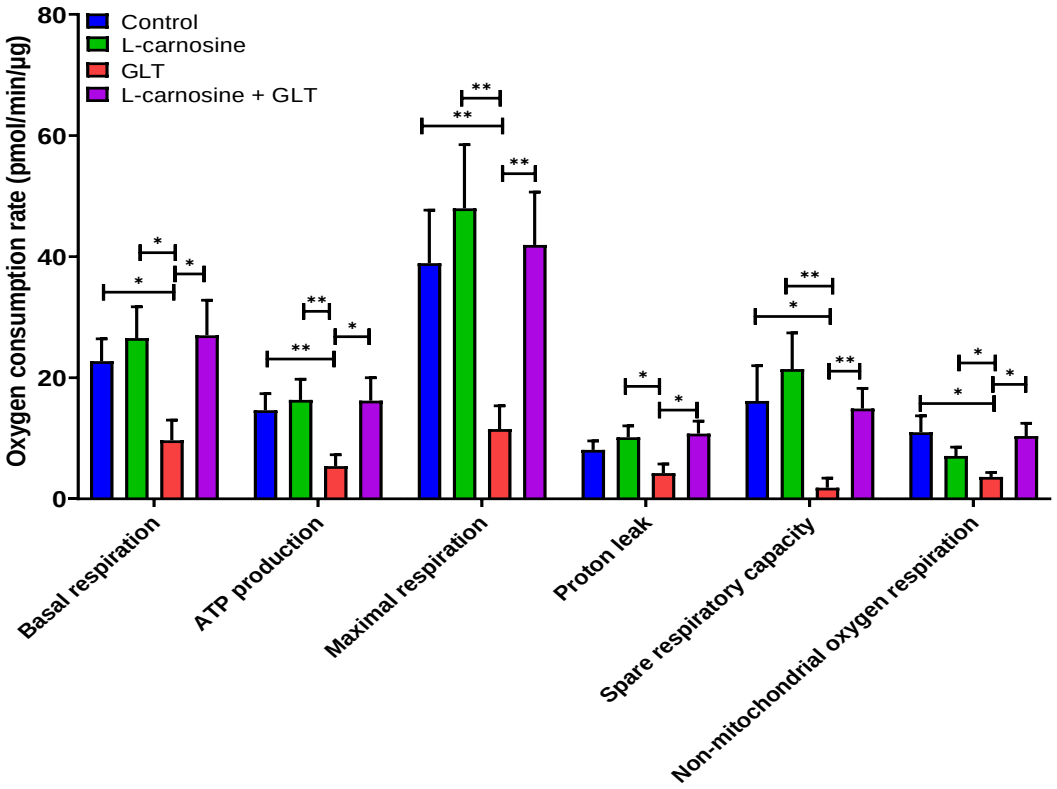

Figure 5.11 Effect of metabolic stress and carnosine on mitochondrial respiration of INS-1cells. (A) Independent traces of various experimental conditions. (B) Individual key parameters of mitochondrial respiration of INS-1 cells exposed to GLT and L-carnosine. INS-1 cells were treated with control medium, glucolipotoxic (GLT) media, L-carnosine, or GLT supplemented L-carnosine for 5 days, changing the medium on the third day. OCR was measured using a Seahorse XFe24 Analyser. Each data point represents a mean normalised OCR measurement from 3 independent experiments. Statistical analyses were carried out by one-way ANOVA followed by Tukey's multiple comparisons test as post hoc test (*p<0.05, **p<0.01).

The individual summary of each key parameter in mitochondrial respiration for INS-1 cells was presented in **Figure 5.11** and was discussed as follows:

For basal respiration, GLT was shown to significantly decrease the basal OCR to 9.67 ± 3.33 pmol/min/µg (p=0.0140, 57.48% reduction) relative to control (22.74 ± 3.70 pmol/min/µg). However, this reduction in basal respiration was increased significantly to 27.01 ± 5.80 pmol/min/µg (p=0.0259, 64.20% increase) upon supplementation of L-carnosine to GLT. Carnosine supplementation of control medium increased basal respiration to 26.55 ± 5.17 pmol/min/µg but no significant difference was observed.

For ATP-linked respiration, GLT was shown to significantly decrease the ATP production to 5.41 ± 1.87 pmol/min/µg (p=0.0099, 63.12% reduction) relative to control (14.67 ± 2.72 pmol/min/µg). However, this reduction in ATP production was increased significantly to 16.23 ± 3.77 pmol/min/µg (p=0.0289, 66.67% increase) upon supplementation of L-carnosine to GLT. Carnosine supplementation of control medium increased ATP production to 16.35 ± 3.41 pmol/min/µg but no significant difference was observed.

For maximal respiration, GLT was shown to significantly decrease the maximal OCR to 11.51 ± 3.86 pmol/min/µg (p=0.0091, 70.42% reduction) relative to control (38.91 ± 8.76 pmol/min/µg). However, this reduction in maximal respiration was increased significantly to 41.92 ± 8.74 pmol/min/µg (p=0.0085, 72.54% increase relative to GLT) upon supplementation of L-carnosine of GLT. Carnosine supplementation of control medium increased maximal respiration to 47.99 ± 10.51 pmol/min/µg.

For proton leak, GLT was shown to decrease the proton leak-linked respiration OCR to 4.26 ± 1.51 pmol/min/µg (47.41% reduction) relative to control (8.10 ± 1.47 pmol/min/µg). However, this was increased significantly to 10.78 ± 2.06 pmol/min/µg (p=0.0237, 60.48% increase) upon supplementation of L-carnosine to

GLT. Carnosine supplementation of control medium increased proton leak to 10.17 ± 1.89 pmol/min/µg.

For spare respiratory capacity, GLT was shown to significantly decreased the reserve respiratory capacity OCR to 1.82 ± 1.59 pmol/min/µg (p=0.0284, 88.74% reduction) relative to control (16.17 ± 5.82 pmol/min/µg). However, spare respiratory capacity was increased significantly to 14.92 ± 3.34 pmol/min/µg (p=0.0036, 87.80% increase) upon supplementation of L-carnosine to GLT. Carnosine supplementation of control medium increased spare respiratory capacity to 21.44 ± 5.96 pmol/min/µg.

GLT was shown to significantly decrease the non-mitochondrial respiration OCR to 3.63 ± 0.72 pmol/min/µg (p=0.0160, 67.00% reduction) relative to control (11.00 ± 2.70 pmol/min/µg). However, this level of non-mitochondrial respiration was increased significantly to 10.37 ± 2.10 pmol/min/µg (p=0.0131, 65.00% increase) upon supplementation of L-carnosine of GLT. Carnosine supplementation of control medium increased non-mitochondrial respiration to 7.08 ± 1.45 pmol/min/µg.

To assess whether L-carnosine affects the damaging impact of GLT on mitochondrial function in skeletal muscle, the oxygen consumption rate (OCR) was measured using an Agilent Seahorse XF analyser. The results shown a reduction of the key parameters of the mitochondrial respiration, as illustrated in **Figure 5.12** for C2C12 myotubes in GLT.

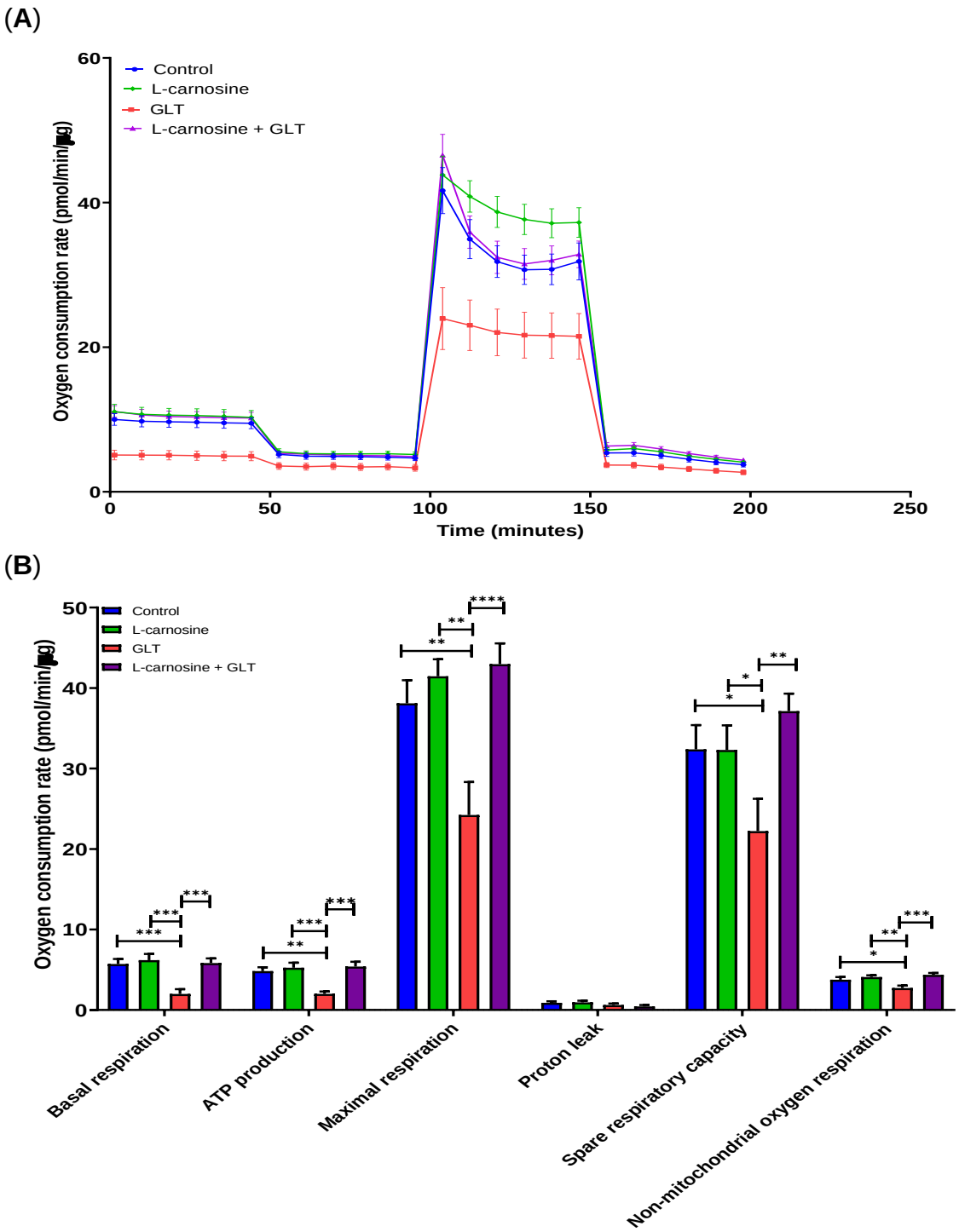

Figure 5.12 Effect of metabolic stress and carnosine on mitochondrial respiration of C2C12 myotubes. (A) Independent traces of various experimental conditions. (B) Individual key parameters of mitochondrial respiration of C2C12 myotubes exposed to GLT and L-carnosine. C2C12 myotubes were treated with control medium, glucolipotoxic (GLT) medium, L-carnosine, or GLT supplemented L-carnosine for 5 days, changing the medium on the third day. OCR was measured using a Seahorse XFe24 Analyser. Each data point represents a mean normalised OCR measurement from 3 independent experiments. Statistical analyses were carried out by one-way ANOVA followed by Tukey's multiple comparisons test as post hoc test (*p<0.05, **p<0.01, ***p<0.001, ****p<0.0001).

The individual summary of each key parameter in mitochondrial respiration for C2C12 myotubes was presented in **Figure 5.12** and was discussed as follows:

For basal respiration, GLT was shown to significantly decrease the basal OCR to 1.86 ± 0.62 pmol/min/µg (p=0.0002, 67.48% reduction) relative to control (5.72 ± 0.61 pmol/min/µg). However, this level of basal respiration was increased significantly to 5.83 ± 0.58 pmol/min/µg (p=0.0006, 68.10% increase relative to GLT) upon supplementation of L-carnosine of GLT. Carnosine supplementation to control medium increased basal respiration to 6.38 ± 0.76 pmol/min/µg.

For ATP-linked respiration, GLT was shown to significantly decrease the ATP production to 1.98 ± 0.33 pmol/min/µg (p=0.0021, 59.01% reduction) relative to control (4.83 ± 0.47 pmol/min/µg). However, this level of in ATP production was increased significantly to 5.39 ± 0.60 pmol/min/µg (p=0.0002, 63.27% increase relative to GLT) upon supplementation of L-carnosine of GLT. Carnosine supplementation to control medium increased ATP production to 5.48 ± 0.62 pmol/min/µg.

For maximal respiration, GLT was shown to significantly decrease the maximal OCR to 22.43 ± 3.99 pmol/min/µg (p=0.0039, 41.13% reduction) relative to control (38.10 ± 2.86 pmol/min/µg). However, this reduction in maximal respiration was increased significantly to 42.97 ± 2.58 pmol/min/µg (p=0.0004, 47.80% increase relative to GLT) upon supplementation of L-carnosine of GLT. Carnosine supplementation to control medium increased maximal respiration to 40.96 ± 2.11 pmol/min/µg.

For proton leak, GLT was shown to decrease the proton leak-linked respiration OCR to 0.55 ± 0.19 pmol/min/µg (38.00% reduction) relative to control (0.89 ± 0.19 pmol/min/µg). Supplementation of L-carnosine to GLT gave an OCR of 0.55 ± 0.19 pmol/min/µg whilst carnosine supplementation of control medium resulted in a proton leak of 0.91 ± 0.21 pmol/min/µg.

For spare respiratory capacity, GLT was shown to significantly decrease the reserve respiratory capacity OCR to 20.57 ± 3.95 pmol/min/µg (p=0.0257, 36.47% reduction) relative to control (32.38 ± 3.01 pmol/min/µg). However, this level of spare respiratory capacity was increased significantly to 37.14 ± 2.17 pmol/min/µg (p=0.0088, 44.61% increase relative to GLT) upon supplementation of L-carnosine of GLT. Carnosine supplementation of control medium increased spare respiratory capacity to 31.43 ± 3.17 pmol/min/µg.

For non-mitochondrial oxygen respiration, GLT was shown to significantly decrease the non-mitochondrial respiration OCR to 2.69 ± 0.32 pmol/min/µg (p=0.0489, 28.46% reduction) relative to control (3.76 ± 0.32 pmol/min/µg). However, this level of non-mitochondrial respiration was increased significantly to 4.37 ± 0.24 pmol/min/µg (p=0.0005, 38.44% increase relative to GLT) upon supplementation of L-carnosine of GLT. Carnosine supplementation to control medium increased non-mitochondrial respiration to 4.15 ± 0.22 pmol/min/µg.

In summary, GLT was shown to reduce all the key parameters in mitochondrial respiration, i.e., basal respiration, ATP production, maximal respiration, proton leak, reserve respiratory capacity and non-mitochondrial oxygen respiration. However, this reduction was shown to either be prevented or else significantly enhanced upon supplementation of GLT medium with L-carnosine both INS-1 and C2C12 myotube cell models.

5.2.4 Effects of β-alanine on the mitochondrial function exposed to glucolipotoxic condition

To assess whether β-alanine affects the damaging impact of GLT on mitochondrial function, the oxygen consumption rate (OCR) was measured using Agilent Seahorse XF analyser. The results shown that there was a reduction in the key parameters of mitochondrial respiration as illustrated in **Figure 5.13** for INS-1 cells in GLT.

(**A**)

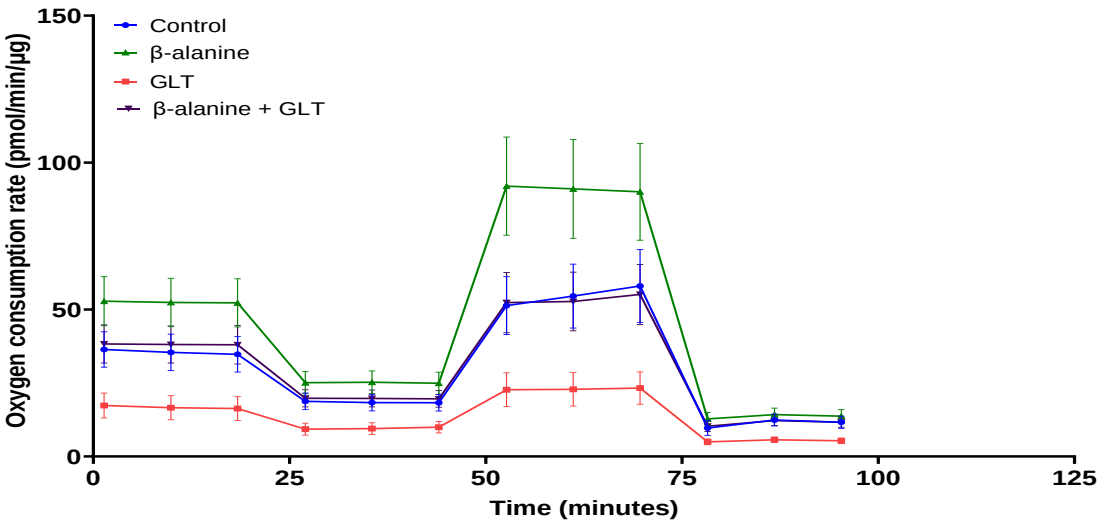

(**B**)

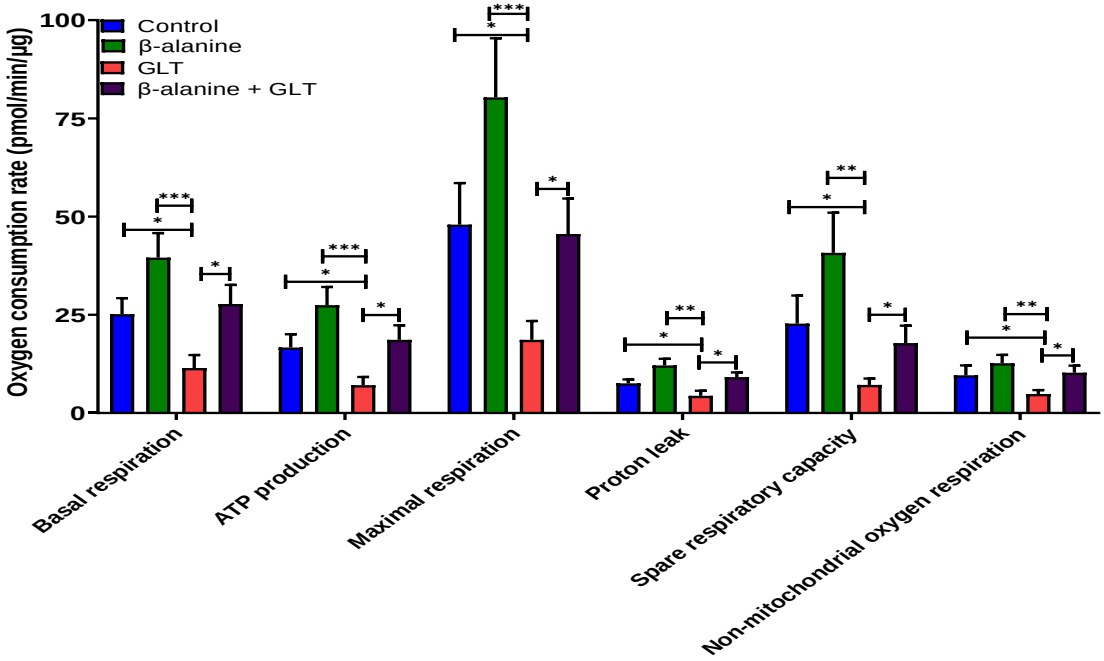

Figure 5.13 Effect of metabolic stress and β-alanine on mitochondrial respiration of INS-1cells. (A) Independent traces of various experimental conditions. (B) Individual key parameters of mitochondrial respiration of INS-1 cells exposed to GLT and β-alanine. INS-1 cells were treated with control medium, glucolipotoxic (GLT) medium, β-alanine, or GLT supplemented β-alanine for 5 days, changing the medium on the third day. OCR was measured using a Seahorse XFe24 Analyser. Each data point represents a mean normalised OCR measurement from 3 independent experiments. Statistical analyses were carried out by one-way ANOVA followed by Tukey's multiple comparisons test as post hoc test (*p<0.05, **p<0.01, ***p<0.001)**.**

The individual summary of each key parameter in mitochondrial respiration for INS-1 cells was presented in **Figure 5.13** and was discussed as follows:

For basal respiration, GLT was shown to significantly decrease the basal OCR to 11.47 ± 3.28 pmol/min/µg (p=0.0155, 54.44% reduction) relative to control (25.18 ± 4.07 pmol/min/µg). However, this level of basal respiration was increased significantly to 27.76 ± 4.86 pmol/min/µg (p=0.0103, 58.68% increase relative to GLT) upon supplementation of β-alanine of GLT. β-alanine supplementation of control media increased basal respiration to 39.57 ± 6.23 pmol/min/µg.

For ATP-linked respiration, GLT was shown to significantly decrease the ATP production to 7.08 ± 2.09 pmol/min/µg (p=0.0247, 57.53% reduction) relative to control (16.67 ± 3.38 pmol/min/µg). However, this level of ATP production was increased significantly to 18.62 ± 3.70 pmol/min/µg (p=0.0113, 61.98% increase relative to GLT) upon supplementation of β-alanine of GLT. β-alanine supplementation of control media increased ATP production to 27.46 ± 4.61 pmol/min/µg.

For maximal respiration, GLT was shown to significantly decrease the maximal OCR to 18.63 ± 4.80 pmol/min/µg (p=0.0193, 61.15% reduction) relative to control (47.95 ± 10.57 pmol/min/µg). However, this reduction in maximal respiration was increased significantly to 45.56 ± 9.05 pmol/min/µg (p=0.0136, 59.11% increase relative to GLT) upon supplementation of β-alanine of GLT. β-alanine supplementation of control media increased maximal respiration to 80.35 ± 15.06 pmol/min/µg.

For proton leak, GLT was shown to significantly decrease the proton leak-linked respiration OCR to 4.38 ± 1.28 pmol/min/µg (p=0.0434, 41.99% reduction) relative to control (7.55 ± 0.99 pmol/min/µg). However, this reduction in proton leak was increased significantly to 9.13 ± 1.21 pmol/min/µg (p=0.0139, 52.03% increase relative to GLT) upon supplementation of β-alanine of GLT. β-alanine

supplementation of control media increased proton leak to 12.10 ± 1.70 pmol/min/µg.

For spare respiratory capacity, GLT was shown to significantly decrease the reserve respiratory capacity OCR to 7.17 ± 1.62 pmol/min/µg (p=0.0444, 68.51% reduction) relative to control (22.77 ± 7.13 pmol/min/µg). However, this reduction in spare respiratory capacity was increased significantly to 17.80 ± 4.43 pmol/min/µg (p=0.0299, 59.72% increase) upon supplementation of β-alanine of GLT. β-alanine supplementation of control media increased the spare respiratory capacity to 40.78 ± 10.21 pmol/min/µg.

For non-mitochondrial oxygen respiration, GLT was shown to significantly decrease the non-mitochondrial respiration OCR to 4.85 ± 0.99 pmol/min/µg (p=0.0467, 49.43% reduction) relative to control (9.59 ± 2.51 pmol/min/µg). However, this reduction in non-mitochondrial respiration was increased significantly to 10.26 ± 1.78 pmol/min/µg (p=0.0131, 52.73% increase relative to GLT) upon supplementation of β-alanine of GLT. β-alanine supplementation of control media increased non-mitochondrial respiration to 12.69 ± 2.11 pmol/min/µg.

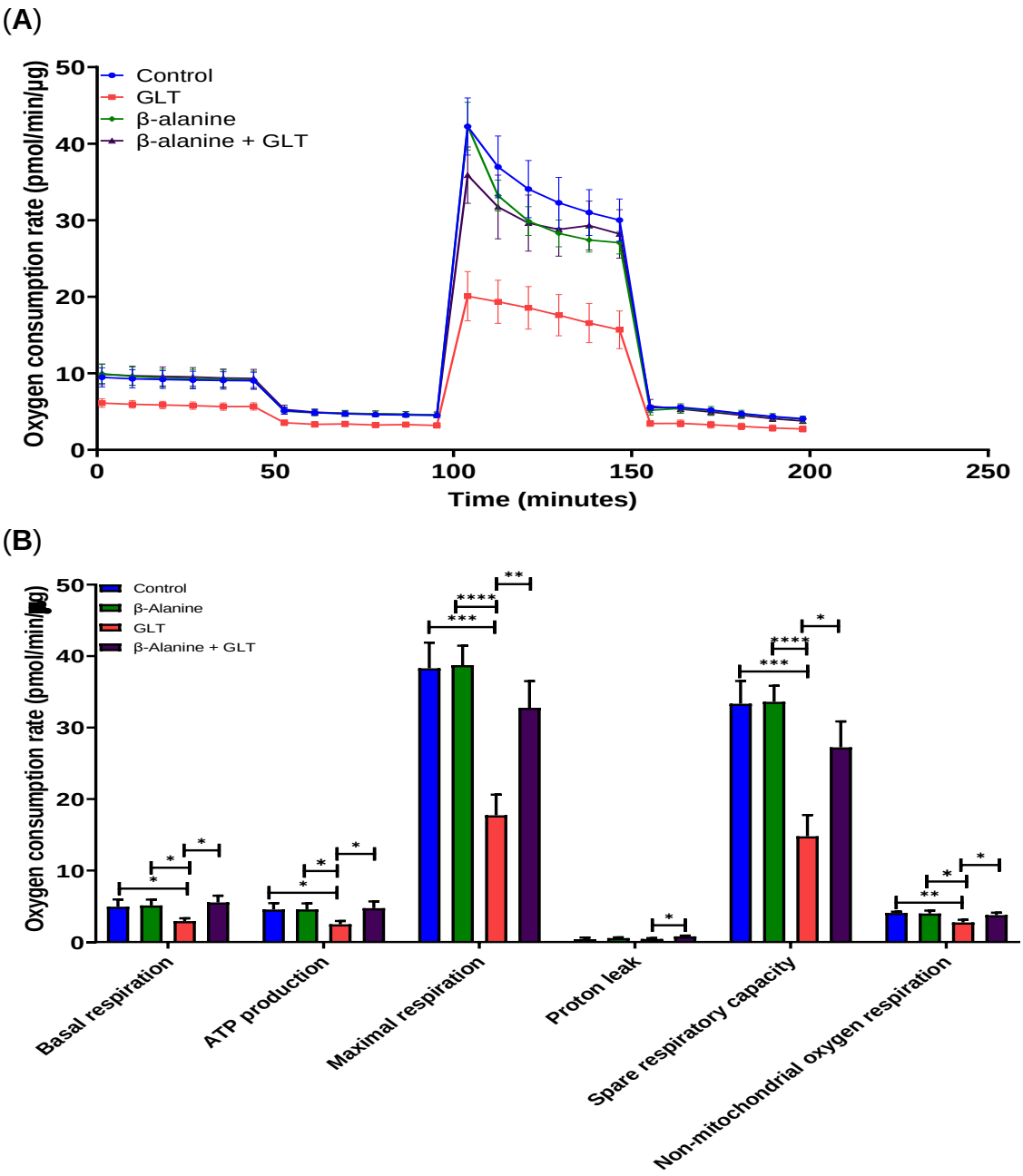

Figure 5.14 Effect of metabolic stress and β-alanine on mitochondrial respiration of C2C12 myotubes. (A) Independent traces of various experimental conditions. (B) Individual key parameters of mitochondrial respiration of C2C12 myotubes exposed to GLT and β-alanine. C2C12 myotubes were treated with control medium, glucolipotoxic (GLT) medium, β-alanine, or GLT supplemented β-alanine for 5 days, changing the medium on the third day. OCR was measured using a Seahorse XFe24 Analyser. Each data point represents a mean normalised OCR measurement from 3 independent experiments. Statistical analyses were carried out by one-way ANOVA followed by Tukey's multiple comparisons test as post hoc test (*p<0.05, **p<0.01, ***p<0.001, ****p<0.0001)**.**

The individual summary of each key parameter in mitochondrial respiration for C2C12 myotubes was presented in **Figure 5.14** and was discussed as follows:

For basal respiration, GLT was shown to significantly decrease the basal OCR to 2.93 ± 0.39 pmol/min/µg (p=0.0402, 40.81% reduction) relative to control (4.95 ± 1.01 pmol/min/µg). However, this reduction in basal respiration was increased significantly to 5.55 ± 0.94 pmol/min/µg (p=0.0480, 47.21% increase relative to GLT) upon supplementation of β-alanine of GLT. β-alanine supplementation of control medium increased basal respiration to 5.13 ± 0.82 pmol/min/µg.

For ATP-linked respiration, GLT was shown to significantly decrease the ATP production to 2.48 ± 0.46 pmol/min/µg (p=0.0276, 45.49% reduction) relative to control (4.55 ± 0.89 pmol/min/µg). However, this reduction in ATP production was increased significantly to 4.75 ± 0.93 pmol/min/µg (p=0.0437, 47.79% increase relative to GLT) upon supplementation of β-alanine of GLT. β-alanine supplementation of control medium increased ATP production to 4.57 ± 0.84 pmol/min/µg.

For maximal respiration, GLT was shown to significantly decrease the maximal OCR to 17.73 ± 2.90 pmol/min/µg (p=0.0004, 53.71% reduction) relative to control (38.30 ± 3.59 pmol/min/µg). However, this reduction in maximal respiration was increased significantly to 32.78 ± 3.72 pmol/min/µg (p=0.0035, 45.91% increase relative to GLT) upon supplementation of β-alanine of GLT. β-alanine supplementation of control medium increased maximal respiration to 38.75 ± 2.72 pmol/min/µg.

For proton leak, GLT was shown to slightly increase the proton leak-linked respiration OCR to 0.44 ± 0.12 pmol/min/µg relative to control (0.40 ± 0.22 pmol/min/µg) but no significant difference was observed. However, the proton leak shown in GLT was increased to 0.80 ± 0.10 pmol/min/µg (p=0.0374, 45.00%

increase relative to GLT) upon supplementation of β-alanine of GLT. β-alanine supplementation of control medium increased proton leak to 0.55 ± 0.11 pmol/min/µg.

For spare respiratory capacity, GLT was shown to significantly decrease the reserve respiratory capacity OCR to 14.80 ± 2.98 pmol/min/µg (p=0.0006, 55.62% reduction) relative to control (33.35 ± 3.18 pmol/min/µg). However, this reduction in spare respiratory capacity was increased significantly to 27.23 ± 3.63 pmol/min/µg (p=0.0175, 45.65% increase relative to GLT) upon supplementation of β-alanine of GLT. β-alanine supplementation of control medium increased spare respiratory capacity to 33.62 ± 2.24 pmol/min/µg.

For non-mitochondrial oxygen respiration, GLT was shown to significantly decrease the non-mitochondrial respiration OCR to 2.74 ± 0.38 pmol/min/µg (p=0.0056, 32.68% reduction) relative to control (4.07 ± 0.17 pmol/min/µg). However, this reduction in non-mitochondrial respiration was increased significantly to 3.78 ± 0.34 pmol/min/µg (p=0.0290, 27.51% increase relative to GLT) upon supplementation of β-alanine of GLT. β-alanine supplementation of control medium have showed no significant difference on non-mitochondrial respiration relative to control.

In summary, GLT has been shown to reduce all the key parameters in the mitochondrial respiration, i.e., basal respiration, ATP production, maximal respiration, proton leak, reserve respiratory capacity and non-mitochondrial oxygen respiration. However, this reduction was shown to either be prevented or else significantly enhanced upon supplementation of medium with β-alanine in both INS-1 and C2C12 myotube cell models.

5.3 Discussion

Mitochondria are double membrane-bound cell organelles. Through mitochondrial oxidative phosphorylation system (OXPHOS), they generate ATP to supply the energy demand of tissues and organs (Manoli et al., 2007). Mitochondria are considered as powerhouses of the cell as they produced ATP required for the normal functions of the cells (Giacomello et al., 2020).

To assess the effects of the L-carnosine and β-alanine supplementation on INS-1 cells and C2C12 myotube viability, calcein-AM assay was conducted. As shown in the results (see **Figures 5.5-5.7**), addition of 10 mM L-carnosine and 10 mM β-alanine to the growth and differentiation media for INS-1 and C2C12 myotubes, respectively, did not affect the health and morphology of the cells. This result indicates that the conditions used in the experiment were not cytotoxic to the cells.

The level of reactive species generated by GLT was evaluated using DCFDA assay (see **Chapter 2 and 6** for more details); it was found that exposure of INS-1 cells and C2C12 myotubes to GLT conditions increased the level of reactive species generated compared to the control. However, when added to the medium L-carnosine and β-alanine were able to scavenge ROS and significantly prevent/reverse the effects of GLT by decreasing the amount of reactive species generated relative to the control condition of each cell model. This means that supplementation of medium with L-carnosine and β-alanine can help in sequestering the excess amount of reactive species generated and prevent its associated toxic effects.

Reactive oxygen species have shown to increase as a result of exposure to high glucose (glucotoxicity) (Tanaka et al., 2002), and high glucose and high fatty acids (GLT) (Barlow and Affourtit, 2013) in β-cell lines and isolated islets. Under normal conditions, the metabolism of glucose and fatty acids generates oxidants.

ROS formed during glucose metabolism in the mitochondrial OXPHOS has been shown to trigger the generation of superoxide anion radical (da-Silva et al., 2004; Nishikawa et al., 2000; Sakai et al., 2003). However, when there is an overproduction of reactive oxygen species this will lead to oxidative stress and cause oxidation damage to proteins, lipids and DNA (St-Pierre et al., 2002; Turrens, 2003) and consequently mitochondrial dysfunction (Brand and Nicholls, 2011).

Glucolipotoxicity has been shown to produce superoxide anion and NO species which react to form peroxynitrite which subsequently forms 3-nitrotyrosine (3-NT) adducts, a biomarker of cell damage and inflammation (Cripps et al., 2017). Also, glucolipotoxicity has been shown to form 4-hydroxynonenal (4-HNE), a product of lipid peroxidation (Cripps et al., 2017). 3-NT and 4-HNE adducts are inducers of oxidative stress and cause oxidative damage to recipient protein or lipids (Chen and Niki, 2006). L-carnosine supplementation to GLT medium has been shown to significantly reduce the production of 3-NT and 4-HNE adducts (Cripps et al., 2017). The formation of these adducts causes oxidative stress and affects the electron transport chain activity as shown in the mitochondrial respiration results presented here.

Defects in the skeletal muscle causing insulin resistance and inhibition of glucose-stimulated insulin secretion by pancreatic β-cells are prominent characteristics of type 2 diabetes which is caused by mitochondrial dysfunction (Gonzalez-Franquesa and Patti, 2017; Lowell and Shulman, 2005). Mitochondrial dysfunction with increased lipid peroxidation product has been reported in the skeletal muscle of insulin-resistant individuals with type 2 diabetes (Kelley et al., 2002) and it has been shown to have decreased muscle oxidative capacity, level of nuclear gene expression involved in oxidative metabolism and mitochondrial electron transport chain activity (Ritov et al., 2010). Mitochondria are multifunctional organelles that have a fundamental role in cellular energy metabolism (McLean et

al., 2014; Wada and Nakatsuka, 2016) and regulation of cell death as a second primary function (Ott et al., 2007). Mitochondria can undergo mitochondrial fusion and fission, mitophagy, and mitochondrial biogenesis (Rovira-Llopis et al., 2017). Mitochondria process the production of ATP via oxidative phosphorylation. This ATP synthesis is commonly assessed through the indirect determination of the amount of mitochondrial oxygen consumption or respiration. The changes observed in the respiratory kinetics in response to specific nutrients/substrates are commonly an indication of alterations in oxidative phosphorylation (Perry et al., 2013).

In type 2 diabetes, it has been shown that there is an excess generation of reactive oxygen species, plus decreased ATP production and mitochondrial dysfunction (Rovira-Llopis et al., 2017). Mitochondrial dysfunction has been reported to play a vital role in the mechanism of type 2 diabetes (Kowluru, 2019; Pinti et al., 2019). Mitochondrial dysfunction is not only observed in type 2 diabetes (Nicholls and Ferguson, 2013) but also in various pathologies such as aging (Terzioglu and Larsson, 2007), cancer (Hsu et al., 2016; Księżakowska-Łakoma et al., 2014) and neurodegenerative diseases (Cho et al., 2010; Nicholls and Ferguson, 2013) including Alzheimer's disease, Parkinson's disease and Huntington's disease. Mitochondrial dysfunction in skeletal muscles has been shown to be involved in the pathogenesis of type 2 diabetes (Bonnard et al., 2008). Rieusset and colleague conducted a study on the effects of high sucrose and high fat diet in mouse muscle mitochondria and it was shown that an increase in ROS production has a negative effect on mitochondrial biogenesis, structure and function (Bonnard et al., 2008). This excess generation of ROS was seen to be involved in mitochondrial alteration; however, they also reported that supplementation with antioxidant compound reverses the effects of ROS and restored mitochondrial integrity (Bonnard et al., 2008). ROS-induced mitochondrial dysfunction can lead to oxidative stress which in turn causes alteration to lipid metabolism, increased production of intracellular lipid

content, and lipid-dependent insulin resistance in muscle cells (Fridlyand and Philipson, 2006).

It has been reported that skeletal muscle myotubes exposed to high glucose or high fatty acid induced-ROS generation show mitochondrial damage (Bonnard et al., 2008). The high-glucose and high-fatty acid induced-ROS production has been shown to cause oxidative stress (Furukawa et al., 2004; Nishikawa et al., 2000). However, it was reported that in the absence of high fatty acid, high glucose was not effective enough to elevate ROS production and trigger mitochondrial dysfunction (Bonnard et al., 2008). However, it was shown that decreasing or normalising the amount of mitochondrial ROS generated could inhibit advanced glycation end-product formation and activation of protein kinase C, build-up of sorbitol and activation of NFκB (Nishikawa et al., 2000).

This study has shown that GLT has generated an excess amount of ROS and reactive nitrogen species (RNS) (see **Chapter 6**). This GLT effect was prevented by the addition of L-carnosine or β-alanine to the cell culture medium. To determine the effects of GLT on mitochondrial function, the Seahorse mito stress assay was conducted. In this assay, parameters such as basal respiration, ATP production, maximal respiration, proton leak, reserve respiratory capacity and non-mitochondrial oxygen respiration were evaluated.

To summarise the results in the mito stress assay, INS-1 cells and C2C12 myotubes exposed for five days in GLT condition significantly decreased their mitochondrial oxygen consumption respiration (OCR) level in all parameters relative to control. However, supplementing their media with L-carnosine or β-alanine prevented this observation by increasing the level of OCR that would otherwise have been inhibited by GLT both in INS-1 cells and C2C12 myotubes.

Basal oxygen consumption is reflective of transport of calcium and other ions across the inner membrane (Duchen, 1992). Mitochondrial dysfunction in type 2

diabetes alters calcium ion transport. This dysregulation of the calcium ion homeostasis is involved in the pathogenesis of type 2 diabetes and insulin sensitivity (Wang et al., 2017).

For ATP-linked respiration, it was found that there was a decrease of ATP production upon exposing INS-1 cells and C2C12 myotubes to GLT. This decrease in ATP-linked oxygen respiration indicates a reduction ATP synthesis (Divakaruni et al., 2014). ATP synthase is a mitochondrial enzyme complex that utilises ADP to form ATP. A study conducted by Köhnke et al. showed that chronic exposure of INS-1 cells to a high concentration of palmitic acid and oleic acid in addition to high glucose, resulted in a significant reduction of ATP synthase β-subunit protein expression (Köhnke et al., 2007). They also found that this reduction was associated with decreasing intracellular ATP content and insulin secretion (Köhnke et al., 2007). The decrease of insulin secretion due to exposure to GLT has also been reported in our group (Cripps et al., 2017). However, this GLT insulin secretion inhibitory effect was reversed by the addition of L-carnosine to the media of INS-1 cells and primary mouse islets (Cripps et al., 2017), data similar to that shown in my results for INS-1 cells (see **Chapter 6**). This study shows that supplementation with either L-carnosine and β-alanine can significantly reverse the ATP-linked oxygen respiration inhibition by GLT.

Proton leak-associated respiration indicates either mitochondrial damage (Dranka et al., 2011) or normal physiological response (Divakaruni and Brand, 2011). It has been shown that GLT significantly reduced the proton leak and indicated mitochondrial damage, and this was reversed significantly upon medium supplementation with L-carnosine and β-alanine. Spare respiratory capacity has also been investigated here, and this parameter displays a response to an increase in ATP demand under stressful conditions. Cells exposed to GLT were shown to

have a significantly lowered reserve capacity and maximal oxygen respiration compared to control, indicating that GLT can drive mitochondrial dysfunction.

A study by Lim and colleagues reported that when β-cells were exposed to high glucose and GLT, there was a significant increase of the mitochondrial electron transport chain complex subunits expression levels, β-cell apoptosis, intracellular lipid accumulation, oxidative stress, endoplasmic reticulum stress, nuclear NF-κB, sterol regulatory element binding protein 1c (SREBP1c) and lipogenic enzymes (Lim et al., 2011). In contrast, there was a significant decrease in citrate synthase activity, glucose-stimulated insulin secretion and intracellular ATP production (Lim et al., 2011). On the other hand, fatty acid β-oxidation has been shown to facilitate the generation of mitochondrial reactive oxygen species (Seifert et al., 2010; St-Pierre et al., 2002; Tahara et al., 2009) and cause endothelial dysfunction during hypoglycaemia (Kajihara et al., 2017), and kidney damage in diabetes (Rosca et al., 2012). But it was also reported that reactive oxygen species generated by free fatty acids originate from peroxisomes instead of from fatty acid β-oxidation (Elsner et al., 2011).

Ashcroft and colleagues have used islets of diabetic βV59M mice exposed to hyperglycaemia and found that multiple genes and proteins implicated in glycolysis and gluconeogenesis pathway were upregulated. In contrast to this upregulation, downregulation of genes and proteins involved in oxidative phosphorylation was seen (Haythorne et al., 2019). These results were also shown when INS-1 β-cells were exposed to high glucose and exhibited a similar significant reduction of mitochondrial metabolism and production of ATP (Haythorne et al., 2019).

Chronic exposure of β-cells with the combination of high glucose and high fatty acids inhibits glucose-stimulated insulin secretion, and lowering the amount of free fatty acid has been shown to lower insulin resistance and hyperinsulinemia (Carpentier et al., 1999; Zhou and Grill, 1994). It was also observed that reducing

the plasma free fatty acid improved the oral glucose tolerance of obese type 2 diabetes patients (Santomauro et al., 1999).

Studies have shown that in addition to β-cell dysfunction resulting from exposure to free fatty acids (Cnop et al., 2001; Lupi et al., 2002), it was also observed that a combination of free fatty acids with glucose amplifies the induction of apoptosis (El-Assaad et al., 2003). It has been seen that GLT drives mitochondrial dysfunction by altering mitochondrial fusion and fission in favour of the loss of the ability to undergo fusion. It was also observed that ATP production decreased and suppressed autophagic turnover (Las et al., 2011), chronic exposure of cells with GLT has been shown to reduce mitochondrial potential and thereby reducing ATP production (El-Assaad et al., 2010; Wikstrom et al., 2007), and oxygen consumption rate decreased (Barlow and Affourtit, 2013).

The radical scavenging effect of β-alanine supplementation presented here can be associated with its utilisation by carnosine synthase to form carnosine. Thereby, β-alanine supplementation has been able to promote the sequestering reactive species and reverse the adverse effects of GLT on the production of radical species and consequently improve mitochondrial function.

5.4 Conclusion

This study has shown that addition of L-carnosine or β-alanine into the media of INS-1 cells and C2C12 myotubes is effective in scavenging reactive species. Also, supplementation with these compounds at 10 mM concentration does not affect the health of both cell models. The effect of GLT on mitochondrial function has been shown to decrease all critical parameters such as basal respiration, maximal respiration, proton leak, spare respiration capacity, non-mitochondrial oxygen consumption and ATP production which is indicative of mitochondrial dysfunction. However, the reduction of all critical parameters in assessing mitochondrial function

were reversed upon medium supplementation with L-carnosine or β-alanine. This suggests that the effectiveness of L-carnosine and β-alanine to prevent mitochondrial dysfunction mediated by GLT is likely due to the ability of these compounds to effectively sequester radical species and thus, result in the protection of mitochondrial function.

Chapter 6

Carnosine, Carnosine Inhibitors and Carnosine Mimetics

6.1 Introduction

Carnosine (β-alanyl-L-histidine) is a natural dipeptide present in mammalian tissues (de Courten et al., 2015; Unno et al., 2008). It was discovered by V.S. Gulewitch, a Russian chemist, in 1900 in Liebig's meat extract (Gulewitsch and Amiradžibi, 1900) as an abundant non-protein nitrogen-containing compound of meat. It is a structurally bioactive compound synthesised by carnosine synthase, EC 6.3.2.11, from β-alanine and L-histidine (Usui et al., 2013).

Carnosine can be found in skeletal muscle where its amount is higher than other tissues (Sale et al., 2013), and it can also be present in brain regions and body fluids. However, carnosine concentration here was 10- to 1000- fold lower than in muscle tissue (Boldyrev et al., 2013). Only skeletal muscle and olfactory bulb in mammals have a carnosine concentration as high as the millimolar range (Boldyrev et al., 2013).

A methylated form of carnosine was found and identified in goose and chicken muscles (anserine), snake muscle (ophidine) and whale muscle (balenine) (Boldyrev et al., 2013). Amongst the mammals, only humans have carnosine and the rest mostly have both carnosine and one of the methylated carnosine. Variable high concentrations of carnosine and anserine in vertebrates were found in skeletal muscle and brain tissue, whilst in marine mammals and reptilian species, balenine was in significant amount (Kwiatkowski et al., 2018). In *Homo sapiens*, carnosine concentration ranges from 12-60 mmol/kg·dm^3 in the vastus lateralis muscle (Sale et al., 2013).

A recent study found that carnosine is considered a scavenger of radical oxygen and nitrogen species (RONS) (Cripps et al., 2017) such as hydroxyl radicals (Tamba and Torreggiani, 1999), peroxy radicals (Kohen et al., 1991), superoxide radicals (Pavlov et al., 1993), and protects against peroxynitrite-induced tyrosine nitration (Fontana et al., 2002), and hypochlorite (Hipkiss et al., 1995). Carnosine

was found to prevent the formation of advanced lipoxidation end-products (ALEs) and advanced glycoxidation end-products (AGEs) (Boldyrev et al., 2013). Carnosine has potential neuroprotective and neurotransmitter functions in the brain (Teufel et al., 2003).

With all the beneficial effects presented here of the endogenous and supplemented carnosine, it was observed to be rapidly hydrolysed in the serum by CN1 and in the intracellular environment by CN2 (Teufel et al., 2003). Human serum carnosinase (CNDP1; CN1) and human tissue carnosinase (also known as cytosolic nonspecific dipeptidase; CNDP2; CN2) are carnosine degrading enzymes and have been identified in human (Teufel et al., 2003) and mouse (Otani et al., 2005).

There are two main strategies proposed to overcome the problem of the hydrolysis of carnosine by carnosinase (Bellia et al., 2014)

1. β-alanine supplementation

Carnosine is synthesised in skeletal muscle from the amino acids β-alanine and L-histidine. β-alanine was reported to be the rate-limiting factor in the synthesis of carnosine (Artioli et al., 2010; Blancquaert et al., 2017; Harris et al., 2006b) as L-histidine has enough supply in the body (Dunnett and Harris, 1999). β-alanine supplementation is shown to increase muscle carnosine (Artioli et al., 2010; Harris et al., 2006; Saunders et al., 2017). Although L-histidine is not the rate-limiting step in the synthesis of carnosine, its amount decreases upon constant supplementation of β-alanine (Blancquaert et al., 2017), but this might not always be the case as it has also been shown that 4 weeks of supplementation of β-alanine did not lead to a reduction of muscle L-histidine content both in men and women (Varanoske et al., 2017).

2. Carnosine derivatisation

The principal objective of carnosine derivatization was to make a non-hydrolysable carnosine analogue. This work was conducted in collaboration with Dr. Christopher Garner, a medicinal chemist in the Department of Chemistry and Forensics, NTU, in order to screen potential chemical compounds that act as carnosinase inhibitors and carnosine mimetics. He used ROCS molecular docking software to identify compounds from the Maybridge library of 53,000 small drug candidates in order to identify those with good fit to the catalytic cleft of both carnosinase enzymes, and which met the criterion of having a molecule with relatively small size and containing 5- or 6-membered aromatic rings linked to an alkyl group to the rest of the molecule. These aromatic rings can be benzene, pyridine, furan, azol, or imidazole.

Calcein AM or calcein acetoxymethyl ester is a cell-permeant dye that can determine cell viability. It is a hydrophobic compound that quickly permeates in plasma membranes of viable cells.

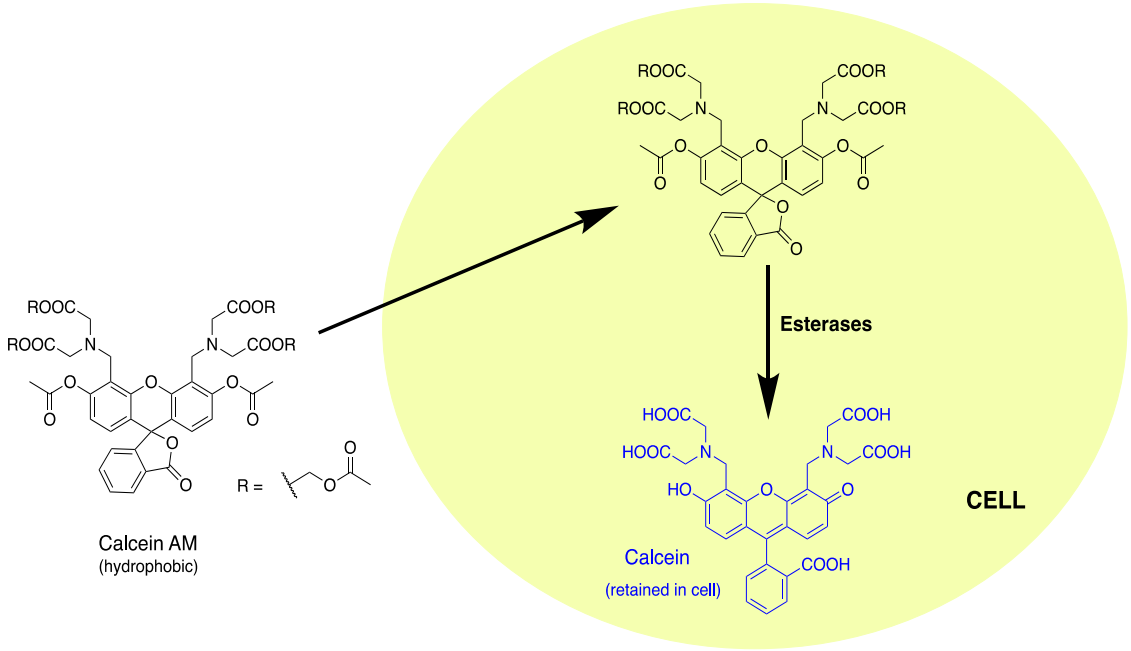

Figure 6.1 Hydrolysis of calcein AM dye to fluorescent calcein by intracellular esterases.

Glucolipotoxicity is a combination of the words glucotoxicity and lipotoxicity (Poitout and Robertson, 2008). Under physiological conditions, glucose and fatty acids are crucial to normal β-cell function. However, when an elevated concentration of glucose and fatty acid either enter or are synthesised within tissues, this can damage it, leading to various disorders including type 2 diabetes (Poitout and Robertson, 2008; Prentki et al., 2002). Prentki et al. suggested that high glucose alone or high fatty acids alone should not have a deleterious effect on the cell since when glucose concentration is high, it will be oxidised. When the free fatty acids are elevated, they will be oxidised instead of glucose (Prentki et al., 2002). When both nutrients levels are high however, it will cause detrimental effects on β-cell function (Poitout and Robertson, 2002) because long-chain acyl-CoA ester level derived from fatty acids is high and will not undergo oxidation due to malonyl-CoA derived from glucose also being high. Malonyl-CoA regulates lipid partitioning by inhibiting the enzymatic action of carnitine palmitoyltransferase-1, a regulating enzyme in mitochondrial fatty acid β-oxidation. This action causes elevation of long-chain acyl-CoA esters in the cytoplasm, which directly or indirectly form ceramide that leads to insulin resistance, dysregulated glucose-stimulated insulin secretion, and apoptosis (Kraegen et al., 2001; Poitout and Robertson, 2002; Prentki et al., 2002).

Other potential effects of glucolipotoxicity on β-cell function include oxidative stress, nitrative stress, and endoplasmic reticulum stress (Weir, 2020). Oxidative stress is caused by the imbalance of the free radical species and antioxidant system initiating insulin secretion reduction (Yaribeygi et al., 2020). Oxidative stress could result from low antioxidants or high production of reactive oxygen and nitrogen species (RONS). On the other hand, the endoplasmic reticulum stress is the build-up of misfolded proteins caused by protein overload and/or variation in the endoplasmic reticulum environment that compromises the efficiency of protein folding (Biden et al., 2014). The generation of high intracellular oxidant levels is able

to damage biological molecules and activate numerous signalling pathways (Myhre et al., 2003).

It has been reported that there is a positive correlation in various pathophysiologies such as Alzheimer's disease, cardiovascular disease, neuroinflammation, and type 2 diabetes with increased oxidative stress and elevation of reactive oxygen species level (Hauck et al., 2019).

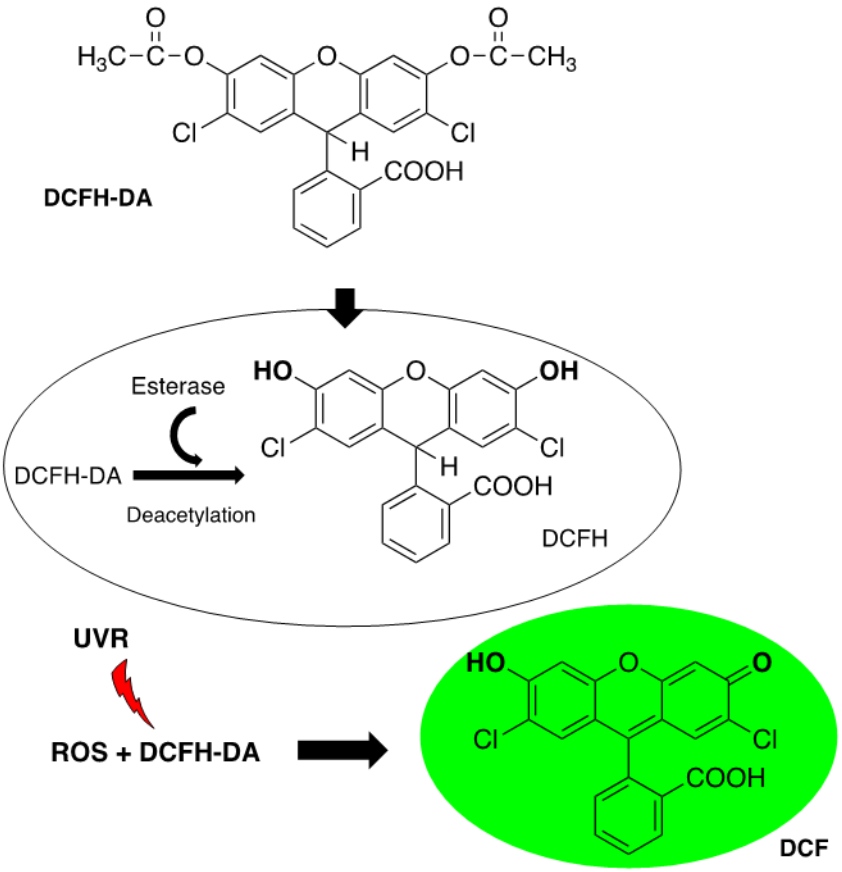

Figure 6.2 Mechanism of action of DCFH-DA in the live cell.

In this study, I screened carnosine analogues with docking scores suggestive of function as carnosinase inhibitors, and carnosine mimetics were also evaluated for their efficacy in reversing the production of reactive species, and thereby their ability to prevent the inhibition of stimulated insulin secretion that is driven by glucolipotoxicity. For this purpose, I used INS-1 rat pancreatic β-cells as a cell model.

6.2 Results

6.2.1 Effects of L-carnosine on glucolipotoxic free radicals and insulin secretion

To assess the cellular health of INS-1 rat pancreatic β-cells exposed to various experimental conditions, cell viability was first determined. Calcein AM Cell Viability Assay is considered more robust than tetrazolium salts or AlamarBlue® Dye, as the cells can be stained and quantified in less than 2 hours (Chen et al., 2017; Miron et al., 2021).

The treated INS-1 cells were visualised using an Olympus CKX53 model microscope at 20x objective before and after the treatment with calcein-AM solution.

As depicted in **Figure 6.3**, INS-1 cells were exposed to the experimental conditions (GLT, carnosine, and GLT + carnosine) and show no observable change in cell morphology relative to control. It was observed that the treatment conditions did not reduce cell adherence onto the surface of the flask. Cells also appeared to have few or no circular/rounded shapes in all conditions. Increased cell death was not significant, and there were few floating cells observed in the flasks.

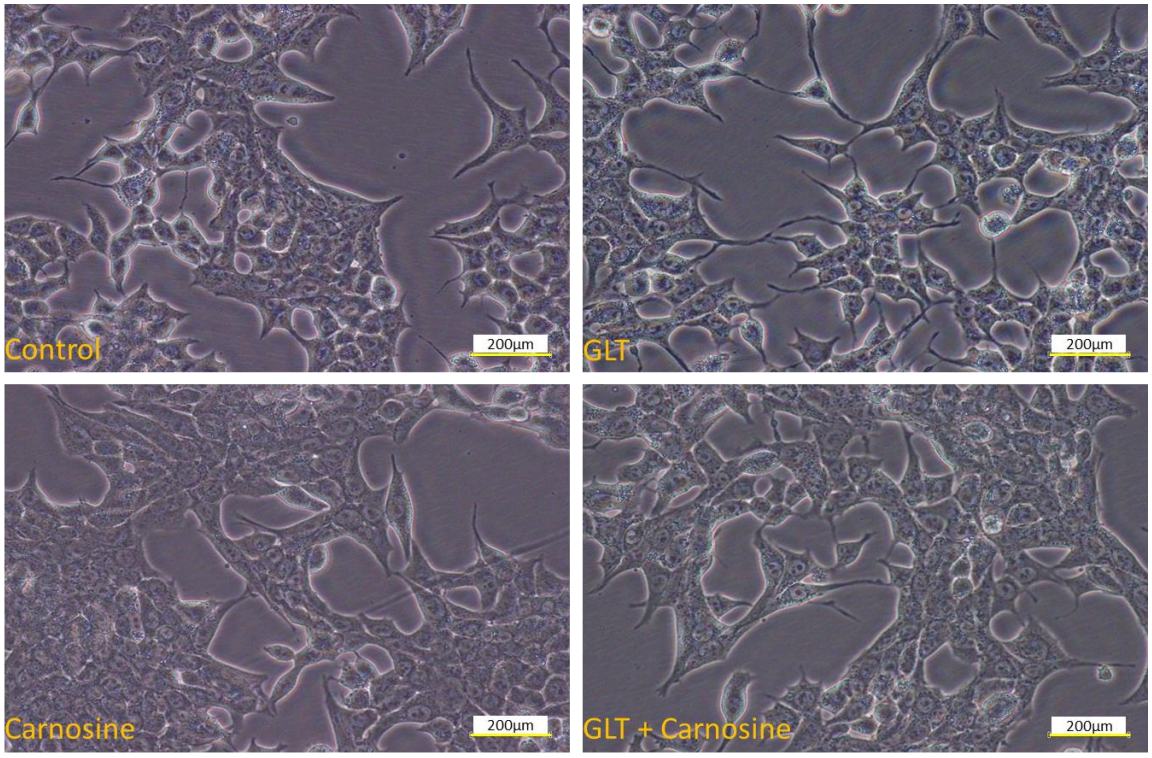

Figure 6.3 Effect of experimental conditions on INS-1 rat pancreatic β-cell morphology. INS-1 cells were incubated for 5 days in complete RPMI-1640 medium ± 10 mM L-carnosine or GLT medium ± 10 mM L-carnosine. Images were taken using an Olympus CKX53 model microscope with camera in a 20x objective.

Functional analysis on INS-1 cell viability was performed using the calcein-AM assay. As depicted in **Figure 6.4**, INS-1 cells treated with various experimental conditions show little or no significant change in viability relative to control, with only a slight change in cell viability following carnosine supplementation found to be significant.

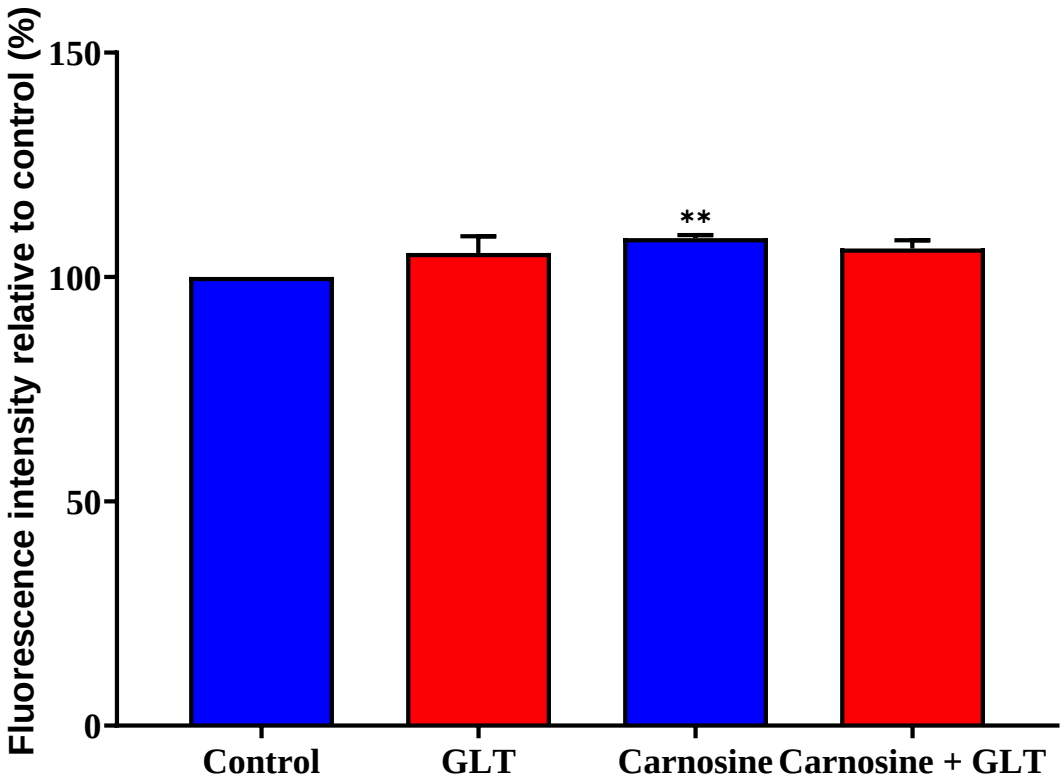

Figure 6.4 Effect of experimental conditions on INS-1 rat pancreatic β-cell viability. INS-1 cells were incubated for 5 days in RPMI-1640 medium ± 10 mM L-carnosine or GLT medium ± 10 mM L-carnosine. After 1 hour incubation with 5 μM solution of calcein-AM, fluorescence intensity was measured using excitation and emission at 490 nm and 520 nm. Cell viability is expressed as percentages of control values ± S.E.M. in comparison to control (=100%) from three independent experiments with two replicates each trial. Statistical analyses were carried out by one-way ANOVA followed by Tukey's multiple comparisons test as post hoc test (**$p<0.01$).

This data show that INS-1 cells treated with GLT had a relative fluorescence of 105.30 ± 3.76% ($p=0.2915$) relative to control, and GLT supplemented with L-carnosine resulted in 106.30 ± 1.86% ($p=0.0762$) relative fluorescence. However, INS-1 rat pancreatic β-cell treated with L-carnosine gave a statistically significant increase in relative fluorescence to 108.7 ± 0.6667% ($p=0.0059$) compared to control. This result suggests that L-carnosine treated cells may have enhanced cell health, albeit there were few floating cells seen under microscope visualisation in any condition.

Glucolipotoxicity has been shown to cause radical species generation, whilst L-carnosine has been seen to potentially sequester carbonyl compounds (Aldini et al., 2005). With this in mind, L-carnosine's potential effect to scavenge radical species generated by GLT was evaluated as shown. Reactive oxygen species (ROS) and reactive nitrogen species (RNS), collectively known as (RONS), are the building blocks for radical carbonyl species (RCS) generation in pancreatic β-cells (Cripps et al., 2017). To determine the level of radical species produced, INS-1 cells were incubated for 5 days in complete RPMI-1640 medium ± 10 mM L-carnosine or GLT (complete RPMI-1640 medium supplemented with 17 mM D-glucose, 200 µM oleic acid, and 200 µM palmitic acid) ± 10 mM L-carnosine. DCFDA (20 µM) was added in Krebs-Ringer buffer solution for 1 hour, and reactive species formation was detected via fluorescence with excitation (495 nm) and emission (530 nm).

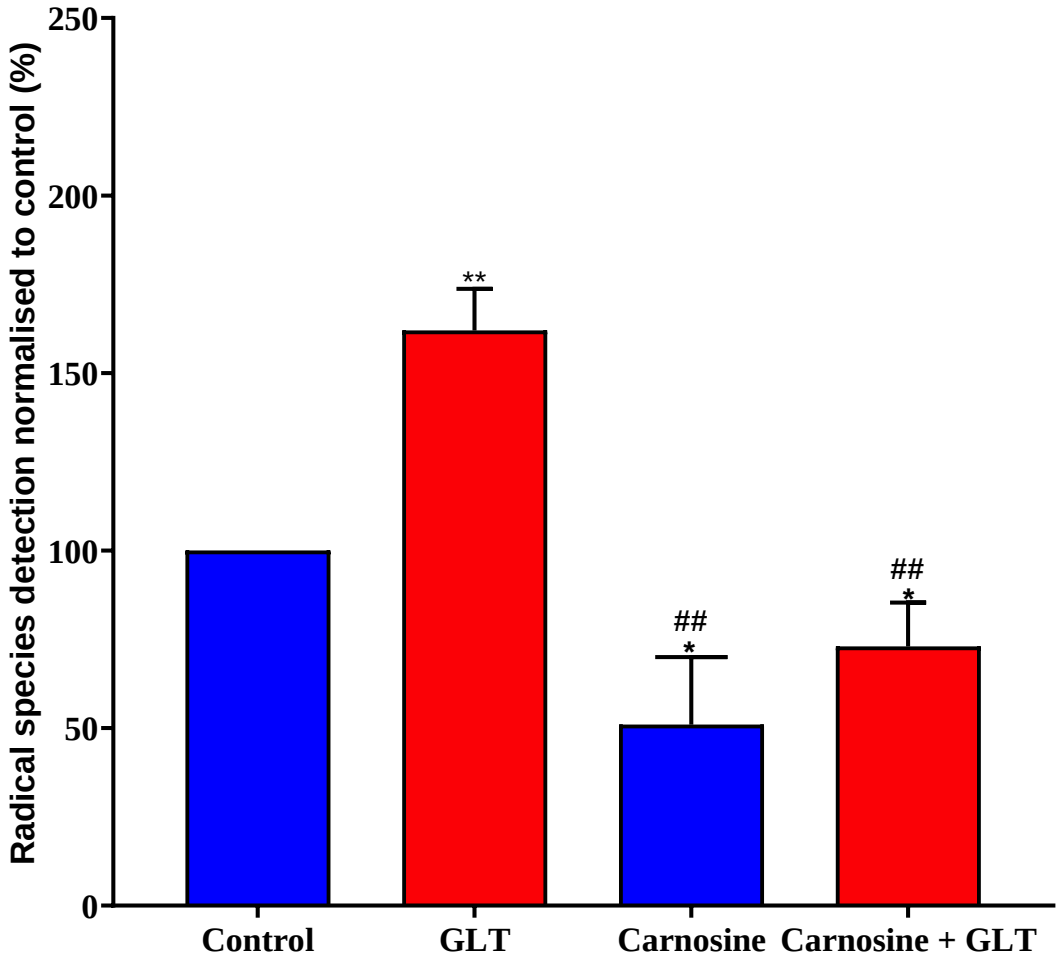

Figure 6.5 Effect of GLT and carnosine on radical species production. INS-1 cells were incubated for 5 days in RPMI-1640 medium ± 10 mM L-carnosine or GLT ± 10 mM L-carnosine. DCFDA was added in Krebs-Ringer buffer solution for 1 hour, and reactive species production was detected via fluorescence with excitation (495 nm) and emission (530 nm). Reactive species are expressed as percentages of control values ± S.E.M. and data presented was from 3 independent experiments with two replicates each trial. Statistical analyses were carried out by one-way ANOVA followed by Tukey's multiple comparisons test as post hoc test (*$p<0.05$, **$p<0.01$ relative to control; $^{\#\#}p<0.01$ relative to GLT).

Figure 6.5 shows the amount of production of radical oxygen species generated in each condition. Exposure of INS-1 cells to GLT resulted in an increase in radical species of 62.03± 11.69 % ($p=0.0061$) relative to control. It was also observed that ROS production in the presence of L-carnosine (51.40 ± 19.20, $p=0.0307$) was significantly lower relative to control, and similarly L-carnosine + GLT (73.13 ± 12.34, $p=0.0064$) ROS production was significantly lower than the GLT (162.03 ± 11.69%).

This indicates the effectiveness of L-carnosine in scavenging ROS in the INS-1 model.

To confirm GLT can also generate RNS in INS-1 cells, iNOS protein expression was determined to validate its effect. To do this, INS-1 cells were incubated for 5 days in RPMI-1640 medium ± GLT. Results show that iNOS was upregulated upon exposure of INS-1 cells with GLT. It was observed to have a highly significant change of approximately 10-fold relative to the control (see **Figure 6.6**).

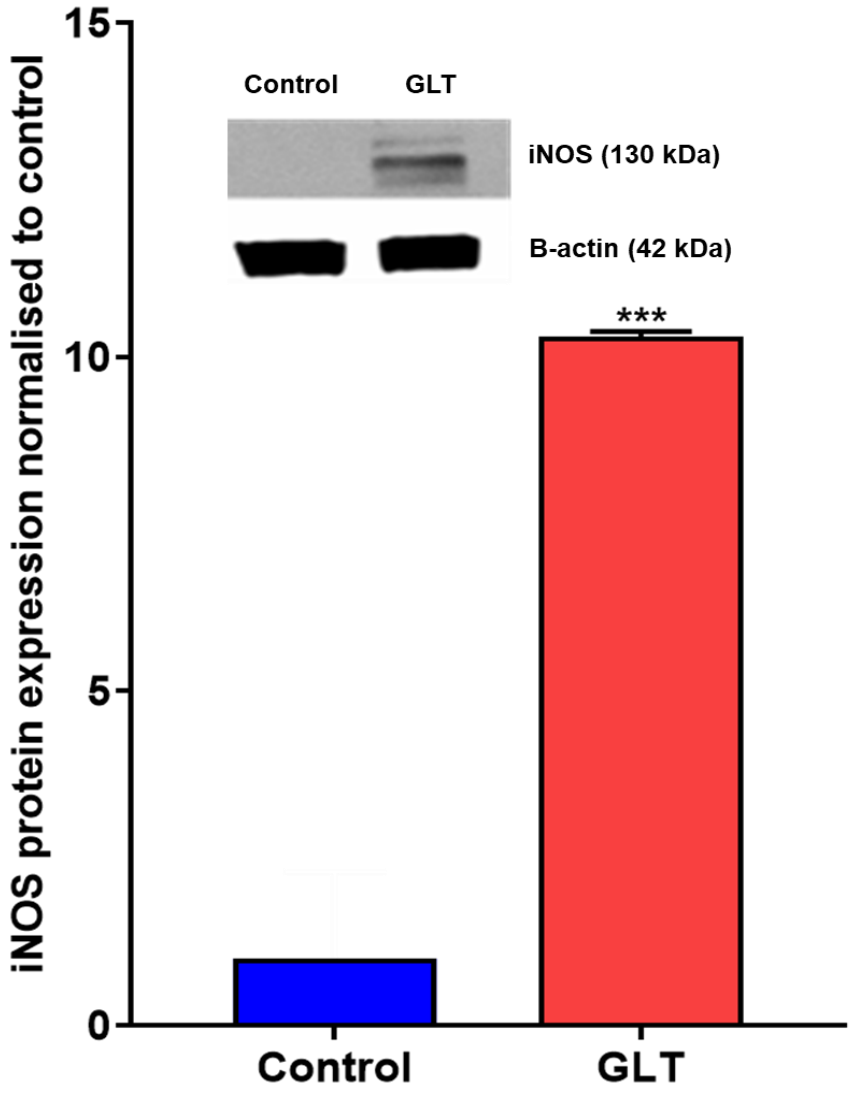

Figure 6.6 iNOs protein expression level. INS-1 cells were incubated for 5 days in RPMI-1640 medium ± GLT. Total cellular protein was separated using 7.5% polyacrylamide gel, transferred to a nitrocellulose membrane, and detected using an anti-iNOS primary antibody (1:1000 dilution). Statistical analysis was carried out by t-test (***p<0.001)

L-carnosine has been shown to have the ability to scavenge radical nitrogen species (RNS) (Hipkiss, 2009). With this, we sought to evaluate the effectiveness of L-carnosine to lower the production of RNS by exposing INS-1 cells for 5 days in RPMI-1640 medium ± 10 mM L-carnosine or GLT ± 10 mM L-carnosine. Total cellular protein was extracted and separated by SDS-PAGE. The separated protein was then transferred onto nitrocellulose membrane and immunoblotted with antibody against inducible nitric oxide synthase (iNOS).

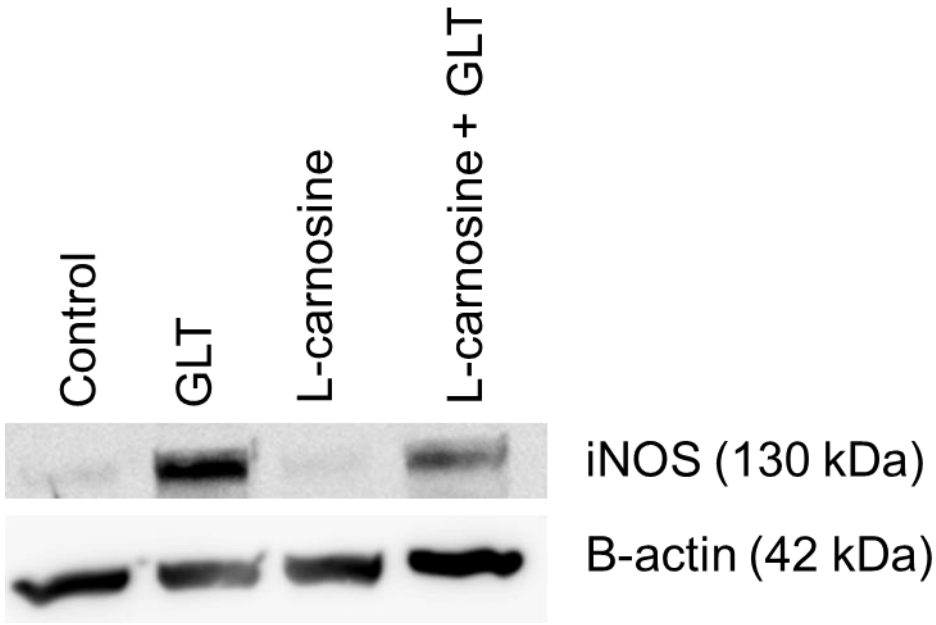

Figure 6.7 Effect of L-carnosine on iNOS protein expression level. INS-1 cells were incubated for 5 days in RPMI-1640 medium ± 10 mM L-carnosine or GLT ± 10 mM L-carnosine. Total cellular protein was separated using 10% polyacrylamide gel, transferred to a nitrocellulose membrane, and detected using an anti-iNOS primary antibody. n=1.

As shown in the result, iNOS protein expression was upregulated in GLT relative to control, and this was effect was reversed by supplementation of L-carnosine to GLT. This observation is similar to that reported previously (Cripps et al., 2017).

Given the potential scavenging effect of L-carnosine against radical species, I next sought to determine its effects on β-cell function, and in particular insulin secretion. Therefore, INS-1 cells were incubated for 5 days in RPMI-1640 medium ± 10 mM L-carnosine or GLT ± 10 mM L-carnosine. After the incubation period, INS-

1 cells were washed twice with Krebs-Ringer buffer solution (KRBS). INS-1 cells were then incubated with KRBS ± secretagogue cocktail for 3 hours. Insulin secretion was measured using Mercodia High Range Rat Insulin ELISA (Sweden).

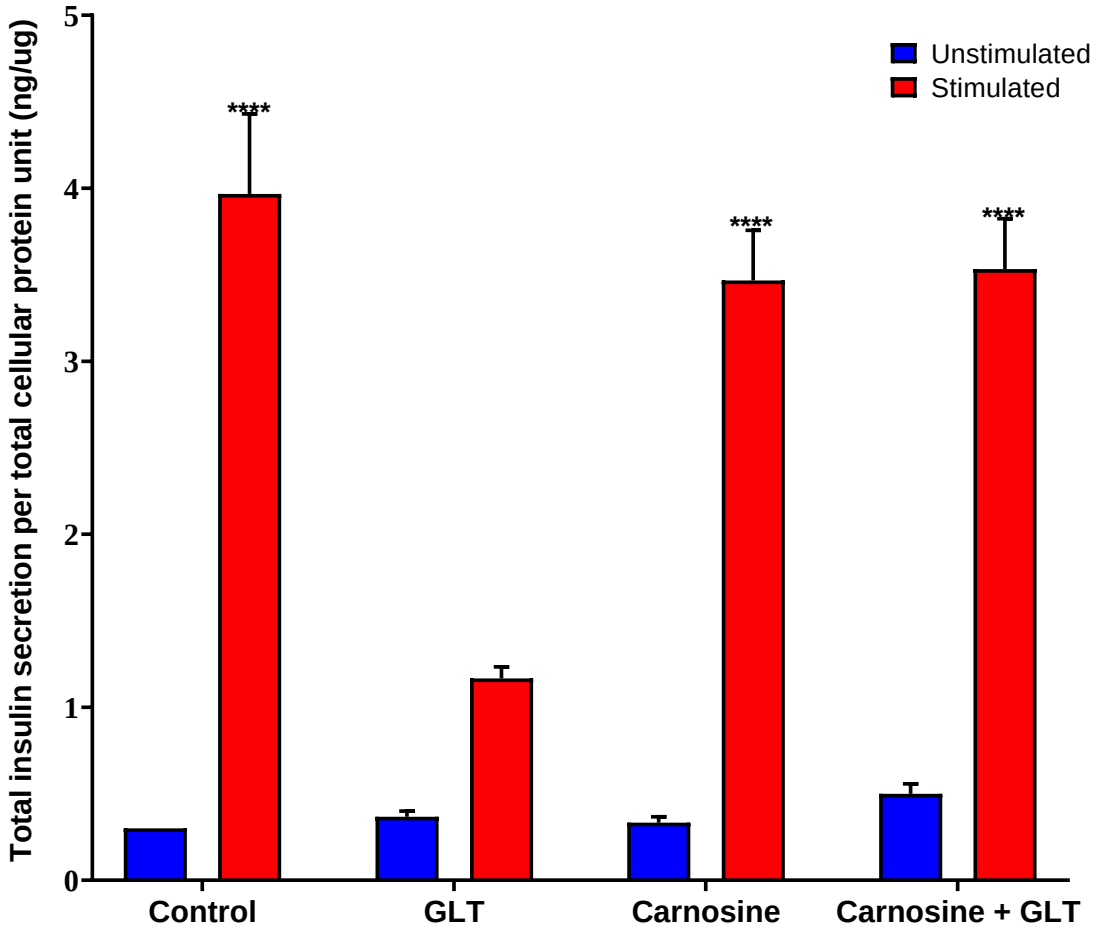

Figure 6.8 Effect of carnosine on insulin secretion to glucolipotoxic treated INS-1 rat pancreatic β-cells. INS-1 cells were incubated for 5 days in complete RPMI-1640 medium ± 10 mM L-carnosine or GLT (RPMI-1640 medium supplemented with 17 mM D-glucose, 200 µM oleic acid and 200 µM palmitic acid) ± 10 mM L-carnosine. High Range Rat Insulin ELISA determined insulin secretion following incubation ± secretagogue cocktail for 3 hours. Unstimulated is in blue colour and stimulated is in red colour with data normalised to total cellular protein. The data shown are of three independent experiments. Statistical analyses were carried out by one-way ANOVA followed by Tukey's multiple comparisons test as post hoc test. ****$p<0.0001$ compared to GLT stimulated sample.

Glucolipotoxicity is shown to decrease insulin secretion significantly in secretagogue-stimulated insulin secretion to 1.17 ± 0.07 ng/µg compared to control

(3.97 ± 0.46 ng/µg, $p<0.0001$). This result indicates that GLT was able to inhibit insulin secretion. On the other hand, I have observed that INS-1 cells exposed to L-carnosine (3.47± 0.29 ng/µg) and L-carnosine + GLT (3.53 ± 0.29 ng/µg) were stimulating insulin secretion significantly, which is relatively similar to the control. This result indicates that L-carnosine enhances insulin secretion and can overturn the inhibitory effect of high glucose and high-fat on insulin secretion. Results presented here were congruent with the published results of Turner Group in 2017 (Cripps et al., 2017).

6.2.2 Carnosinase inhibitors as potential scavengers of reactive species and their effect on insulin secretion

As shown, L-carnosine, is able to scavenge radical species and reverse the inhibitory effect of GLT on insulin secretion. However, it was reported by Pavlin et al. that the enzyme carnosinase could rapidly hydrolyse it into its amino acid components, L-histidine and β-alanine (Pavlin et al., 2016). This might affect its aforementioned beneficial properties. However, Bellia et al. (2014) proposed a strategy to combat carnosinase's hydrolytic activity by derivatising L-carnosine structure into a carnosinase resistant compound. Putative carnosinase inhibitors screened using pharmacophore modelling strategies conducted by Dr. Garner's group in the Department of Chemistry and Forensics, NTU were therefore utilised to test this hypothesis. Carnosinase inhibitors were screened to fit into the active site perfectly and considered to have a relatively weak bonding interaction of the enzyme carnosinase. This interaction would result in a conformational change of the enzyme's active site and the substrate's weak interaction.

There were 50 compounds screened as potential carnosinase inhibitors. Out of the 50 compounds, 14 compounds passed the rapidly overlay for chemical structures test. This is a test used to measure the shape similarity of the molecules

(Hawkins et al., 2007; Rush et al., 2005). Only the top 5 compounds were used in this study as initial screening using C2C12 myotubes by a colleague in the lab shown that the other compounds were toxic. The potential carnosinase inhibitors were evaluated on their effect on cell viability, radical species production, and insulin secretion.

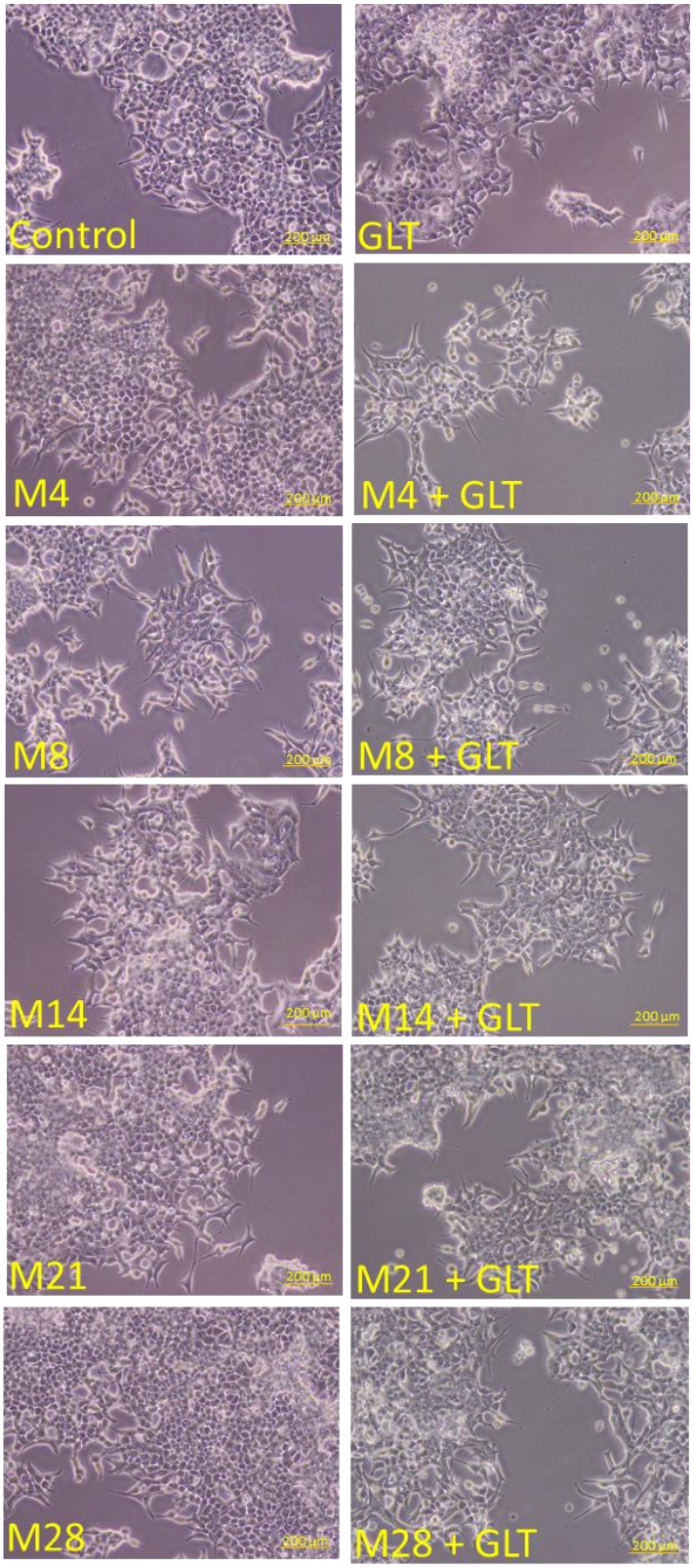

Figure 6.9 Morphological effect of carnosinase inhibitors to INS-1 rat pancreatic β-cells. INS-1 cells were incubated for 5 days in RPMI-1640 medium ± 10 mM L-carnosine or RPMI-1640 medium ± 100 μM carnosinase inhibitors or GLT medium ± 10 mM L-carnosine or GLT media ± 100 μM carnosinase inhibitors. Images were taken using an Olympus CKX53 model microscope with a camera in a 10x objective.

INS-1 cells were incubated for 5 days in RPMI-1640 ± 10 mM L-carnosine or RPMI-1640 ± 100 µM carnosinase inhibitors or GLT medium ± 10 mM L-carnosine or GLT medium ± 100 µM carnosinase inhibitors. INS-1 cells were shown to be not affected by the presence of the carnosinase inhibitors as their cellular shape was not round or circular. Few floating cells were observed, but this effect was not significantly different from the control (**Figure 6.9**). However, it was shown that amongst the Maybridge compound treatments, M8 supplemented to GLT resulted in a slight increase in calcein-AM fluorescence (102.67 ± 0.33 %) that was statistically significantly compared to control ($p=0.0153$) (shown in **Figure 6.10**).

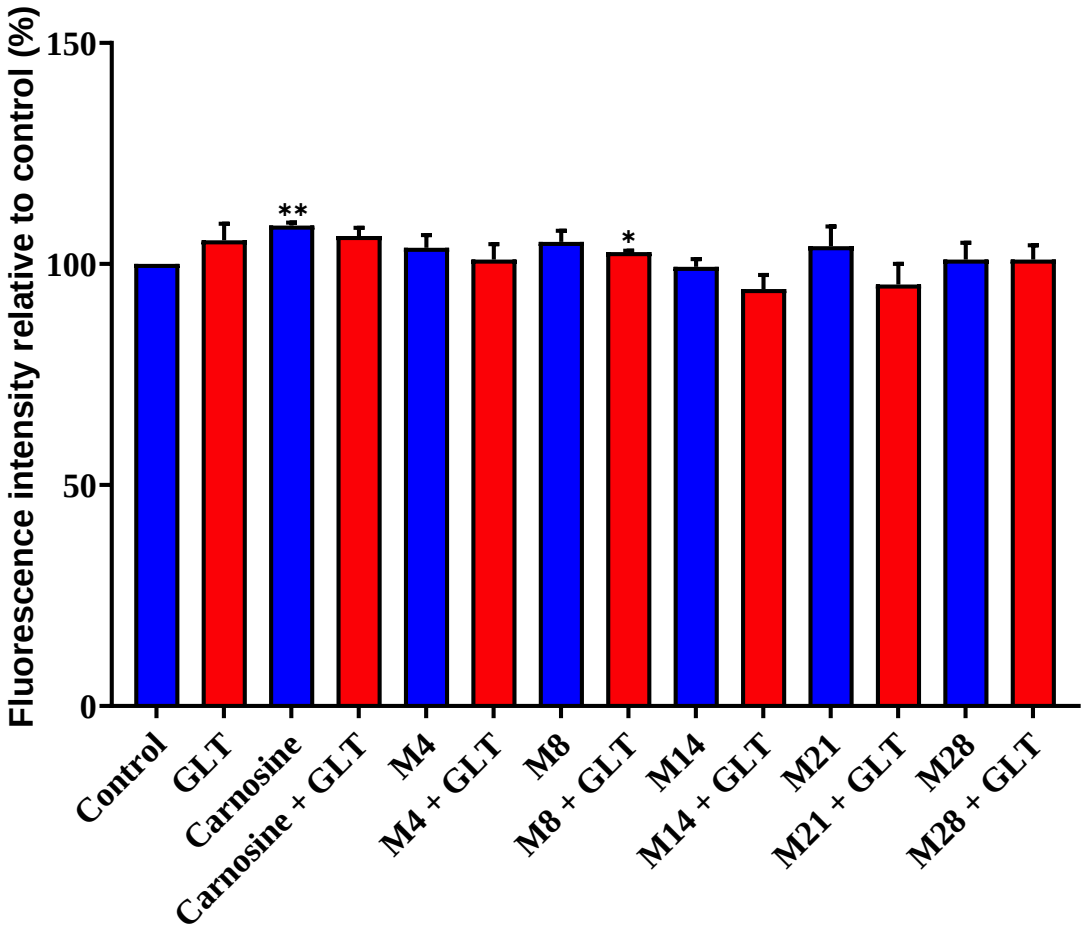

Figure 6.10 Effect of carnosinase inhibitors on INS-1 rat pancreatic β-cell health. INS-1 cells were incubated for 5 days in RPMI-1640 ± 10 mM L-carnosine or RPMI-1640 ± 100 µM carnosinase inhibitors or GLT medium ± 10 mM carnosine or GLT medium ± 100 µM carnosinase inhibitors. Cell viability is expressed as percentage change ± S.E.M. in comparison to control from 3 independent experiments. Statistical analyses were carried out by one-way ANOVA followed by Tukey's multiple comparisons test as post hoc test. $p<0.05$*, $p<0.01$** relative to control.

Carnosinase inhibitor potential to effectively inhibit carnosinase's hydrolytic action, could, in turn, result in an increase in endogenous carnosine levels, thereby enhancing the potential to effectively scavenge radical species without being hydrolysed, and was therefore evaluated along with β-cell insulin secretion.

To measure reactive species, INS-1 cells were incubated for 5 days in RPMI-1640 ± 10 mM L-carnosine or RPMI-1640 ± 100 µM carnosinase inhibitors or GLT medium ± 10 mM L-carnosine or GLT media ± 100 µM carnosinase inhibitors (**Figure 6.11**). All the Maybridge compounds tested reduced reactive species levels.

However, with the exception of M8, this was not statistically significant from control ($p>0.05$). M8 + GLT by contrast significantly decreased reactive species levels to 61.67 ± 29.28 % ($p= 0.0335$) of control, whereas GLT without carnosine increased the level to 162.00 ± 11.72 %. Thus, M8 is potentially an effective inhibitor of carnosinase and, thereby may increase endogenous carnosine levels sufficiently to scavenge ROS.

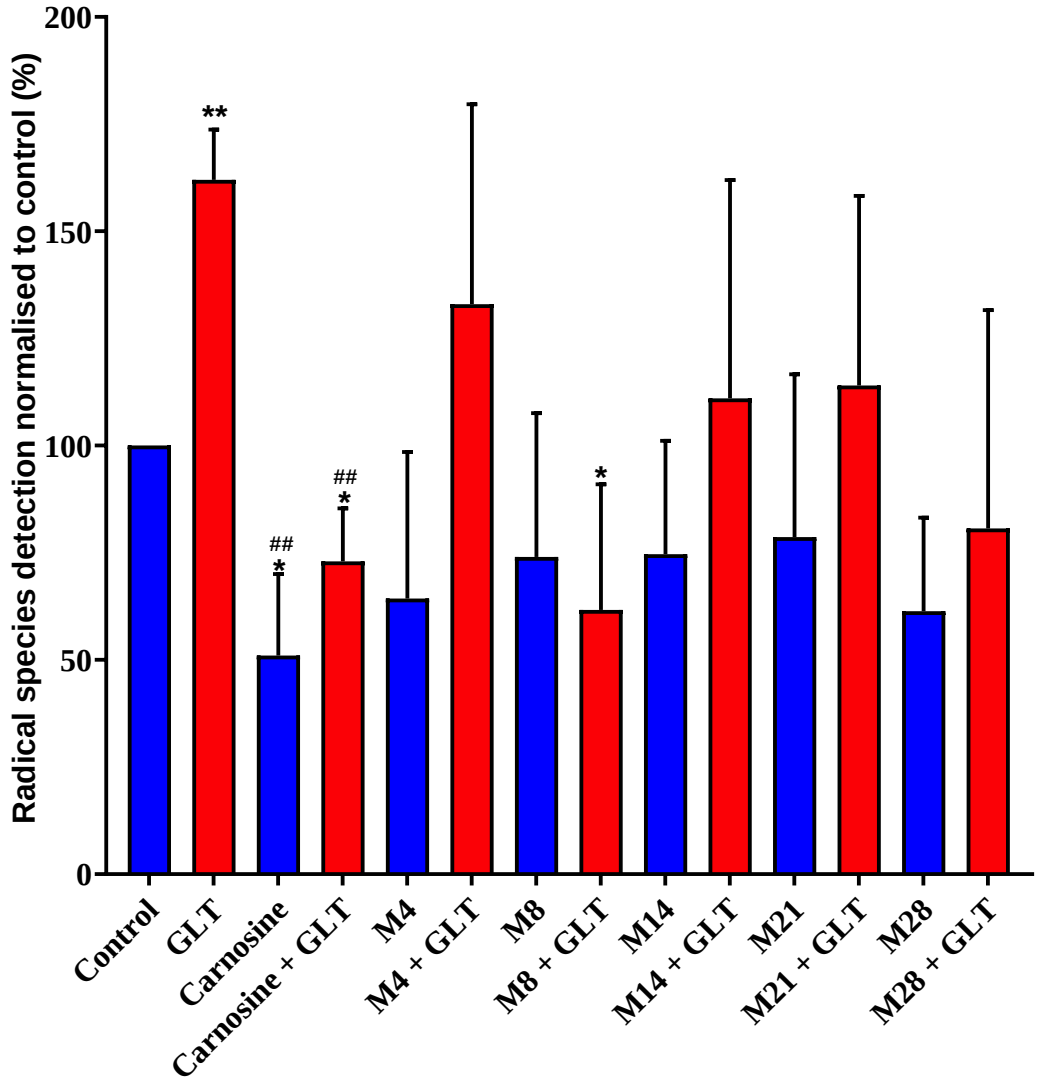

Figure 6.11 Effect of carnosinase inhibitors on GLT ROS production. INS-1 cells were incubated for 5 days in RPMI-1640 ± 10 mM L-carnosine or RPMI-1640 ± 100 µM carnosinase inhibitors or GLT medium ± 10 mM L-carnosine or GLT medium ± 100 µM carnosinase inhibitors. Twenty (20) µM DCFDA was loaded in Krebs-Ringer buffer solution for 1h and reactive species detected via fluorescence with excitation and emission of 495 nm and 530 nm, respectively. Reactive species are expressed as percentages of control values ± S.E.M. in comparison to control from 3 independent experiments. *p<0.05, **p<0.01 relative to control; ##p<0.01 relative to GLT.

Radical species production is a hallmark of type 2 diabetes. Thus, Maybridge carnosinase inhibitors' effect on insulin secretion was evaluated based on the result that it has the potential to decrease the ROS generated by GLT. INS-1 cells were incubated for 5 days in RPMI-1640 ± 10 mM L-carnosine or RPMI-1640 ± 100 µM carnosinase inhibitors or GLT medium ± 10 mM L-carnosine or GLT medium ± 100 µM carnosinase inhibitors. After the incubation period, INS-1 cells were washed twice with KRBS and incubated for 2 hours with KRBS ± secretagogue cocktail.

Maybridge carnosinase inhibitors, in general, shown a slight increase in insulin secretion relative to GLT (**Figure 6.12**); however, they did not manifest a significant positive effect on reversing the insulin secretion inhibited by GLT upon its supplementation to GLT.

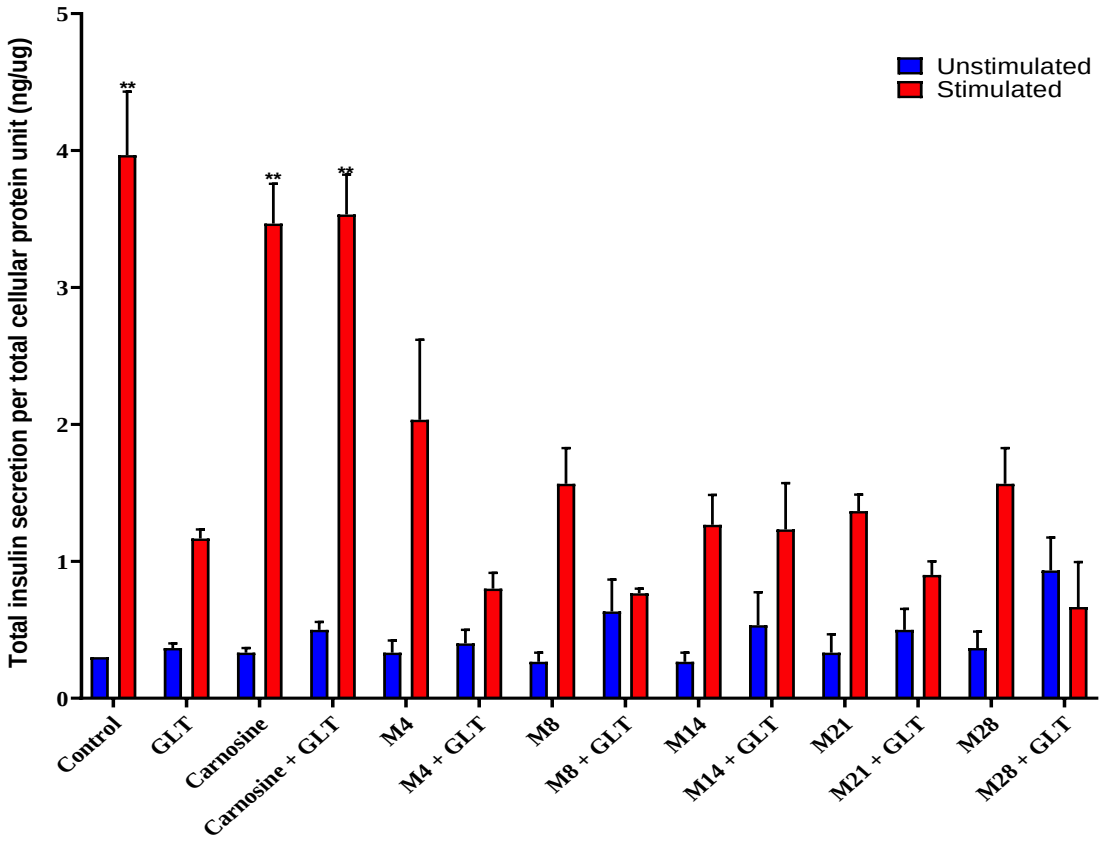

Figure 6.12 Effect of carnosinase inhibitors on insulin secretion to glucolipotoxic treated INS-1 rat pancreatic β-cells. INS-1 cells were incubated for 5 days in RPMI-1640 medium ± 10 mM L-carnosine or RPMI-1640 ± 100 µM carnosinase inhibitors or GLT medium ± 10 mM L-carnosine or GLT medium ± 100 µM carnosinase inhibitors. Insulin secretion was determined using Mercodia High Range Rat Insulin ELISA following incubation ± secretagogue cocktail for 3 hours. Unstimulated is in blue colour and stimulated is in red colour with data normalised to total cellular protein. The data shown are from three independent experiments. **p<0.0001 compared to GLT stimulated sample.

6.2.3 Carnosine mimetics as a potential scavenger of reactive species and their effect on insulin secretion

Another strategy that we proposed in battling the hydrolytic activity of carnosinase was to synthesise slowly-hydrolysable carnosine mimetics. These compounds were designed and synthesised to have the same biological function and action exhibited by L-carnosine. Through collaboration with Dr. Garner's research group in the Department of Chemistry and Forensics, three carnosine mimetics (E1, E2, and E3)

were synthesised. The names of these compounds remain confidential due to pending IP and patent consideration.

To determine the potential beneficial effects of carnosine mimetics, cell viability and functional assays were conducted. To evaluate the effect of carnosine mimetics on cell viability, INS-1 cells were incubated for 5 days in RPMI-1640 medium ± 10 mM L-carnosine or RPMI-1640 ± 10 mM carnosine mimetics or GLT medium ± 10 mM carnosine or GLT medium ± 10 mM carnosine mimetics. After the incubation period, cell morphology was evaluated under a microscope using a 10x objective **(Figure 6.13**). INS-1 cells were observed not to be in a rounded or circular shape. There were a few floating cells seen not adhering onto the flask's surface, but this does not affect the cells' total cell viability (see **Figure 6.14**).

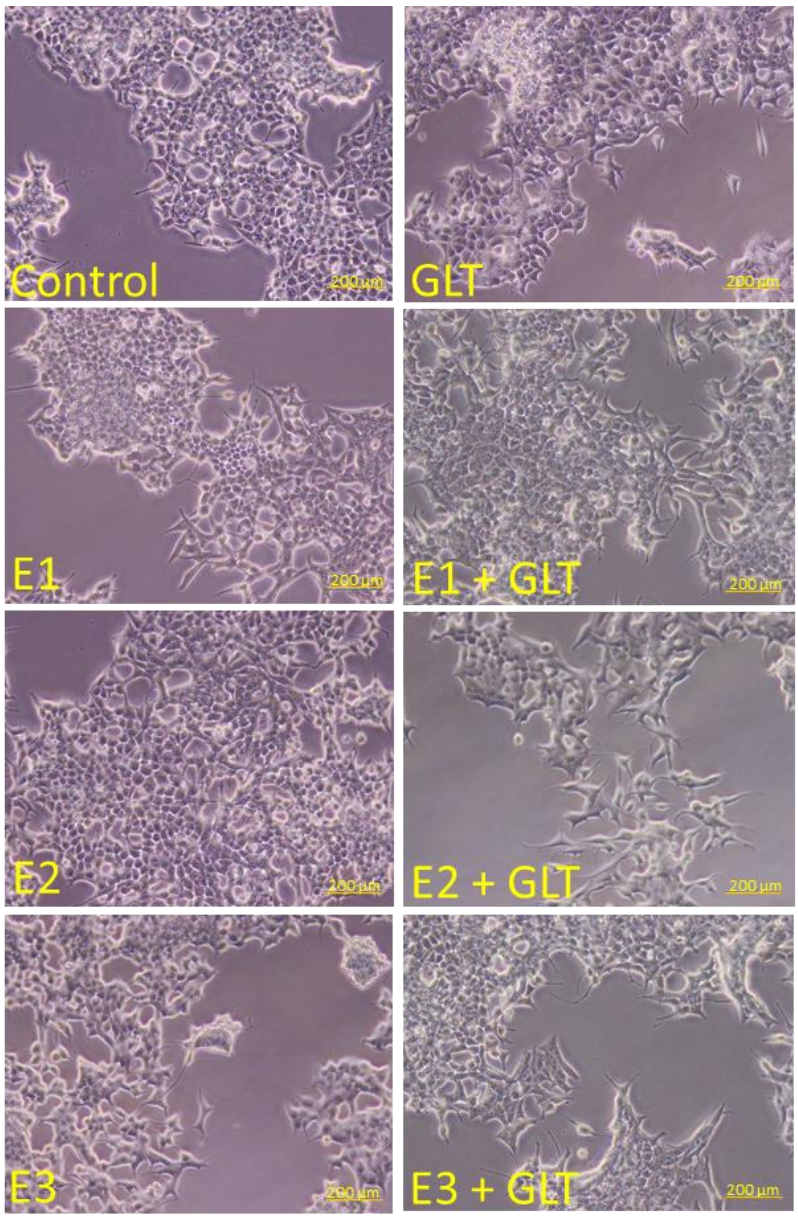

Figure 6.13 INS-1 cells treated with carnosine mimetics. INS-1 cells were incubated for 5 days in RPMI-1640 ± 10 mM L-carnosine or RPMI-1640 ± 100 µM carnosine mimetics or GLT medium ± 10mM L-carnosine or GLT medium ± 100 µM carnosine mimetics. Images were taken using an Olympus CKX53 model microscope with a camera using a 10x objective.

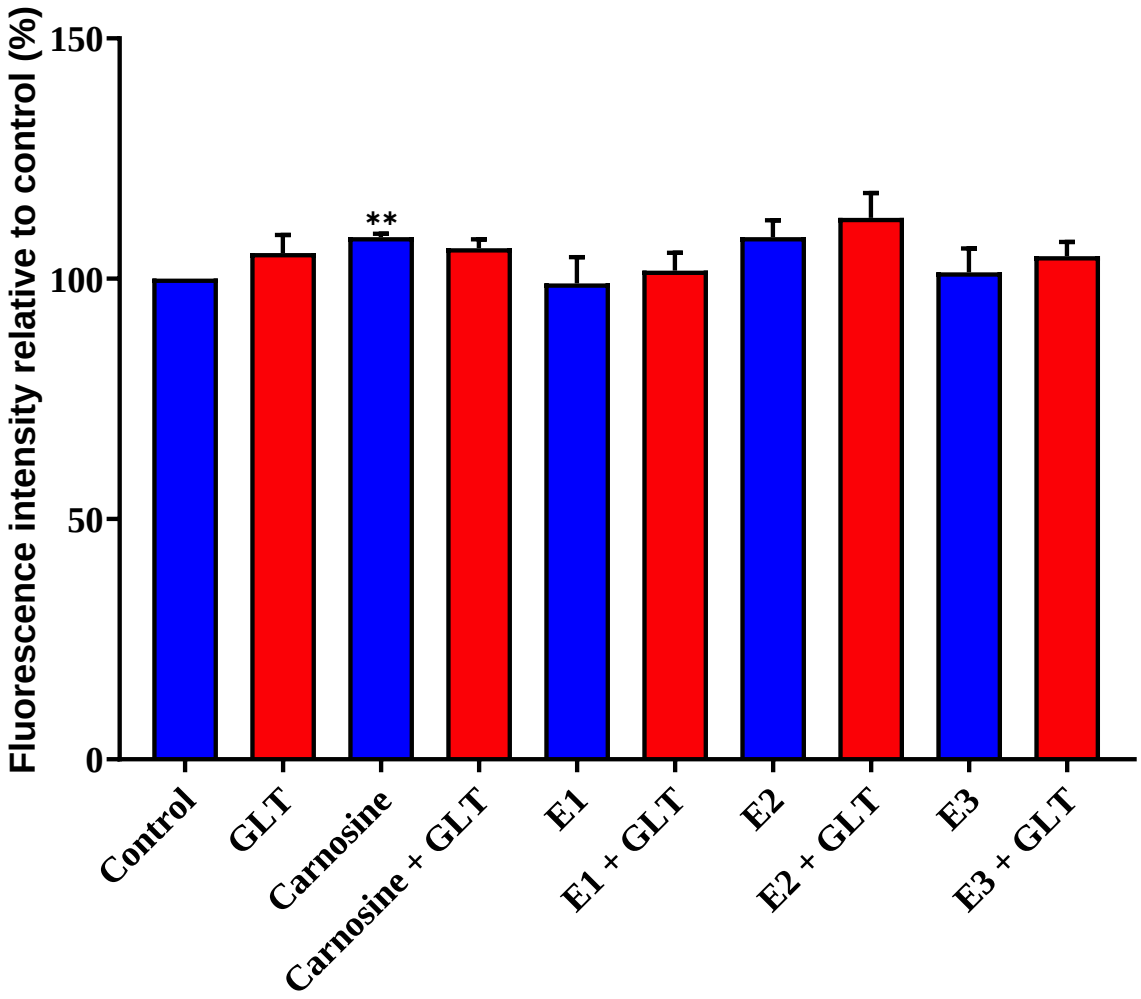

Figure 6.14 Effect of carnosine esters on INS-1 rat pancreatic β-cell health. INS-1 cells were incubated for 5 days in RPMI-1640 medium ± 10 mM L-carnosine or RPMI-1640 ± 100 µM carnosine mimetics or GLT medium ± 10 mM L-carnosine or GLT medium ± 100 µM carnosine mimetics. Cell viability is expressed as percentages of control values ± S.E.M. in comparison to control from 3 independent experiments. Statistical analyses were carried out by one-way ANOVA followed by Tukey's multiple comparisons test as post hoc test. $p<0.01$** relative to control.

Depicted in **Figure 6.14**, for the most part, INS-1 cells treated with carnosine mimetics show that reactive species levels were non-significantly different relative to control ($p>0.05$). However, E2 did decrease the reactive species level to 77.33 ± 6.89% compared to control ($p=0.0302$).

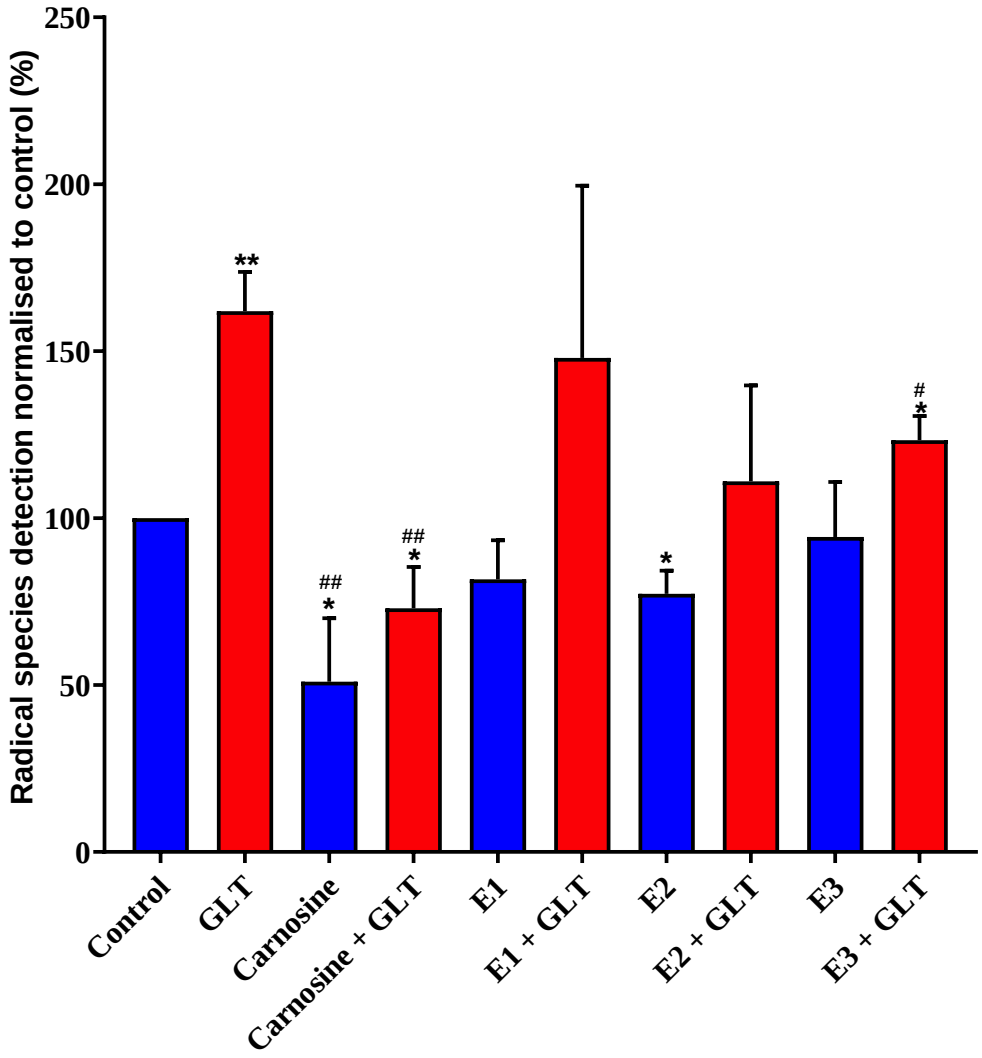

Figure 6.15 Effect of carnosine mimetics on GLT ROS production. INS-1 cells were incubated for 5 days in RPMI-1640 ± 10 mM L-carnosine or RPMI-1640 medium ± 100 µM carnosine mimetics or GLT medium ± 10 mM L-carnosine or GLT medium ± 100 µM carnosine mimetics. Twenty (20) µM DCFDA was loaded in Krebs-Ringer buffer for 1h, and reactive species production was detected via fluorescence with excitation and emission of 495nm and 530nm, respectively. Reactive species are expressed as percentages of control values ± S.E.M. in comparison to control from 3 independent experiments. *p<0.05, **p<0.01 relative to control; $^{\#}$p<0.05, $^{\#\#}$p<0.01 relative to GLT.

Glucolipotoxicity is shown to increase reactive species to 162.00 ± 11.72 % the level of control cells (p=0.0339). The supplementation of carnosine mimetics lowered this level, E1 (148.00 ± 51.54 %, p=0.4500) and E2 (111.00 ± 28.75, p=0.7388), although the results exhibited by these carnosine mimetics were shown not to be significantly different to GLT. By contrast, E3 supplementation of GLT medium did

significantly lowered reactive species to 123.33 ± 7.26 % (p=0.0486) compared with reactive species levels generated by GLT (162.00 ± 11.72 %).

Even with the significant decrease of ROS level generated by E3 supplementation to GLT (123.33 ± 7.26 %), it was still shown that its ROS production remained significantly higher compared to control. This result indicates that E3 can scavenge radical species but is not as effective as L-carnosine's scavenging activity in these cells.

To compare the capacity of carnosine mimetics to L-carnosine in stimulating insulin secretion against GLT insulin secretion inhibition, INS-1 cells were incubated for 5 days in RPMI-1640 medium ± 10 mM L-carnosine or RPMI-1640 medium ± 100 µM carnosine mimetics or GLT medium ± 10 mM L-carnosine or GLT medium ± 100 µM carnosine mimetics.

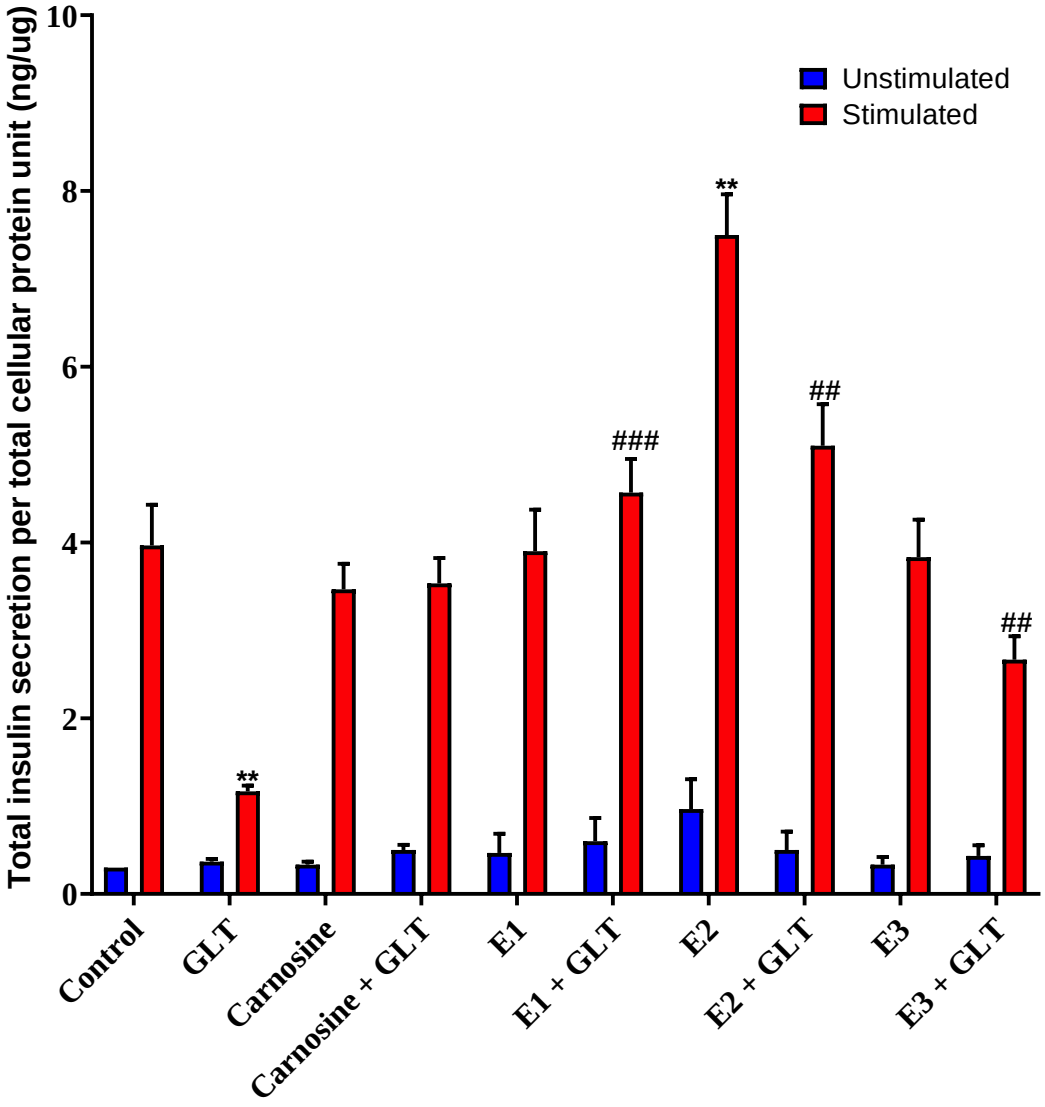

Figure 6.16 Effect of carnosine on insulin secretion to glucolipotoxic treated INS-1 rat pancreatic β-cells. INS-1 cells were incubated for 5 days in RPMI-1640 medium ± 10 mM L-carnosine or RPMI-1640 medium ± 100 µM carnosine mimetics or GLT medium ± 10 mM L-carnosine or GLT medium ± 100 µM carnosine mimetics. Mercodia High Range Rat Insulin ELISA determined insulin secretion following incubation ± secretagogue cocktail for 3 hours. Unstimulated is in blue colour and stimulated is in red colour with data normalised to total cellular protein. The data shown are from three independent experiments. **p<0.01 relative to control; $^{\#\#}$p<0.01, $^{\#\#\#}$p<0.001 relative to GLT.

After the 5-day incubation period, amongst the carnosine mimetics, only E2 has been observed to have a significant increase (7.50 ± 0.46 ng/µg, p=0.0057) in insulin secretion relative to control. And the other two mimetics, E1 (3.90 ± 0.47 ng/µg) and E3 (3.83 ± 0.43 ng/µg), were found to be similar to the control in increasing

insulin secretion. Whilst GLT decreased insulin secretion significantly compared to control (3.5 ± 0.50 ng/µg, p=0.0039), this was reversed by supplementation with carnosine mimetics. It was shown that the addition of carnosine mimetics to GLT was able to reverse GLT's insulin secretion inhibition effect. E1 + GLT (4.57 ± 0.38 ng/µg, p=0.0010), E2 + GLT (5.10 ± 0.47 ng/µg, p=0.0012), and E3 + GLT (2.67 ± 0.27 ng/µg, p=0.0055) increased significantly the stimulated insulin secretion level inhibited by GLT. This indicates that these synthesised non-hydrolysable carnosine mimetics could exhibit potential to increase the stimulated insulin secretion inhibited by GLT.

6.2.4 Effect of carnosinase inhibitor and carnosine mimetic on 4-hydroxynonenal level

4-hydroxynonenal (4-HNE) is a biomarker for oxidative stress caused by forming a covalent bond to proteins, DNA, and phospholipids containing amino moiety (Zhong and Yin, 2015). Amongst the carnosinase inhibitors and carnosine mimetics, M8 and E3 were chosen as the top potential drug candidate molecules based on their efficacy to lower radical species in both INS-1 cells and C2C12 myotubes, and crucially in terms of the functional impact that they had in stimulating glucose uptake into C2C12 myotubes (unpublished data by Dr. Charlie A. Lavilla, Jr, a fellow PhD student in the Turner group).

In collaboration with Dr. Paul W. Caton and Dr. Sophie Sayers from King's College London, control and high fat-fed CD-1 mice had their drinking water supplemented with or without M8 (100 µM) and E3 (100 µM) for 10 weeks (with local Ethics Board approval). The animals had their weight checked weekly, and at the conclusion of the study they also underwent a glucose tolerance test. M8 was found to be effective at reducing weight gain in the high fat-fed mice, whilst E3 significantly enhanced glucose tolerance in these animals (Lavilla et al, unpublished data). Blood

samples were then taken, frozen, and shipped to NTU for analysis of systemic reactive species scavenging effectiveness. This was determined by measuring 4-HNE and 3-NT levels (see next section) following ELISA kit manufacturer's protocols (Mercodia, Uppsala, Sweden).

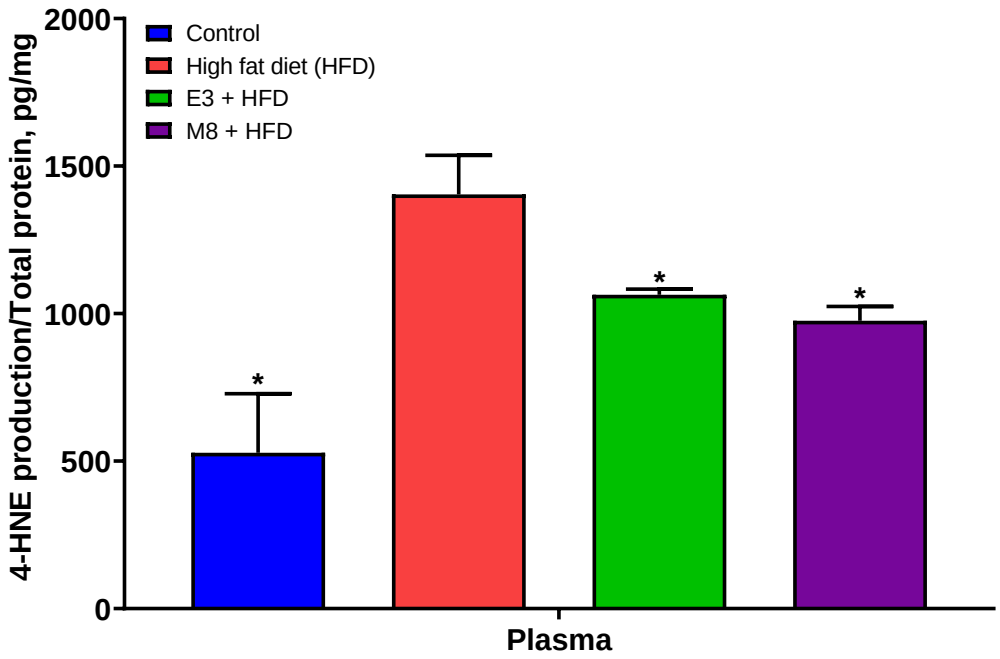

Figure 6.17 Effect of M8 and E3 on 4-hydroxynonenal production. The plasma was added with heparin as anticoagulant and the samples were centrifuged for 5 minutes at 1,000 x g at 4 ^{o}C. The supernatant was collected and assayed immediately following manufacturer's 4-HNE ELISA kit protocol (Fine test, Wuhan Fine Biotech Co., Ltd.). The data shown are from three independent experiments. The total protein concentration of the supernatant was determined using BCA protein assay. Statistical analyses were carried out by one-way ANOVA followed by Tukey's multiple comparisons test as post hoc test. *$p<0.05$ compared to a high-fat diet.

High-fat diet (HFD) was shown to significantly increase the 4-HNE level to 1403.80 ± 132.85 pg/mg ($p=0.0109$) relative to control (528.06 ± 200.17 pg/mg). However, the 4-HNE level was significantly reduced upon supplementation of drinking water with E3 to 1063.74 ± 19.33 pg/mg ($p=0.0322$). This represents a 24.22% decrease in 4-HNE level. M8 supplementation to drinking water of HFD mice had a similar

effect on 4-HNE level, which was decreased to 975.61 ± 48.56 pg/mg (p=0.0194). This represents a 30.50% decrease in the total 4-HNE level.

6.2.5 Effect of carnosinase inhibitor and carnosine mimetic on 3-nitrotyrosine level

3-Nitrotyrosine is considered as a classical biomarker of nitro-oxidative stress formed due to nitration of protein-bound (S-glutathiolation and S-oxidation of cysteine) and tyrosine residues by reactive peroxynitrite or peroxonitrite (ONOO-) ions (Daiber et al., 2021; Pirro et al., 2007; Teixeira et al., 2016a).

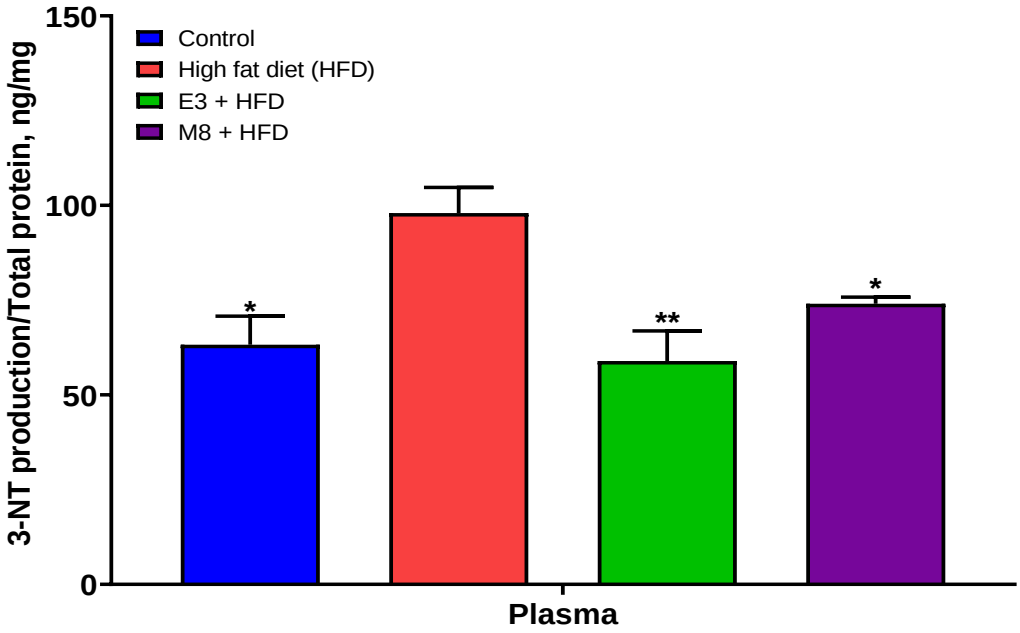

Figure 6.18 Effect of M8 and E3 on 3-nitrotyrosine production. The plasma was added with heparin as anticoagulant and the samples were centrifuged for 5 minutes at 1,000 x g at 4 ^{o}C. The supernatant was collected and assayed immediately following manufacturer's 3-NT ELISA kit protocol (Fine test, Wuhan Fine Biotech Co., Ltd.). The data shown are from three independent experiments. The total protein concentration of the supernatant was determined using BCA protein assay. Statistical analyses were carried out by one-way ANOVA followed by Tukey's multiple comparisons test as post hoc test. **p<0.05 compared to a high-fat diet.

High-fat diet (HFD) was shown to significantly increase the 3-NT level to 97.97 ± 6.75 pg/mg (p=0.0132) relative to control (63.23 ± 7.53 pg/mg). However, this increase was significantly reduced upon drinking water supplementation with E3 to 58.95 ± 7.92 pg/mg (p=0.0100). This represents a 39.83% reduction in total 3-NT species level, and importantly complete protection against the HFD-associated increase in 3-NT from control level. M8 supplementation also reduced 3-NT level, and this was decreased to 74.03 ± 1.75 pg/mg (p=0.0132). This represents a 24.44% reduction in total 3-NT species level, and a 68.92% reduction in the HFD-associated increase in 3-NT from control.

6.3 Discussion

Cell viability is very useful in evaluating compounds for their cytotoxicity. By this, cell viability assay can be used to determine the effects of compounds on cell health and to optimise cell culture and experimental conditions. As shown in the results, experimental conditions under investigation (GLT, L-carnosine, and L-carnosine + GLT) did not have a negative effect on INS-1 cell health over the duration of these experiments. Similar results were observed for INS-1 cells when exposed to carnosinase inhibitors ± GLT and carnosine mimetics ± GLT.

This study has shown that GLT generated a significant amount of reactive oxygen and nitrogen species (RONS). 2',7'-Dichlorofluorescin diacetate (DCFH-DA) or 2',7'-dichlorodihydrofluorescin diacetate (DCFH2-DA), a non-fluorescent cell-permeable probe that diffuses easily on the plasma membrane, was used to detect intracellular oxidative stress (Reiniers et al., 2017). Although DCFH-DA is commonly used to measure reactive oxygen species (Eruslanov and Kusmartsev, 2010), it can also detect some nitrogen species (Kalyanaraman et al., 2012). Importantly, enzymes such as glutathione peroxidase, catalase, thioredoxin, and superoxide dismutase that can detoxify and remove RONS (Evans et al., 2003; Newsholme et

al., 2016; Tiedge et al., 1997) are found in relatively low abundance in pancreatic β-cells, thereby allowing accumulation of RONS (Tiedge et al., 1997).

The introduction of antioxidants can be used to strategically minimised the harmful excess production of RONS by GLT. Carnosine and its related histidine-containing dipeptides (homocarnosine, balenine, and anserine) effectively reduce reactive and cytotoxic carbonyl species by forming adducts (Aldini et al., 2005; Vistoli et al., 2009) through carnosinylation, resulting in their deactivation and removal of damaged proteins (Brownson and Hipkiss, 2000). These carnosinylated proteins were suggested to have the following fates: first, they stay within the cell as lipofuscin (age-pigment) as observed predominantly in nerve, brain, and muscle. Second, they can be degraded by the proteasomal or lysosomal systems. Lastly, they can be eliminated by exocytosis, possibly be endocytosed by scavenging receptors, and destroyed by the lysosomal system (Hipkiss et al., 2001). Hence, carnosine helps in protecting biomolecules from oxidative stress (Prokopieva et al., 2016). Boldyrev reported that L-carnosine was able to inhibit the formation of advanced glycoxidation end-products (AGEs) and advanced lipoxidation end products (ALEs), of which both are involved in the ageing process (Boldyrev, 2012). My data shows that L-carnosine effectively lowers the level of radical oxygen and nitrogen species (RONS) generated by glucolipotoxicity, consistent with previously reported carnosine action as an effective scavenger of intracellular RONS, the building blocks of reactive carbonyl species (RCS) in pancreatic β-cell (Cripps et al., 2017).

At physiological pH, amino and carboxyl groups of β-alanine in L-carnosine is in zwitterionic form and can sequester protons; however, L-carnosine owes its buffering activity to its imidazole ring (Tamba and Torreggiani, 1999). It was reported that L-carnosine tautomers are formed at pH 7 and 9. At pH 7, the positively charged and neutral forms of imidazole ring exist, i.e., tautomer 1 and 2 are present. At pH

7 also enables to react with protons efficiently as L-carnosine pKa value is close to 7.0 (Tamba and Torreggiani, 1999). However, tautomer 1 is predominantly present at this slight alkaline condition (pH 9) as tautomer 2 is energetically less stable compared to tautomer 1 (**Figure 6.19**). Looking at the imidazole ring of L-carnosine, C2 and C4 are the preferred sites for OH radical addition as both are negatively charged.

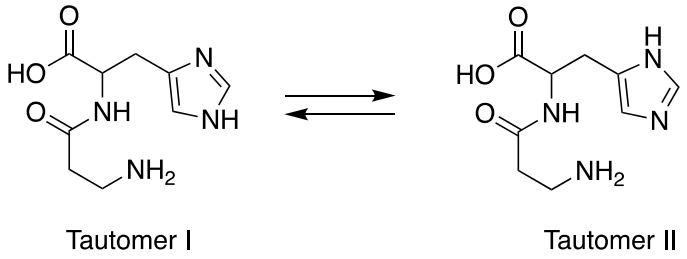

Figure 6.19 Tautomeric forms of L-carnosine. Tautomer I is predominantly present at slightly alkaline conditions at pH 7 and 9.

Several studies have presented the antioxidant activity of L-carnosine in scavenging radical oxygen species (Decker et al., 2000; Fontana et al., 2002; Klebanov et al., 1997; Kohen et al., 1988; Pavlov et al., 1993; Tamba and Torreggiani, 1999; Zhou et al., 1998) and the mechanism in sequestering this radical oxygen species can be illustrated in the reaction below.

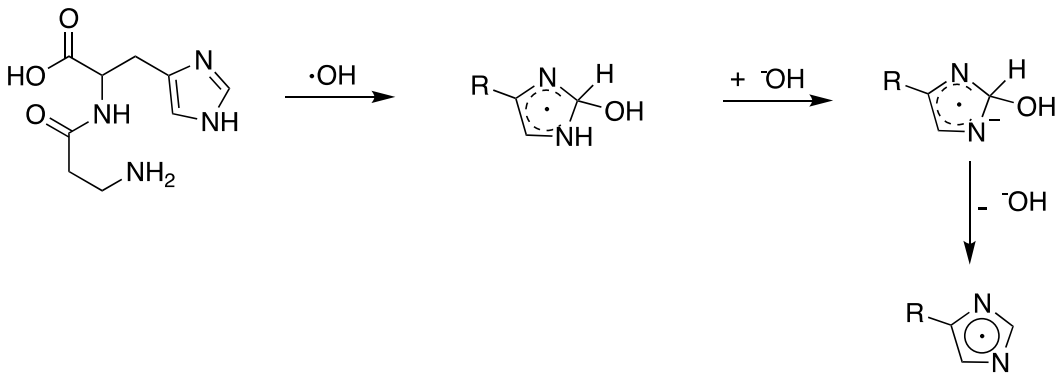

Figure 6.20 Reaction mechanism of L-carnosine towards hydroxyl radicals.

In this reaction, OH radical prefers to attack the C2 site and form a stable intermediate radical (**Figure 6.20**), which disables it from reacting with other biomolecules and, therefore, less reactive than OH radical. The transient intermediate is obtained by the elimination of water through a based-catalysed reaction. Hence, the scavenging effect of L-carnosine towards ROS can be illustrated by this mechanism.

Inducible nitric oxide synthase (iNOS) is a Ca^{2+}-independent enzyme that generates nitric oxide from L-arginine conversion to citrulline (Aktan, 2004; Lechner et al., 2005; Vannini et al., 2015). Diabetic islets displayed impaired insulin and glucagon responses to glucose, disturbed cAMP generation, and high inducible nitric oxide synthase (iNOS) mRNA and protein expression (Muhammed et al., 2012). Inducible nitric oxide synthase (iNOS) is considered to contribute to oxidative stress/nitrative stress and plays a central role in altering glucose metabolism during inflammation (Anavi and Tirosh, 2020). Expression of iNOS results in nitric oxide and peroxynitrite species production, which can form 3-nitrotyrosine from protein tyrosyl residues (Anavi and Tirosh, 2020). In this study, iNOS protein expression was significantly upregulated upon exposing INS-1 cells with high glucose and high fatty acid diet. However, this was shown to be downregulated by the addition of L-carnosine. This indicates that L-carnosine was able to scavenge RNS.

Insulin is the principal peptide hormone secreted by the β-cells of Langerhans' pancreatic islets (Wilcox, 2005). It is responsible for controlling glucose metabolism by facilitating cellular glucose uptake and regulating carbohydrates, lipid, and protein (Muoio and Newgard, 2008). Its principal function is to control the uptake and utilisation of glucose in peripheral tissues via the glucose transporter (Leto and Saltiel, 2012). As mentioned, glucolipotoxicity was reported to impair glucose-stimulated insulin secretion (Kraegen et al., 2001; Poitout and Robertson, 2002). My data shows that glucolipotoxicity significantly inhibited stimulated insulin secretion,

but that this could be reversed upon L-carnosine supplementation. This indicates that L-carnosine scavenging of RONS could normalise β-cell function and enhance insulin secretion.

Carnosinase is an enzyme that is able to hydrolyse carnosine (Boldyrev, 2012; Peters et al., 2018; Sauerhöfer et al., 2007). Quantification and identification of carnosinase was conducted by Michael J. Cripps, PhD, a colleague in the Turner group, and he identified through immunoblotting that carnosinase is present in INS-1 cells. Hence, this presence of carnosinase could affect the full biological action of carnosine. Having this premise, one option to combat the hydrolytic action of carnosinase is to increase the carnosine supplement concentration, but this seems impractical. It was observed that a higher concentration (100- and 500 mM) of L-carnosine has a deleterious effect on INS-1 cell morphology, as seen in the preliminary results (n=3) that a higher concentration of L-carnosine killed INS-1 cells (results not shown in the thesis). Another strategy found was to screen potential carnosinase inhibitors and carnosine mimetics. Our results found that M8, a putative carnosinase inhibitor, lowered ROS generated by GLT significantly. Although M8 was shown to reverse the stimulated insulin secretion inhibited by GLT slightly, it was shown not to be a statistically significant effect. With carnosine mimetics (E1, E2, and E3), it was found that these compounds were not only able to decrease ROS generated by GLT, but were also able to significantly reverse the inhibition of stimulated insulin secretion caused by GLT. This result indicates a potentially effective strategy to combat the hydrolytic activity of carnosinase and offer a RONS scavenging potential, which consequently increases insulin secretion in β-cells. However, more tests are needed to conduct to fully understand the action of these compounds and to know if they are better than L-carnosine.

Results presented here also shown that M8 and E3 were able to significantly reduce the 3-NT and 4-HNE adduct formation generated in the plasma of CD-1 mice

fed a high-fat diet. The possible explanation for this effect is the potential scavenging activity of these compounds. This effect is likely a consequence of the same reaction mechanism of L-carnosine shown in **Figure 6.20,** and the quenching effect of L-carnosine shown in **Figure 6.21**.

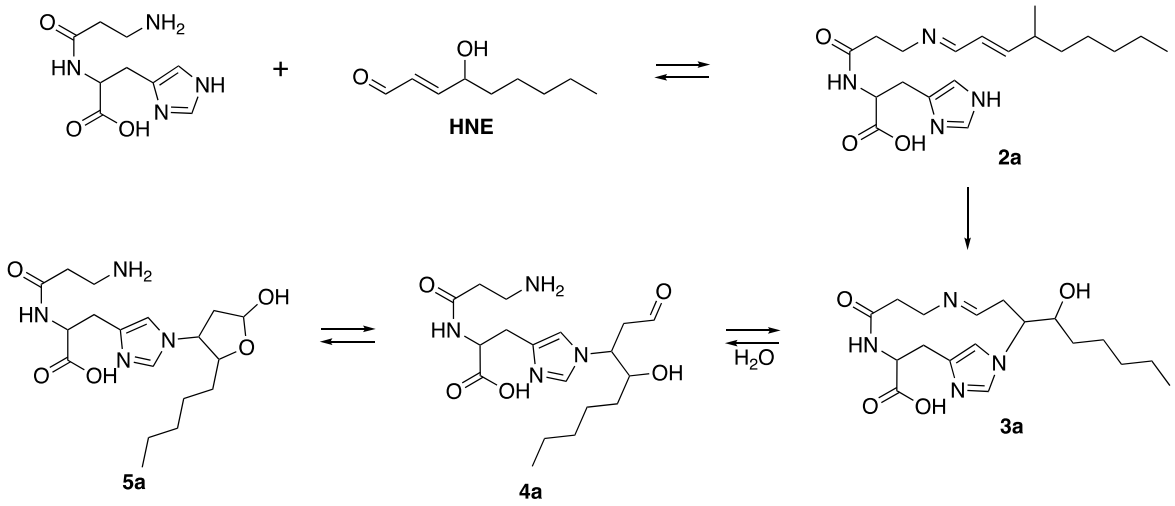

Figure 6.21 Proposed reaction mechanism of L-carnosine with 4-HNE.

The amino group of L-carnosine reacts with the ketone moiety of HNE to form a reversible α,β-unsaturated imine (**2a**), which will subsequently undergo a ring closure through intramolecular Michael addition reaction (**3a**). Hydration of **3a** hydrolysed the imine group (**4a**), and this is followed by cyclisation reaction leading to the formation of a hemiacetal derivative (**5a**) (Aldini et al., 2002; Aldini et al., 2005; Boldyrev et al., 2013; Fotouhi et al., 2018).

4-Hydroxynonenal (4-HNE), one of the major products of lipid peroxidation, can interact with DNA and cause a genotoxic effect even at a micromolar concentration (Eckl et al., 1993). This reactivity of 4-HNE is due to the interaction of the double bond, aldehyde group, and hydroxyl group, which are near to each other (Witz, 1989). During elevated ROS and oxidative stress, 4-HNE is highly generated, and this can react with DNA, proteins, and membrane lipids and could potentially

cause mitochondrial dysfunction (Xiao et al., 2017). 4-HNE, an oxidative stress marker, was observed to be elevated in human patients with diabetic retinopathy (Oruc et al., 2020), in diabetic rat kidneys (Liu et al., 2016), and in type 2 diabetic patients with nephropathy (Calabrese et al., 2007). Jaganjac et al. determined an elevated amount of 4-HNE adducts in the blood of obese men with type 2 diabetes (Jaganjac et al., 2017).

3-Nitrotyrosine (3-NT) results from the interaction of free L-tyrosine and RNS such as nitric oxide, peroxynitrite, peroxynitrous acid, and nitrogen dioxide radicals (Seeley et al., 2014). This can result in a post-translational modification of proteins which could eventually lead to various physiological and pathological conditions (Teixeira et al., 2016), including oxidative stress, inflammation, neurodegenerative and cardiovascular conditions (Surmeli et al., 2010). It was also observed that peroxynitrite interaction with proteins could lead to systemic lupus (Ahsan, 2013; Pan et al., 2020; Shah et al., 2014).

3-NT level in plasma was observed to be higher in patients with coronary artery diseases (Pourfarzam et al., 2013; Shishehbor et al., 2003), and shown to accumulate during atherogenesis (Upmacis, 2008) and seen to be predominant in atherosclerotic blood vessels (Sucu et al., 2003). 3-NT levels in diabetic patients (de Bandeira et al., 2013; Jialal et al., 2012), nephropathic diabetic patients (Thuraisingham et al., 2000), and diabetic patients with microvascular complications and inflammation (Devaraj et al., 2007) were observed to be high. The 3-NT level was determined to be high in animal models with rheumatoid arthritis and osteoarthritis (Nemirovskiy et al., 2009).

In this study, it was observed that supplementation of M8 and E3 to the drinking water of high-fat mice significantly reduced 4-HNE and 3-NT formation. This result indicates that these compounds can potentially reduce oxidative stress by

effectively scavenging RONS, which is considered one of the mechanisms involved in the progression of type 2 diabetes and insulin resistance.

6.4 Conclusion

L-carnosine was shown to effectively sequester reactive oxygen and nitrogen species (RONS) generated by glucolipotoxicity. L-carnosine was also shown to reverse the inhibitory action of GLT on stimulated insulin secretion. Screened carnosinase inhibitors were not observed to scavenge ROS significantly and did not show a reversal effect of the stimulated insulin-secretion inhibitory effect of GLT. However, carnosine mimetics (E1, E2, and E3) were shown to sequester ROS, and E3 was seen to have a high efficacy significantly in decreasing ROS. All carnosine mimetics have been shown to efficiently reverse the stimulated insulin secretion inhibitory effect of GLT, thus enhancing insulin secretion with a high effect even at a relatively low concentration of 100 μM. Carnosine inhibitor, M8, and carnosine mimetic, E3 were shown to reduce significantly the generated 4-HNE and 3-NT adducts in plasma of mice fed a high-fat diet. With these results, L-carnosine, M8, and E3 are compounds that could potentially be used to combat complications of type 2 diabetes and enhance insulin secretion.

Chapter 7

General Discussion, Summary, and Conclusion

7.1 General discussion and summary

Diabetes is a primary cause of kidney failure, stroke, lower limb amputation and blindness if not prevented and treated. Obesity is the main modifiable risk factor, with studies confirming that up to 90% of patients with T2D are overweight or obese, and that obese people are at the highest risk of developing T2D (Wilding, 2014). Intensive lifestyle interventions are, however, resource-intensive and difficult to sustain. Alternatively, it is feasible that by manipulating molecules and pathways central to the induction of diabetogenesis, we might offer an improved clinical prognosis to millions of patients who have diabetes.

Visceral adipose tissue (VAT) is also thought to be linked to the pathophysiology of type 2 diabetes. There are many differences between visceral adipose tissue and subcutaneous adipose tissue. VAT is found mainly in the abdomen area, namely the mesentery and omentum, and it drains directly through the portal circulation to the liver. It is known that VAT contains more inflammatory and immune cells, and it is more metabolically active. In addition, VAT can generate more free fatty acids (Ibrahim, 2010) and amplify the underlining pathophysiology of T2D. In addition to being known as a metabolic disorder, type 2 diabetes is also now thought of as an inflammatory disease (Turner et al., 2014).

The initial failure of β-cell can be attributed to the following processes: oxidative stress, endoplasmic reticulum stress, mitochondrial dysfunction and glucolipotoxicity (Prentki et al., 2006). When hyperglycaemia has developed, β-cell function failure is increased by the addition of amyloid deposition, O-linked glycosylation and islet inflammation, which all affect loss of β-cell mass by inducing apoptosis (Prentki and Nolan, 2006). Furthermore, Butler et al. also reported that β-cell volume decreases in obese and lean patients with T2D (Butler et al., 2003).

To understand the molecular basis underpinning diabetogenesis, and to identify potential novel drug targets, this doctoral project focused on the combined and

damaging effect of elevated glucose and increased free fatty acid levels. This combination is termed glucolipotoxicity (GLT). T2D is characterised by elevated blood sugar levels resulting from insulin deficiency, insulin resistance and β-cell mass reduction. Pancreatic β-cells are the primary cell-type used in this project, as they produce and secrete insulin in response to increased blood sugar levels and are therefore affected in the onset of T2D. The glucolipotoxic environment has been created in the INS-1 β-cell line model by supplementing RPMI-1640 media with D-glucose, sodium oleate and palmitic acid (Marshall et al., 2007).

This study was divided into four chapters that investigated the impact of high-glucose and high-fatty acid diet on INS-1 rat pancreatic β-cell, mice primary islet cell and skeletal muscle C2C12 myotubes. In addition, L-carnosine and β-alanine on the production of radical species generated by glucolipotoxicity have also been determined and its effects on the mitochondrial function were conducted.

In chapter 3, the effects of GLT on HNF4α expression was evaluated. Using transcriptomic analysis and MetacoreTM technology, it was determined that HNF4α is the central regulator of various multiple protein trafficking genes such as syntaxin 17 and Rab genes (Rab1b, Rab2a, Rab4b and Rab10) that are implicated in the secretory trafficking pathway in pancreatic b-cells. Furthermore, it was also shown that the downregulation of HNF4α, Rab genes, and syntaxin 17 was driven by GLT metabolic stress. expression HNF1α was also shown to be transcriptionally activated by HNF4α (Sel et al., 1996). This result shows that HNF4α affects HNF1α expression, and this result is in congruent with the idea that HNF1α is transcriptionally activated by HNF4α (Sel et al., 1996).

In chapter 4, the effects of GLT on extracellular matrix proteins was determined, and cytoskeletal remodelling was suggested to be linked to MMP-14, MMP-15, MMP16, CD44 and ErbB4 expression. Matrix metalloproteinases (MMPs) are zinc-dependent extracellular matrix endopeptidases (Cui et al., 2017) that have

previously been suggested to be involved in the development of complications of type 2 diabetes (Abreu et al., 2016). From both previous microarray data from the Turner group, and current Illumina-HiSeq gene expression data, it was shown that cell adhesion-ECM remodelling, cell adhesion-cell matrix glycoconjugates and cell adhesion-integrin inside-out signalling in neutrophils were significantly downregulated when INS-1 cells were exposed to GLT. When MMP14, CD44 and ErbB4 were knocked down and gene expression reduced, it was shown that this reduced insulin secretion. This result suggests that MMP14, CD44 and ErbB4 play a vital role in the regulation of insulin secretion observed in type 2 diabetes.

In chapter 5, the effect of GLT on mitochondrial function was investigated. β-cell dysfunction is a characteristic of type 2 diabetes that is linked to the action of high glucose and high fatty acid diet (GLT) through mechanisms such as islet inflammation, endoplasmic reticulum stress, oxidative stress and mitochondrial dysfunction (van Raalte and Diamant, 2011). Mitochondria generate approximately 90% of cellular reactive oxygen species (ROS) (Dan Dunn et al., 2015; Rocha et al., 2016). The imbalance between increased mitochondrial reactive oxygen species production and decreased antioxidant defence activity results in oxidative stress, thereby damaging cellular components such as lipids, proteins and DNA (Xiao et al., 2017).

Previous studies have reported that high glucose, and high fatty acids significantly increase mitochondrial reactive oxygen species (Seifert et al., 2010; St-Pierre et al., 2002; Tahara et al., 2009) and consequently increase mitochondrial electron transport chain complex subunits expression levels, β-cell apoptosis, intracellular lipid accumulation, oxidative stress, endoplasmic reticulum stress, and nuclear NF-κB (Lim et al., 2011). GLT has also been shown to affect mitochondrial function by altering mitochondrial fusion and fission in favour of the loss of its ability to undergo fusion (Las et al., 2011). Furthermore, it has also been shown that ATP

production decreases (Haythorne et al., 2019; Köhnke et al., 2007; Las et al., 2011; Lim et al., 2011) autophagy is suppressed (Las et al., 2011), the mitochondrial membrane altered (Wikstrom et al., 2007), and oxygen consumption rate decreased (Barlow and Affourtit, 2013). I therefore sought to determine whether carnosine and β-alanine might be able to counter these damaging effects of GLT on mitochondrial function Supplementation of carnosine or β-alanine to GLT media significantly protected cells against GLT-mediated mitochondrial dysfunction. This reversal effect of carnosine and β-alanine to the deleterious effect of GLT is likely associated with the ability of carnosine to sequester the excess mitochondrial radical species generated by the introduction of GLT. β-alanine alone (Boldyrev, 2012) cannot sequester radical species however, but instead is thought to react with intracellular histidine to form carnosine.

In chapter 6, carnosine was shown to be an effective scavenger of HNE, α- and β-unsaturated aldehydes associated with lipid peroxidation and oxidative stress (Guiotto et al., 2005). However, presence of carnosinase enzymes in both sera and intracellular environments cause the hydrolysis of carnosine into its amino acid components (Sauerhöfer et al., 2007). Hence, in collaboration with Dr. Garner and his team from NTU Department of Chemistry and Forensics, potential carnosine inhibitors and carnosine mimetics (which are slowly-hydrolysable by carnosinase) were generated. GLT generates significant amounts of radical oxygen and nitrogen species (RONS), and has also been shown to inhibit secretagogue-stimulated insulin secretion. However, this effect of GLT was prevented by the supplementation of carnosine, which weas shown to sequester excess generated RONS. This reversal effect of carnosine was also mirrored by carnosine mimetics (E1, E2 and E3) at 2 orders of magnitude lower concentration. Furthermore, M8 and E3, significantly reduced 3-NT and 4-HNE adduct formation in plasma of CD-1 mice fed with high-fat diet. The reversal effect of carnosine and its analogues on RONS

generation and inhibition of insulin secretion of GLT suggests that these compounds could potentially be used in the future treatment of type 2 diabetes and insulin resistance.

In summary, GLT has been shown to drive dysregulation of gene expression, as well as to generate significant amounts of radical species that eventually drive oxidative stress, nitrosative stress, and mitochondrial dysfunction, events which consequently inhibit stimulated insulin secretion. However, the presence of carnosine, its analogues, or β-alanine can reverse many of the damaging effects of GLT effectively, thereby making these molecules attractive candidates for therapeutic development.

Chapter 8

Future Work

8.1 Histone acetylation

In a parallel transcriptomic study (currently unpublished) conducted in the Turner research group, it was shown that glucolipotoxicity alters metabolic pathways by significantly downregulating IDH2, SC4MOL, FASN and insulin gene expression in INS-1 cells. IDH2 catalyses the reversible oxidative decarboxylation of isocitrate to α-ketoglutarate in mitochondria and reduction of $NADP^+$ to NADPH (Molenaar et al., 2018). Sterol-C4-methyl oxidase like (SC4MOL) is involved in catalysing the demethylation of C4-methysterols in the cholesterol biosynthesis pathway (Sukhanova et al., 2013). Fatty acid synthase (FASN) is involved in fatty acid synthesis from acetyl-CoA and NADPH (Kuhajda, 2006).

Glucolipotoxicity was also shown to increase intracellular acetyl CoA levels, and this then led to histone H3 and H4 acetylation. Histone acetylation is one of the epigenetic mechanisms involved in diabetes (Li et al., 2016). Histone acetylation plays a role in regulating gene expression based on external factors (Lee and Grant, 2019).

In collaboration with Dr. Paul W. Caton and Dr. Sophie Sayers from King's College London, I sought to determine whether these findings from INS-1 cell-line experiments could be replicated in primary cells. In brief, pancreatic islet cells from CD-1 mice were isolated and cultured *ex vivo* in RPMI-1640 media, or RPMI-1640 media supplemented with 17 mM D-glucose, 200 µM oleic acid and 200 µM palmitic acid. Cells were lysed, then RNA extracted and reverse transcribed, and RT-qPCR performed using primers specific for the target genes.

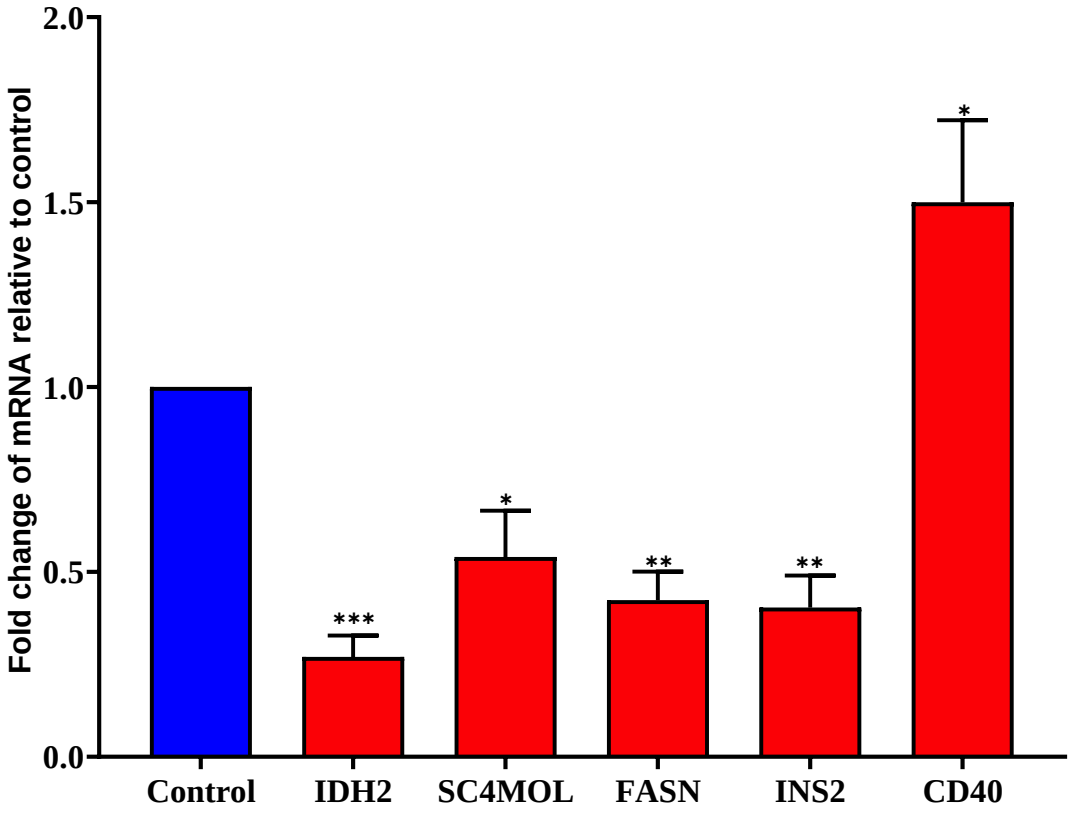

Figure 8.1 qPCR validation of genes involved in TCA, fatty acid and cholesterol synthesis. The pancreas was surgically removed from mice and islets were isolated, then cultured for 72h in RPMI-1640 medium or RPMI-1640 medium supplemented with 17 mM D-glucose, 200 μM oleic acid, and 200 μM palmitic acid. Cells were then lysed, RNA extracted, and cDNA synthesised, and RT-qPCR was performed using primers specific for the target genes. Data represented as ΔΔCt values expressed as a fold change compared to cells grown in control medium. Data shown is the mean ± S.E.M. of three independent experiments. *p<0.05, **p<0.01, ***p<0.001.

As shown in **Figure 8.1**, IDH2, SC4MOL, FASN and insulin mRNA expression levels were significantly reduced to 0.27 ± 0.06 (p=0.0002), 0.54 ± 0.13 (p=0.0217), 0.42 ± 0.08 (p=0.0017), and 0.40 ± 0.09 (p=0.0024), respectively, relative to control pancreatic islets. This downregulation of gene expression closely resembles the data generated using INS-1 cells, and thereby validates the gene expression data generated using INS-1 cells.

Decreased IDH2 expression results in a decrease of NAPDH generation and inhibition of insulin secretion. I therefore sought to determine whether reversing the

effect of GLT on IDH2 expression by overexpressing IDH2 mRNA could reverse this deleterious action of GLT on pancreatic b-cells. This part of the study was conducted in collaboration with Dr. Sergio L. Colombo at NTU.

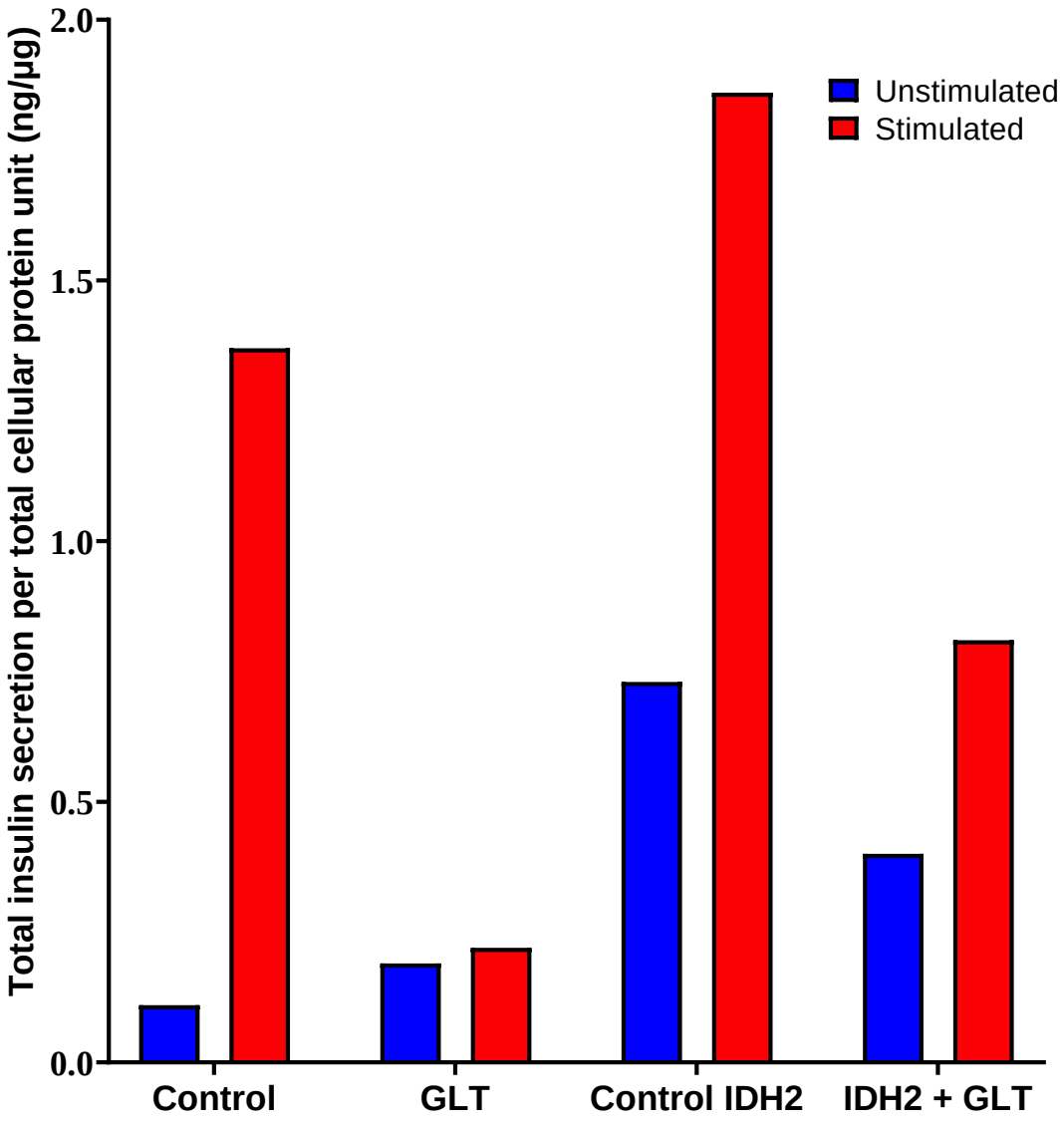

Figure 8.2 Effect of glucolipotoxicity inhibited insulin secretion to IDH2 overexpressed INS-1 cells. INS-1 rat pancreatic β-cells were incubated for 5 days in complete RPMI-1640 or RPMI-1640 control supplemented with 27 mM glucose, 200 µM oleic acid and 200 µM palmitic acid or RPMI-1640 control supplemented with 27 mM glucose, 200 µM oleic acid, 200 µM palmitic acid and 10mM carnosine. Insulin secretion was determined by High Range Rat Insulin ELISA following incubation ± secretagogue cocktail for 2h [(-) blue, (+) red] with data normalised to total cellular protein content.

Results show that IDH2 overexpressing INS-1 rat pancreatic β-cells secrete more insulin than control cells. Furthermore, IDH2 overexpressing INS-1 rat pancreatic β-

cells exposed to GLT did partially recover their secretory capacity. This data is however currently based on n=1, and further repeats are necessary to confirm these findings.

8.2 Olfactory receptor agonist ligands its implication to glucolipotoxicity inhibition of insulin secretion

G protein-coupled receptors (GPCRs) are the main target in drug development programs. They are primarily involved in cell communication and are encoded by the largest family in our genome (Alexander et al., 2019; Kobilka, 2007; Møller et al., 2017). Olfactory receptors (ORs), identified by Buck and Axel in 1991 (Buck and Axel, 1991) are GPCRs that mediate olfactory chemoreception (Leem et al., 2018) and are able to elevate intracellular cAMP (Dalesio et al., 2018). Olfactory receptors are not only expressed in olfactory sensory neurons but also in many tissues including skin, lung, intestine, testis, and blood (Maßberg and Hatt, 2018). Olfactory receptors have been seen to function in cell-cell recognition, migration, proliferation, the apoptotic cycle, exocytosis, and pathfinding processes (Maßberg and Hatt, 2018) however largely of their functions are not yet fully known (Leem et al., 2018).

Vertebrate olfactory receptors are composed of four different families of G protein-coupled receptors (Mombaerts, 2004):

1. Olfactory receptor family: approximately1000 functional members in some mammalian species is the largest amongst the families (Zhang et al., 2004).
2. Trace amine-associated receptors with <20 members (Liberles and Buck, 2006);
3. V1R vomeronasal receptors with approximately with 150 members (Pfister and Rodriguez, 2005; Zhang et al., 2004);
4. V2R vomeronasal receptors with approximately 60 members (Yang et al., 2005).

C family of GPCRs contains 22 members including V2R vomeronasal receptors (Pin et al., 2003), calcium-sensing receptor (CaS), eight metabotropic glutamate ($mGlu_{1-8}$) receptors, GABA-B receptors ($GABA_{B1}$ and $GABA_{B2}$), and taste receptors (T1R1-T1R3) (Fredriksson et al., 2003).

In 2008, Triballeau et al identified V2R-like receptor, called receptor 5.24, from goldfish olfactory epithelium was activated by 20 natural amino acids (Triballeau et al., 2008). Amongst the amino acids, receptor 5.24 has a higher affinity towards lysine and arginine, classified as basic amino acids. Because of the diverse function of receptor 5.24 as an odourant receptor, it enables the olfactory system to detect various odourants based on ligand selectivity. Using the virtual high-throughput screening (vHTS), Triballeau et al 2008 was able to identify novel compounds, amongst are L-glutamic acid-y-p-nitroanilide, L-canavanine and LL-diaminopimelic acid, for exploring the C class of GPCR and examine the olfactory function in vivo (Triballeau et al., 2008).

In this study, I sought to determine whether olfactory receptors are dysregulated by exposure to glucolipotoxicity, and whether olfactory receptor agonist ligands, L-glutamic acid-y-p-nitroanilide, L-canavanine and LL-diaminopimelic acid affect the glucolipotoxic inhibition of insulin secretion. Utilising existing Illumina HiSeq data within the Turner group, where INS-1 rat pancreatic ß-cells were incubated in complete RPMI-1640 media (control) and GLT for 72hrs, all olfactory receptor RNA read counts were measured in both experimental conditions. It was observed that 734 out of 1199 olfactory receptors were significantly downregulated upon exposure to glucolipotoxicity. Only the top 20 olfactory receptors with a p-value <0.001 were considered (unpublished data in Turner group).

Cell functional analyses, i.e., cell viability and insulin secretion assay, were conducted to olfactory receptor (OLRs) agonists. On cell morphology, results show that there was no observable change in cell morphology and cells do not show non-

adherence onto the plate and assume a rounded shape. Increased cell death is not significant as their only a few floating cells observe. Cell viability was conducted to assess the cells' metabolic activity which reflects the number of viable cells in the treatment.

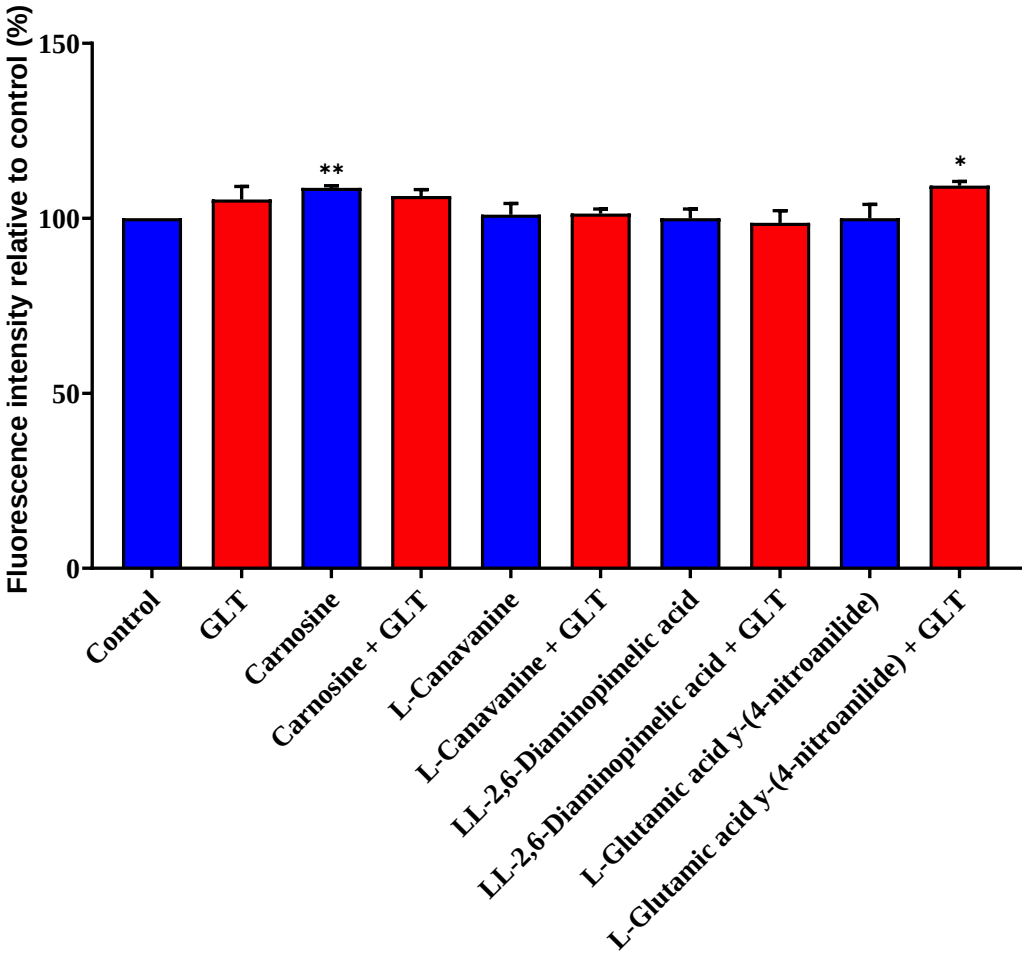

Figure 8.3 Effect of OLRs on INS-1 rat pancreatic β-cell health. INS-1 cells were incubated for 5 days in RPMI-1640 medium ± 10 mM L-carnosine or RPMI-1640 ± 100 µM OLRs or GLT medium ± 10 mM L-carnosine or GLT medium ± 100 µM OLRs. Cell viability is expressed as percentage change ± S.E.M. in comparison to control from 3 independent experiments. $p<0.05$*, $p<0.01$** relative to control.

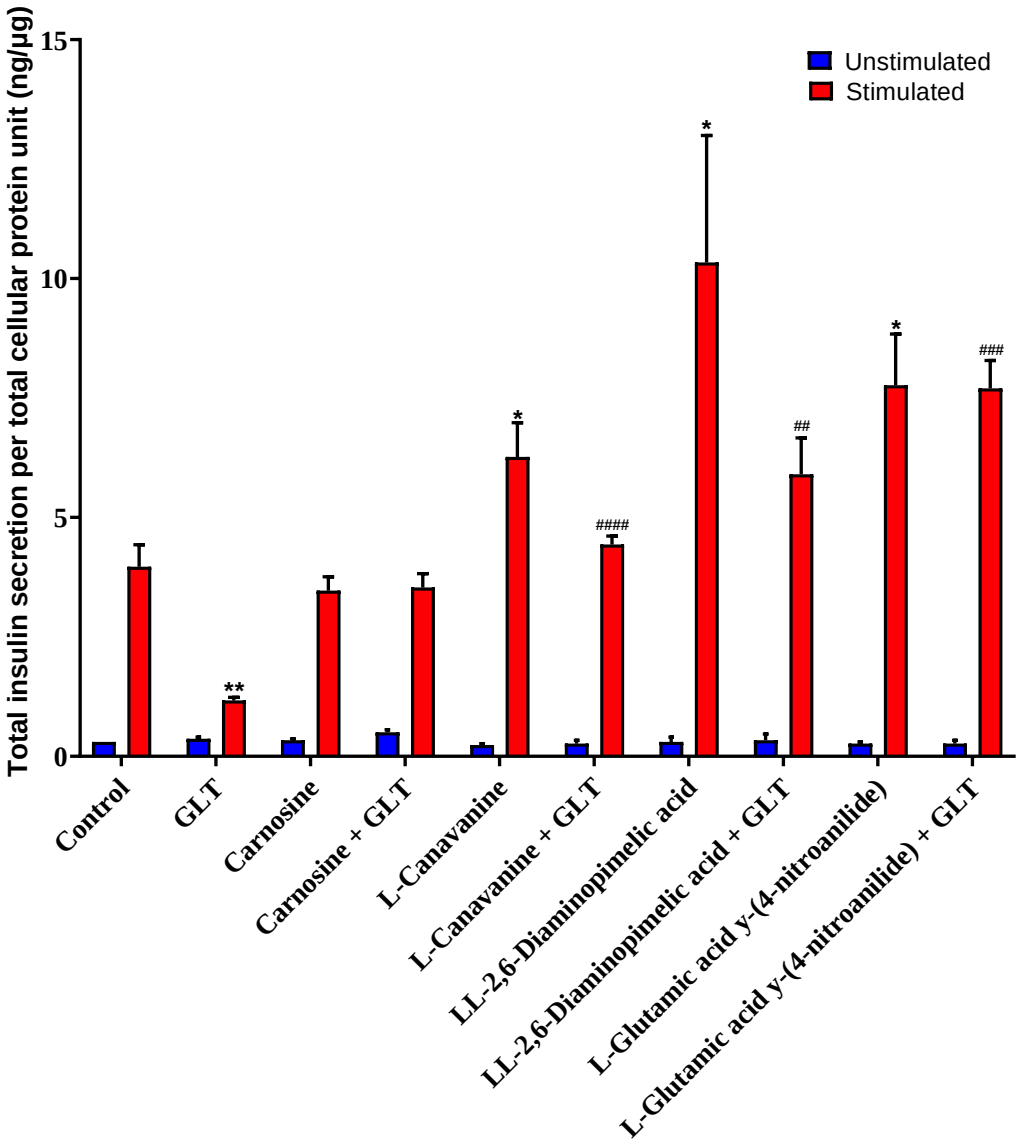

Figure 8.4 Effect of OLRs on insulin secretion to glucolipotoxic treated INS-1 rat pancreatic β-cells. INS-1 cells were incubated for 5 days in RPMI-1640 medium ± 10 mM L-carnosine or RPMI-1640 media ± 100 µM OLRs or GLT medium ± 10 mM L-carnosine or GLT medium ± 100 µM OLRs. Mercodia High Range Rat Insulin ELISA determined insulin secretion following incubation ± secretagogue cocktail for 3 hours. Unstimulated is in blue colour and stimulated is in red colour with data normalised to total cellular protein. The data shown are from three independent experiments. *p<0.05, **p<0.01 relative to control; ##p<0.01, ###p<0.001, ####p<0.0001 relative to GLT.

After the 5-day incubation period, it was shown that L-canavanine, L,L-2,6-Diaminopimelic acid, and L-glutamic acid γ-(4-nitroanilide) significantly increased insulin secretion to 6.27 ± 0.72 ng/µg (p=0.0272), 10.33 ± 2.66 ng/µg (p=0.0389), and 7.77 ± 1.07 ng/µg (p=0.0157), respectively, relative to control (3.97 ± 0.46

ng/µg). It can be shown also in the results that GLT effectively inhibited insulin secretion, but this inhibition could be reversed by addition of OLR agonists. Specifically, L-canavanine + GLT, L,L-2,6-Diaminopimelic acid + GLT, and L-glutamic acid γ-(4-nitroanilide) + GLT significantly increased secretagogue-stimulated insulin secretion to 4.43 ± 0.18 ng/µg (p=0.0001), 5.90 ± 0.76 ng/µg (p=0.0035), and 7.70 ± 0.59 ng/µg (p=0.0004), respectively, relative to GLT (1.17 ± 0.07 ng/µg). This result suggests that OLRs ligand agonist are able to significantly enhance insulin secretion.

As one of the four members of the GPCR family, it was found TAARs are mainly expressed in olfactory epithelium except for TAAR1 (Christian and Berry, 2018; Johnson et al., 2012; Liberles and Buck, 2006). However, other TAARs, except TAAR1, are classified as olfactory TAARs (Liberles and Buck, 2006). This data complements a previous report that that GPCR exposed to trace amines such as *p*-tyramine, β-phenethylamine, tryptamine, and octopamine were able to increase the production of cAMP (Bunzow et al., 2001). More specifically, a colleague in the Turner group found that TAARs 1-4, were activated by the physiological TAAR ligands isopentylamine, 2-phenylethylamine, *p*-tyramine, and agmatine. This resulted in significantly increased intracellular cAMP and significantly enhanced insulin secretion.

With most of the TAARs functioning as olfactory TAARs, olfactory receptor agonist ligands, L-glutamic acid-y-p-nitroanilide, L-canavanine and LL-diaminopimelic acid were screened for their potential to augment insulin secretion. Results show that olfactory receptor agonist ligands were able to stimulate insulin secretion at the control level, and that these ligands also were able to reverse the glucolipotoxic inhibition to insulin secretion. As olfactory TAARs are coupled to olfactory G protein, G_{olf} activation by adenylate cyclase III, they can increase intracellular cAMP levels and hence amplify insulin secretion (Phang et al., 1984).

It has been previously reported in Turner's group that glucolipotoxicity (GLT) effectively inhibits stimulated insulin secretion using INS-1 rat pancreatic β-cells. It has also been established in Turner's lab that carnosine has a great potential to reverse the harmful effects of GLT, i.e., carnosine was able to reverse glucolipotoxic inhibition of insulin secretion (Cripps et al., 2017) and also the results shown in Chapter 6 of this thesis. Unpublished data in Turner group found that GLT downregulated olfactory receptor RNA expression. This was assessed by exposing INS-1 cells to a 5 day in GLT and then RNA was extracted and conducted Illumina HiSeq sequencing. TAARs, except for TAAR1, have been shown to couple to olfactory G protein (G_{olf}) (Ebrahimi and Chess, 1998). Activated G_{olf} then dissociates from Gβγ and then activates adenylate cyclase III, resulting in an increase in intracellular cAMP (Ebrahimi and Chess, 1998). With this, the binding of the OLRs ligands to the olfactory receptor activates adenylate cyclase III, thereby increasing cAMP and consequently increase insulin secretion triggered by the elevation of Ca^{2+} in INS-1 cells. The data presented here thus demonstrates that OLR agonists are effective agents to enhance insulin secretion. As such they could potentially form another class of therapeutic agent that could be developed to enhance insulin secretion and treat T2D. This hypothesis forms the basis for future studies in the Turner group.

References

Abbasi, F., Lamendola, C., Harris, C.S., Harris, V., Tsai, M., Tripathi, P., Abbas, F., Reaven, G.M., Reaven, P.D., Snyder, M.P., Kim, S.H., and Knowles, J.W. (2021). Statins Are Associated With Increased Insulin Resistance and Secretion. Arterioscler Thromb Vasc Biol *41,* 2786-2797.

Abdelgani, S., Puckett, C., Adams, J., Triplitt, C., DeFronzo, R.A., and Abdul-Ghani, M. (2021). Insulin secretion is a strong predictor for need of insulin therapy in patients with new-onset diabetes and HbA1c of more than 10%: A post hoc analysis of the EDICT study. Diabetes Obes Metab *23,* 1631-1639.

Abdelmoez, A.M., Sardón Puig, L., Smith, J.A.B., Gabriel, B.M., Savikj, M., Dollet, L., Chibalin, A.V., Krook, A., Zierath, J.R., and Pillon, N.J. (2020). Comparative profiling of skeletal muscle models reveals heterogeneity of transcriptome and metabolism. Am J Physiol Cell Physiol *318,* C615-C626.

Abreu, B.J., and de Brito Vieira, Wouber Hérickson. (2016). Metalloproteinase Changes in Diabetes. Adv Exp Med Biol *920,* 185-190.

Abu-Soud, H.M., and Stuehr, D.J. (1993). Nitric oxide synthases reveal a role for calmodulin in controlling electron transfer. Proc Natl Acad Sci U S A *90,* 10769-10772.

Ahmad, W., Ijaz, B., Shabbiri, K., Ahmed, F., and Rehman, S. (2017). Oxidative toxicity in diabetes and Alzheimer's disease: mechanisms behind ROS/ RNS generation. J Biomed Sci *24,* 76.

Ahsan, H. (2013). 3-Nitrotyrosine: A biomarker of nitrogen free radical species modified proteins in systemic autoimmunogenic conditions. Hum Immunol *74,* 1392-1399.

Aktan, F. (2004). iNOS-mediated nitric oxide production and its regulation. Life Sciences *75,* 639-653.

Aldini, G., Carini, M., Beretta, G., Bradamante, S., and Facino, R.M. (2002). Carnosine is a quencher of 4-hydroxy-nonenal: through what mechanism of reaction? Biochem Biophys Res Commun *298,* 699-706.

Aldini, G., Facino, R.M., Beretta, G., and Carini, M. (2005). Carnosine and related dipeptides as quenchers of reactive carbonyl species: From structural studies to therapeutic perspectives. BioFactors *24,* 77-87.

Alexander, S.P.H., Christopoulos, A., Davenport, A.P., Kelly, E., Mathie, A., Peters, J.A., Veale, E.L., Armstrong, J.F., Faccenda, E., Harding, S.D*., et al.* (2019). THE CONCISE GUIDE TO PHARMACOLOGY 2019/20: G protein-coupled receptors. Br J Pharmacol *176 Suppl 1,* S21-S141.

Alumets, J., Håkanson, R., and Sundler, F. (1978). Distribution, ontogeny and ultrastructure of pancreatic polypeptide (PP) cells in the pancreas and gut of the chicken. Cell Tissue Res *194,* 377-386.

Amălinei, C., Căruntu, I.D., Giuşcă, S.E., and Bălan, R.A. (2010). Matrix metalloproteinases involvement in pathologic conditions. Rom J Morphol Embryol *51,* 215-228.

Amanat, S., Ghahri, S., Dianatinasab, A., Fararouei, M., and Dianatinasab, M. (2020). Exercise and Type 2 Diabetes. Adv Exp Med Biol *1228,* 91-105.

American Diabetes Association. (2013). Economic costs of diabetes in the U.S. in 2012. Diabetes Care *36,* 1033-1046.

American Diabetes Association. (2002). American Diabetes Association: clinical practice recommendations 2002. Diabetes Care *25 Suppl 1,* 1.

Anavi, S., and Tirosh, O. (2020). iNOS as a metabolic enzyme under stress conditions. Free Radic Biol Med *146,* 16-35.

Angermüller, S., Bruder, G., Völkl, A., Wesch, H., and Fahimi, H.D. (1987). Localization of xanthine oxidase in crystalline cores of peroxisomes. A cytochemical and biochemical study. Eur J Cell Biol *45,* 137-144.

Ansurudeen, I., Sunkari, V.G., Grünler, J., Peters, V., Schmitt, C.P., Catrina, S., Brismar, K., and Forsberg, E.A. (2012). Carnosine enhances diabetic wound healing in the db/db mouse model of type 2 diabetes. Amino Acids *43,* 127-134.

Antonenkov, V.D., Grunau, S., Ohlmeier, S., and Hiltunen, J.K. (2010). Peroxisomes are oxidative organelles. Antioxid Redox Signal *13,* 525-537.

Ao, C., Huo, Y., Qi, L., Xiong, Z., Xue, L., and Qi, Y. (2010). Pioglitazone suppresses the lipopolysaccharide-induced production of inflammatory factors in mouse macrophages by inactivating NF-κB. Cell Biology International *34,* 723-730.

Aragón, F., Karaca, M., Novials, A., Maldonado, R., Maechler, P., and Rubí, B. (2015). Pancreatic polypeptide regulates glucagon release through PPYR1 receptors expressed in mouse and human alpha-cells. Biochim Biophys Acta *1850,* 343-351.

Arena, E.T., Rueden, C.T., Hiner, M.C., Wang, S., Yuan, M., and Eliceiri, K.W. (2017). Quantitating the cell: turning images into numbers with ImageJ. WIREs Developmental Biology *6,* e260.

Arimura, A., Sato, H., Dupont, A., Nishi, N., and Schally, A.V. (1975). Somatostatin: abundance of immunoreactive hormone in rat stomach and pancreas. Science *189,* 1007-1009.

Arneth, B., Arneth, R., and Shams, M. (2019). Metabolomics of Type 1 and Type 2 Diabetes. Int J Mol Sci *20,*

Arora, K., Liyanage, P., Zhong, Q., and Naren, A.P. (2021). A SNARE protein Syntaxin 17 captures CFTR to potentiate autophagosomal clearance under stress. Faseb J *35,* e21185.

Arosio, M., Ronchi, C.L., Gebbia, C., Cappiello, V., Beck-Peccoz, P., and Peracchi, M. (2003). Stimulatory effects of ghrelin on circulating somatostatin and pancreatic polypeptide levels. J Clin Endocrinol Metab *88,* 701-704.

Artioli, G.G., Gualano, B., Smith, A., Stout, J., and Lancha, A.H. (2010). Role of beta-alanine supplementation on muscle carnosine and exercise performance. Med Sci Sports Exerc *42,* 1162-1173.

Asfari, M., Janjic, D., Meda, P., Li, G., Halban, P.A., and Wollheim, C.B. (1992). Establishment of 2-mercaptoethanol-dependent differentiated insulin-secreting cell lines. Endocrinology *130,* 167-178.

Ashcroft, F.M., Proks, P., Smith, P.A., Ämmälä, C., Bokvist, K., and Rorsman, P. (1994). Stimulus–secretion coupling in pancreatic β cells. Journal of Cellular Biochemistry *55,* 54-65.

Auer, H., Lyianarachchi, S., Newsom, D., Klisovic, M.I., Marcucci, U., and Kornacker, K. (2003). Chipping away at the chip bias: RNA degradation in microarray analysis. Nature Genetics *35,* 292-293.

Babizhayev, M.A., Burke, L., Micans, P., and Richer, S.P. (2009). N-Acetylcarnosine sustained drug delivery eye drops to control the signs of ageless vision: Glare sensitivity, cataract amelioration and quality of vision currently available treatment for the challenging 50,000-patient population. Clin Interv Aging *4,* 31-50.

Backes, T.M., Langfermann, D.S., Lesch, A., Rössler, O.G., Laschke, M.W., Vinson, C., and Thiel, G. (2021). Regulation and function of AP-1 in insulinoma cells and pancreatic β-cells. Biochem Pharmacol *193,* 114748.

Bae, Y., You, J.H., Cho, N.H., Kim, L.E., Shim, H.M., Park, J., and Cho, H.C. (2021). Association of Protein Z with Prediabetes and Type 2 Diabetes. Endocrinol Metab (Seoul) *36,* 637-646.

Baetens, D., Malaisse-Lagae, F., Perrelet, A., and Orci, L. (1979). Endocrine pancreas: three-dimensional reconstruction shows two types of islets of langerhans. Science *206,* 1323-1325.

Bagnati, M., Ogunkolade, B.W., Marshall, C., Tucci, C., Hanna, K., Jones, T.A., Bugliani, M., Nedjai, B., Caton, P.W., Kieswich, J.*, et al.* (2016). Glucolipotoxicity initiates pancreatic β-cell death through TNFR5/CD40-mediated STAT1 and NF-κB activation. Cell Death Dis *7,* e2329.

Baguet, A., Koppo, K., Pottier, A., and Derave, W. (2010). Beta-alanine supplementation reduces acidosis but not oxygen uptake response during high-intensity cycling exercise. Eur J Appl Physiol *108,* 495-503.

Bähr, I., Bazwinsky-Wutschke, I., Wolgast, S., Hofmann, K., Streck, S., Mühlbauer, E., Wedekind, D., and Peschke, E. (2012). GLUT4 in the endocrine pancreas--indicating an impact in pancreatic islet cell physiology? Horm Metab Res *44,* 442-450.

Bailey, C.J. (1992). Biguanides and NIDDM. Diabetes Care *15,* 755-772.

Bailey, C.J., and Turner, R.C. (1996). Metformin. New England Journal of Medicine *334,* 574-579.

Bainor, A., Chang, L., McQuade, T.J., Webb, B., and Gestwicki, J.E. (2011). Bicinchoninic acid (BCA) assay in low volume. Analytical Biochemistry *410,* 310-312.

Balaban, R.S., Nemoto, S., and Finkel, T. (2005). Mitochondria, oxidants, and aging. Cell *120,* 483-495.

Barlow, J., and Affourtit, C. (2013). Novel insights into pancreatic β-cell glucolipotoxicity from real-time functional analysis of mitochondrial energy metabolism in INS-1E insulinoma cells. Biochem J *456,* 417-426.

Barter, P.J., Cochran, B.J., and Rye, K. (2018). CETP inhibition, statins and diabetes. Atherosclerosis *278,* 143-146.

Beckman, J.S., Beckman, T.W., Chen, J., Marshall, P.A., and Freeman, B.A. (1990). Apparent hydroxyl radical production by peroxynitrite: implications for endothelial injury from nitric oxide and superoxide. Proc Natl Acad Sci U S A *87,* 1620-1624.

Bedard, K., and Krause, K. (2007). The NOX Family of ROS-Generating NADPH Oxidases: Physiology and Pathophysiology. Physiological Reviews *87,* 245-313.

Bellia, F., Vecchio, G., and Rizzarelli, E. (2014). Carnosinases, Their Substrates and Diseases. Molecules *19,* 2299-2329.

Berts, A., Ball, A., Dryselius, G., Gylfe, E., and Hellman, B. (1996). Glucose stimulation of somatostatin-producing islet cells involves oscillatory Ca2+ signaling. Endocrinology *137,* 693-697.

Betteridge, D.J. (2000). What is oxidative stress? Metabolism *49,* 3-8.

Bhardwaj, G., Penniman, C.M., Jena, J., Suarez Beltran, P.A., Foster, C., Poro, K., Junck, T.L., Hinton, A.O. Jr, Souvenir, R., Fuqua, J.D., Morales, P.E., Bravo-Sagua, R., Sivitz, W.I., Lira, V.A., Abel, E.D., and O'Neill, B.T. (2021). Insulin and IGF-1 receptors regulate complex I-dependent mitochondrial bioenergetics and supercomplexes via FoxOs in muscle. J Clin Invest *131,*

Biden, T.J., Boslem, E., Chu, K.Y., and Sue, N. (2014). Lipotoxic endoplasmic reticulum stress, β cell failure, and type 2 diabetes mellitus. Trends Endocrinol Metab *25,* 389-398.

Bindokas, V.P., Kuznetsov, A., Sreenan, S., Polonsky, K.S., Roe, M.W., and Philipson, L.H. (2003). Visualizing superoxide production in normal and diabetic rat islets of Langerhans. J Biol Chem *278,* 9796-9801.

Blancquaert, L., Everaert, I., Missinne, M., Baguet, A., Stegen, S., Volkaert, A., Petrovic, M., Vervaet, C., Achten, E., DE Maeyer, M., DE Henauw, S., and Derave, W. (2017). Effects of Histidine and β-alanine Supplementation on Human Muscle Carnosine Storage. Med Sci Sports Exerc *49,* 602-609.

Blough, N.V., and Zafiriou, O.C. (2002). Reaction of superoxide with nitric oxide to form peroxonitrite in alkaline aqueous solution.*2021,*

Blüher, M. (2019). Neuregulin 4: A "Hotline" Between Brown Fat and Liver. Obesity (Silver Spring) *27,* 1555-1557.

Bogdan, C. (2001). Nitric oxide and the regulation of gene expression. Trends Cell Biol *11,* 66-75.

Bogdan, C., Röllinghoff, M., and Diefenbach, A. (2000). Reactive oxygen and reactive nitrogen intermediates in innate and specific immunity. Current Opinion in Immunology *12,* 64-76.

Böger, C.A., and Sedor, J.R. (2012). GWAS of diabetic nephropathy: is the GENIE out of the bottle? PLoS Genet *8,* e1002989.

Boj, S.F., Parrizas, M., Maestro, M.A., and Ferrer, J. (2001). A transcription factor regulatory circuit in differentiated pancreatic cells. Proc Natl Acad Sci U S A *98,* 14481-14486.

Boldyrev, A.A. (2012). Carnosine: new concept for the function of an old molecule. Biochemistry (Mosc) *77,* 313-326.

Boldyrev, A.A., Aldini, G., and Derave, W. (2013). Physiology and pathophysiology of carnosine. Physiol Rev *93,* 1803-1845.

Bonnans, C., Chou, J., and Werb, Z. (2014). Remodelling the extracellular matrix in development and disease. Nat Rev Mol Cell Biol *15,* 786-801.

Bonnard, C., Durand, A., Peyrol, S., Chanseaume, E., Chauvin, M., Morio, B., Vidal, H., and Rieusset, J. (2008). Mitochondrial dysfunction results from oxidative stress in the skeletal muscle of diet-induced insulin-resistant mice. J Clin Invest *118,* 789-800.

Bonner, C., Kerr-Conte, J., Gmyr, V., Queniat, G., Moerman, E., Thévenet, J., Beaucamps, C., Delalleau, N., Popescu, I., Malaisse, W.J. and Sener, A. (2015). Inhibition of the glucose transporter SGLT2 with dapagliflozin in pancreatic alpha cells triggers glucagon secretion. Nat Med *21,* 512-517.

Bordi, C., Ferrari, C., D'Adda, T., Pilato, F., Carfagna, G., Bertelé, A., and Missale, G. (1986). Ultrastructural characterization of fundic endocrine cell hyperplasia associated with atrophic gastritis and hypergastrinaemia. Virchows Arch A Pathol Anat Histopathol *409,* 335-347.

Boucher, E., Mayer, G., Londono, I., and Bendayan, M. (2006). Expression and localization of MT1-MMP and furin in the glomerular wall of short- and long-term diabetic rats. Kidney Int *69,* 1570-1577.

Brand, M.D., and Esteves, T.C. (2005). Physiological functions of the mitochondrial uncoupling proteins UCP2 and UCP3. Cell Metab *2,* 85-93.

Brand, M.D., and Nicholls, D.G. (2011). Assessing mitochondrial dysfunction in cells. Biochem J *435,* 297-312.

Braun, M., Ramracheya, R., Amisten, S., Bengtsson, M., Moritoh, Y., Zhang, Q., Johnson, P.R., and Rorsman, P. (2009). Somatostatin release, electrical activity, membrane currents and exocytosis in human pancreatic delta cells. Diabetologia *52,* 1566-1578.

Brenner, T.K., Posa-Markaryan, K., Hercher, D., Sperger, S., Heimel, P., Keibl, C., Nürnberger, S., Grillari, J., Redl, H., and Hacobian, A. (2021). Evaluation of BMP2/miRNA co-expression systems for potent therapeutic efficacy in bone-tissue regeneration. Eur Cell Mater *41,* 245-268.

Brereton, M.F., Vergari, E., Zhang, Q., and Clark, A. (2015). Alpha-, Delta- and PP-cells. J Histochem Cytochem *63,* 575-591.

Briaud, I., Harmon, J.S., Kelpe, C.L., Segu, V.B., and Poitout, V. (2001). Lipotoxicity of the pancreatic beta-cell is associated with glucose-dependent esterification of fatty acids into neutral lipids. Diabetes *50,* 315-321.

Briaud, I., Kelpe, C.L., Johnson, L.M., Tran, P.O.T., and Poitout, V. (2002). Differential effects of hyperlipidemia on insulin secretion in islets of langerhans from hyperglycemic versus normoglycemic rats. Diabetes *51,* 662-668.

Brieger, K., Schiavone, S., Miller, F.J., and Krause, K. (2012). Reactive oxygen species: from health to disease. Swiss Med Wkly *142,* w13659.

Broglio, F., Arvat, E., Benso, A., Gottero, C., Muccioli, G., Papotti, M., van der Lely, A. J., Deghenghi, R., and Ghigo, E. (2001). Ghrelin, a natural GH secretagogue produced by the stomach, induces hyperglycemia and reduces insulin secretion in humans. J Clin Endocrinol Metab *86,* 5083-5086.

Broglio, F., Gottero, C., Benso, A., Prodam, F., Destefanis, S., Gauna, C., Maccario, M., Deghenghi, R., van der Lely, A. J., and Ghigo, E. (2003). Effects of ghrelin on the insulin and glycemic responses to glucose, arginine, or free fatty acids load in humans. J Clin Endocrinol Metab *88,* 4268-4272.

Brown, E., Heerspink, H.J.L., Cuthbertson, D.J., and Wilding, J.P.H. (2021). SGLT2 inhibitors and GLP-1 receptor agonists: established and emerging indications. The Lancet *398,* 262-276.

Brownson, C., and Hipkiss, A.R. (2000). Carnosine reacts with a glycated protein. Free Radical Biology and Medicine *28,* 1564-1570.

Brubaker, P.L., and Drucker, D.J. (2004). Minireview: Glucagon-like peptides regulate cell proliferation and apoptosis in the pancreas, gut, and central nervous system. Endocrinology *145,* 2653-2659.

Brun, T., Roche, E., Assimacopoulos-Jeannet, F., Corkey, B.E., Kim, K.H., and Prentki, M. (1996). Evidence for an anaplerotic/malonyl-CoA pathway in pancreatic beta-cell nutrient signaling. Diabetes *45,* 190-198.

Buck, L., and Axel, R. (1991). A novel multigene family may encode odorant receptors: a molecular basis for odor recognition. Cell *65,* 175-187.

Bunzow, J.R., Sonders, M.S., Arttamangkul, S., Harrison, L.M., Zhang, G.E., Quigley, D.I., Darland, T., Suchland, K.L., Pasumamula, S., Kennedy, J.L. and Olson, S.B. (2001). Amphetamine, 3,4-methylenedioxymethamphetamine, lysergic acid diethylamide, and metabolites of the catecholamine neurotransmitters are agonists of a rat trace amine receptor. Mol Pharmacol *60,* 1181-1188.

Butler, A.E., Janson, J., Bonner-Weir, S., Ritzel, R., Rizza, R.A., and Butler, P.C. (2003). Beta-cell deficit and increased beta-cell apoptosis in humans with type 2 diabetes. Diabetes *52,* 102-110.

Butler, G.S., and Overall, C.M. (2009). Proteomic identification of multitasking proteins in unexpected locations complicates drug targeting. Nat Rev Drug Discov *8,* 935-948.

Cabral-Pacheco, G.A., Garza-Veloz, I., Castruita-De la Rosa, C., Ramirez-Acuña, J.M., Perez-Romero, B.A., Guerrero-Rodriguez, J.F., Martinez-Avila, N., and Martinez-Fierro, M.L. (2020). The Roles of Matrix Metalloproteinases and Their Inhibitors in Human Diseases. Int J Mol Sci *21,*

Cadenas, E., and Davies, K.J. (2000). Mitochondrial free radical generation, oxidative stress, and aging. Free Radic Biol Med *29,* 222-230.

Calabrese, V., Mancuso, C., Sapienza, M., Puleo, E., Calafato, S., Cornelius, C., Finocchiaro, M., Mangiameli, A., Di Mauro, M., Stella, A.M.G., and Castellino, P. (2007). Oxidative stress and cellular stress response in diabetic nephropathy. Cell Stress Chaperones *12,* 299-306.

Calcaterra, V., Verduci, E., Cena, H., Magenes, V.C., Todisco, C.F., Tenuta, E., Gregorio, C., De Giuseppe, R., Bosetti, A., Di Profio, E., and Zuccotti, G. (2021). Polycystic Ovary Syndrome in Insulin-Resistant Adolescents with Obesity: The Role of Nutrition Therapy and Food Supplements as a Strategy to Protect Fertility. Nutrients *13,*

Campbell, I.W., and Mariz, S. (2007). β-Cell preservation with thiazolidinediones. Diabetes Research and Clinical Practice *76,* 163-176.

Capella, C., Hage, E., Solcia, E., and Usellini, L. (1978). Ultrastructural similarity of endocrine-like cells of the human lung and some related cells of the gut. Cell Tissue Res *186,* 25-37.

Carpentier, A., Mittelman, S.D., Lamarche, B., Bergman, R.N., Giacca, A., and Lewis, G.F. (1999). Acute enhancement of insulin secretion by FFA in humans is lost with prolonged FFA elevation. Am J Physiol *276,* 1055.

Carrington, C.A., Rubery, E.D., Pearson, E.C., and Hales, C.N. (1986). Five new insulin-producing cell lines with differing secretory properties. J Endocrinol *109,* 193-200.

Castillo-Martín, M., Bonet, S., Morató, R., and Yeste, M. (2014). Comparative effects of adding β-mercaptoethanol or L-ascorbic acid to culture or vitrification-warming media on IVF porcine embryos. Reprod Fertil Dev *26,* 875-882.

Castrillo, A., Pennington, D.J., Otto, F., Parker, P.J., Owen, M.J., and Boscá, L. (2001). Protein kinase Cepsilon is required for macrophage activation and defense against bacterial infection. J Exp Med *194,* 1231-1242.

Cauwe, B., and Opdenakker, G. (2010). Intracellular substrate cleavage: a novel dimension in the biochemistry, biology and pathology of matrix metalloproteinases. Crit Rev Biochem Mol Biol *45,* 351-423.

Cazares, V.A., Subramani, A., Saldate, J.J., Hoerauf, W., and Stuenkel, E.L. (2014). Distinct actions of Rab3 and Rab27 GTPases on late stages of exocytosis of insulin. Traffic *15,* 997-1015.

Cereghini, S. (1996). Liver-enriched transcription factors and hepatocyte differentiation. Faseb J *10,* 267-282.

Chang, J.J., Stanfill, A., and Pourmotabbed, T. (2016). The Role of Matrix Metalloproteinase Polymorphisms in Ischemic Stroke. Int J Mol Sci *17,*

Chavrier, P., Parton, R.G., Hauri, H.P., Simons, K., and Zerial, M. (1990). Localization of low molecular weight GTP binding proteins to exocytic and endocytic compartments. Cell *62,* 317-329.

Cheeseman, K.H., and Slater, T.F. (1993). An introduction to free radical biochemistry. Br Med Bull *49,* 481-493.

Chen, L., Chen, L., Wan, L., Huo, Y., Huang, J., Li, J., Lu, J., Xin, B., Yang, Q., and Guo, C. (2019). Matrine improves skeletal muscle atrophy by inhibiting E3 ubiquitin ligases and activating the Akt/mTOR/FoxO3α signaling pathway in C2C12 myotubes and mice. Oncol Rep *42,* 479-494.

Chen, S., Lv, X., Hu, B., Shao, Z., Wang, B., Ma, K., Lin, H., and Cui, M. (2017). RIPK1/RIPK3/MLKL-mediated necroptosis contributes to compression-induced rat nucleus pulposus cells death. Apoptosis *22,* 626-638.

Chen, Y., and Lippincott-Schwartz, J. (2013). Rab10 delivers GLUT4 storage vesicles to the plasma membrane. Commun Integr Biol *6,* e23779.

Chen, Y., Wang, Y., Zhang, J., Deng, Y., Jiang, L., Song, E., Wu, X.S., Hammer, J.A., Xu, T., and Lippincott-Schwartz, J. (2012). Rab10 and myosin-Va mediate insulin-stimulated GLUT4 storage vesicle translocation in adipocytes. J Cell Biol *198,* 545-560.

Chen, Z., and Niki, E. (2006). 4-hydroxynonenal (4-HNE) has been widely accepted as an inducer of oxidative stress. Is this the whole truth about it or can 4-HNE also exert protective effects? IUBMB Life *58,* 372-373.

Cheng, C., Li, Z., Zhang, M., and Chen, D. (2021). Jateorhizine alleviates insulin resistance by promoting adipolysis and glucose uptake in adipocytes. J Recept Signal Transduct Res *41,* 255-262.

Cheng, H.M., and González, R.G. (1986). The effect of high glucose and oxidative stress on lens metabolism, aldose reductase, and senile cataractogenesis. Metabolism *35,* 10-14.

Cheng, K.W., Lahad, J.P., Kuo, W., Lapuk, A., Yamada, K., Auersperg, N., Liu, J., Smith-McCune, K., Lu, K.H., Fishman, D., Gray, J.W., and Mills, G.B. (2004). The RAB25 small GTPase determines aggressiveness of ovarian and breast cancers. Nat Med *10,* 1251-1256.

Chera, S., Baronnier, D., Ghila, L., Cigliola, V., Jensen, J.N., Gu, G., Furuyama, K., Thorel, F., Gribble, F.M., Reimann, F., and Herrera, P.L. (2014). Diabetes recovery

by age-dependent conversion of pancreatic δ-cells into insulin producers. Nature *514,* 503-507.

Chiasson, J., Josse, R.G., Gomis, R., Hanefeld, M., Karasik, A., and Laakso, M. (2003). Acarbose Treatment and the Risk of Cardiovascular Disease and Hypertension in Patients With Impaired Glucose ToleranceThe STOP-NIDDM Trial. Jama *290,* 486-494.

Chinnery, P.F., and Schon, E.A. (2003). Mitochondria. J Neurol Neurosurg Psychiatry *74,* 1188-1199.

Cho, D., Nakamura, T., and Lipton, S.A. (2010). Mitochondrial dynamics in cell death and neurodegeneration. Cell Mol Life Sci *67,* 3435-3447.

Cho, Y.M., and Kieffer, T.J. (2011). New aspects of an old drug: metformin as a glucagon-like peptide 1 (GLP-1) enhancer and sensitiser. Diabetologia *54,* 219-222.

Chouchani, E.T., Kazak, L., Jedrychowski, M.P., Lu, G.Z., Erickson, B.K., Szpyt, J., Pierce, K.A., Laznik-Bogoslavski, D., Vetrivelan, R., Clish, C.B. and Robinson, A.J. (2016). Mitochondrial ROS regulate thermogenic energy expenditure and sulfenylation of UCP1. Nature *532,* 112-116.

Chouchani, E.T., Pell, V.R., Gaude, E., Aksentijević, D., Sundier, S.Y., Robb, E.L., Logan, A., Nadtochiy, S.M., Ord, E.N., Smith, A.C. and Eyassu, F. (2014). Ischaemic accumulation of succinate controls reperfusion injury through mitochondrial ROS. Nature *515,* 431-435.

Christian, M. (2015). Transcriptional fingerprinting of "browning" white fat identifies NRG4 as a novel adipokine. Adipocyte *4,* 50-54.

Christian, S.L., and Berry, M.D. (2018). Trace Amine-Associated Receptors as Novel Therapeutic Targets for Immunomodulatory Disorders. Front Pharmacol *9,* 680.

Chueire, V.B., and Muscelli, E. (2021). Effect of free fatty acids on insulin secretion, insulin sensitivity and incretin effect - a narrative review. Arch Endocrinol Metab *65,* 24-31.

Chung, A.W.Y., Hsiang, Y.N., Matzke, L.A., McManus, B.M., van Breeman, C., and Okon, E.B. (2006). Reduced Expression of Vascular Endothelial Growth Factor Paralleled With the Increased Angiostatin Expression Resulting From the Upregulated Activities of Matrix Metalloproteinase-2 and -9 in Human Type 2 Diabetic Arterial Vasculature. Circulation Research *99,* 140-148.

Clark, A., Wells, C.A., Buley, I.D., Cruickshank, J.K., Vanhegan, R.I., Matthews, D.R., Cooper, G.J., Holman, R.R., and Turner, R.C. (1988). Islet amyloid, increased A-cells, reduced B-cells and exocrine fibrosis: quantitative changes in the pancreas in type 2 diabetes. Diabetes Res *9,* 151-159.

Clark, S.A., Burnham, B.L., and Chick, W.L. (1990). Modulation of glucose-induced insulin secretion from a rat clonal beta-cell line. Endocrinology *127,* 2779-2788.

Cnop, M., Hannaert, J.C., Hoorens, A., Eizirik, D.L., and Pipeleers, D.G. (2001). Inverse Relationship between Cytotoxicity of Free Fatty Acids in Pancreatic Islet Cells and Cellular Triglyceride Accumulation. Diabetes *50,* 1771-1777.

Collombat, P., Xu, X., Heimberg, H., and Mansouri, A. (2010). Pancreatic beta-cells: From generation to regeneration. Semin. Cell Dev. Biol. *21,* 838-844.

Colombo, M., Gregersen, S., Xiao, J., and Hermansen, K. (2003). Effects of ghrelin and other neuropeptides (CART, MCH, orexin A and B, and GLP-1) on the release of insulin from isolated rat islets. Pancreas *27,* 161-166.

Commoner, B., Townsend, J., and Pake, G.E. (1954). Free radicals in biological materials. Nature *174,* 689-691.

Corbeel, L., and Freson, K. (2008). Rab proteins and Rab-associated proteins: major actors in the mechanism of protein-trafficking disorders. Eur J Pediatr *167,* 723-729.

Cowie, M.R., and Fisher, M. (2020). SGLT2 inhibitors: mechanisms of cardiovascular benefit beyond glycaemic control. Nat Rev Cardiol *17,* 761-772.

Cripps, M.J., Hanna, K., Lavilla, C., Sayers, S.R., Caton, P.W., Sims, C., De Girolamo, L., Sale, C., and Turner, M.D. (2017). Carnosine scavenging of glucolipotoxic free radicals enhances insulin secretion and glucose uptake. Sci Rep *7,*

Cryer, P.E. (2012). Minireview: Glucagon in the pathogenesis of hypoglycemia and hyperglycemia in diabetes. Endocrinology *153,* 1039-1048.

Cui, N., Hu, M., and Khalil, R.A. (2017). Biochemical and Biological Attributes of Matrix Metalloproteinases. Prog Mol Biol Transl Sci *147,* 1-73.

da Silva Rosa, Simone C., Martens, M.D., Field, J.T., Nguyen, L., Kereliuk, S.M., Hai, Y., Chapman, D., Diehl-Jones, W., Aliani, M., West, A.R.*, et al.* (2021). BNIP3L/Nix-induced mitochondrial fission, mitophagy, and impaired myocyte glucose uptake are abrogated by PRKA/PKA phosphorylation. Autophagy *17,* 2257-2272.

Da Silva Xavier, G. (2018). The Cells of the Islets of Langerhans. J Clin Med *7,*

Daiber, A., Hahad, O., Andreadou, I., Steven, S., Daub, S., and Munzel, T. (2021). Redox-related biomarkers in human cardiovascular disease-classical footprints and beyond." *Redox Biology* 42 (2021): 101875

Dalesio, N.M., Barreto Ortiz, S.F., Pluznick, J.L., and Berkowitz, D.E. (2018). Olfactory, Taste, and Photo Sensory Receptors in Non-sensory Organs: It Just Makes Sense. Front Physiol *9,* 1673.

Damsbo, P., Clauson, P., Marbury, T.C., and Windfeld, K. (1999). A double-blind randomized comparison of meal-related glycemic control by repaglinide and glyburide in well-controlled type 2 diabetic patients. Diabetes Care *22,* 789-794.

Dan Dunn, J., Alvarez, L.A., Zhang, X., and Soldati, T. (2015). Reactive oxygen species and mitochondria: A nexus of cellular homeostasis. Redox Biol *6,* 472-485.

da-Silva, W.S., Gómez-Puyou, A., de Gómez-Puyou, M.T., Moreno-Sanchez, R., De Felice, F.G., de Meis, L., Oliveira, M.F., and Galina, A. (2004). Mitochondrial bound hexokinase activity as a preventive antioxidant defense: steady-state ADP formation as a regulatory mechanism of membrane potential and reactive oxygen species generation in mitochondria. J Biol Chem *279,* 39846-39855.

de Courten, B., Kurdiova, T., de Courten, Maximilian P. J., Belan, V., Everaert, I., Vician, M., Teede, H., Gasperikova, D., Aldini, G., Derave, W., Ukropec, J., and Ukropcova, B. (2015). Muscle Carnosine Is Associated with Cardiometabolic Risk Factors in Humans. *PloS one* 10, no. 10 (2015): e0138707.

De Grandis, R.A., Oliveira, K.M., Guedes, A.P.M., Dos Santos, Patrick W. S., Aissa, A.F., Batista, A.A., and Pavan, F.R. (2021). A Novel Ruthenium(II) Complex With Lapachol Induces G2/M Phase Arrest Through Aurora-B Kinase Down-Regulation and ROS-Mediated Apoptosis in Human Prostate Adenocarcinoma Cells. Front Oncol *11,* 682968.

de Bandeira, S., da Fonseca, Lucas José S., da S Guedes, G., Rabelo, L.A., Goulart, M.O.F., and Vasconcelos, S.M.L. (2013). Oxidative stress as an underlying contributor in the development of chronic complications in diabetes mellitus. Int J Mol Sci *14,* 3265-3284.

Dean, R.A., Cox, J.H., Bellac, C.L., Doucet, A., Starr, A.E., and Overall, C.M. (2008). Macrophage-specific metalloelastase (MMP-12) truncates and inactivates ELR+ CXC chemokines and generates CCL2, -7, -8, and -13 antagonists: potential role of the macrophage in terminating polymorphonuclear leukocyte influx. Blood *112,* 3455-3464.

Decker, E.A., Livisay, S.A., and Zhou, S. (2000). A re-evaluation of the antioxidant activity of purified carnosine. Biochemistry (Mosc) *65,* 766-770.

DeFronzo, R.A., and Goodman, A.M. (1995). Efficacy of metformin in patients with non-insulin-dependent diabetes mellitus. The Multicenter Metformin Study Group. N Engl J Med *333,* 541-549.

Derave, W., Ozdemir, M.S., Harris, R.C., Pottier, A., Reyngoudt, H., Koppo, K., Wise, J.A., and Achten, E. (2007). Beta-Alanine supplementation augments muscle carnosine content and attenuates fatigue during repeated isokinetic contraction bouts in trained sprinters. J Appl Physiol (1985) *103,* 1736-1743.

Derosa, G., Maffioli, P., Salvadeo, S., Ferrari, I., Ragonesi, P., Querci, F., Franzetti, I., Gadaleta, G., Ciccarelli, L., Piccinni, M., D'Angelo, A., and Cicero, A. (2010). Exenatide Versus Glibenclamide in Patients with Diabetes. Diabetes Technology & Therapeutics *12,* 233-240.

Derosa, G., and Maffioli, P. (2012). α-Glucosidase inhibitors and their use in clinical practice. Arch Med Sci *8,* 899-906.

Derosa, G., Putignano, P., Bossi, A.C., Bonaventura, A., Querci, F., Franzetti, I.G., Guazzini, B., Testori, G., Fogari, E., and Maffioli, P. (2011). Exenatide or glimepiride added to metformin on metabolic control and on insulin resistance in type 2 diabetic patients. European Journal of Pharmacology *666,* 251-256.

Derveaux, S., Vandesompele, J., and Hellemans, J. (2010). How to do successful gene expression analysis using real-time PCR. Methods *50,* 227-230.

Devaraj, S., Cheung, A.T., Jialal, I., Griffen, S.C., Nguyen, D., Glaser, N., and Aoki, T. (2007). Evidence of increased inflammation and microcirculatory abnormalities in patients with type 1 diabetes and their role in microvascular complications. Diabetes *56,* 2790-2796.

DeWitt, D.E., and Hirsch, I.B. (2003). Outpatient insulin therapy in type 1 and type 2 diabetes mellitus: scientific review. Jama *289,* 2254-2264.

Dezaki, K., Sone, H., and Yada, T. (2008). Ghrelin is a physiological regulator of insulin release in pancreatic islets and glucose homeostasis. Pharmacol Ther *118,* 239-249.

Di Meo, S., Reed, T.T., Venditti, P., and Victor, V.M. (2016). Role of ROS and RNS Sources in Physiological and Pathological Conditions. Oxid Med Cell Longev *2016,*

Diani, A.R., Sawada, G., Wyse, B., Murray, F.T., and Khan, M. (2004). Pioglitazone preserves pancreatic islet structure and insulin secretory function in three murine models of type 2 diabetes. American Journal of Physiology-Endocrinology and Metabolism *286,* E116-E122.

DiNicolantonio, J.J., McCarty, M.F., and OKeefe, J.H. (2018). Role of dietary histidine in the prevention of obesity and metabolic syndrome. Open Heart *5,* e000676.

Diokmetzidou, A., Tsikitis, M., Nikouli, S., Kloukina, I., Tsoupri, E., Papathanasiou, S., Psarras, S., Mavroidis, M., and Capetanaki, Y. (2016). Strategies to Study Desmin in Cardiac Muscle and Culture Systems. Methods Enzymol *568,* 427-459.

Divakaruni, A.S., and Brand, M.D. (2011). The regulation and physiology of mitochondrial proton leak. Physiology (Bethesda) *26,* 192-205.

Divakaruni, A.S., Paradyse, A., Ferrick, D.A., Murphy, A.N., and Jastroch, M. (2014). Chapter Sixteen - Analysis and Interpretation of Microplate-Based Oxygen Consumption and pH Data. In Methods in Enzymology, Murphy, Anne N., and Chan, David C. eds., Academic Press) pp. 309-354.

Dodson, G., and Steiner, D. (1998). The role of assembly in insulin's biosynthesis. Curr Opin Struct Biol *8,* 189-194.

Dolan, V., Hensey, C., and Brady, H.R. (2003). Diabetic nephropathy: renal development gone awry? Pediatr Nephrol *18,* 75-84.

Doliba, N., Qin, W., Najafi, H., Liu, C., Buettger, C., Sotiris, J., Collins, H., Li, C., Stanley, C., Wilson, D., and Grimsby, J. (2012). Glucokinase activation repairs defective bioenergetics of islets of Langerhans isolated from type 2 diabetics. Am J Physiol Endocrinol Metab *302,* E87-E102.

Donath, M.Y., Dinarello, C.A., and Mandrup-Poulsen, T. (2019). Targeting innate immune mediators in type 1 and type 2 diabetes. Nat Rev Immunol *19,* 734-746.

Donath, M.Y., and Shoelson, S.E. (2011). Type 2 diabetes as an inflammatory disease. Nat Rev Immunol *11,* 98-107.

de la Cour, C., Björkqvist, M., Sandvik, A., Bakke, I., Zhao, C., Chen, D., and Håkanson, R. (2001). A-like cells in the rat stomach contain ghrelin and do not operate under gastrin control. Regul Pept *99,* 141-150.

Dranka, B., Benavides, G., Diers, A., Giordano, S., Zelickson, B., Reily, C., Zou, L., Chatham, J., Hill, B., Zhang, J., Landar, A., and Darley-Usmar, V. (2011). Assessing bioenergetic function in response to oxidative stress by metabolic profiling. Free Radic Biol Med *51,* 1621-1635.

Du, L., and Novick, P. (2001). 11 - Purification and Properties of a GTPase-Activating Protein for Yeast Rab GTPases. In Methods in Enzymology, Balch, W. E., Der, Channing J. and Hall, Alan eds., Academic Press) pp. 91-99.

Duchen, M. (1992). Ca(2+)-dependent changes in the mitochondrial energetics in single dissociated mouse sensory neurons. Biochem J *283,* 41-50.

Dufour, A. (2015). Degradomics of matrix metalloproteinases in inflammatory diseases. Front Biosci (Schol Ed) *7,* 150-167.

Dufour, A., Bellac, C., Eckhard, U., Solis, N., Klein, T., Kappelhoff, R., Fortelny, N., Jobin, P., Rozmus, J., Mark, J. and Pavlidis, P. (2018). C-terminal truncation of IFN-γ inhibits proinflammatory macrophage responses and is deficient in autoimmune disease. Nat Commun *9,* 2416.

Dunnett, M., and Harris, R.C. (1999). Influence of oral beta-alanine and L-histidine supplementation on the carnosine content of the gluteus medius. Equine Veterinary Journal. Supplement *30,* 499-504.

Easom, R.A. (2000). Beta-granule transport and exocytosis. Semin Cell Dev Biol *11,* 253-266.

Ebrahimi, F.A., and Chess, A. (1998). Olfactory G proteins: simple and complex signal transduction. Curr Biol *8,* 431.

Eckl, P.M., Ortner, A., and Esterbauer, H. (1993). Genotoxic properties of 4-hydroxyalkenals and analogous aldehydes. Mutat Res *290,* 183-192.

Edelman, J.J.B., Seco, M., Dunne, B., Matzelle, S.J., Murphy, M., Joshi, P., Yan, T.D., Wilson, M.K., Bannon, P.G., Vallely, M.P., and Passage, J. (2013). Custodiol for myocardial protection and preservation: a systematic review. Ann Cardiothorac Surg *2,* 717-728.

Egido, E.M., Rodriguez-Gallardo, J., Silvestre, R.A., and Marco, J. (2002). Inhibitory effect of ghrelin on insulin and pancreatic somatostatin secretion. Eur J Endocrinol *146,* 241-244.

El-Assaad, W., Buteau, J., Peyot, M., Nolan, C., Roduit, R., Hardy, S., Joly, E., Dbaibo, G., Rosenberg, L., and Prentki, M. (2003). Saturated fatty acids synergize with elevated glucose to cause pancreatic beta-cell death. Endocrinology *144,* 4154-4163.

El-Assaad, W., Joly, E., Barbeau, A., Sladek, R., Buteau, J., Maestre, I., Pepin, E., Zhao, S., Iglesias, J., Roche, E., and Prentki, M. (2010). Glucolipotoxicity alters lipid partitioning and causes mitochondrial dysfunction, cholesterol, and ceramide

deposition and reactive oxygen species production in INS832/13 ss-cells. Endocrinology *151,* 3061-3073.

Ellard, S., Bellanné-Chantelot, C., and Hattersley, A.T. (2008). Best practice guidelines for the molecular genetic diagnosis of maturity-onset diabetes of the young. Diabetologia *51,* 546-553.

Ellard, S., and Colclough, K. (2006). Mutations in the genes encoding the transcription factors hepatocyte nuclear factor 1 alpha (HNF1A) and 4 alpha (HNF4A) in maturity-onset diabetes of the young. Human Mutation *27,* 854-869.

El-Mir, M., Nogueira, V., Fontaine, E., Avéret, N., Rigoulet, M., and Leverve, X. (2000). Dimethylbiguanide Inhibits Cell Respiration via an Indirect Effect Targeted on the Respiratory Chain Complex I *. Journal of Biological Chemistry *275,* 223-228.

Elsner, M., Gehrmann, W., and Lenzen, S. (2011). Peroxisome-generated hydrogen peroxide as important mediator of lipotoxicity in insulin-producing cells. Diabetes *60,* 200-208.

Ensinck, J., Laschansky, E., Vogel, R., Simonowitz, D., Roos, B., and Francis, B. (1989). Circulating prosomatostatin-derived peptides. Differential responses to food ingestion. J Clin Invest *83,* 1580-1589.

Eruslanov, E., and Kusmartsev, S. (2010). Identification of ROS using oxidized DCFDA and flow-cytometry. Methods Mol Biol *594,* 57-72.

Evans, J., Goldfine, I., Maddux, B., and Grodsky, G. (2003). Are oxidative stress-activated signaling pathways mediators of insulin resistance and beta-cell dysfunction? Diabetes *52,* 1-8.

Everaert, I., Mooyaart, A., Baguet, A., Zutinic, A., Baelde, H., Achten, E., Taes, Y., De Heer, E., and Derave, W. (2011). Vegetarianism, female gender and increasing age, but not CNDP1 genotype, are associated with reduced muscle carnosine levels in humans. Amino Acids *40,* 1221-1229.

Farilla, L., Hui, H., Bertolotto, C., Kang, E., Bulotta, A., Di Mario, U., and Perfetti, R. (2002). Glucagon-Like Peptide-1 Promotes Islet Cell Growth and Inhibits Apoptosis in Zucker Diabetic Rats. Endocrinology *143,* 4397-4408.

Farnsworth, N., and Benninger, R. (2014). New insights into the role of connexins in pancreatic islet function and diabetes. FEBS Letters *588,* 1278-1287.

Fehmann, H., Göke, R., and Göke, B. (1995). Cell and molecular biology of the incretin hormones glucagon-like peptide-I and glucose-dependent insulin releasing polypeptide. Endocr Rev *16,* 390-410.

Fontana, M., Pinnen, F., Lucente, G., and Pecci, L. (2002). Prevention of peroxynitrite-dependent damage by carnosine and related sulphonamido pseudodipeptides. Cell Mol Life Sci *59,* 546-551.

Fontés, G., Zarrouki, B., Hagman, D., Latour, M., Semache, M., Roskens, V., Moore, P., Prentki, M., Rhodes, C., Jetton, T., and Poitout, V. (2010). Glucolipotoxicity age-dependently impairs beta cell function in rats despite a marked increase in beta cell mass. Diabetologia *53,* 2369-2379.

Ford, A., and Rajagopalan, P. (2018). Extracellular matrix remodeling in 3D: implications in tissue homeostasis and disease progression. Wiley Interdiscip Rev Nanomed Nanobiotechnol *10,* e1503.

Förstermann, U., and Sessa, W. (2012). Nitric oxide synthases: regulation and function. Eur Heart J *33,* 829-837d.

Fotouhi, L., Heravi, M., Zadsirjan, V., and Atoi, P. (2018). Electrochemically Induced Michael Addition Reaction: An Overview. The Chemical Record *18,* 1633-1657.

Fredriksson, R., Lagerström, M., Lundin, L., and Schiöth, H. (2003). The G-protein-coupled receptors in the human genome form five main families. Phylogenetic analysis, paralogon groups, and fingerprints. Mol Pharmacol *63,* 1256-1272.

Freeman, B., and Crapo, J. (1982). Biology of disease: free radicals and tissue injury. Lab Invest *47,* 412-426.

Fridlyand, L., and Philipson, L. (2006). Reactive species and early manifestation of insulin resistance in type 2 diabetes. Diabetes Obes Metab *8,* 136-145.

Friebe, A., Sandner, P., and Schmidtko, A. (2020). cGMP: a unique 2nd messenger molecule - recent developments in cGMP research and development. Naunyn Schmiedebergs Arch Pharmacol *393,* 287-302.

Fuchs, A., Samovski, D., Smith, G., Cifarelli, V., Farabi, S., Yoshino, J., Pietka, T., Chang, S., Ghosh, S., Myckatyn, T., and Klein, S. (2021). Associations Among Adipose Tissue Immunology, Inflammation, Exosomes and Insulin Sensitivity in People With Obesity and Nonalcoholic Fatty Liver Disease. Gastroenterology *161,* 968-981.e12.

Fuller, A., Neuberger, A., and Webster, T. (1947). Histidine deficiency in the rat and its effect on the carnosine and anserine content of muscle. Biochem J *41,* 11-19.

Furuhashi, M., Koyama, M., Higashiura, Y., Murase, T., Nakamura, T., Matsumoto, M., Sakai, A., Ohnishi, H., Tanaka, M., Saitoh, S. and Moniwa, N. (2020). Differential regulation of hypoxanthine and xanthine by obesity in a general population. J Diabetes Investig *11,* 878-887.

Furukawa, S., Fujita, T., Shimabukuro, M., Iwaki, M., Yamada, Y., Nakajima, Y., Nakayama, O., Makishima, M., Matsuda, M., and Shimomura, I. (2004). Increased oxidative stress in obesity and its impact on metabolic syndrome. J Clin Invest *114,* 1752-1761.

Gadsby, R. (2007). New treatments for type 2 diabetes—The DPP4 inhibitors. Primary Care Diabetes *1,* 209-211.

Galliera, E., Tacchini, L., and Romanelli, M. (2015). Matrix metalloproteinases as biomarkers of disease: updates and new insights. Clin Chem Lab Med *53,* 349-355.

Gangji, A., Cukierman, T., Gerstein, H., Goldsmith, C., and Clase, C. (2007). A systematic review and meta-analysis of hypoglycemia and cardiovascular events: a comparison of glyburide with other secretagogues and with insulin. Diabetes Care *30,* 389-394.

García-Irigoyen, O., Latasa, M., Carotti, S., Uriarte, I., Elizalde, M., Urtasun, R., Vespasiani-Gentilucci, U., Morini, S., Benito, P., Ladero, J., and Rodriguez, J. (2015). Matrix metalloproteinase 10 contributes to hepatocarcinogenesis in a novel crosstalk with the stromal derived factor 1/C-X-C chemokine receptor 4 axis. Hepatology *62,* 166-178.

Garvey, W., Maianu, L., Zhu, J., Brechtel-Hook, G., Wallace, P., and Baron, A. (1998). Evidence for defects in the trafficking and translocation of GLUT4 glucose

transporters in skeletal muscle as a cause of human insulin resistance. J Clin Invest *101,* 2377-2386.

Gavaldà-Navarro, A., Villarroya, J., Cereijo, R., Giralt, M., and Villarroya, F. (2022). The endocrine role of brown adipose tissue: An update on actors and actions. Rev Endocr Metab Disord *23,* 31-41.

Gerich, J.E. (1988). Lilly lecture 1988. Glucose counterregulation and its impact on diabetes mellitus. Diabetes *37,* 1608-1617.

Gerich, J., Raskin, P., Jean-Louis, L., Purkayastha, D., and Baron, M. (2005). Preserve-beta: two-year efficacy and safety of initial combination therapy with nateglinide or glyburide plus metformin. Diabetes Care *28,* 2093-2099.

Giacomello, M., Pyakurel, A., Glytsou, C., and Scorrano, L. (2020). The cell biology of mitochondrial membrane dynamics. Nat Rev Mol Cell Biol *21,* 204-224.

Ginsberg, S., Alldred, M., Counts, S., Cataldo, A., Neve, R., Jiang, Y., Wuu, J., Chao, M., Mufson, E., Nixon, R., and Che, S. (2010). Microarray analysis of hippocampal CA1 neurons implicates early endosomal dysfunction during Alzheimer's disease progression. Biol Psychiatry *68,* 885-893.

Goldenring, J., Aron, L., Lapierre, L., Navarre, J., and Casanova, J. (2001). 23 - Expression and Properties of Rab25 in Polarized Madin-Darby Canine Kidney Cells. In Methods in Enzymology, Balch, W. E., Der, Channing J. and Hall, Alan eds., Academic Press) pp. 225-234.

Gomberg, M. (1900). An instance of trivalent carbon: triphenylmethyl. J. Am. Chem. Soc. *22,* 757-771.

Gonzalez, A., Sochor, M., Hothersall, J., and McLean, P. (1986). Effect of aldose reductase inhibitor (sorbinil) on integration of polyol pathway, pentose phosphate pathway, and glycolytic route in diabetic rat lens. Diabetes *35,* 1200-1205.

Gonzalez, F.J. (2005). Role of cytochromes P450 in chemical toxicity and oxidative stress: studies with CYP2E1. Mutat Res *569,* 101-110.

Gonzalez-Franquesa, A., and Patti, M. (2017). Insulin Resistance and Mitochondrial Dysfunction. Adv Exp Med Biol *982,* 465-520.

Göpel, S., Kanno, T., Barg, S., Galvanovskis, J., and Rorsman, P. (1999). Voltage-gated and resting membrane currents recorded from B-cells in intact mouse pancreatic islets. J Physiol *521 Pt 3,* 717-728.

Greco, D., Broussard, J., and Peterson, M. (1995). Insulin therapy. Vet Clin North Am Small Anim Pract *25,* 677-689.

Gross, J., and Lapiere, C. (1962). Collagenolytic activity in amphibian tissues: a tissue culture assay. Proc Natl Acad Sci U S A *48,* 1014-1022.

Gryczyńska, W., Litvinov, N., Bitew, B., Bartosz, Z., Kośmider, W., Bogdański, P., and Skrypnik, D. (2021). Excess Body Mass-A Factor Leading to the Deterioration of COVID-19 and Its Complications-A Narrative Review. Viruses *13,*

Guber, K., Pemmasani, G., Malik, A., Aronow, W., Yandrapalli, S., and Frishman, W. (2021). Statins and Higher Diabetes Mellitus Risk: Incidence, Proposed Mechanisms, and Clinical Implications. Cardiol Rev *29,* 314-322.

Guiotto, A., Calderan, A., Ruzza, P., and Borin, G. (2005). Carnosine and carnosine-related antioxidants: a review. Curr Med Chem *12,* 2293-2315.

Gulewitsch, W., and Amiradžibi, S. (1900). Ueber das Carnosin, eine neue organische Base des Fleischextractes. Berichte Der Deutschen Chemischen Gesellschaft *33,* 1902-1903.

Gunton, J., Kulkarni, R., Yim, S., Okada, T., Hawthorne, W., Tseng, Y., Roberson, R., Ricordi, C., O'Connell, P., Gonzalez, F., and Kahn, C. (2005). Loss of ARNT/HIF1β Mediates Altered Gene Expression and Pancreatic-Islet Dysfunction in Human Type 2 Diabetes. Cell *122,* 337-349.

Guo, S., and Lu, H. (2019). Novel Mechanisms of Regulation of the Expression and Transcriptional Activity of HNF4α. J Cell Biochem *120,* 519-532.

Hagman, D., Hays, L., Parazzoli, S., and Poitout, V. (2005). Palmitate inhibits insulin gene expression by altering PDX-1 nuclear localization and reducing MafA expression in isolated rat islets of Langerhans. J Biol Chem *280,* 32413-32418.

Haliyur, R., Tong, X., Sanyoura, M., Shrestha, S., Lindner, J., Saunders, D., Aramandla, R., Poffenberger, G., Redick, S., Bottino, R. and Prasad, N. (2019).

Human islets expressing HNF1A variant have defective β cell transcriptional regulatory networks. J Clin Invest *129,* 246-251.

Halliwell, B. (1997). What nitrates tyrosine? Is nitrotyrosine specific as a biomarker of peroxynitrite formation in vivo? FEBS Letters *411,* 157-160.

Han, S., Jee, Y., Han, K., Kang, Y., Kim, H., Han, J., Kim, Y., and Cha, D. (2006). An imbalance between matrix metalloproteinase-2 and tissue inhibitor of matrix metalloproteinase-2 contributes to the development of early diabetic nephropathy. Nephrol Dial Transplant *21,* 2406-2416.

Hansen, S., Párrizas, M., Jensen, M., Pruhova, S., Ek, J., Boj, S.F., Johansen, A., Maestro, M., Rivera, F., Eiberg, H. and Andel, M. (2002). Genetic evidence that HNF-1alpha-dependent transcriptional control of HNF-4alpha is essential for human pancreatic beta cell function. J Clin Invest *110,* 827-833.

Hanusch, B., Sinningen, K., Brinkmann, F., Dillenhöfer, S., Frank, M., Jöckel, K.H., Koerner-Rettberg, C., Holtmann, M., Legenbauer, T., Langrock, C. and Reinehr, T. (2022). Characterization of the L-Arginine/Nitric Oxide Pathway and Oxidative Stress in Pediatric Patients with Atopic Diseases. Int J Mol Sci *23,*

Harmon, J.S., Gleason, C.E., Tanaka, Y., Poitout, V., and Robertson, R.P. (2001). Antecedent hyperglycemia, not hyperlipidemia, is associated with increased islet triacylglycerol content and decreased insulin gene mRNA level in Zucker diabetic fatty rats. Diabetes *50,* 2481-2486.

Harris, R., Tallon, M., Dunnett, M., Boobis, L., Coakley, J., Kim, H., Fallowfield, J., Hill, C., Sale, C., and Wise, J. (2006). The absorption of orally supplied beta-alanine and its effect on muscle carnosine synthesis in human vastus lateralis. Amino Acids *30,* 279-289.

Harrison, R. (2004). Physiological roles of xanthine oxidoreductase. Drug Metab Rev *36,* 363-375.

Hauck, A., Huang, Y., Hertzel, A., and Bernlohr, D. (2019). Adipose oxidative stress and protein carbonylation. J Biol Chem *294,* 1083-1088.

Hauge-Evans, A., King, A., Carmignac, D., Richardson, C., Robinson, I., Low, M., Christie, M., Persaud, S., and Jones, P. (2009). Somatostatin secreted by islet delta-

cells fulfills multiple roles as a paracrine regulator of islet function. Diabetes *58,* 403-411.

Hausladen, A., and Stamler, J. (1999). Nitrosative stress. Methods Enzymol *300,* 389-395.

Hawkins, P., Skillman, A., and Nicholls, A. (2007). Comparison of shape-matching and docking as virtual screening tools. J Med Chem *50,* 74-82.

Haythorne, E., Rohm, M., van de Bunt, M., Brereton, M., Tarasov, A., Blacker, T., Sachse, G., Silva dos Santos, M., Terron Exposito, R., Davis, S. and Baba, O. (2019). Diabetes causes marked inhibition of mitochondrial metabolism in pancreatic β-cells. *Nature communications*, *10*(1), pp.1-17.

Hayward, R., Manning, W., Kaplan, S., Wagner, E., and Greenfield, S. (1997). Starting insulin therapy in patients with type 2 diabetes: effectiveness, complications, and resource utilization. Jama *278,* 1663-1669.

He, Y., and Häder, D. (2002). Reactive oxygen species and UV-B: effect on cyanobacteria. Photochem. Photobiol. Sci. *1,* 729-736.

Heimberg, H., De Vos, A., Pipeleers, D., Thorens, B., and Schuit, F. (1995). Differences in glucose transporter gene expression between rat pancreatic alpha- and beta-cells are correlated to differences in glucose transport but not in glucose utilization. J Biol Chem *270,* 8971-8975.

Helms, C., and Kim-Shapiro, D. (2013). Hemoglobin-mediated nitric oxide signaling. Free Radic Biol Med *61,* 464-472.

Herst, P., Rowe, M., Carson, G., and Berridge, M. (2017). Functional Mitochondria in Health and Disease. Front Endocrinol (Lausanne) *8,* 296.

Hill, C., Harris, R., Kim, H., Harris, B., Sale, C., Boobis, L., Kim, C., and Wise, J. (2007). Influence of beta-alanine supplementation on skeletal muscle carnosine concentrations and high intensity cycling capacity. Amino Acids *32,* 225-233.

Hipkiss, A., Brownson, C., and Carrier, M. (2001). Carnosine, the anti-ageing, anti-oxidant dipeptide, may react with protein carbonyl groups. Mech Ageing Dev *122,* 1431-1445.

Hipkiss, A.R. (2009). Carnosine and its possible roles in nutrition and health. Adv Food Nutr Res *57,* 87-154.

Hipkiss, A.R., Michaelis, J., and Syrris, P. (1995). Non-enzymatic glycosylation of the dipeptide l-carnosine, a potential anti-protein-cross-linking agent. FEBS Letters *371,* 81-85.

Hirakawa, S., Kojima, T., Obata, K., Okabayashi, T., Yokota, S., Nomura, K., Obonai, T., Fuchimoto, J., Himi, T., Tsutsumi, H., and Sawada, N. (2013). Marked induction of matrix metalloproteinase-10 by respiratory syncytial virus infection in human nasal epithelial cells. J Med Virol *85,* 2141-2150.

Hirst, J., Farmer, A., Dyar, A., Lung, T., and Stevens, R. (2013). Estimating the effect of sulfonylurea on HbA1c in diabetes: a systematic review and meta-analysis. Diabetologia *56,* 973-984.

Hökfelt, T., Johansson, O., Efendic, S., Luft, R., and Arimura, A. (1975). Are there somatostatin-containing nerves in the rat gut? Immunohistochemical evidence for a new type of peripheral nerves. Experientia *31,* 852-854.

Holliday, R., and McFarland, G. (2000). A role for carnosine in cellular maintenance. Biochemistry (Mosc) *65,* 843-848.

Holmbeck, K., Bianco, P., Caterina, J., Yamada, S., Kromer, M., Kuznetsov, S., Mankani, M., Robey, P., Poole, A., Pidoux, I., Ward, J., and Birkedal-Hansen, H. (1999). MT1-MMP-deficient mice develop dwarfism, osteopenia, arthritis, and connective tissue disease due to inadequate collagen turnover. Cell *99,* 81-92.

Holst, J., and Orskov, C. (2004). The incretin approach for diabetes treatment: modulation of islet hormone release by GLP-1 agonism. Diabetes *53 Suppl 3,* 197.

Holst, N. (1999). Glucagon-like Peptide 1 (GLP-1): An Intestinal Hormone, Signalling Nutritional Abundance, with an Unusual Therapeutic Potential. Trends Endocrinol Metab *10,* 229-235.

Holstein, A., Plaschke, A., and Egberts, E. (2001). Lower incidence of severe hypoglycaemia in patients with type 2 diabetes treated with glimepiride versus glibenclamide. Diabetes/Metabolism Research and Reviews *17,* 467-473.

Home, P., Pocock, S., Beck-Nielsen, H., Gomis, R., Hanefeld, M., Jones, N., Komajda, M., and McMurray, J. (2007). Rosiglitazone Evaluated for Cardiovascular Outcomes — An Interim Analysis. New England Journal of Medicine *357,* 28-38.

Horinishi, H., Grillo, M., and Margolis, F. (1978). Purification and characterization of carnosine synthetase from mouse olfactory bulbs. J Neurochem *31,* 909-919.

Hotamisligil, G. (2010). Endoplasmic reticulum stress and the inflammatory basis of metabolic disease. Cell *140,* 900-917.

Hsu, C., Tseng, L., and Lee, H. (2016). Role of mitochondrial dysfunction in cancer progression. Exp Biol Med (Maywood) *241,* 1281-1295.

Hu, J., Van den Steen, P., Sang, Q., and Opdenakker, G. (2007). Matrix metalloproteinase inhibitors as therapy for inflammatory and vascular diseases. Nat Rev Drug Discov *6,* 480-498.

Hu, R., Xia, C., Butfiloski, E., and Clare-Salzler, M. (2018). Effect of high glucose on cytokine production by human peripheral blood immune cells and type I interferon signaling in monocytes: Implications for the role of hyperglycemia in the diabetes inflammatory process and host defense against infection. Clin Immunol *195,* 139-148.

Hu, Y., Gao, Y., Zhang, M., Deng, K., Singh, R., Tian, Q., Gong, Y., Pan, Z., Liu, Q., Boisclair, Y.R., and Long, Q. (2019). Endoplasmic Reticulum-Associated Degradation (ERAD) Has a Critical Role in Supporting Glucose-Stimulated Insulin Secretion in Pancreatic β-Cells. Diabetes *68,* 733-746.

Huang, L., Shen, H., Atkinson, M., and Kennedy, R. (1995). Detection of exocytosis at individual pancreatic beta cells by amperometry at a chemically modified microelectrode. Proc Natl Acad Sci U S A *92,* 9608-9612.

Huang, S., and Czech, M. (2007). The GLUT4 glucose transporter. Cell Metab *5,* 237-252.

Ibrahim, M. (2010). Subcutaneous and visceral adipose tissue: structural and functional differences. Obes Rev *11,* 11-18.

Ignarro, L., Buga, ., Wood, K., Byrns, R., and Chaudhuri, G. (1987). Endothelium-derived relaxing factor produced and released from artery and vein is nitric oxide. Proc Natl Acad Sci U S A *84,* 9265-9269.

Ihara, A., Yamagata, K., Nammo, T., Miura, A., Yuan, M., Tanaka, T., Sladek, F., Matsuzawa, Y., Miyagawa, J., and Shimomura, I. (2005). Functional characterization of the HNF4α isoform (HNF4α8) expressed in pancreatic β-cells. Biochemical and Biophysical Research Communications *329,* 984-990.

Inaba, W., Mizukami, H., Kamata, K., Takahashi, K., Tsuboi, K., and Yagihashi, S. (2012). Effects of long-term treatment with the dipeptidyl peptidase-4 inhibitor vildagliptin on islet endocrine cells in non-obese type 2 diabetic Goto-Kakizaki rats. European Journal of Pharmacology *691,* 297-306.

Inada, A., Nagai, K., Arai, H., Miyazaki, J., Nomura, K., Kanamori, H., Toyokuni, S., Yamada, Y., Bonner-Weir, S., Weir, G., Fukatsu, A., and Seino, Y. (2005). Establishment of a diabetic mouse model with progressive diabetic nephropathy. Am J Pathol *167,* 327-336.

Irwin, N., and Flatt, P. (2013). Enteroendocrine hormone mimetics for the treatment of obesity and diabetes. Curr Opin Pharmacol *13,* 989-995.

Ishida, H., Takizawa, M., Ozawa, S., Nakamichi, Y., Yamaguchi, S., Katsuta, H., Tanaka, T., Maruyama, M., Katahira, H., Yoshimoto, K., Itagaki, E., and Nagamatsu, S. (2004). Pioglitazone improves insulin secretory capacity and prevents the loss of β-cell mass in obese diabetic db/db mice: possible protection of β cells from oxidative stress. Metabolism *53,* 488-494.

Ishii, T., Sugita, Y., and Bannai, S. (1987). Regulation of glutathione levels in mouse spleen lymphocytes by transport of cysteine. Journal of Cellular Physiology *133,* 330-336.

Ishikawa, K., Takenaga, K., Akimoto, M., Koshikawa, N., Yamaguchi, A., Imanishi, H., Nakada, K., Honma, Y., and Hayashi, J. (2008). ROS-generating mitochondrial DNA mutations can regulate tumor cell metastasis. Science *320,* 661-664.

Itakura, E., and Mizushima, N. (2013). Syntaxin 17. Autophagy *9,* 917-919.

Jacqueminet, S., Briaud, I., Rouault, C., Reach, G., and Poitout, V. (2000). Inhibition of insulin gene expression by long-term exposure of pancreatic beta cells to palmitate is dependent on the presence of a stimulatory glucose concentration. Metabolism *49,* 532-536.

Jaganjac, M., Almuraikhy, S., Al-Khelaifi, F., Al-Jaber, M., Bashah, M., Mazloum, N.A., Zarkovic, K., Zarkovic, N., Waeg, G., Kafienah, W., and Elrayess, M. (2017). Combined metformin and insulin treatment reverses metabolically impaired omental adipogenesis and accumulation of 4-hydroxynonenal in obese diabetic patients. Redox Biol *12,* 483-490.

James, D., Stöckli, J., and Birnbaum, M. (2021). The aetiology and molecular landscape of insulin resistance. Nat Rev Mol Cell Biol *22,* 751-771.

Jang, K. (2020). Maturity-onset diabetes of the young: update and perspectives on diagnosis and treatment. Yeungnam Univ J Med *37,* 13-21.

Jensen, T., Karlsson, P., Gylfadottir, S., Andersen, S., Bennett, D., Tankisi, H., Finnerup, N., Terkelsen, A., Khan, K., Themistocleous, A. and Kristensen, A. (2021). Painful and non-painful diabetic neuropathy, diagnostic challenges and implications for future management. Brain *144,* 1632-1645.

Jia, J., Zhang, X., Ge, C., and Jois, M. (2009). The polymorphisms of UCP2 and UCP3 genes associated with fat metabolism, obesity and diabetes. Obes Rev *10,* 519-526.

Jialal, I., Devaraj, S., Adams-Huet, B., Chen, X., and Kaur, H. (2012). Increased cellular and circulating biomarkers of oxidative stress in nascent metabolic syndrome. J Clin Endocrinol Metab *97,* 1844.

Johnson, M., Tsai, L., Roy, D., Valenzuela, D., Mosley, C., Magklara, A., Lomvardas, S., Liberles, S., and Barnea, G. (2012). Neurons expressing trace amine-associated receptors project to discrete glomeruli and constitute an olfactory subsystem. Proc Natl Acad Sci U S A *109,* 13410-13415.

Juneja, R., Hirsch, I., Naik, R., Brooks-Worrell, B., Greenbaum, C., and Palmer, J. (2001). Islet cell antibodies and glutamic acid decarboxylase antibodies, but not the

clinical phenotype, help to identify type 1(1/2) diabetes in patients presenting with type 2 diabetes. Metabolism *50,* 1008-1013.

Kadota, Y., Kawakami, T., Takasaki, S., Sato, M., and Suzuki, S. (2016). Gene expression related to lipid and glucose metabolism in white adipose tissue. Obes Res Clin Pract *10,* 85-93.

Kahn, S. (2003). The relative contributions of insulin resistance and beta-cell dysfunction to the pathophysiology of Type 2 diabetes. Diabetologia *46,* 3-19.

Kailey, B., van de Bunt, M., Cheley, S., Johnson, P., MacDonald, P., Gloyn, A., Rorsman, P., and Braun, M. (2012). SSTR2 is the functionally dominant somatostatin receptor in human pancreatic β- and α-cells. Am J Physiol Endocrinol Metab *303,* 1107.

Kajihara, N., Kukidome, D., Sada, K., Motoshima, H., Furukawa, N., Matsumura, T., Nishikawa, T., and Araki, E. (2017). Low glucose induces mitochondrial reactive oxygen species via fatty acid oxidation in bovine aortic endothelial cells. J Diabetes Investig *8,* 750-761.

Kalyanaraman, B., Darley-Usmar, V., Davies, K., Dennery, P., Forman, H., Grisham, M., Mann, G., Moore, K., Roberts, L., and Ischiropoulos, H. (2012). Measuring reactive oxygen and nitrogen species with fluorescent probes: challenges and limitations. Free Radical Biology and Medicine *52,* 1-6.

Kamran, H., Kupferstein, E., Sharma, N., Karam, J., Myers, A., Youssef, I., Sowers, J., Gustafson, D., Salifu, M., and McFarlane, S. (2018). Statins and New-Onset Diabetes in Cardiovascular and Kidney Disease Cohorts: A Meta-Analysis. Cardiorenal Med *8,* 105-112.

Kanno, T., Göpel, S.O., Rorsman, P., and Wakui, M. (2002). Cellular function in multicellular system for hormone-secretion: electrophysiological aspect of studies on α-, β- and δ-cells of the pancreatic islet. Neuroscience Research *42,* 79-90.

Karkabounas, S., Papadopoulos, N., Anastasiadou, C., Gubili, C., Peschos, D., Daskalou, T., Fikioris, N., Simos, Y.V., Kontargiris, E., Gianakopoulos, X., Ragos, V., and Chatzidimitriou, M. (2018). Effects of α-Lipoic Acid, Carnosine, and Thiamine

Supplementation in Obese Patients with Type 2 Diabetes Mellitus: A Randomized, Double-Blind Study. J Med Food *21,* 1197-1203.

Kaur, G., Lakshmi, P., Rastogi, A., Bhansali, A., Jain, S., Teerawattananon, Y., Bano, H., and Prinja, S. (2020). Diagnostic accuracy of tests for type 2 diabetes and prediabetes: A systematic review and meta-analysis. PLoS One *15,* e0242415.

Kawasaki, F., Matsuda, M., Kanda, Y., Inoue, H., and Kaku, K. (2005). Structural and functional analysis of pancreatic islets preserved by pioglitazone in db/db mice. American Journal of Physiology-Endocrinology and Metabolism *288,* E510-E518.

Kazda, C., Ding, Y., Kelly, R., Garhyan, P., Shi, C., Lim, C., Fu, H., Watson, D., Lewin, A., Landschulz, W., and Deeg, M. (2017). Erratum. Evaluation of Efficacy and Safety of the Glucagon Receptor Antagonist LY2409021 in Patients With Type 2 Diabetes: 12- and 24-Week Phase 2 Studies. Diabetes Care 2016;39:1241-1249. Diabetes Care *40,* 808.

Kehrer, J., and Klotz, L. (2015). Free radicals and related reactive species as mediators of tissue injury and disease: implications for Health. Crit Rev Toxicol *45,* 765-798.

Kelley, D., He, J., Menshikova, E., and Ritov, V. (2002). Dysfunction of mitochondria in human skeletal muscle in type 2 diabetes. Diabetes *51,* 2944-2950.

Kelpe, C., Moore, P., Parazzoli, S., Wicksteed, B., Rhodes, C., and Poitout, V. (2003). Palmitate inhibition of insulin gene expression is mediated at the transcriptional level via ceramide synthesis. J Biol Chem *278,* 30015-30021.

Kersten, S., Desvergne, B., and Wahli, W. (2000). Roles of PPARs in health and disease. Nature *405,* 421-424.

Klatt, P., and Lamas, S. (2000). Regulation of protein function by S-glutathiolation in response to oxidative and nitrosative stress. Eur J Biochem *267,* 4928-4944.

Klebanov, G., YuO, N., Babenkova, I., Popov, I., Levin, G., Tyulina, O., Boldyrev, A., and Yua, N. (1997). Evidence for a direct interaction of superoxide anion radical with carnosine. Biochem Mol Biol Int *43,* 99-106.

Knop, F., Vilsbøll, T., Madsbad, S., Holst, J., and Krarup, T. (2007). Inappropriate suppression of glucagon during OGTT but not during isoglycaemic i.v. glucose infusion contributes to the reduced incretin effect in type 2 diabetes mellitus. Diabetologia *50,* 797-805.

Knott, A., and Bossy-Wetzel, E. (2010). Impact of nitric oxide on metabolism in health and age-related disease. Diabetes Obes Metab *12 Suppl 2,* 126-133.

Kobayashi, M., and Zochodne, D. (2018). Diabetic neuropathy and the sensory neuron: New aspects of pathogenesis and their treatment implications. J Diabetes Investig *9,* 1239-1254.

Kobilka, B. (2007). G protein coupled receptor structure and activation. Biochim Biophys Acta *1768,* 794-807.

Kohen, R., Misgav, R., and Ginsburg, I. (1991). The SOD like activity of copper:carnosine, copper:anserine and copper:homocarnosine complexes. Free Radic Res Commun *12-13 Pt 1,* 179-185.

Kohen, R., Yamamoto, Y., Cundy, K., and Ames, B. (1988). Antioxidant activity of carnosine, homocarnosine, and anserine present in muscle and brain. Proc Natl Acad Sci U S A *85,* 3175-3179.

Köhnke, R., Mei, J., Park, M., York, D., and Erlanson-Albertsson, C. (2007). Fatty acids and glucose in high concentration down-regulates ATP synthase beta-subunit protein expression in INS-1 cells. Nutr Neurosci *10,* 273-278.

Koivisto, V. (1993). Insulin therapy in type II diabetes. Diabetes Care *16 Suppl 3,* 29-39.

Korbonits, M., Goldstone, A., Gueorguiev, M., and Grossman, A. (2004). Ghrelin--a hormone with multiple functions. Front Neuroendocrinol *25,* 27-68.

Kouidrat, Y., Pizzol, D., Cosco, T., Thompson, T., Carnaghi, M., Bertoldo, A., Solmi, M., Stubbs, B., and Veronese, N. (2017). High prevalence of erectile dysfunction in diabetes: a systematic review and meta-analysis of 145 studies. Diabet Med *34,* 1185-1192.

Kowluru, R. (2019). Mitochondrial Stability in Diabetic Retinopathy: Lessons Learned From Epigenetics. Diabetes *68,* 241-247.

Kraegen, E., Cooney, G., Ye, J., Thompson, A., and Furler, S. (2001). The role of lipids in the pathogenesis of muscle insulin resistance and beta cell failure in type II diabetes and obesity. Exp Clin Endocrinol Diabetes *109 Suppl 2,* 189.

Księżakowska-Łakoma, K., Żyła, M., and Wilczyński, J. (2014). Mitochondrial dysfunction in cancer. Prz Menopauzalny *13,* 136-144.

Kuhajda, F. (2006). Fatty acid synthase and cancer: new application of an old pathway. Cancer Res *66,* 5977-5980.

Kumar, S., Narwal, S., Kumar, V., and Prakash, O. (2011). α-glucosidase inhibitors from plants: A natural approach to treat diabetes. Pharmacogn Rev *5,* 19-29.

Kurutas, E. (2016). The importance of antioxidants which play the role in cellular response against oxidative/nitrosative stress: current state. Nutr J *15,* 71.

Kwiatkowski, S., Kiersztan, A., and Drozak, J. (2018). Biosynthesis of Carnosine and Related Dipeptides in Vertebrates. Curr Protein Pept Sci *19,* 771-789.

Kwon, J., Lee, S., Yang, K., Ahn, Y., Kim, Y.J., Stadtman, E., and Rhee, S. (2004). Reversible oxidation and inactivation of the tumor suppressor PTEN in cells stimulated with peptide growth factors. Proc Natl Acad Sci U S A *101,* 16419-16424.

Lacey, R., Berrow, N., London, N., Lake, S., James, R., Scarpello, J., and Morgan, N. (1990). Differential effects of beta-adrenergic agonists on insulin secretion from pancreatic islets isolated from rat and man. J Mol Endocrinol *5,* 49-54.

Las, G., Serada, S., Wikstrom, J., Twig, G., and Shirihai, O. (2011). Fatty acids suppress autophagic turnover in β-cells. Journal of Biological Chemistry *286,* 42534-42544.

Lavine, J., Raess, P., Stapleton, D., Rabaglia, M., Suhonen, J., Schueler, K., Koltes, J., Dawson, J., Yandell, B., Samuelson, L., and Beinfeld, M. (2010). Cholecystokinin is up-regulated in obese mouse islets and expands beta-cell mass by increasing beta-cell survival. Endocrinology *151,* 3577-3588.

Law, B., Fowlkes, V., Goldsmith, J., Carver, W., and Goldsmith, E. (2012). Diabetes-Induced Alterations in the Extracellular Matrix and Their Impact on Myocardial Function. Microsc Microanal *18,* 22-34.

Lawrence, M. (2021). Understanding insulin and its receptor from their three-dimensional structures. Mol Metab *52,* 101255.

Lechner, M., Lirk, P., and Rieder, J. (2005). Inducible nitric oxide synthase (iNOS) in tumor biology: The two sides of the same coin. Seminars in Cancer Biology *15,* 277-289.

Lee, C., and Grant, P. (2019). Chapter 1-1 - Role of Histone Acetylation and Acetyltransferases in Gene Regulation. In Toxicoepigenetics, McCullough, Shaun D., and Dolinoy, Dana C. eds., Academic Press) pp. 3-30.

Lee, H., and Wei, Y. (2000). Mitochondrial role in life and death of the cell. J Biomed Sci *7,* 2-15.

Lee, J., Zhao, L., Youn, H., Weatherill, A., Tapping, R., Feng, L., Lee, W., Fitzgerald, K., and Hwang, D. (2004). Saturated Fatty Acid Activates but Polyunsaturated Fatty Acid Inhibits Toll-like Receptor 2 Dimerized with Toll-like Receptor 6 or 1*. Journal of Biological Chemistry *279,* 16971-16979.

Lee-Huang, S., Huang, P., and Huang, P. (2021). Endothelial Nitric Oxide Synthase Knockdown in Human Stem Cells Impacts Mitochondrial Biogenesis and Adipogenesis: Live-Cell Real-Time Fluorescence Imaging. J Clin Med *10,*

Leem, J., Shim, H., Cho, H., and Park, J. (2018). Octanoic acid potentiates glucose-stimulated insulin secretion and expression of glucokinase through the olfactory receptor in pancreatic β-cells. Biochem Biophys Res Commun *503,* 278-284.

Lehto, M., Bitzén, P., Isomaa, B., Wipemo, C., Wessman, Y., Forsblom, C., Tuomi, T., Taskinen, M., and Groop, L. (1999). Mutation in the HNF-4alpha gene affects insulin secretion and triglyceride metabolism. Diabetes *48,* 423-425.

Leloup, C., Tourrel-Cuzin, C., Magnan, C., Karaca, M., Castel, J., Carneiro, L., Colombani, A., Ktorza, A., Casteilla, L., and Pénicaud, L. (2009). Mitochondrial reactive oxygen species are obligatory signals for glucose-induced insulin secretion. Diabetes *58,* 673-681.

Lencioni, C., Lupi, R., and Del Prato, S. (2008). Beta-cell failure in type 2 diabetes mellitus. Curr Diab Rep *8,* 179-184.

Lenz, O., Elliot, S., and Stetler-Stevenson, W. (2000). Matrix Metalloproteinases in Renal Development and Disease. Jasn *11,* 574-581.

Leto, D., and Saltiel, A. (2012). Regulation of glucose transport by insulin: traffic control of GLUT4. Nature Reviews Molecular Cell Biology *13,* 383-396.

Leung, N., Sakaue, T., Carpentier, A., Uffelman, K., Giacca, A., and Lewis, G. (2004). Prolonged increase of plasma non-esterified fatty acids fully abolishes the stimulatory effect of 24 hours of moderate hyperglycaemia on insulin sensitivity and pancreatic beta-cell function in obese men. Diabetologia *47,* 204-213.

Lewandowski, K., Banach, E., Bieńkiewicz, M., and Lewiński, A. (2011). Clinical research Matrix metalloproteinases in type 2 diabetes and non-diabetic controls: effects of short-term and chronic hyperglycaemia. Arch Med Sci *7,* 294-303.

Li, G., and Marlin, M. (2015). Rab Family of GTPases. Methods Mol Biol *1298,* 1-15.

Li, J., Ning, G., and Duncan, S. (2000). Mammalian hepatocyte differentiation requires the transcription factor HNF-4α. Genes Dev *14,* 464-474.

Li, X., Li, C., and Sun, G. (2016). Histone Acetylation and Its Modifiers in the Pathogenesis of Diabetic Nephropathy. J Diabetes Res *2016,* 4065382.

Liberles, S., and Buck, L. (2006). A second class of chemosensory receptors in the olfactory epithelium. Nature *442,* 645-650.

Lim, S., Rashid, M.A., Jang, M., Kim, Y., Won, H., Lee, J., Woo, J., Kim, Y., Murphy, M., Ali, L., Ha, J., and Kim, S. (2011). Mitochondria-targeted antioxidants protect pancreatic β-cells against oxidative stress and improve insulin secretion in glucotoxicity and glucolipotoxicity. Cell Physiol Biochem *28,* 873-886.

Linn, T., Ortac, K., Laube, H., and Federlin, K. (1996). Intensive therapy in adult insulin-dependent diabetes mellitus is associated with improved insulin sensitivity and reserve: a randomized, controlled, prospective study over 5 years in newly diagnosed patients. Metabolism *45,* 1508-1513.

Liu, G., Ji, W., Huang, J., Liu, L., and Wang, Y. (2016). 4-HNE expression in diabetic rat kidneys and the protective effects of probucol. J Endocrinol Invest *39,* 865-873.

Liu, T., Sun, L., Zhang, Y., Wang, Y., and Zheng, J. (2022). Imbalanced GSH/ROS and sequential cell death. J Biochem Mol Toxicol *36,* e22942.

Liu, X., Wang, Z., Yang, Y., Li, Q., Zeng, R., Kang, J., and Wu, J. (2016). Rab1A mediates proinsulin to insulin conversion in β-cells by maintaining Golgi stability through interactions with golgin-84. Protein Cell *7,* 692-696.

Livak, K., and Schmittgen, T. (2001). Analysis of relative gene expression data using real-time quantitative PCR and the 2(-Delta Delta C(T)) Method. Methods *25,* 402-408.

Lizcano, J., and Alessi, D. (2002). The insulin signalling pathway. Current Biology *12,* R236-R238.

Ljubicic, S., Bezzi, P., Brajkovic, S., Nesca, V., Guay, C., Ohbayashi, N., Fukuda, M., Abderrhamani, A., and Regazzi, R. (2013). The GTPase Rab37 Participates in the Control of Insulin Exocytosis. PLoS One *8,* e68255.

Llacua, L., Faas, M., and de Vos, P. (2018). Extracellular matrix molecules and their potential contribution to the function of transplanted pancreatic islets. Diabetologia *61,* 1261-1272.

Locke, A., Kahali, B., Berndt, S., Justice, A., Pers, T., Day, F., Powell, C., Vedantam, S., Buchkovich, M., Yang, J. and Croteau-Chonka, D. (2015). Genetic studies of body mass index yield new insights for obesity biology. Nature *518,* 197-206.

López-Soldado, I., Niisuke, K., Veiga, C., Adrover, A., Manzano, A., Martínez-Redondo, V., Camps, M., Bartrons, R., Zorzano, A., and Gumà, A. (2016). Neuregulin improves response to glucose tolerance test in control and diabetic rats. Am J Physiol Endocrinol Metab *310,* 440.

Lowell, B., and Shulman, G. (2005). Mitochondrial dysfunction and type 2 diabetes. Science *307,* 384-387.

Luft, R., Efendić, S., and Hökfelt, T. (1978). Somatostatin--both hormone and neurotransmitter? Diabetologia *14,* 1-13.

Lupi, R., Dotta, F., Marselli, L., Del Guerra, S., Masini, M., Santangelo, C., Patané, G., Boggi, U., Piro, S., Anello, M. and Bergamini, E. (2002). Prolonged exposure to free fatty acids has cytostatic and pro-apoptotic effects on human pancreatic islets: evidence that beta-cell death is caspase mediated, partially dependent on ceramide pathway, and Bcl-2 regulated. Diabetes *51,* 1437-1442.

Ma, Y., Gao, M., and Liu, D. (2016). Preventing High Fat Diet-induced Obesity and Improving Insulin Sensitivity through Neuregulin 4 Gene Transfer. Sci Rep *6,* 26242.

Mabley, J., Southan, G., Salzman, A., and Szabó, C. (2004). The combined inducible nitric oxide synthase inhibitor and free radical scavenger guanidinoethyldisulfide prevents multiple low-dose streptozotocin-induced diabetes in vivo and interleukin-1beta-induced suppression of islet insulin secretion in vitro. Pancreas *28,* 39.

Maeda, S., Imamura, M., Kurashige, M., Araki, S., Suzuki, D., Babazono, T., Uzu, T., Umezono, T., Toyoda, M., Kawai, K. and Imanishi, M. (2013). Replication study for the association of 3 SNP loci identified in a genome-wide association study for diabetic nephropathy in European type 1 diabetes with diabetic nephropathy in Japanese patients with type 2 diabetes. Clin Exp Nephrol *17,* 866-871.

Maestre, I., Jordán, J., Calvo, S., Reig, J., Ceña, V., Soria, B., Prentki, M., and Roche, E. (2003). Mitochondrial dysfunction is involved in apoptosis induced by serum withdrawal and fatty acids in the beta-cell line INS-1. Endocrinology *144,* 335-345.

Malaisse, W. (2003). Pharmacology of the meglitinide analogs: new treatment options for type 2 diabetes mellitus. Treat Endocrinol *2,* 401-414.

Malik, F., and Taplin, C. (2014). Insulin therapy in children and adolescents with type 1 diabetes. Paediatr Drugs *16,* 141-150.

Malmberg, K. (1997). Prospective randomised study of intensive insulin treatment on long term survival after acute myocardial infarction in patients with diabetes mellitus. DIGAMI (Diabetes Mellitus, Insulin Glucose Infusion in Acute Myocardial Infarction) Study Group. Bmj *314,* 1512-1515.

Manoli, I., Alesci, S., Blackman, M., Su, Y., Rennert, O., and Chrousos, G. (2007). Mitochondria as key components of the stress response. Trends Endocrinol Metab *18,* 190-198.

Marchant, D., Bellac, C., Moraes, T., Wadsworth, S., Dufour, A., Butler, G., Bilawchuk, L., Hendry, R., Robertson, A., Cheung, C. and Ng, J. (2014). A new transcriptional role for matrix metalloproteinase-12 in antiviral immunity. Nat Med *20,* 493-502.

Marchetti, P., Del Guerra, S., Marselli, L., Lupi, R., Masini, M., Pollera, M., Bugliani, M., Boggi, U., Vistoli, F., Mosca, F., and Del Prato, S. (2004). Pancreatic Islets from Type 2 Diabetic Patients Have Functional Defects and Increased Apoptosis That Are Ameliorated by Metformin. The Journal of Clinical Endocrinology & Metabolism *89,* 5535-5541.

Maritim, A., Sanders, R., and Watkins, J. (2003). Diabetes, oxidative stress, and antioxidants: a review. J Biochem Mol Toxicol *17,* 24-38.

Marshall, C., Hitman, G., Cassell, P., and Turner, M. (2007). Effect of glucolipotoxicity and rosiglitazone upon insulin secretion. Biochemical and Biophysical Research Communications *356,* 756-762.

Maßberg, D., and Hatt, H. (2018). Human Olfactory Receptors: Novel Cellular Functions Outside of the Nose. Physiol Rev *98,* 1739-1763.

Mathiesen, D., Bagger, J., Bergmann, N., Lund, A., Christensen, M., Vilsbøll, T., and Knop, F. (2019). The Effects of Dual GLP-1/GIP Receptor Agonism on Glucagon Secretion—A Review. Int J Mol Sci *20,*

Mauris, J., Woodward, A., Cao, Z., Panjwani, N., and Argüeso, P. (2014). Molecular basis for MMP9 induction and disruption of epithelial cell-cell contacts by galectin-3. J Cell Sci *127,* 3141-3148.

McCaffrey, M., and Lindsay, A. (2013). Rab Family. In Encyclopedia of Biological Chemistry (Second Edition), Lennarz, William J., and Lane, M. Daniel eds., (Waltham: Academic Press) pp. 1-6.

McCord, J., Roy, R., and Schaffer, S. (1985). Free radicals and myocardial ischemia. The role of xanthine oxidase. Adv Myocardiol *5,* 183-189.

McCulloch, L., van de Bunt, M., Braun, M., Frayn, K., Clark, A., and Gloyn, A. (2011). GLUT2 (SLC2A2) is not the principal glucose transporter in human pancreatic beta cells: implications for understanding genetic association signals at this locus. Mol Genet Metab *104,* 648-653.

McDonald, T., and Ellard, S. (2013). Maturity onset diabetes of the young: identification and diagnosis. Ann Clin Biochem *50,* 403-415.

McLean, J., Moylan, J., and Andrade, F. (2014). Mitochondria dysfunction in lung cancer-induced muscle wasting in C2C12 myotubes. Front Physiol *5,* 503.

McLennan, S., Martell, S., and Yue, D. (2002). Effects of mesangium glycation on matrix metalloproteinase activities: possible role in diabetic nephropathy. Diabetes *51,* 2612-2618.

McVean, J., and Miller, J. (2021). MiniMedTM780G Insulin pump system with smartphone connectivity for the treatment of type 1 diabetes: overview of its safety and efficacy. Expert Rev Med Devices *18,* 499-504.

Meda, P., Bosco, D., Chanson, M., Giordano, E., Vallar, L., Wollheim, C., and Orci, L. (1990). Rapid and reversible secretion changes during uncoupling of rat insulin-producing cells. J Clin Invest *86,* 759-768.

Mehta, V., Kumar, A., Jaggi, A., and Singh, N. (2020). Restoration of the Attenuated Neuroprotective Effect of Ischemic Postconditioning in Diabetic Mice by SGLT Inhibitor Phlorizin. Curr Neurovasc Res *17,* 706-718.

Meijles, D., Fuller, S., Cull, J., Alharbi, H., Cooper, S., Sugden, P., and Clerk, A. (2021). The insulin receptor family and protein kinase B (Akt) are activated in the heart by alkaline pH and α1-adrenergic receptors. Biochem J *478,* 2059-2079.

Miedzybrodzka, Z., Hattersley, A., Ellard, S., Pearson, D., de Silva, D., Harvey, R., and Haites, N. (1999). Non-penetrance in a MODY 3 family with a mutation in the hepatic nuclear factor 1alpha gene: implications for predictive testing. Eur J Hum Genet *7,* 729-732.

Mîinea, C., Sano, H., Kane, S., Sano, E., Fukuda, M., Peränen, J., Lane, W., and Lienhard, G. (2005). AS160, the Akt substrate regulating GLUT4 translocation, has a functional Rab GTPase-activating protein domain. Biochem J *391,* 87-93.

Miron, A., Sajet, A., Groeneveld-van Beek, E., Kok, J., Dedeci, M., de Jong, M., Amo-Addae, V., Melles, G., Oellerich, S., and van der Wees, J. (2021). Endothelial Cell Viability after DMEK Graft Preparation. Curr Eye Res *46,* 1621-1630.

Mittal, C., and Murad, F. (1977). Activation of guanylate cyclase by superoxide dismutase and hydroxyl radical: a physiological regulator of guanosine 3',5'-monophosphate formation. Proc Natl Acad Sci U S A *74,* 4360-4364.

Mittal, R., Patel, A., Debs, L., Nguyen, D., Patel, K., Grati, M., Mittal, J., Yan, D., Chapagain, P., and Liu, X. (2016). Intricate Functions of Matrix Metalloproteinases in Physiological and Pathological Conditions. J Cell Physiol *231,* 2599-2621.

Miyazaki, Y., and DeFronzo, R. (2008). Rosiglitazone and pioglitazone similarly improve insulin sensitivity and secretion, glucose tolerance and adipocytokines in type 2 diabetic patients. Diabetes, Obesity and Metabolism *10,* 1204-1211.

Moelands, S., Lucassen, P., Akkermans, R., De Grauw, W. and Van de Laar, F., (2018). Alpha-glucosidase inhibitors for prevention or delay of type 2 diabetes mellitus and its associated complications in people at increased risk of developing type 2 diabetes mellitus. Cochrane Database of Systematic Reviews, (12)

Mohamed, A., Bierhaus, A., Schiekofer, S., Tritschler, H., Ziegler, R., and Nawroth, P. (1999). The role of oxidative stress and NF-kappaB activation in late diabetic complications. Biofactors *10,* 157-167.

Moldéus, P. (1993). Toxicity induced by nitrogen dioxide in experimental animals and isolated cell systems. Scand J Work Environ Health *19 Suppl 2,* 28-36.

Molenaar, R., Maciejewski, J., Wilmink, J., and van Noorden, C. (2018). Wild-type and mutated IDH1/2 enzymes and therapy responses. Oncogene *37,* 1949-1960.

Møller, T.C., Moreno-Delgado, D., Pin, J., and Kniazeff, J. (2017). Class C G protein-coupled receptors: reviving old couples with new partners. Biophys Rep *3,* 57-63.

Mombaerts, P. (2004). Odorant receptor gene choice in olfactory sensory neurons: the one receptor-one neuron hypothesis revisited. Curr Opin Neurobiol *14,* 31-36.

Monti, L., Lucotti, P., Setola, E., Rossodivita, A., Pala, M., Galluccio, E., LaCanna, G., Castiglioni, A., Cannoletta, M., Meloni, C. and Zavaroni, I. (2012). Effects of

chronic elevation of atrial natriuretic peptide and free fatty acid levels in the induction of type 2 diabetes mellitus and insulin resistance in patients with mitral valve disease. Nutr Metab Cardiovasc Dis *22,* 58-65.

Morrissey, S., Zhang, F., Ding, C., Montoya-Durango, D., Hu, X., Yang, C., Wang, Z., Yuan, F., Fox, M., Zhang, H. and Guo, H. (2021). Tumor-derived exosomes drive immunosuppressive macrophages in a pre-metastatic niche through glycolytic dominant metabolic reprogramming. *Cell metabolism*, *33*(10), pp.2040-2058.

Muhammed, S., Lundquist, I., and Salehi, A. (2012). Pancreatic β-cell dysfunction, expression of iNOS and the effect of phosphodiesterase inhibitors in human pancreatic islets of type 2 diabetes. Diabetes, Obesity and Metabolism *14,* 1010-1019.

Muoio, D., and Newgard, C. (2008). Mechanisms of disease:Molecular and metabolic mechanisms of insulin resistance and beta-cell failure in type 2 diabetes. Nat Rev Mol Cell Biol *9,* 193-205.

Muri, J., and Kopf, M. (2021). Redox regulation of immunometabolism. Nat Rev Immunol *21,* 363-381.

Myhre, O., Andersen, J., Aarnes, H., and Fonnum, F. (2003). Evaluation of the probes 2′,7′-dichlorofluorescin diacetate, luminol, and lucigenin as indicators of reactive species formation. Biochemical Pharmacology *65,* 1575-1582.

Nagase, H., Visse, R., and Murphy, G. (2006). Structure and function of matrix metalloproteinases and TIMPs. Cardiovascular Research *69,* 562-573.

Nagy, T., Blaylock, M., and Garvey, W. (2004). Role of UCP2 and UCP3 in nutrition and obesity. Nutrition *20,* 139-144.

Nam, K., Lee, H., Smith, J., Lapierre, L., Kamath, V., Chen, X., Aronow, B., Yeatman, T., Bhartur, S., Calhoun, B. and Condie, B. (2010). Loss of Rab25 promotes the development of intestinal neoplasia in mice and is associated with human colorectal adenocarcinomas. *The Journal of clinical investigation*, *120*(3), pp.840-849.

Naor, D., Sionov, R., and Ish-Shalom, D. (1997). CD44: structure, function, and association with the malignant process. Adv Cancer Res *71,* 241-319.

Naseri, M., Sereshki, Z., Ghavami, B., Zangii, B., Kamalinejad, M., Moghaddam, P., Asghari, M., Nejad, S., Emadi, F., and Ghaffari, F. (2021). Preliminary results of effect of barley (*Hordeum vulgare L*.) extract on liver, pancreas, kidneys and cardiac tissues in streptozotocin induced diabetic rats. Eur J Transl Myol *32,*

Nathan, D., Buse, J., Davidson, M., Ferrannini, E., Holman, R., Sherwin, R., and Zinman, B. (2009). Medical management of hyperglycemia in type 2 diabetes: a consensus algorithm for the initiation and adjustment of therapy: a consensus statement of the American Diabetes Association and the European Association for the Study of Diabetes. Diabetes Care *32,* 193-203.

Nauck, M., and Meier, J. (2018). Incretin hormones: Their role in health and disease. Diabetes Obes Metab *20 Suppl 1,* 5-21.

Nemirovskiy, O., Radabaugh, M., Aggarwal, P., Funckes-Shippy, C., Mnich, S., Meyer, D., Sunyer, T., Mathews, W., and Misko, T. (2009). Plasma 3-nitrotyrosine is a biomarker in animal models of arthritis: Pharmacological dissection of iNOS' role in disease. Nitric Oxide *20,* 150-156.

Nestler, J. (2008). Metformin in the treatment of infertility in polycystic ovarian syndrome: an alternative perspective. Fertility and Sterility *90,* 14-16.

Neuen, B., Young, T., Heerspink, H., Neal, B., Perkovic, V., Billot, L., Mahaffey, K., Charytan, D., Wheeler, D., Arnott, C. and Bompoint, S. (2019). SGLT2 inhibitors for the prevention of kidney failure in patients with type 2 diabetes: a systematic review and meta-analysis. The Lancet Diabetes & endocrinology, 7(11), pp.845-854.

Ng, R., and Marshall, F. (1978). Regional and subcellular distribution of homocarnosine-carnosine synthetase in the central nervous system of rats. J Neurochem *30,* 87.

Nguyen, M., Favelyukis, S., Nguyen, A., Reichart, D., Scott, P., Jenn, A., Liu-Bryan, R., Glass, C., Neels, J., and Olefsky, J. (2007). A subpopulation of macrophages infiltrates hypertrophic adipose tissue and is activated by free fatty acids via Toll-like receptors 2 and 4 and JNK-dependent pathways. J Biol Chem *282,* 35279-35292.

Nicholls, D., and Ferguson, S. (2013). 12 - Mitochondria in Physiology and Pathology. In Bioenergetics (Fourth Edition), Nicholls, David G., and Ferguson, Stuart J. eds., (Boston: Academic Press) pp. 345-386.

Nishikawa, T., Edelstein, D., Du, X., Yamagishi, S., Matsumura, T., Kaneda, Y., Yorek, M., Beebe, D., Oates, P., Hammes, H., Giardino, I., and Brownlee, M. (2000). Normalizing mitochondrial superoxide production blocks three pathways of hyperglycaemic damage. Nature *404,* 787-790.

Nissen, S., and Wolski, K. (2007). Effect of rosiglitazone on the risk of myocardial infarction and death from cardiovascular causes. N Engl J Med *356,* 2457-2471.

Nkonge, K., Nkonge, D., and Nkonge, T. (2020). The epidemiology, molecular pathogenesis, diagnosis, and treatment of maturity-onset diabetes of the young (MODY). Clin Diabetes Endocrinol *6,* 20.

Nolan, T., Hands, R., and Bustin, S. (2006). Quantification of mRNA using real-time RT-PCR. Nat Protoc *1,* 1559-1582.

Novick, P., and Zerial, M. (1997). The diversity of Rab proteins in vesicle transport. Current Opinion in Cell Biology *9,* 496-504.

Numazawa, S., Sakaguchi, H., Aoki, R., Taira, T., and Yoshida, T. (2008). Regulation of the susceptibility to oxidative stress by cysteine availability in pancreatic beta-cells. Am J Physiol Cell Physiol *295,* 468.

Nunnari, J., and Suomalainen, A. (2012). Mitochondria: in sickness and in health. Cell *148,* 1145-1159.

Odom, D., Zizlsperger, N., Gordon, D., Bell, G., Rinaldi, N., Murray, H., Volkert, T., Schreiber, J., Rolfe, P., Gifford, D. and Fraenkel, E. (2004). Control of pancreas and liver gene expression by HNF transcription factors. *Science*, *303*(5662), pp.1378-1381.

Oh, E., Ahn, M., Afelik, S., Becker, T., Roep, B., and Thurmond, D. (2018). Syntaxin 4 Expression in Pancreatic β-Cells Promotes Islet Function and Protects Functional β-Cell Mass. Diabetes *67,* 2626-2639.

Oh, E., Stull, N., Mirmira, R., and Thurmond, D. (2014). Syntaxin 4 Up-Regulation Increases Efficiency of Insulin Release in Pancreatic Islets From Humans With and Without Type 2 Diabetes Mellitus. J Clin Endocrinol Metab *99,* E866-E870.

O'Harte, F., Mooney, M., Kelly, C., and Flatt, P.. (1998). Glycated cholecystokinin-8 has an enhanced satiating activity and is protected against enzymatic degradation. Diabetes *47,* 1619-1624.

Okuno, D., Iino, R., and Noji, H. (2011). Rotation and structure of FoF1-ATP synthase. J Biochem *149,* 655-664.

Olayioye, M., Neve, R., Lane, H., and Hynes, N. (2000). New EMBO members' review. Embo J *19,* 3159-3167.

Olofsson, C., Collins, S., Bengtsson, M., Eliasson, L., Salehi, A., Shimomura, K., Tarasov, A., Holm, C., Ashcroft, F., and Rorsman, P. (2007). Long-term exposure to glucose and lipids inhibits glucose-induced insulin secretion downstream of granule fusion with plasma membrane. Diabetes *56,* 1888-1897.

Olofsson, C., Göpel, S., Barg, S., Galvanovskis, J., Ma, X., Salehi, A., Rorsman, P., and Eliasson, L. (2002). Fast insulin secretion reflects exocytosis of docked granules in mouse pancreatic B-cells. Pflugers Arch *444,* 43-51.

Olson, B., and Markwell, J. (2007). Assays for Determination of Protein Concentration. Current Protocols in Protein Science *48,* 3.4.1-3.4.29.

Oruc, Y., Celik, F., Ozgur, G., Beyazyildiz, E., Ugur, K., Yardim, M., Sahin, I., Akkoc, R.F. and Aydin, S. (2020). Altered blood and aqueous humor levels of asprosin, 4-hydroxynonenal, and 8-hydroxy-deoxyguanosine in patients with diabetes mellitus and cataract with and without diabetic retinopathy. *Retina*, *40*(12), pp.2410-2416.

Osborn, O., and Olefsky, J. (2012). The cellular and signaling networks linking the immune system and metabolism in disease. Nat Med *18,* 363-374.

Otani, H., Okumura, N., Hashida-Okumura, A., and Nagai, K. (2005). Identification and characterization of a mouse dipeptidase that hydrolyzes L-carnosine. J Biochem *137,* 167-175.

Ott, M., Rey-Campos, J., Cereghini, S., and Yaniv, M. (1991). vHNF1 is expressed in epithelial cells of distinct embryonic origin during development and precedes HNF1 expression. Mech Dev *36,* 47-58.

Ott, M., Gogvadze, V., Orrenius, S., and Zhivotovsky, B. (2007). Mitochondria, oxidative stress and cell death. Apoptosis *12,* 913-922.

Owen, K., Skupien, J., and Malecki, M. (2009). The clinical application of non-genetic biomarkers for differential diagnosis of monogenic diabetes. Diabetes Res Clin Pract *86 Suppl 1,* 15.

Owen, M., Doran, E., and Halestrap, A. (2000). Evidence that metformin exerts its anti-diabetic effects through inhibition of complex 1 of the mitochondrial respiratory chain. Biochemical Journal *348,* 607-614.

Owora, A. (2018). Commentary: Diagnostic Validity and Clinical Utility of HbA1c Tests for Type 2 Diabetes Mellitus. Curr Diabetes Rev *14,* 196-199.

Pacher, P., Beckman, J., and Liaudet, L. (2007). Nitric oxide and peroxynitrite in health and disease. Physiol Rev *87,* 315-424.

Pan, L., Yang, S., Wang, J., Xu, M., Wang, S., and Yi, H. (2020). Inducible nitric oxide synthase and systemic lupus erythematosus: a systematic review and meta-analysis. BMC Immunol *21,* 6.

Pan, X., Wang, L., and Pan, A. (2021). Epidemiology and determinants of obesity in China. Lancet Diabetes Endocrinol *9,* 373-392.

Paniccia, A., and Schulick, R. (2017). Chapter 4 - Pancreatic Physiology and Functional Assessment. In Blumgart's Surgery of the Liver, Biliary Tract and Pancreas, 2-Volume Set (Sixth Edition), Jarnagin, William R. ed., (Philadelphia: Elsevier) pp. 66-76.e3.

Paolisso, G., Gambardella, A., Amato, L., Tortoriello, R., D'Amore, A., Varricchio, M., and D'Onofrio, F. (1995). Opposite effects of short- and long-term fatty acid infusion on insulin secretion in healthy subjects. Diabetologia *38,* 1295-1299.

Paradies, G., Petrosillo, G., Paradies, V., and Ruggiero, F. (2010). Oxidative stress, mitochondrial bioenergetics, and cardiolipin in aging. Free Radical Biology and Medicine *48,* 1286-1295.

Park, W. (2021). Enhanced cell death effects of MAP kinase inhibitors in propyl gallate-treated lung cancer cells are related to increased ROS levels and GSH depletion. Toxicol in Vitro *74,* 105176.

Patanè, G., Piro, S., Rabuazzo, A., Anello, M., Vigneri, R., and Purrello, F. (2000). Metformin restores insulin secretion altered by chronic exposure to free fatty acids or high glucose: a direct metformin effect on pancreatic beta-cells. Diabetes *49,* 735-740.

Pavlin, M., Rossetti, G., De Vivo, M., and Carloni, P. (2016). Carnosine and Homocarnosine Degradation Mechanisms by the Human Carnosinase Enzyme CN1: Insights from Multiscale Simulations. Biochemistry *55,* 2772-2784.

Pavlov, A., Revina, A., Dupin, A., Boldyrev, A., and Yaropolov, A. (1993). The mechanism of interaction of carnosine with superoxide radicals in water solutions. Biochim Biophys Acta *1157,* 304-312.

Pepper, M. (2001). Extracellular proteolysis and angiogenesis. Thromb Haemost *86,* 346-355.

Pérez, A., Ramos, A., and Carreras, G. (2020). Insulin Therapy in Hospitalized Patients. Am J Ther *27,* e71-e78.

Perfetti, R., Zhou, J., Doyle, M., and Egan, J. (2000). Glucagon-Like Peptide-1 Induces Cell Proliferation and Pancreatic-Duodenum Homeobox-1 Expression and Increases Endocrine Cell Mass in the Pancreas of Old, Glucose-Intolerant Rats. Endocrinology *141,* 4600-4605.

Perkins, B., Sherr, J., and Mathieu, C. (2021). Type 1 diabetes glycemic management: Insulin therapy, glucose monitoring, and automation. Science *373,* 522-527.

Perry, C., Kane, D., Lanza, I., and Neufer, P. (2013). Methods for assessing mitochondrial function in diabetes. Diabetes *62,* 1041-1053.

Persinger, R., Poynter, M., Ckless, K., and Janssen-Heininger, Y. (2002). Molecular mechanisms of nitrogen dioxide induced epithelial injury in the lung. Mol Cell Biochem *234-235,* 71-80.

Peters, V., Zschocke, J., and Schmitt, C. (2018). Carnosinase, diabetes mellitus and the potential relevance of carnosinase deficiency. J Inherit Metab Dis *41,* 39-47.

Petersen, M., and Shulman, G. (2018). Mechanisms of Insulin Action and Insulin Resistance. Physiol Rev *98,* 2133-2223.

Pfister, P., and Rodriguez, I. (2005). Olfactory expression of a single and highly variable V1r pheromone receptor-like gene in fish species. Proc Natl Acad Sci U S A *102,* 5489-5494.

Phang, W., Domboski, L., Krausz, Y., and Sharp, G. (1984). Mechanisms of synergism between glucose and cAMP on stimulation of insulin release. Am J Physiol *247,* 701.

Picciano, A., and Crane, B. (2019). A nitric oxide synthase-like protein from Synechococcus produces NO/NO3 - from l-arginine and NADPH in a tetrahydrobiopterin- and Ca2+-dependent manner. J Biol Chem *294,* 10708-10719.

Pihoker, C., Gilliam, L., Ellard, S., Dabelea, D., Davis, C., Dolan, L., Greenbaum, C., Imperatore, G., Lawrence, J., Marcovina, S. and Mayer-Davis, E. (2013). Prevalence, characteristics and clinical diagnosis of maturity onset diabetes of the young due to mutations in HNF1A, HNF4A, and glucokinase: results from the SEARCH for Diabetes in Youth. The Journal of Clinical Endocrinology & Metabolism, 98(10), pp.4055-4062.

Pin, J., Galvez, T., and Prézeau, L. (2003). Evolution, structure, and activation mechanism of family 3/C G-protein-coupled receptors. Pharmacol Ther *98,* 325-354.

Pinal-Fernandez, I., Casal-Dominguez, M., and Mammen, A. (2018). Statins: pros and cons. Med Clin (Barc) *150,* 398-402.

Pinti, M., Fink, G., Hathaway, Q., Durr, A., Kunovac, A., and Hollander, J. (2019). Mitochondrial dysfunction in type 2 diabetes mellitus: an organ-based analysis. Am J Physiol Endocrinol Metab *316,* E268-E285.

Pirro, M., Schillaci, G., Mannarino, M., Savarese, G., Vaudo, G., Siepi, D., Paltriccia, R., and Mannarino, E. (2007). Effects of rosuvastatin on 3-nitrotyrosine and aortic stiffness in hypercholesterolemia. Nutrition, Metabolism and Cardiovascular Diseases *17,* 436-441.

Pitocco, D., Zaccardi, F., Di Stasio, E., Romitelli, F., Santini, S., Zuppi, C., and Ghirlanda, G. (2010). Oxidative stress, nitric oxide, and diabetes. Rev Diabet Stud *7,* 15-25.

Poitout, V. (2008). Glucolipotoxicity of the pancreatic beta-cell: Myth or reality? Biochem Soc Trans *36,* 901-904.

Poitout, V., Amyot, J., Semache, M., Zarrouki, B., Hagman, D., and Fontés, G. (2010). Glucolipotoxicity of the pancreatic beta cell. Biochimica Et Biophysica Acta (BBA) - Molecular and Cell Biology of Lipids *1801,* 289-298.

Poitout, V., and Robertson, R. (2008). Glucolipotoxicity: fuel excess and beta-cell dysfunction. Endocr Rev *29,* 351-366.

Poitout, V., and Robertson, R. (2002). Minireview: Secondary beta-cell failure in type 2 diabetes--a convergence of glucotoxicity and lipotoxicity. Endocrinology *143,* 339-342.

Ponta, H., Sherman, L., and Herrlich, P. (2003). CD44: From adhesion molecules to signalling regulators. Nature Reviews Molecular Cell Biology *4,* 33-45.

Pontoglio, M., Prié, D., Cheret, C., Doyen, A., Leroy, C., Froguel, P., Velho, G., Yaniv, M., and Friedlander, G. (2000). HNF1alpha controls renal glucose reabsorption in mouse and man. EMBO Rep *1,* 359-365.

Portik-Dobos, V., Anstadt, M., Hutchinson, J., Bannan, M., and Ergul, A. (2002). Evidence for a matrix metalloproteinase induction/activation system in arterial vasculature and decreased synthesis and activity in diabetes. Diabetes *51,* 3063-3068.

Pospisilik, J., Martin, J., Doty, T., Ehses, J., Pamir, N., Lynn, F.C., Piteau, S., Demuth, H., McIntosh, C., and Pederson, R. (2003). Dipeptidyl peptidase IV inhibitor treatment stimulates beta-cell survival and islet neogenesis in streptozotocin-induced diabetic rats. Diabetes *52,* 741-750.

Pourfarzam, M., Movahedian, A., Sarrafzadegan, N., Basati, G., and Samsamshariat, S. (2013). Association between Plasma Myeloperoxidase and Free 3-Nitrotyrosine Levels in Patients with Coronary Artery Disease.*2013,*

Prentki, M., and Corkey, B. (1996). Are the beta-cell signaling molecules malonyl-CoA and cystolic long-chain acyl-CoA implicated in multiple tissue defects of obesity and NIDDM? Diabetes *45,* 273-283.

Prentki, M., Joly, E., El-Assaad, W., and Roduit, R. (2002). Malonyl-CoA signaling, lipid partitioning, and glucolipotoxicity: role in beta-cell adaptation and failure in the etiology of diabetes. Diabetes *51 Suppl 3,* 405.

Prentki, M., and Nolan, C.J. (2006). Islet beta cell failure in type 2 diabetes. J Clin Invest *116,* 1802-1812.

Pritchard, K.A., Ackerman, A.W., Gross, E., Stepp, D., Shi, Y., Fontana, J., Baker, J., and Sessa, W. (2001). Heat shock protein 90 mediates the balance of nitric oxide and superoxide anion from endothelial nitric-oxide synthase. J Biol Chem *276,* 17621-17624.

Prokopieva, V., Yarygina, E., Bokhan, N., and Ivanova, S. (2016). Use of Carnosine for Oxidative Stress Reduction in Different Pathologies. Oxid Med Cell Longev *2016,*

Pruett, S., Obiri, N., and Kiel, J. (1989). Involvement and relative importance of at least two distinct mechanisms in the effects of 2-mercaptoethanol on murine lymphocytes in culture. Journal of Cellular Physiology *141,* 40-45.

Puddu, A., Sanguineti, R., Mach, F., Dallegri, F., Viviani, G., and Montecucco, F. (2013). Update on the Protective Molecular Pathways Improving Pancreatic Beta-Cell Dysfunction. Mediators of Inflammation *2013,* e750540.

Raffetto, J., and Khalil, R. (2008). Matrix metalloproteinases and their inhibitors in vascular remodeling and vascular disease. Biochem Pharmacol *75,* 346-359.

Rani, V., Deep, G., Singh, R., Palle, K., and Yadav, U. (2016). Oxidative stress and metabolic disorders: Pathogenesis and therapeutic strategies. Life Sciences *148,* 183-193.

Rao, X., Huang, X., Zhou, Z., and Lin, X. (2013). An improvement of the 2ˆ(-delta delta CT) method for quantitative real-time polymerase chain reaction data analysis. Biostat Bioinforma Biomath *3,* 71-85.

Rath, A., Glibowicka, M., Nadeau, V., Chen, G., and Deber, C. (2009). Detergent binding explains anomalous SDS-PAGE migration of membrane proteins. Pnas *106,* 1760-1765.

Reimer, M., Pacini, G., and Ahrén, B. (2003). Dose-dependent inhibition by ghrelin of insulin secretion in the mouse. Endocrinology *144,* 916-921.

Reiniers, M., van Golen, R., Bonnet, S., Broekgaarden, M., van Gulik, T., Egmond, M., and Heger, M. (2017). Preparation and Practical Applications of 2′,7′-Dichlorodihydrofluorescein in Redox Assays. Anal. Chem. *89,* 3853-3857.

Renström, E., Ding, W., Bokvist, K., and Rorsman, P. (1996). Neurotransmitter-induced inhibition of exocytosis in insulin-secreting beta cells by activation of calcineurin. Neuron *17,* 513-522.

Rhee, S., Yang, K., Kang, S., Woo, H., and Chang, T. (2005). Controlled elimination of intracellular H(2)O(2): regulation of peroxiredoxin, catalase, and glutathione peroxidase via post-translational modification. Antioxid Redox Signal *7,* 619-626.

Richter, B., Bandeira-Echtler, E., Bergerhoff, K., and Lerch, C.L. (2008). Dipeptidyl peptidase-4 (DPP-4) inhibitors for type 2 diabetes mellitus. Cochrane Database Syst Rev CD006739.

Rieg, T., and Vallon, V. (2018). Development of SGLT1 and SGLT2 inhibitors. Diabetologia *61,* 2079-2086.

Rindi, G., Necchi, V., Savio, A., Torsello, A., Zoli, M., Locatelli, V., Raimondo, F., Cocchi, D., and Solcia, E. (2002). Characterisation of gastric ghrelin cells in man and other mammals: studies in adult and fetal tissues. Histochem Cell Biol *117,* 511-519.

Rindi, G., Savio, A., Torsello, A., Zoli, M., Locatelli, V., Cocchi, D., Paolotti, D., and Solcia, E. (2002). Ghrelin expression in gut endocrine growths. Histochem Cell Biol *117,* 521-525.

Ritov, V., Menshikova, E., Azuma, K., Wood, R., Toledo, F., Goodpaster, B., Ruderman, N., and Kelley, D. (2010). Deficiency of electron transport chain in human skeletal muscle mitochondria in type 2 diabetes mellitus and obesity. Am J Physiol Endocrinol Metab *298,* 49.

Rivellese, A., Patti, L., Romano, G., Innelli, F., Di Marino, L., Annuzzi, G., Iavicoli, M., Coronel, G., and Riccardi, G. (2000). Effect of insulin and sulfonylurea therapy, at the same level of blood glucose control, on low density lipoprotein subfractions in type 2 diabetic patients. J Clin Endocrinol Metab *85,* 4188-4192.

Robbins, G., Wen, H., and Ting, J. (2014). Inflammasomes and metabolic disorders: old genes in modern diseases. Mol Cell *54,* 297-308.

Robertson, R., Harmon, J., Tran, P., Tanaka, Y., and Takahashi, H. (2003). Glucose toxicity in beta-cells: type 2 diabetes, good radicals gone bad, and the glutathione connection. Diabetes *52,* 581-587.

Rocha, M., Apostolova, N., Diaz-Rua, R., Muntane, J., and Victor, V. (2020). Mitochondria and T2D: Role of Autophagy, ER Stress, and Inflammasome. Trends in Endocrinology & Metabolism *31,* 725-741.

Rocha, M., Diaz-Morales, N., Rovira-Llopis, S., Escribano-Lopez, I., Bañuls, C., Hernandez-Mijares, A., Diamanti-Kandarakis, E., and Victor, V. (2016). Mitochondrial Dysfunction and Endoplasmic Reticulum Stress in Diabetes. Curr Pharm Des *22,* 2640-2649.

Roche, E., Farfari, S., Witters, L., Assimacopoulos-Jeannet, F., Thumelin, S., Brun, T., Corkey, B., Saha, A., and Prentki, M. (1998). Long-term exposure of beta-INS cells to high glucose concentrations increases anaplerosis, lipogenesis, and lipogenic gene expression. Diabetes *47,* 1086-1094.

Rorsman, P., and Renström, E. (2003). Insulin granule dynamics in pancreatic beta cells. Diabetologia *46,* 1029-1045.

Rorsman, P., and Ashcroft, F. (2018). Pancreatic β-Cell Electrical Activity and Insulin Secretion: Of Mice and Men. Physiol Rev *98,* 117-214.

Rosca, M., Vazquez, E., Chen, Q., Kerner, J., Kern, T., and Hoppel, C. (2012). Oxidation of fatty acids is the source of increased mitochondrial reactive oxygen

species production in kidney cortical tubules in early diabetes. Diabetes *61,* 2074-2083.

Rosenstock, J., Hassman, D., Madder, R., Brazinsky, S., Farrell, J., Khutoryansky, N., and Hale, P. (2004). Repaglinide versus nateglinide monotherapy: a randomized, multicenter study. Diabetes Care *27,* 1265-1270.

Roskoski, R. (2019). Small molecule inhibitors targeting the EGFR/ErbB family of protein-tyrosine kinases in human cancers. Pharmacological Research *139,* 395-411.

Roskoski, R. (2014). The ErbB/HER family of protein-tyrosine kinases and cancer. Pharmacological Research *79,* 34-74.

Rovira-Llopis, S., Bañuls, C., Diaz-Morales, N., Hernandez-Mijares, A., Rocha, M., and Victor, V. (2017). Mitochondrial dynamics in type 2 diabetes: Pathophysiological implications. Redox Biol *11,* 637-645.

Rueden, C., Schindelin, J., Hiner, M., DeZonia, B., Walter, A., Arena, E., and Eliceiri, K. (2017). ImageJ2: ImageJ for the next generation of scientific image data. BMC Bioinformatics *18,* 529.

Rush, T., Grant, J., Mosyak, L., and Nicholls, A. (2005). A shape-based 3-D scaffold hopping method and its application to a bacterial protein-protein interaction. J Med Chem *48,* 1489-1495.

Ryffel, G. (2001). Mutations in the human genes encoding the transcription factors of the hepatocyte nuclear factor (HNF)1 and HNF4 families: functional and pathological consequences. J Mol Endocrinol *27,* 11-29.

Sagai, M., Ichinose, T., and Kubota, K. (1984). Studies on the biochemical effects of nitrogen dioxide. IV. Relation between the change of lipid peroxidation and the antioxidative protective system in rat lungs upon life span exposure to low levels of NO2. Toxicol Appl Pharmacol *73,* 444-456.

Saini, D., Kochar, A., and Poonia, R. (2021). Clinical correlation of diabetic retinopathy with nephropathy and neuropathy. Indian J Ophthalmol *69,* 3364-3368.

Saitoh, Y., Chun-ping, C., Noma, K., Ueno, H., Mizuta, M., and Nakazato, M. (2008). Pioglitazone attenuates fatty acid–induced oxidative stress and apoptosis in pancreatic β-cells. Diabetes, Obesity and Metabolism *10,* 564-573.

Sakai, K., Matsumoto, K., Nishikawa, T., Suefuji, M., Nakamaru, K., Hirashima, Y., Kawashima, J., Shirotani, T., Ichinose, K., Brownlee, M., and Araki, E. (2003). Mitochondrial reactive oxygen species reduce insulin secretion by pancreatic beta-cells. Biochem Biophys Res Commun *300,* 216-222.

Sale, C., Artioli, G., Gualano, B., Saunders, B., Hobson, R., and Harris, R. (2013). Carnosine: from exercise performance to health. Amino Acids *44,* 1477-1491.

Sale, C., Saunders, B., and Harris, R. (2010). Effect of beta-alanine supplementation on muscle carnosine concentrations and exercise performance. Amino Acids *39,* 321-333.

Saltiel, A., and Kahn, C. (2001). Insulin signalling and the regulation of glucose and lipid metabolism. Nature *414,* 799-806.

Santangelo, L., Marchetti, A., Cicchini, C., Conigliaro, A., Conti, B., Mancone, C., Bonzo, J., Gonzalez, F., Alonzi, T., Amicone, L., and Tripodi, M. (2011). The Stable Repression of Mesenchymal Program Is Required for Hepatocyte Identity: A Novel Role for Hepatocyte Nuclear Factor 4α. Hepatology *53,* 2063-2074.

Santomauro, A., Boden, G., Silva, M., Rocha, D., Santos, R., Ursich, M., Strassmann, P., and Wajchenberg, B. (1999). Overnight lowering of free fatty acids with Acipimox improves insulin resistance and glucose tolerance in obese diabetic and nondiabetic subjects. Diabetes *48,* 1836-1841.

Santos, J., Tewari, S., Lin, J., and Kowluru, R. (2013). Interrelationship between activation of matrix metalloproteinases and mitochondrial dysfunction in the development of diabetic retinopathy. Biochemical and Biophysical Research Communications *438,* 760-764.

Sanvee, G., Panajatovic, M., Bouitbir, J., and Krähenbühl, S. (2019). Mechanisms of insulin resistance by simvastatin in C2C12 myotubes and in mouse skeletal muscle. Biochem Pharmacol *164,* 23-33.

Saraswathy, N., and Ramalingam, P. (2011). 10 - Introduction to proteomics. In Concepts and Techniques in Genomics and Proteomics, Saraswathy, Nachimuthu, and Ramalingam, Ponnusamy eds., Woodhead Publishing) pp. 147-158.

Sarmiento-Ortega, V., Moroni-González, D., Díaz, A., Eduardo, B., and Samuel, T. (2021). Oral Subacute Exposure to Cadmium LOAEL Dose Induces Insulin Resistance and Impairment of the Hormonal and Metabolic Liver-Adipose Axis in Wistar Rats. Biol Trace Elem Res

Sauerhöfer, S., Yuan, G., Braun, G., Deinzer, M., Neumaier, M., Gretz, N., Floege, J., Kriz, W., van der Woude, F., and Moeller, M. (2007). L-carnosine, a substrate of carnosinase-1, influences glucose metabolism. Diabetes *56,* 2425-2432.

Saunders, B., de Salles Painelli, V., De Oliveira, L., da Eira Silva, V., Da Silva, R., Riani, L., Franchi, M., de Souza Gonçalves, L., Harris, R., Roschel, H. and Artioli, G. (2017). Twenty-four weeks of β-alanine supplementation on carnosine content, related genes, and exercise. *Medicine & Science in Sports & Exercise*, *49*(5), pp.896-906.

Saunders, B., Elliott-Sale, K., Artioli, G., Swinton, P., Dolan, E., Roschel, H., Sale, C., and Gualano, B. (2017). β-alanine supplementation to improve exercise capacity and performance: a systematic review and meta-analysis. Br J Sports Med *51,* 658-669.

Scamrov, A., and Beabealashvilli, R. (1988). The influence of a double-stranded hindrance on DNA synthesis performed by DNA polymerase alpha, T4 DNA polymerase, DNA polymerase I (Klenow fragment) and AMV reverse transcriptase. FEBS Lett *228,* 144-148.

Schafer, F., and Buettner, G. (2001). Redox environment of the cell as viewed through the redox state of the glutathione disulfide/glutathione couple. Free Radic Biol Med *30,* 1191-1212.

Schneider, C., Rasband, W., and Eliceiri, K. (2012). NIH Image to ImageJ: 25 years of image analysis. Nature Methods *9,* 671-675.

Schrader, M., and Fahimi, H. (2004). Mammalian peroxisomes and reactive oxygen species. Histochem Cell Biol *122,* 383-393.

Schroeder, A., Mueller, O., Stocker, S., Salowsky, R., Leiber, M., Gassmann, M., Lightfoot, S., Menzel, W., Granzow, M., and Ragg, T. (2006). The RIN: an RNA integrity number for assigning integrity values to RNA measurements. BMC Mol Biol *7,* 3.

Sędzikowska, A., and Szablewski, L. (2021). Insulin and Insulin Resistance in Alzheimer's Disease. Int J Mol Sci *22,*

Seeley, K., Fertig, A., Dufresne, C., Pinho, J., and Stevens, S. (2014). Evaluation of a method for nitrotyrosine site identification and relative quantitation using a stable isotope-labeled nitrated spike-in standard and high resolution fourier transform MS and MS/MS analysis. Int J Mol Sci *15,* 6265-6285.

Seifert, E., Estey, C., Xuan, J., and Harper, M. (2010). Electron transport chain-dependent and -independent mechanisms of mitochondrial H2O2 emission during long-chain fatty acid oxidation. J Biol Chem *285,* 5748-5758.

Sel, S., Ebert, T., Ryffel, G., and Drewes, T. (1996). Human renal cell carcinogenesis is accompanied by a coordinate loss of the tissue specific transcription factors HNF4 alpha and HNF1 alpha. Cancer Lett *101,* 205-210.

Senbanjo, L., and Chellaiah, M. (2017). CD44: A Multifunctional Cell Surface Adhesion Receptor Is a Regulator of Progression and Metastasis of Cancer Cells. Front Cell Dev Biol *5,* 18.

Senn, J. (2006). Toll-like receptor-2 is essential for the development of palmitate-induced insulin resistance in myotubes. J Biol Chem *281,* 26865-26875.

Seto, S., Tsujimura, K., Horii, T., and Koide, Y. (2014). Chapter 10 - Mycobacterial Survival in Alveolar Macrophages as a Result of Coronin-1a Inhibition of Autophagosome Formation. In Autophagy: Cancer, Other Pathologies, Inflammation, Immunity, Infection, and Aging, Hayat, M. A. ed., (Amsterdam: Academic Press) pp. 161-170.

Seufert, J., Kieffer, T., Leech, C., Holz, G., Moritz, W., Ricordi, C., and Habener, J. (1999). Leptin suppression of insulin secretion and gene expression in human pancreatic islets: implications for the development of adipogenic diabetes mellitus. J Clin Endocrinol Metab *84,* 670-676.

Shah, D., Mahajan, N., Sah, S., Nath, S., and Paudyal, B. (2014). Oxidative stress and its biomarkers in systemic lupus erythematosus. J Biomed Sci *21,* 23.

She, L., Li, W., Guo, Y., Zhou, J., Liu, J., Zheng, W., Dai, A., Chen, X., Wang, P., He, H. and Zhang, P. (2022). Association of glucokinase gene and glucokinase regulatory protein gene polymorphisms with gestational diabetes mellitus: A case–control study. Gene, 824, p.146378.

Shen, S., Liao, Q., Zhang, T., Pan, R., and Lin, L. (2019). Myricanol modulates skeletal muscle-adipose tissue crosstalk to alleviate high-fat diet-induced obesity and insulin resistance. Br J Pharmacol *176,* 3983-4001.

Shi, H., Kokoeva, M.V., Inouye, K., Tzameli, I., Yin, H., and Flier, J. (2006). TLR4 links innate immunity and fatty acid-induced insulin resistance. J Clin Invest *116,* 3015-3025.

Shields, B., Shepherd, M., Hudson, M., McDonald, T.J., Colclough, K., Peters, J., Knight, B., Hyde, C., Ellard, S., Pearson, E., and Hattersley, A. (2017). Population-Based Assessment of a Biomarker-Based Screening Pathway to Aid Diagnosis of Monogenic Diabetes in Young-Onset Patients. Diabetes Care *40,* 1017-1025.

Shih, D., Screenan, S., Munoz, K., Philipson, L., Pontoglio, M., Yaniv, M., Polonsky, K., and Stoffel, M. (2001). Loss of HNF-1alpha function in mice leads to abnormal expression of genes involved in pancreatic islet development and metabolism. Diabetes *50,* 2472-2480.

Shimabukuro, M., Zhou, Y., Levi, M., and Unger, R. (1998). Fatty acid-induced beta cell apoptosis: a link between obesity and diabetes. Proc Natl Acad Sci U S A *95,* 2498-2502.

Shishehbor, M., Aviles, R., Brennan, M., Fu, X., Goormastic, M., Pearce, G., Gokce, N., Keaney, J., Penn, M., Sprecher, D., Vita, J., and Hazen, S. (2003). Association of nitrotyrosine levels with cardiovascular disease and modulation by statin therapy. Jama *289,* 1675-1680.

Sies, H. (1997). Oxidative stress: oxidants and antioxidants. Exp Physiol *82,* 291-295.

Sies, H. (2015). Oxidative stress: a concept in redox biology and medicine. Redox Biol *4,* 180-183.

Singh, I. (1997). Biochemistry of peroxisomes in health and disease. Mol Cell Biochem *167,* 1-29.

Singh, P., Mahadi, F., Roy, A., and Sharma, P. (2009). Reactive oxygen species, reactive nitrogen species and antioxidants in etiopathogenesis of diabetes mellitus type-2. Indian J Clin Biochem *24,* 324-342.

Singh, S., Loke, Y., and Furberg, C. (2007). Long-term risk of cardiovascular events with rosiglitazone: a meta-analysis. Jama *298,* 1189-1195.

Skaper, S., Das, S., and Marshall, F. (1973). Some properties of a homocarnosine-carnosine synthetase isolated from rat brain. J Neurochem *21,* 1429-1445.

Sladek, F. (1994). Orphan receptor HNF-4 and liver-specific gene expression. Receptor *4,* 64.

Sladek, F., Zhong, W., Lai, E., and Darnell, J. (1990). Liver-enriched transcription factor HNF-4 is a novel member of the steroid hormone receptor superfamily. Genes Dev *4,* 2353-2365.

Sliwkowski, M., and Yarden, Y. (2001). Untangling the ErbB signalling network. Nature Reviews. Molecular Cell Biology *2,* 127-137.

Smith, P., Krohn, R., Hermanson, G., Mallia, A., Gartner, F., Provenzano, M., Fujimoto, E., Goeke, N., Olson, B., and Klenk, D. (1985). Measurement of protein using bicinchoninic acid. Analytical Biochemistry *150,* 76-85.

Sola, D., Rossi, L., Schianca, G., Maffioli, P., Bigliocca, M., Mella, R., Corlianò, F., Fra, G., Bartoli, E., and Derosa, G. (2015). Sulfonylureas and their use in clinical practice. Arch Med Sci *11,* 840-848.

Solcia, E., Usellini, L., Buffa, R., Rindi, G., Villani, L., Zampatti, C., and Silini, E. (1987). Endocrine cells producing regulatory peptides. Experientia *43,* 839-850.

Solis-Herrera, C., Triplitt, C., Cersosimo, E. and DeFronzo, R., (2021). Pathogenesis of type 2 diabetes mellitus. Endotext [Internet].

Song, M., Kim, K., Yoon, J., and Kim, J. (2006). Activation of Toll-like receptor 4 is associated with insulin resistance in adipocytes. Biochem Biophys Res Commun *346,* 739-745.

Spiegelman, B. (1998). PPAR-gamma: adipogenic regulator and thiazolidinedione receptor. Diabetes *47,* 507-514.

Starr, A., Dufour, A., Maier, J., and Overall, C. (2012). Biochemical analysis of matrix metalloproteinase activation of chemokines CCL15 and CCL23 and increased glycosaminoglycan binding of CCL16. J Biol Chem *287,* 5848-5860.

Stefan, Y., Orci, L., Malaisse-Lagae, F., Perrelet, A., Patel, Y., and Unger, R. (1982). Quantitation of endocrine cell content in the pancreas of nondiabetic and diabetic humans. Diabetes *31,* 694-700.

Stenvers, D., Scheer, F., Schrauwen, P., la Fleur, S., and Kalsbeek, A. (2019). Circadian clocks and insulin resistance. Nat Rev Endocrinol *15,* 75-89.

Stock, D., Leslie, A., and Walker, J. (1999). Molecular architecture of the rotary motor in ATP synthase. Science *286,* 1700-1705.

Stoffel, M., and Duncan, S. (1997). The maturity-onset diabetes of the young (MODY1) transcription factor HNF4alpha regulates expression of genes required for glucose transport and metabolism. Proc Natl Acad Sci U S A *94,* 13209-13214.

Stoffers, D., Kieffer, T., Hussain, M., Drucker, D., Bonner-Weir, S., Habener, J., and Egan, J. (2000). Insulinotropic glucagon-like peptide 1 agonists stimulate expression of homeodomain protein IDX-1 and increase islet size in mouse pancreas. Diabetes *49,* 741-748.

Stolz, D., Zamora, R., Vodovotz, Y., Loughran, P., Billiar, T., Kim, Y., Simmons, R., and Watkins, S. (2002). Peroxisomal localization of inducible nitric oxide synthase in hepatocytes. Hepatology *36,* 81-93.

St-Pierre, J., Buckingham, J., Roebuck, S., and Brand, M. (2002). Topology of superoxide production from different sites in the mitochondrial electron transport chain. J Biol Chem *277,* 44784-44790.

Suarez-Pinzon, W., Mabley, J., Strynadka, K., Power, R., Szabó, C., and Rabinovitch, A. (2001). An inhibitor of inducible nitric oxide synthase and scavenger of peroxynitrite prevents diabetes development in NOD mice. J Autoimmun *16,* 449-455.

Suarez-Pinzon, W., Szabó, C., and Rabinovitch, A. (1997). Development of autoimmune diabetes in NOD mice is associated with the formation of peroxynitrite in pancreatic islet beta-cells. Diabetes *46,* 907-911.

Sucu, N., Unlü, A., Tamer, L., Aytacoglu, B., Ercan, B., Dikmengil, M., and Atik, U. (2003). 3-Nitrotyrosine in atherosclerotic blood vessels. Clin Chem Lab Med *41,* 23-25.

Sugawara, K., Shibasaki, T., Mizoguchi, A., Saito, T., and Seino, S. (2009). Rab11 and its effector Rip11 participate in regulation of insulin granule exocytosis. Genes Cells *14,* 445-456.

Sugawara, T., Kano, F., and Murata, M. (2014). Rab2A is a pivotal switch protein that promotes either secretion or ER-associated degradation of (pro)insulin in insulin-secreting cells. Sci Rep *4,* 6952.

Sukhanova, A., Gorin, A., Serebriiskii, I., Gabitova, L., Zheng, H., Restifo, D., Egleston, B., Cunningham, D., Bagnyukova, T., Liu, H. and Nikonova, A. (2013). Targeting C4-Demethylating Genes in the Cholesterol Pathway Sensitizes Cancer Cells to EGF Receptor Inhibitors via Increased EGF Receptor DegradationSterol Pathway Genes Regulate Tumor Response to Anti-EGFR. Cancer discovery, 3(1), pp.96-111.

Sulkin, T., Bosman, D., and Krentz, A. (1997). Contraindications to metformin therapy in patients with NIDDM. Diabetes Care *20,* 925-928.

Sundler, F., Håkanson, R., and Larsson, L. (1977). Ontogeny of rat pancreatic polypeptide (PP) cells. Cell Tissue Res *178,* 303-306.

Surmeli, N., Litterman, N., Miller, A., and Groves, J. (2010). Peroxynitrite mediates active site tyrosine nitration in manganese superoxide dismutase. Evidence of a role for the carbonate radical anion. J Am Chem Soc *132,* 17174-17185.

Svendsen, B., Larsen, O., Gabe, M., Christiansen, C., Rosenkilde, M., Drucker, D., and Holst, J. (2018). Insulin Secretion Depends on Intra-islet Glucagon Signaling. Cell Reports *25,* 1127-1134.e2.

Szabó, C., Mabley, J., Moeller, S., Shimanovich, R., Pacher, P., Virag, L., Soriano, F., Van Duzer, J., Williams, W., Salzman, A., and Groves, J. (2002). Part I: pathogenetic role of peroxynitrite in the development of diabetes and diabetic vascular complications: studies with FP15, a novel potent peroxynitrite decomposition catalyst. Mol Med *8,* 571-580.

Tahara, E., Navarete, F., and Kowaltowski, A. (2009). Tissue-, substrate-, and site-specific characteristics of mitochondrial reactive oxygen species generation. Free Radic Biol Med *46,* 1283-1297.

Takahashi, Y., Sarkar, J., Yamada, J., Matsunaga, Y., Nonaka, Y., Banjo, M., Sakaguchi, R., Shinya, T., and Hatta, H. (2021). Enhanced skeletal muscle glycogen repletion after endurance exercise is associated with higher plasma insulin and skeletal muscle hexokinase 2 protein levels in mice: comparison of level running and downhill running model. J Physiol Biochem *77,* 469-480.

Tallant, C., Marrero, A., and Gomis-Rüth, F. (2010). Matrix metalloproteinases: Fold and function of their catalytic domains. Biochimica Et Biophysica Acta (BBA) - Molecular Cell Research *1803,* 20-28.

Tamba, M., and Torreggiani, A. (1999). Hydroxyl radical scavenging by carnosine and Cu(II)-carnosine complexes: a pulse-radiolysis and spectroscopic study. Int J Radiat Biol *75,* 1177-1188.

Tamborlane, W., and Amiel, S. (1992). Hypoglycemia in the treated diabetic patient. A risk of intensive insulin therapy. Endocrinol Metab Clin North Am *21,* 313-327.

Tanaka, Y., Tran, P., Harmon, J., and Robertson, R. (2002). A role for glutathione peroxidase in protecting pancreatic beta cells against oxidative stress in a model of glucose toxicity. Proc Natl Acad Sci U S A *99,* 12363-12368.

Tannous, M., Rabini, R., Vignini, A., Moretti, N., Fumelli, P., Zielinski, B., Mazzanti, L., and Mutus, B. (1999). Evidence for iNOS-dependent peroxynitrite production in diabetic platelets. Diabetologia *42,* 539-544.

Taylor, R. (2021). Type 2 diabetes and remission: practical management guided by pathophysiology. J Intern Med *289,* 754-770.

Taylor, S., Yazdi, Z., and Beitelshees, A. (2021). Pharmacological treatment of hyperglycemia in type 2 diabetes. J Clin Invest *131,*

Teixeira, D., Fernandes, R., Prudêncio, C., and Vieira, M. (2016). 3-Nitrotyrosine quantification methods: Current concepts and future challenges. Biochimie *125,* 1-11.

Terzioglu, M., and Larsson, N. (2007). Mitochondrial dysfunction in mammalian ageing. Novartis found Symp *287,* 197-213.

Teufel, M., Saudek, V., Ledig, J., Bernhardt, A., Boularand, S., Carreau, A., Cairns, N., Carter, C., Cowley, D., Duverger, D. and Ganzhorn, A., 2003. Sequence identification and characterization of human carnosinase and a closely related non-specific dipeptidase. Journal of Biological Chemistry, 278(8), pp.6521-6531.

Thanabalasingham, G., Pal, A., Selwood, M., Dudley, C., Fisher, K., Bingley, P., Ellard, S., Farmer, A., McCarthy, M., and Owen, K. (2012). Systematic assessment of etiology in adults with a clinical diagnosis of young-onset type 2 diabetes is a successful strategy for identifying maturity-onset diabetes of the young. Diabetes Care *35,* 1206-1212.

Thannickal, V., and Fanburg, B. (2000). Reactive oxygen species in cell signaling. Am J Physiol Lung Cell Mol Physiol *279,* 1005.

Theocharis, A., Skandalis, S., Gialeli, C., and Karamanos, N. (2016). Extracellular matrix structure. Adv Drug Deliv Rev *97,* 4-27.

Thirumalai, A., Holing, E., Brown, Z., and Gilliam, L. (2013). A case of hepatocyte nuclear factor-1β (TCF2) maturity onset diabetes of the young misdiagnosed as type 1 diabetes and treated unnecessarily with insulin. J Diabetes *5,* 462-464.

Thomas, H., Jaschkowitz, K., Bulman, M., Frayling, T., Mitchell, S., Roosen, S., Lingott-Frieg, A., Tack, C., Ellard, S., Ryffel, G., and Hattersley, A. (2001). A distant upstream promoter of the HNF-4alpha gene connects the transcription factors involved in maturity-onset diabetes of the young. Hum Mol Genet *10,* 2089-2097.

Thompson, D., and Gill, G. (1985). The EGF receptor: structure, regulation and potential role in malignancy. Cancer Surveys *4,* 767-788.

Thrailkill, K., Bunn, R., and Fowlkes, J. (2009). Matrix metalloproteinases: their potential role in the pathogenesis of diabetic nephropathy. Endocrine *35,* 1-10.

Thuraisingham, R., Nott, C., Dodd, S., and Yaqoob, M. (2000). Increased nitrotyrosine staining in kidneys from patients with diabetic nephropathy. Kidney Int *57,* 1968-1972.

Tiedge, M., Lortz, S., Drinkgern, J., and Lenzen, S. (1997). Relation between antioxidant enzyme gene expression and antioxidative defense status of insulin-producing cells. Diabetes *46,* 1733-1742.

Tisdale, E., and Balch, W. (1996). Rab2 is essential for the maturation of pre-Golgi intermediates. J Biol Chem *271,* 29372-29379.

Tomas, A., Yermen, B., Min, L., Pessin, J., and Halban, P. (2006). Regulation of pancreatic beta-cell insulin secretion by actin cytoskeleton remodelling: role of gelsolin and cooperation with the MAPK signalling pathway. J Cell Sci *119,* 2156-2167.

Torreggiani, A., Tamba, M., and Fini, G. (2000). Binding of copper(II) to carnosine: Raman and IR spectroscopic study. Biopolymers *57,* 149-159.

Toshinai, K., Mondal, M., Nakazato, M., Date, Y., Murakami, N., Kojima, M., Kangawa, K., and Matsukura, S. (2001). Upregulation of Ghrelin expression in the stomach upon fasting, insulin-induced hypoglycemia, and leptin administration. Biochem Biophys Res Commun *281,* 1220-1225.

Tourrel, C., Bailbe, D., Lacorne, M., Meile, M., Kergoat, M., and Portha, B. (2002). Persistent improvement of type 2 diabetes in the Goto-Kakizaki rat model by expansion of the beta-cell mass during the prediabetic period with glucagon-like peptide-1 or exendin-4. Diabetes *51,* 1443-1452.

Townsend, S., and Gannon, M. (2019). Extracellular Matrix-Associated Factors Play Critical Roles in Regulating Pancreatic β-Cell Proliferation and Survival. Endocrinology *160,* 1885-1894.

Tremblay, P., Fortin, C., and Sirard, M. (2021). Gene cascade analysis in human granulosa tumor cells (KGN) following exposure to high levels of free fatty acids and insulin. J Ovarian Res *14,* 178.

Trexler, E., Smith-Ryan, A., Stout, J., Hoffman, J., Wilborn, C., Sale, C., Kreider, R., Jäger, R., Earnest, C., Bannock, L. and Campbell, B. (2015). International society of sports nutrition position stand: Beta-Alanine. Journal of the International Society of Sports Nutrition, 12(1), p.30.

Triballeau, N., Van Name, E., Laslier, G., Cai, D., Paillard, G., Sorensen, P., Hoffmann, R., Bertrand, H., Ngai, J., and Acher, F. (2008). High-potency olfactory receptor agonists discovered by virtual high-throughput screening: molecular probes for receptor structure and olfactory function. Neuron *60,* 767-774.

Triposkiadis, F., Xanthopoulos, A., Bargiota, A., Kitai, T., Katsiki, N., Farmakis, D., Skoularigis, J., Starling, R., and Iliodromitis, E. (2021). Diabetes Mellitus and Heart Failure. J Clin Med *10,*

Tschöp, M., Smiley, D., and Heiman, M. (2000). Ghrelin induces adiposity in rodents. Nature *407,* 908-913.

Tsikas, D., and Duncan, M. (2014). Mass spectrometry and 3-nitrotyrosine: strategies, controversies, and our current perspective. Mass Spectrom Rev *33,* 237-276.

Turner, M., Nedjai, B., Hurst, T., and Pennington, D. (2014). Cytokines and chemokines: At the crossroads of cell signalling and inflammatory disease. Biochim Biophys Acta *1843,* 2563-2582.

Turrens, J. (2003). Mitochondrial formation of reactive oxygen species. J Physiol *552,* 335-344.

UKPDS. (1998). United Kingdom Prospective Diabetes Study 24: a 6-year, randomized, controlled trial comparing sulfonylurea, insulin, and metformin therapy in patients with newly diagnosed type 2 diabetes that could not be controlled with diet therapy. United Kingdom Prospective Diabetes Study Group. Ann Intern Med *128,* 165-175.

Unger, R. (1995). Lipotoxicity in the pathogenesis of obesity-dependent NIDDM. Genetic and clinical implications. Diabetes *44,* 863-870.

Unger, R., and Grundy, S. (1985). Hyperglycaemia as an inducer as well as a consequence of impaired islet cell function and insulin resistance: implications for the management of diabetes. Diabetologia *28,* 119-121.

Unger, R., and Orci, L. (1975). The essential role of glucagon in the pathogenesis of diabetes mellitus. Lancet *1,* 14-16.

Unger, R. (2010). Glucagon Physiology and Pathophysiology.*2021,*

Unno, H., Yamashita, T., Ujita, S., Okumura, N., Otani, H., Okumura, A., Nagai, K., and Kusunoki, M. (2008). Structural basis for substrate recognition and hydrolysis by mouse carnosinase CN2. J Biol Chem *283,* 27289-27299.

Upmacis, R. (2008). Atherosclerosis: A Link Between Lipid Intake and Protein Tyrosine Nitration. Lipid Insights *2008,* 75.

Usui, T., Kubo, Y., Akanuma, S., and Hosoya, K. (2013). β-Alanine and l-histidine transport across the inner blood-retinal barrier: Potential involvement in l-carnosine supply. Experimental Eye Research *113,* 135-142.

Valko, M., Leibfritz, D., Moncol, J., Cronin, M., Mazur, M., and Telser, J. (2007). Free radicals and antioxidants in normal physiological functions and human disease. Int J Biochem Cell Biol *39,* 44-84.

Valkovicova, T., Skopkova, M., Stanik, J., and Gasperikova, D. (2019). Novel insights into genetics and clinics of the HNF1A-MODY. Endocr Regul *53,* 110-134.

Vallon, V., and Verma, S. (2021). Effects of SGLT2 Inhibitors on Kidney and Cardiovascular Function. Annu Rev Physiol *83,* 503-528.

van de Laar, Floris A., Lucassen, P., Akkermans, R., van de Lisdonk, Eloy H., Rutten, G., and van Weel, C. (2005). Alpha-glucosidase inhibitors for patients with type 2 diabetes: results from a Cochrane systematic review and meta-analysis. Diabetes Care *28,* 154-163.

Van Geest, R., Klaassen, I., Lesnik-Oberstein, S., Tan, H., Mura, M., Goldschmeding, R., Van Noorden, Cornelis J., and Schlingemann, R. (2013). Vitreous TIMP-1 levels associate with neovascularization and TGF-β2 levels but not with fibrosis in the clinical course of proliferative diabetic retinopathy. J Cell Commun Signal *7,* 1-9.

van Raalte, D., and Diamant, M. (2011). Glucolipotoxicity and beta cells in type 2 diabetes mellitus: target for durable therapy? Diabetes Res Clin Pract *93 Suppl 1,* 37.

Vannini, F., Kashfi, K., and Nath, N. (2015). The dual role of iNOS in cancer. Redox Biology *6,* 334-343.

Varanoske, A., Hoffman, J., Church, D., Coker, N., Baker, K., Dodd, S., Oliveira, L., Dawson, V., Wang, R., Fukuda, D., and Stout, J. (2017). ScienceDirect. Journal of Environmental Sciences (China) 125-126.

Venditti, P., Napolitano, G., and Di Meo, S. (2015). Role of Mitochondria and Other ROS Sources in Hyperthyroidism-Linked Oxidative Stress. Immunology, Endocrine & Metabolic Agents - Medicinal ChemistryCurrent Medicinal Chemistry - Immunology, Endocrine & Metabolic Agents) *15,* 5-36.

Vető, B., Bojcsuk, D., Bacquet, C., Kiss, J., Sipeki, S., Martin, L., Buday, L., Bálint, B.L., and Arányi, T. (2017). The transcriptional activity of hepatocyte nuclear factor 4 alpha is inhibited via phosphorylation by ERK1/2. Plos One *12,* e0172020.

Visse, R., and Nagase, H. (2003). Matrix Metalloproteinases and Tissue Inhibitors of Metalloproteinases. Circulation Research *92,* 827-839.

Vistoli, G., Orioli, M., Pedretti, A., Regazzoni, L., Canevotti, R., Negrisoli, G., Carini, M., and Aldini, G. (2009). Design, Synthesis, and Evaluation of Carnosine Derivatives as Selective and Efficient Sequestering Agents of Cytotoxic Reactive Carbonyl Species. ChemMedChem *4,* 967-975.

Vranas, M., Wohlwend, D., Qiu, D., Gerhardt, S., Trncik, C., Pervaiz, M., Ritter, K., Steimle, S., Randazzo, A., Einsle, O. and Günther, S. (2021). Structural Basis for Inhibition of ROS-Producing Respiratory Complex I by NADH-OH. *Angewandte Chemie*, *133*(52), pp.27483-27487.

Wada, J., and Nakatsuka, A. (2016). Mitochondrial Dynamics and Mitochondrial Dysfunction in Diabetes. Acta Med Okayama *70,* 151-158.

Wall, S., Sampson, M., Levell, N., and Murphy, G. (2003). Elevated matrix metalloproteinase-2 and -3 production from human diabetic dermal fibroblasts. Br J Dermatol *149,* 13-16.

Wallemacq, C. (2019). [Statins and new-onset diabetes : benefit-risk balance]. Rev Med Suisse *15,* 1454-1457.

Wang, C., and Wei, Y. (2017). Role of mitochondrial dysfunction and dysregulation of Ca2+ homeostasis in the pathophysiology of insulin resistance and type 2 diabetes. J Biomed Sci *24,* 70.

Wang, G., Zhao, X., Meng, Z., Kern, M., Dietrich, A., Chen, Z., Cozacov, Z., Zhou, D., Okunade, A., Su, X. and Li, S. (2014). The brown fat–enriched secreted factor Nrg4 preserves metabolic homeostasis through attenuation of hepatic lipogenesis. Nature medicine, 20(12), pp.1436-1443.

Wang, H., Maechler, P., Antinozzi, P., Hagenfeldt, K., and Wollheim, C. (2000). Hepatocyte nuclear factor 4alpha regulates the expression of pancreatic beta -cell genes implicated in glucose metabolism and nutrient-induced insulin secretion. J Biol Chem *275,* 35953-35959.

Wang, Q., and Brubaker, P. (2002). Glucagon-like peptide-1 treatment delays the onset of diabetes in 8 week-old db/db mice. Diabetologia *45,* 1263-1273.

Wang, X., and Hai, C. (2011). ROS acts as a double-edged sword in the pathogenesis of type 2 diabetes mellitus: is Nrf2 a potential target for the treatment? Mini Rev Med Chem *11,* 1082-1092.

Wang, X., and Khalil,. (2018). Matrix Metalloproteinases, Vascular Remodeling, and Vascular Disease. Adv Pharmacol *81,* 241-330.

Wang, Y., Liu, Q., Kang, S., Huang, K., and Tong, T. (2021). Dietary Bioactive Ingredients Modulating the cAMP Signaling in Diabetes Treatment. Nutrients *13,*

Wang, Z., Gao, Z., Wang, A., Jia, L., Zhang, X., Fang, M., Yi, K., Li, Q., and Hu, H. (2019). Comparative oral and intravenous pharmacokinetics of phlorizin in rats

having type 2 diabetes and in normal rats based on phase II metabolism. Food Funct *10,* 1582-1594.

Wang, Z. (2017). ErbB Receptors and Cancer. Methods Mol Biol *1652,* 3-35.

Wei, Y., and Lee, H. (2002). Oxidative stress, mitochondrial DNA mutation, and impairment of antioxidant enzymes in aging. Exp Biol Med (Maywood) *227,* 671-682.

Weir, G., Samols, E., Loo, S., Patel, Y., and Gabbay, K. (1979). Somatostatin and pancreatic polypeptide secretion: effects of glucagon, insulin, and arginine. Diabetes *28,* 35-40.

Weir, G. (2020). Glucolipotoxicity, β-Cells, and Diabetes: The Emperor Has No Clothes. Diabetes *69,* 273-278.

Weiss, M., Steiner, D. and Philipson, L. (2015). Insulin biosynthesis, secretion, structure, and structure-activity relationships.

Wenzl, F., Ambrosini, S., Mohammed, S., Kraler, S., Lüscher, T., Costantino, S., and Paneni, F. (2021). Inflammation in Metabolic Cardiomyopathy. Front Cardiovasc Med *8,* 742178.

White, P., McGarrah, R., Herman, M., Bain, J., Shah, S., and Newgard, C. (2021). Insulin action, type 2 diabetes, and branched-chain amino acids: A two-way street. Mol Metab *52,* 101261.

Wierup, N., and Sundler, F. (2004). Circulating levels of ghrelin in human fetuses. Eur J Endocrinol *150,* 405.

Wierup, N., Svensson, H., Mulder, H., and Sundler, F. (2002). The ghrelin cell: a novel developmentally regulated islet cell in the human pancreas. Regul Pept *107,* 63-69.

Wierup, N., Björkqvist, M., Weström, B., Pierzynowski, S., Sundler, F., and Sjölund, K. (2007). Ghrelin and motilin are cosecreted from a prominent endocrine cell population in the small intestine. J Clin Endocrinol Metab *92,* 3573-3581.

Wierup, N., Sundler, F., and Heller, R. (2014). The islet ghrelin cell. J Mol Endocrinol *52,* 35.

Wikstrom, J., Katzman, S., Mohamed, H., Twig, G., Graf, S., Heart, E., Molina, A., Corkey, B., De Vargas, L., Danial, N., Collins, S., and Shirihai, O. (2007). β-Cell mitochondria exhibit membrane potential heterogeneity that can be altered by stimulatory or toxic fuel levels. Diabetes *56,* 2569-2578.

Wilcox, G. (2005). Insulin and insulin resistance. Clin Biochem Rev *26,* 19-39.

Wilding, J. (2014). The importance of weight management in type 2 diabetes mellitus. Int J Clin Pract *68,* 682-691.

Witz, G. (1989). Biological interactions of α,β-unsaturated aldehydes. Free Radical Biology and Medicine *7,* 333-349.

Wong, C., Al-Salami, H., and Dass, C. (2020). C2C12 cell model: its role in understanding of insulin resistance at the molecular level and pharmaceutical development at the preclinical stage. J Pharm Pharmacol *72,* 1667-1693.

Wright, J., Richards, T., and Becker, D. (2012). Connexins and Diabetes.*2021,*

Xiao, M., Zhong, H., Xia, L., Tao, Y., and Yin, H. (2017). Pathophysiology of mitochondrial lipid oxidation: Role of 4-hydroxynonenal (4-HNE) and other bioactive lipids in mitochondria. Free Radical Biology and Medicine *111,* 316-327.

Xiong, Q., Yu, C., Zhang, Y., Ling, L., Wang, L., and Gao, J. (2017). Key proteins involved in insulin vesicle exocytosis and secretion (Review). Biomedical Reports *6,* 134-139.

Xu, H. (2013). Obesity and metabolic inflammation. Drug Discov Today Dis Mech *10,*

Yamagata, K., Oda, N., Kaisaki, P., Menzel, S., Furuta, H., Vaxillaire, M., Southam, L., Cox, R., Lathrop, G., Boriraj, V. and Chen, X. (1996). Mutations in the hepatocyte nuclear factor-1α gene in maturity-onset diabetes of the young (MODY3). Nature, 384(6608), pp.455-458.

Yan, P., Xu, Y., Wan, Q., Feng, J., Li, H., Gao, C., Yang, J., Zhong, H., and Zhang, Z. (2017). Decreased plasma neuregulin 4 concentration is associated with increased high-sensitivity C-reactive protein in newly diagnosed type 2 diabetes mellitus patients: a cross-sectional study. Acta Diabetol *54,* 1091-1099.

Yandrapalli, S., Malik, A., Guber, K., Rochlani, Y., Pemmasani, G., Jasti, M., and Aronow, W.S. (2019). Statins and the potential for higher diabetes mellitus risk. Expert Rev Clin Pharmacol *12,* 825-830.

Yang, H., Shi, P., Zhang, Y., and Zhang, J. (2005). Composition and evolution of the V2r vomeronasal receptor gene repertoire in mice and rats. Genomics *86,* 306-315.

Yang, S., and Lian, G. (2020). ROS and diseases: role in metabolism and energy supply. Mol Cell Biochem *467,* 1-12.

Yang, Y., and LiCata, V. (2018). Pol I DNA polymerases stimulate DNA end-joining by Escherichia coli DNA ligase. Biochem Biophys Res Commun *497,* 13-18.

Yang, Y., Kwak, S., and Park, K. (2020). Update on Monogenic Diabetes in Korea. Diabetes Metab J *44,* 627-639.

Yao, X., Carlson, D., Sun, Y., Ma, L., Wolf, S., Minei, J., and Zang, Q. (2015). Mitochondrial ROS Induces Cardiac Inflammation via a Pathway through mtDNA Damage in a Pneumonia-Related Sepsis Model. PLoS One *10,* e0139416.

Yap, C., and Winckler, B. (2009). Vesicular Sorting to Axons and Dendrites. In Encyclopedia of Neuroscience, Squire, Larry R. ed., (Oxford: Academic Press) pp. 115-120.

Yaribeygi, H., Sathyapalan, T., Atkin, S.L., and Sahebkar, A. (2020). Molecular Mechanisms Linking Oxidative Stress and Diabetes Mellitus. Oxid Med Cell Longev *2020,* 8609213.

Yi, Z., Yokota, H., Torii, S., Aoki, T., Hosaka, M., Zhao, S., Takata, K., Takeuchi, T., and Izumi, T. (2002). The Rab27a/granuphilin complex regulates the exocytosis of insulin-containing dense-core granules. Mol Cell Biol *22,* 1858-1867.

Yin, Z., Zhang, W., Feng, F., Zhang, Y., and Kang, W. (2014). α-Glucosidase inhibitors isolated from medicinal plants. Food Science and Human Wellness *3,* 136-174.

Yoon, T., and Munson, M. (2018). SNARE complex assembly and disassembly. Current Biology *28,* R397-R401.

Yu, W., Woessner, J., McNeish, J., and Stamenkovic, I. (2002). CD44 anchors the assembly of matrilysin/MMP-7 with heparin-binding epidermal growth factor precursor and ErbB4 and regulates female reproductive organ remodeling. Genes Dev *16,* 307-323.

Zapol, W. (2019). Nitric Oxide Story. Anesthesiology *130,* 435-440.

Zeender, E., Maedler, K., Bosco, D., Berney, T., Donath, M., and Halban, P. (2004). Pioglitazone and Sodium Salicylate Protect Human β-Cells against Apoptosis and Impaired Function Induced by Glucose and Interleukin-1β. The Journal of Clinical Endocrinology & Metabolism *89,* 5059-5066.

Zeng, Q., Li, N., Pan, X., Chen, L., and Pan, A. (2021). Clinical management and treatment of obesity in China. Lancet Diabetes Endocrinol *9,* 393-405.

Zhang, Q., Bengtsson, M., Partridge, C., Salehi, A., Braun, M., Cox, R., Eliasson, L., Johnson, P., Renström, E., Schneider, T. and Berggren, P. (2007). R-type Ca2+-channel-evoked CICR regulates glucose-induced somatostatin secretion. Nature cell biology, 9(4), pp.453-460.

Zhang, S., Lachance, B., Mattson, M., and Jia, X. (2021). Glucose metabolic crosstalk and regulation in brain function and diseases. Prog Neurobiol *204,* 102089.

Zhang, X., Rogers, M., Tian, H., Zhang, X., Zou, D., Liu, J., Ma, M., Shepherd, G., and Firestein, S. (2004). High-throughput microarray detection of olfactory receptor gene expression in the mouse. Proc Natl Acad Sci U S A *101,* 14168-14173.

Zhao, S., Zhang, Y., Gamini, R., Zhang, B., and von Schack, D. (2018). Evaluation of two main RNA-seq approaches for gene quantification in clinical RNA sequencing: polyA+ selection versus rRNA depletion. Sci Rep *8,* 4781.

Zhong, H., and Yin, H. (2015). Role of lipid peroxidation derived 4-hydroxynonenal (4-HNE) in cancer: Focusing on mitochondria. Redox Biology *4,* 193-199.

Zhou, G., Myers, R., Li, Y., Chen, Y., Shen, X., Fenyk-Melody, J., Wu, M., Ventre, J., Doebber, T., Fujii, N. and Musi, N. (2001). Role of AMP-activated protein kinase in mechanism of metformin action. The Journal of clinical investigation, 108(8), pp.1167-1174.

Zhou, S., Dickinson, L., Yang, L., and Decker, E. (1998). Identification of hydrazine in commercial preparations of carnosine and its influence on carnosine's antioxidative properties. Anal Biochem *261,* 79-86.

Zhou, Y., and Grill, V. (1994). Long-term exposure of rat pancreatic islets to fatty acids inhibits glucose-induced insulin secretion and biosynthesis through a glucose fatty acid cycle. J Clin Invest *93,* 870-876.

Zitka, O., Skalickova, S., Gumulec, J., Masarik, M., Adam, V., Hubalek, J., Trnkova, L., Kruseova, J., Eckschlager, T., and Kizek, R. (2012). Redox status expressed as GSH:GSSG ratio as a marker for oxidative stress in paediatric tumour patients. Oncol Lett *4,* 1247-1253.

Zito, E. (2015). ERO1: A protein disulfide oxidase and H2O2 producer. Free Radic Biol Med *83,* 299-304.

Zorov, D., Juhaszova, M., and Sollott, S. (2014). Mitochondrial reactive oxygen species (ROS) and ROS-induced ROS release. Physiol Rev *94,* 909-950.

Appendices

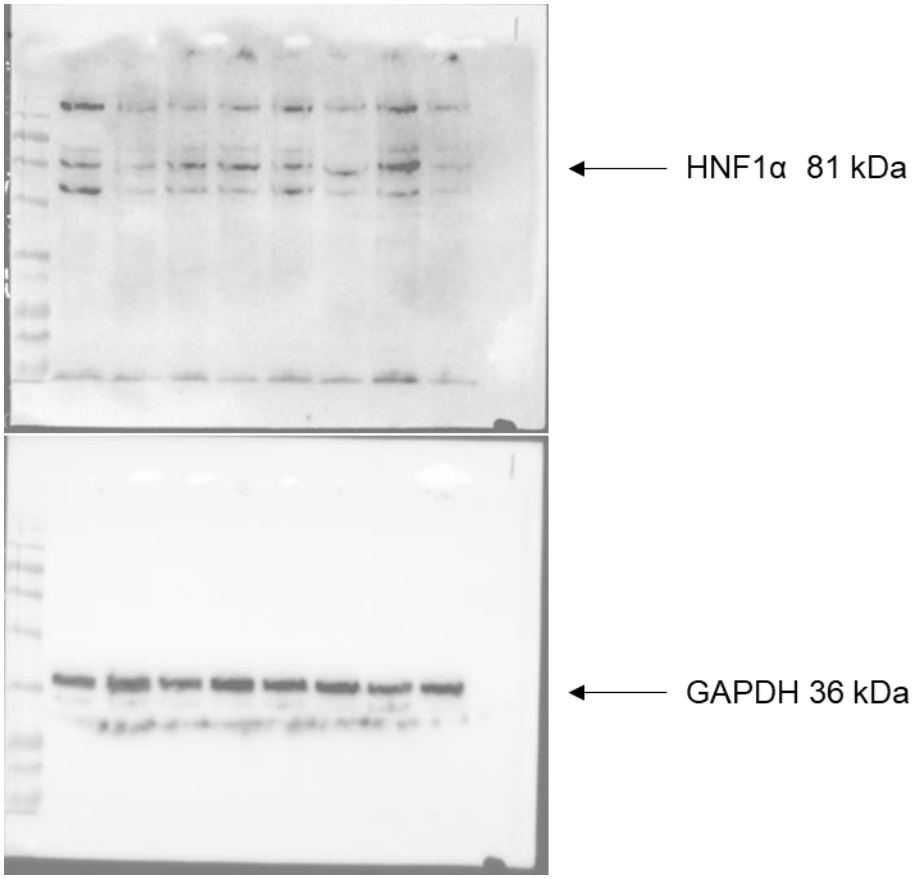

Figure A1. HNF1α. Control (1st lane, 3rd lane, 5th lane and 7th lane) and GLT (2nd lane, 4th lane, 6th lane and 8th lane)

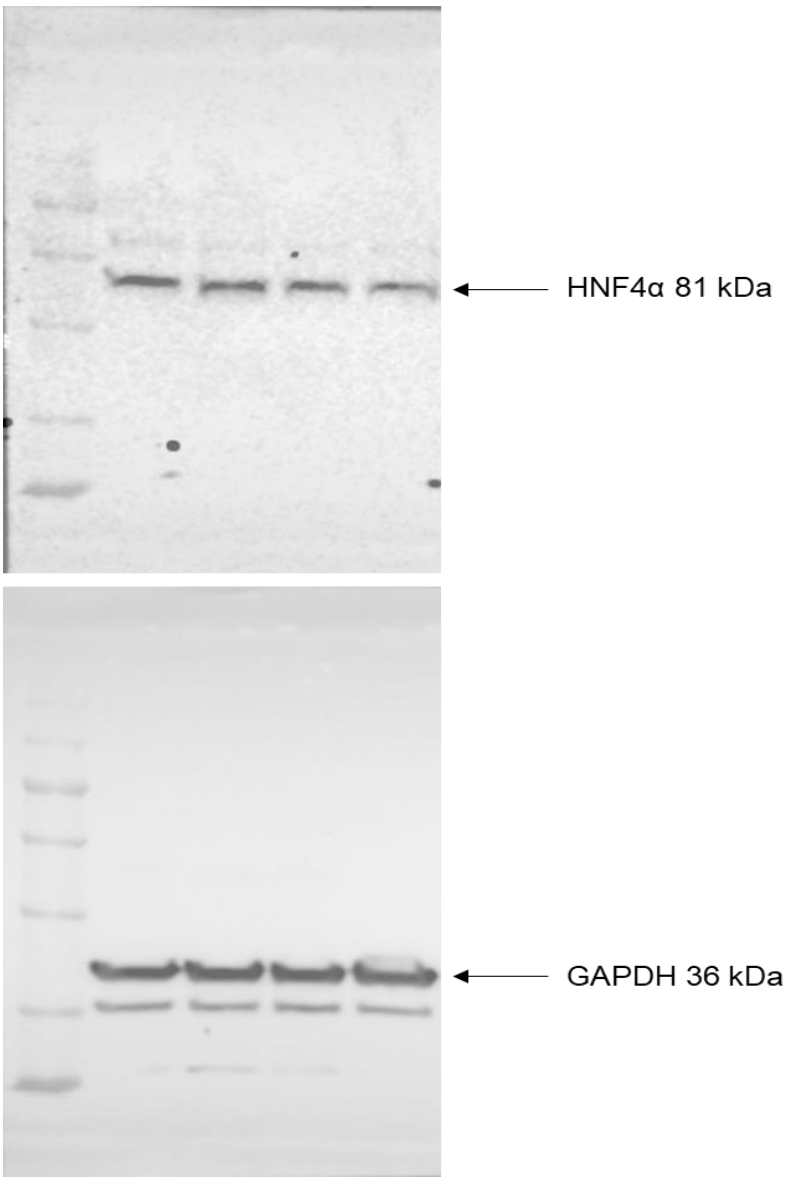

Figure A2. HNF4α. Control (1st lane and 3rd lane) and GLT (2nd lane, and 4th lane)

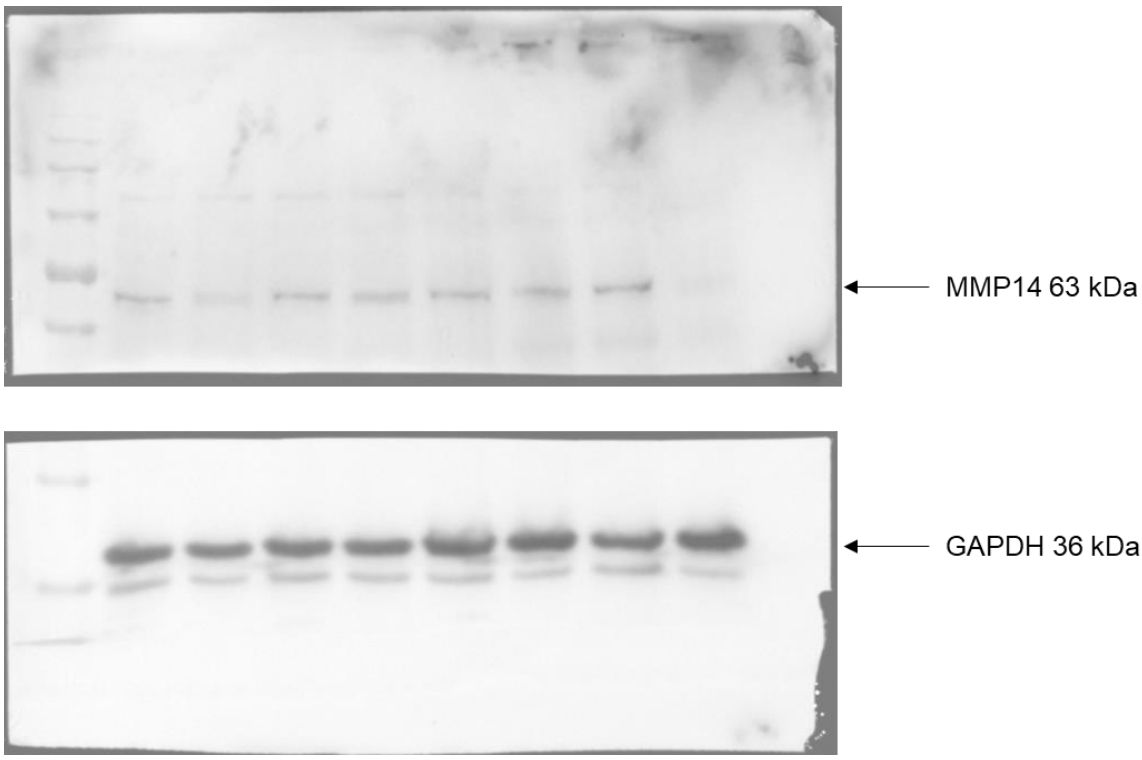

Figure A3. MMP14. Control (1st lane, 3rd lane, 5th lane and 7th lane) and GLT (2nd lane, 4th lane, 6th lane and 8th lane)

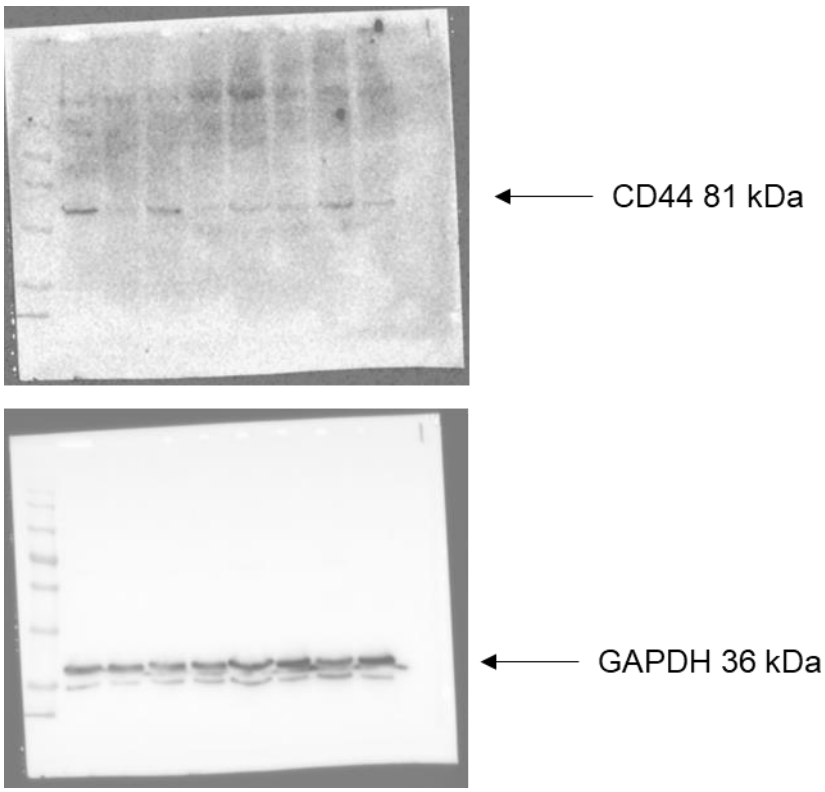

Figure A4. CD44. Control (1st lane, 3rd lane, 5th lane and 7th lane) and GLT (2nd lane, 4th lane, 6th lane and 8th lane)

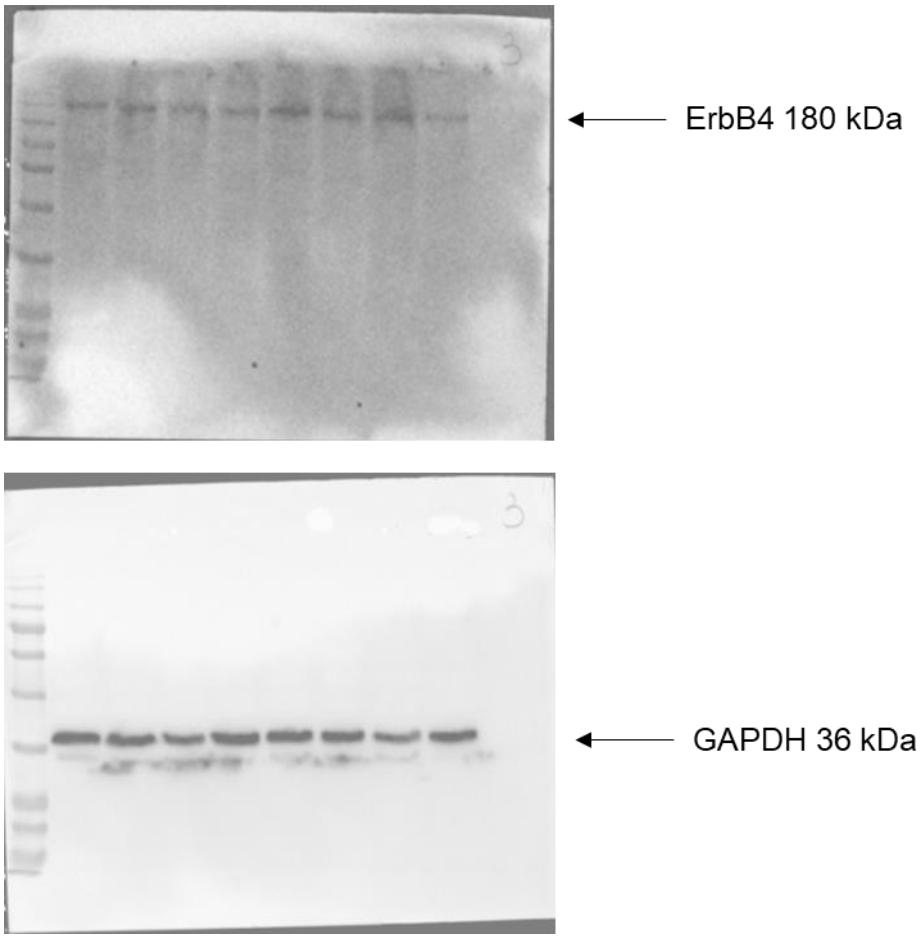

Figure A5. ErbB4. Control (1st lane, 3rd lane, 5th lane and 7th lane) and GLT (2nd lane, 4th lane, 6th lane and 8th lane)

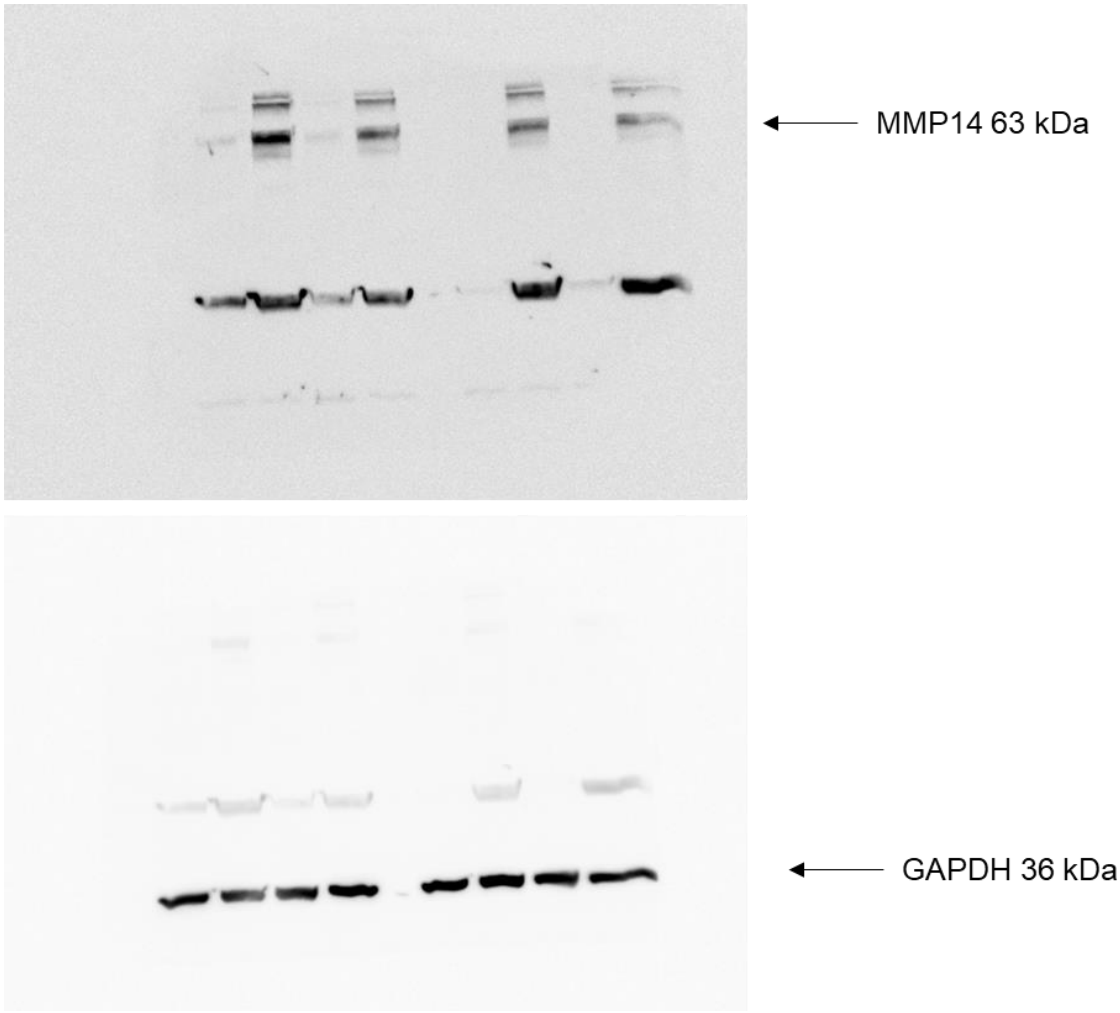

Figure A6. iNOS. Control (1st and 6th lane), GLT (2nd and 7th lane), carnosine (3rd and 8th lane) and GLT + carnosine (4th and 9th lane)